Identification of breast carcinogens based on PPARγ antagonism

Ardenkjær-Skinnerup, Jacob

Publication date:
2023

Document Version
Publisher's PDF, also known as Version of record

Title: Identification of breast carcinogens based on PPARγ antagonism
Name: Jacob Ardenkjær-Skinnerup
University: Technical University of Denmark
Institute: National Food Institute
Group: Research Group for Risk Benefit
Submission date: 25/10/2023

Supervisors:

Gitte Ravn-Haren, Senior Scientist
National Food Institute, Technical University of Denmark

Ulla B. Vogel, Professor
National Research Centre for the Working Environment

Niels Hadrup, Senior Scientist
National Research Centre for the Working Environment

Assessment committee:

Sari Mäkelä, Professor
Institute of Biomedicine, University of Turku

Jakob Bo Hansen, Associate Professor
Department of Biology, University of Copenhagen

Hanna Katarina Lilith Johansson, Senior Researcher
National Food Institute, Technical University of Denmark

Table of contents

Preface

This thesis is submitted in partial fulfillment of the requirements for obtaining the PhD degree at the Technical University of Denmark. The present PhD project was a collaboration between the National Food Institute at the Technical University of Denmark and the National Research Centre for the Working Environment. The main supervisor was Gitte Ravn-Haren from the National Food Institute, and the co-supervisors were Ulla Vogel and Niels Hadrup from the National Research Centre for the Working Environment. The project was partially funded by the Focused Research Effort on Chemicals in the Working Environment (FFIKA) from the Danish Government. The research was supervised and conducted from April 2020 to October 2023 at the Technical University of Denmark, the National Research Centre for the Working Environment, the University of Copenhagen, and Cornell University. The thesis is based on three unpublished manuscripts and includes work carried out by collaborators, which is specified in the methods section.

Acknowledgements

I would like to thank my supervisors, Gitte Ravn-Haren, Ulla Vogel, and Niels Hadrup, for excellent supervision and support during my PhD project. Their guidance and insightful feedback have been very helpful throughout my project. I would also like to thank Terje Svingen, Brice Emanuelli, and Kristy A. Brown for inviting me to conduct part of my research in their laboratories and providing supervision. In addition, I would like to thank the National Food Institute, the National Research Centre for the Working Environment, the Novo Nordisk Foundation Center for Basic Metabolic Research, and Weill Cornell Medicine, where I have conducted my research during my PhD, for being great research environments and offering resources, facilities, and academic support. Also, thanks to the research group members at these institutions for excellent ideas, constructive feedback, and a positive working atmosphere.

The work I have done during my project has been greatly influenced by support and contributions from collaborators. I would like to thank all the collaborators on the project for their interest and for sharing their expertise: Eva Bay Wedebye, Ana Caroline Vasconcelos Engedal Nissen, Nikolai Georgiev Nikolov, Martin Smieško, Sofie Christiansen, Mikael Pedersen, Patricia S. S. Petersen, Birthe B. Kragelund, and Daniel Saar. Also, I am very thankful for the laboratory assistance I received from Anne-Karin Asp, Dorte Lykkegaard Korsbech, Heidi Broksø Letting, Lillian Sztuk, and Maud Bering Andersen.

I would like to express appreciation to FFIKA (Focused Research Effort on Chemicals in the Working Environment, from the Danish Government) for funding my research. I also highly appreciate the travel grants I received for my research stay in New York (Idella Foundation, William Demant Foundation, and Christian and Ottilia Brorsons Travel Grant) and my conference attendance at the Annual Meeting of the Endocrine Society 2023 in Chicago (William Demant Foundation and Familien Hede Nielsens Foundation).

My parents and sister have also given me lots of support, particularly in the last tough months. I would like to thank them for their encouragement and understanding, and also for taking care of the kids sometimes, allowing me to get a proper night's sleep. Finally, I would like to thank my supportive wife, Nicoline. I am grateful that she has motivated and backed me throughout my project, and I appreciate the sacrifices she has made, especially during our stay in New York. Thanks to Nicoline and our kids, Milan and Mikkel, for their patience and love, and for all the fun we have together even in the most difficult times.

Summary

The protein peroxisome proliferator-activated receptor gamma (PPARγ) is a transcription factor highly expressed in adipose tissue where it is crucial for the development of fat cells (adipocytes) through the process of adipogenesis. In addition, PPARγ is involved in the production of hormones and signaling molecules in adipose tissue. The function of PPARγ can be modified by exogenous chemicals through agonistic or antagonistic effects on PPARγ activity, which can lead to disruption of metabolism and the endocrine system. The focus of this project was to study how exposure to foreign chemicals can impact breast cancer development via PPARγ antagonism, as the regulation and balance of hormones play a significant role in this. While there is evidence suggesting that PPARγ can act as a tumor suppressor, particularly in the breast, the exact mechanisms are not yet fully understood.

The hormone estrogen is produced by the enzyme aromatase in the adipose tissue, where it signals locally to the cells of the breast tissue and stimulates cell division. It has been shown that PPARγ represses the expression of aromatase, suggesting that exposure to PPARγ-inhibiting chemicals in the environment may lead to overexpression of aromatase in the adipose tissue. Increased aromatase expression is associated with an elevated level of circulating estrogens – a well-known risk factor for breast cancer. That is why medical treatment with aromatase inhibitors is an effective strategy to reduce estrogen production and consequently prevent cancer growth. The connection between PPARγ, aromatase, and their influence on metabolic disease and cancer is thus an important area of study.

The primary aim of the project was to identify chemicals that inhibit PPARγ and investigate if they affect estrogen production in the adipose tissue and thereby potentially promote breast cancer. Modulation of PPARγ activity in response to environmental and occupational chemical exposure has been studied extensively, yet experimental results are often inconsistent. Therefore, previously identified PPARγ inhibitors were confirmed in an orthogonal analysis assessing the effects of 25 chemicals on the transcriptional activity of PPARγ. Additional PPARγ antagonists were discovered by similar testing of chemicals predicted to inhibit PPARγ based on a quantitative structure-activity relationship (QSAR) model developed by collaborators. NMR spectroscopy performed by other collaborators showed that two of the confirmed PPARγ antagonists directly interact with and inhibit PPARγ. To complement these results, it was demonstrated that seven of the chemicals could block adipogenesis, which PPARγ is essential for. An interesting observation was that the expression of aromatase was greater in the pre-adipocytes than in the fully developed adipocytes. This led to investigation of whether impaired adipogenesis in response to PPARγ inhibitors would affect aromatase expression. The results indicated that PPARγ inhibition prevented adipogenesis-induced downregulation of aromatase.

A short-term effect of PPARγ inhibition on aromatase expression was studied in human pre-adipocytes and adipocytes. The results revealed no effect of PPARγ-inhibiting chemicals in the pre-adipocytes, where the PPARγ level is low, but increased aromatase expression in mature adipocytes, where PPARγ is abundant. Consistent with this, ectopic overexpression of PPARγ, as well as stimulation with a PPARγ activator, decreased the expression of aromatase in pre-adipocytes. In breast adipose tissue explants, activation and inhibition of PPARγ had similar effects as in adipocytes. Short-term exposure of female rats to PPARγ inhibitors, including alcohol, however, did not affect aromatase expression in the adipose tissue.

It can be concluded that PPARγ inhibitors could be identified among environmental chemicals, and these inhibitors elevated aromatase expression both indirectly by impairing adipogenesis and via a more acute mechanism, which is yet to be defined. Increased adipose tissue aromatase expression will supposedly lead to increased local estrogen production, which can potentially promote breast tumor growth.

Summary (in Danish)

Proteinet peroxisomproliferator-aktiveret receptor gamma (PPARγ) er en transkriptionsfaktor som er højt udtrykt i fedtvæv, hvor det er afgørende for udviklingen af fedtceller (adipocytter) gennem processen, adipogenese. Derudover er PPARγ involveret i produktionen af hormoner og signalmolekyler i fedtvævet. Funktionen af PPARγ kan påvirkes af eksogene stoffer gennem agonistiske eller antagonistiske effekter på PPARγ aktivitet, hvilket kan føre til forstyrrelse af stofskiftet og hormonsystemet. Dette projekt fokuserer på at undersøge, hvordan eksponering over for fremmede stoffer kan påvirke udviklingen af brystkræft via PPARγ antagonisme, da hormonregulering og -balance spiller en væsentlig rolle for dette. Mens der er evidens for, at PPARγ kan virke tumorundertrykkende, især i brystet, er de præcise mekanismer endnu ikke fuldt ud forstået.

Hormonet østrogen bliver produceret af enzymet aromatase i fedtvævet, hvor det signalerer lokalt til cellerne i brystvævet og stimulerer celledeling. Det er vist, at PPARγ undertrykker ekspressionen af aromatase, hvilket tyder på, at eksponering over for PPARγ-hæmmende stoffer i miljøet kan føre til overudtrykkelse af aromatase i fedtvævet. Øget aromatase-ekspression er forbundet med forhøjet niveau af cirkulerende østrogener – en velkendt risikofaktor for brystkræft. Derfor er medicinsk behandling med aromatase-hæmmere også en effektiv strategi til at nedsætte østrogenproduktionen og dermed forhindre kræftvækst. Forbindelsen mellem PPARγ, aromatase og deres indflydelse på metabolisk sygdom og kræft er altså et vigtigt forskningsområde.

Det overordnede formål med projektet var at identificere stoffer, der hæmmer PPARγ, samt undersøge om de påvirker østrogenproduktionen i fedtvævet og dermed potentielt virker brystkræftfremkaldende. Modulering af PPARγ aktivitet som reaktion på eksponering over for stoffer i miljøet og på arbejdspladsen har været undersøgt udførligt, men alligevel er eksperimentelle resultater ofte inkonsistente. Derfor blev tidligere identificerede PPARγ-hæmmere bekræftet i en orthogonal analyse, der vurderede 25 stoffers virkninger på den transskriptionelle aktivitet af PPARγ. Yderligere PPARγ-antagonister blev opdaget ved en lignende test af stoffer, der forventes at hæmme PPARγ baseret på en kvantitativ struktur-aktivitetsrelationsmodel (QSAR-model) udviklet af samarbejdspartnere. NMR-spektroskopi udført af andre samarbejdspartnere viste, at to af de bekræftede PPARγ-antagonister direkte interagerer med og hæmmer PPARγ. For at supplere disse resultater blev det påvist, at syv af stofferne kunne blokere adipogenese, som PPARγ er afgørende for. En interessant observation var, at udtrykkelsen af aromatase var højere i præ-adipocytter end i de fuldt udviklede adipocytter. Dette førte til undersøgelse af, om nedsat adipogenese som reaktion på PPARγ-hæmmere ville påvirke aromatase-ekspression. Resultaterne indikerede, at PPARγ-hæmning forhindrede adipogenese-induceret nedregulering af aromatase.

En kortsigtet effekt af PPARγ-hæmning på aromatase-udtrykkelse blev undersøgt i humane præ-adipocytter og adipocytter. Resultaterne viste ingen effekt af PPARγ-hæmmende stoffer i præ-adipocytterne, hvor PPARγ-niveauet er lavt, men øget aromatase-ekspression i de fuldtudviklede adipocytter, hvor der er højt PPARγ-niveau. Dette er i overensstemmelse med, at ektopisk overekspression af PPARγ, såvel som stimulering med en PPARγ-aktivator, reducerede ekspressionen af aromatase i præ-adipocytter. I eksplantater fra brystfedtvæv havde aktivering og hæmning af PPARγ lignende virkninger som i adipocytter. Kortvarig eksponering af hunrotter for PPARγ-hæmmere, inklusive alkohol, påvirkede imidlertid ikke aromatase-ekspression i fedtvævet.

Det kan konkluderes, at PPARγ-hæmmere kunne identificeres blandt stoffer i miljøet, og disse hæmmere forhøjede aromatase-ekspression både indirekte ved at svække adipogenese og via en mere akut mekanisme, som endnu ikke er defineret. Øget aromatase-ekspression i fedtvævet vil angiveligt føre til øget lokal østrogenproduktion, som potentielt kan fremme brysttumorvækst.

List of manuscripts

Manuscript I
"Orthogonal Assay and QSAR Modeling of Tox21 PPARγ Antagonist In Vitro High-Throughput Screening Assay". Jacob Ardenkjær-Skinnerup, Ana Caroline Vasconcelos Engedal Nissen, Nikolai Georgiev Nikolov, Martin Smieško, Niels Hadrup, Gitte Ravn-Haren, Eva Bay Wedebye, Ulla Vogel.

Manuscript II
"PPARγ Antagonists Induce Aromatase Transcription in Adipose Tissue Cultures". Jacob Ardenkjær-Skinnerup, Daniel Saar, Patricia S. S. Petersen, Mikael Pedersen, Terje Svingen, Birthe B. Kragelund, Niels Hadrup, Gitte Ravn-Haren, Brice Emanuelli, Kristy A. Brown, Ulla B. Vogel.

Manuscript III
"PPARγ-mediated effect of ethanol and ethylene glycol on aromatase expression in adipose tissue." Jacob Ardenkjær-Skinnerup, Daniel Saar, Sofie Christiansen, Terje Svingen, Niels Hadrup, Kristy A. Brown, Brice Emanuelli, Birthe B. Kragelund, Gitte Ravn-Haren, Ulla B. Vogel.

List of abbreviations

15d-PGJ2	15-deoxy-$\Delta^{12,14}$-prostaglandin J_2
3' SC	self 3' complementarity
9cRA	9-*cis*-retinoic acid
abs.	absolute
AC_{50}	half-maximal activity concentration
ADH	alcohol dehydrogenase
AF1	activation function 1
AF2	activation function 2
ALDH	aldehyde dehydrogenase
ALT	alanine aminotransferase
ANOVA	analysis of variance
ANS	8-anilino-1-naphthalenesulfonic acid
aP2	adipocyte protein 2
AR	androgen receptor
ASC	adipose stromal cell
AU	arbitrary units
BA	balanced accuracy
BADGE	bisphenol A diglycidyl ether
BMI	body mass index
bp	base pairs
BRCA1	breast cancer gene 1
C/EBP	CCAAT/enhancer binding protein
CALUX	chemically activated luciferase gene expression
CAS	Chemical Abstracts Service
cDNA	complementary DNA
CI	confidence interval
CRISPR	clustered regularly interspaced short palindromic repeats
DBD	DNA-binding domain
DEHP	di-(2-ethylhexyl)-phthalate
DEHPA	di-(2-ethylhexyl)-phosphoric acid
DHEA	dehydroepiandrosterone
DHT	dihydrotestosterone
DMBA	7,12-dimethylbenzanthracene
DMEM	Dulbecco's Modified Eagle Medium
DMSO	dimethyl sulfoxide
DNA	deoxyribonucleic acid
DPhP	diphenyl phthalate
DSS	4,4-dimethyl-4-silapentane-1-sulfonic acid
DTU	Technical University of Denmark
DTU Food	National Food Institute at the Technical University of Denmark
EC_{50}	half maximal effective concentration
E_{max}	maximal effect
ERα	estrogen receptor alpha
ESI	electrospray ionization
EV	empty vector
FBS	fetal bovine serum
FLuc	firefly luciferase
FN	false negative
FP	false positive

FPLD3	familial partial lipodystrophy subtype 3
FSH	follicle stimulating hormone
FSK	forskolin
GC%	guanine-cytosine percentage
GFP	green fluorescent protein
GR	glucocorticoid receptor
HEK293	human embryonic kidney 293
HSQC	heteronuclear single quantum coherence
IATA	Integrated Approaches to Testing and Assessments
IBMX	3-isobutyl-1-methylxanthine
IC_{50}	half-maximal activity concentration
IRB	Institutional Review Board
ITC	isothermal titration calorimetry (ITC
K_{aw}	partition coefficient between air and water
K_i	inhibitory constant
K_{ow}	partition coefficient between octanol and water
LBD	ligand-binding domain
LC-MS/MS	liquid chromatography with tandem mass spectrometry
LDH	lactate dehydrogenase
LH	luteinizing hormone
LOD	limit of detection
LOQ	limit of quantification
LPDM	Leadscope® Predictive Data Miner
MEHP	mono-(2-ethylhexyl)-phthalate
mRNA	messenger RNA
ND	not detected
NIH	National Institutes of Health
NMR	nuclear magnetic resonance
NMU	N-methyl-N-nitrosourea
NUL	no upper limit
OD	optical density
PACM	PPAR-associated conserved motif
PBS	phosphate-buffered saline
PCR	polymerase chain reaction
PFAS	polyfluoroalkyl substance
PKA	protein kinase A
PKC	protein kinase C
PMA	phorbol 12-myristate 13-acetate
POP	persistent organic pollutant
PPAR	peroxisome proliferator-activated receptor
PPARγ	peroxisome proliferator-activated receptor gamma
PPRE	PPAR-responsive regulatory element
PR-B	progesterone receptor B
PVDF	polyvinylidene difluoride
qPCR	quantitative PCR
QSAR	quantitative structure-activity relationship
RAR	retinoic acid receptor
RARE2	retinoic acid response element 2
REACH	Registration, Evaluation, Authorization and Restriction of Chemicals (EU regulation)
RNA	ribonucleic acid
RT-qPCR	quantitative reverse transcription PCR

RXR	retinoid X receptor
SC	self complementarity
SD	standard deviation
SDS-PAGE	sodium dodecyl sulfate-polyacrylamide gel electrophoresis
SEM	standard error of the mean
SGBS	Simpson-Golabi-Behmel syndrome
SID	substance identifier
SNP	single nucleotide polymorphism
SPR	surface plasmon resonance
SUMO	small ubiquitin-like modifier
sWAT	subcutaneous white adipose tissue
T3	triiodothyronine
TBBPA	tetrabromobisphenol A
TCBPA	tetrachlorobisphenol A
T_m	melting temperature
TN	true negative
Tox21	Toxicology in the 21st Century
TP	true positive
TRβ	thyroid receptor beta
TSA	thermal shift assay
UAS	upstream activation sequence
UCPH	University of Copenhagen
UHPLC	ultra high performance liquid chromatography
vWAT	visceral white adipose tissue

Introduction

Peroxisome proliferator-activated receptor gamma (PPARγ) is a nuclear receptor involved in a wide range of cellular functions, and its dysregulation can contribute to several adverse outcomes, such as diabetes, obesity, cancer, and cardiovascular disease.[1–4] A large number of chemicals in the domestic and occupational environments can bind to PPARγ and affect its activity.[5] Activation of PPARγ by agonists may promote osteoporosis,[6] heart failure,[2] and weight gain,[7] while inhibition of PPARγ by antagonists may lead to development of insulin resistance,[8] cancer,[1,9] and pulmonary fibrosis.[10,11]

This project focused on the tumor suppressing role of PPARγ in mammary carcinogenesis, and particularly the effect of impaired PPARγ signaling on adipose tissue estrogen production. Exposure to environmental pollutants that modulate PPARγ function can potentially disrupt metabolism and the endocrine system.[12–14] Epidemiological studies indicate that metabolic disorders are often associated with an increased risk of certain cancers, such as breast cancer.[15] Accordingly, when activated by agonists in adipose stromal cells (ASCs), PPARγ has been shown to be a repressor of aromatase,[16,17] the rate-limiting enzyme in estrogen synthesis, suggesting that exposure to PPARγ antagonists may cause a derepression of aromatase and thus act as mammary carcinogens. Very little is currently known about the effect of PPARγ antagonists on aromatase expression, and the involvement of PPARγ in metabolic disease and cancer is important to study to better understand the mechanisms of action, and to ultimately help prevent disease.

Breast cancer is the most commonly diagnosed cancer worldwide and is the fourth most common cause of cancer-related death.[18] Modifiable risk factors for breast cancer include obesity, physical inactivity, hormone therapy, and alcohol consumption.[19] Genetic epidemiological studies found interaction between alcohol intake and the functional polymorphism *PPARG* Pro12Ala,[20,21] suggesting that ethanol promotes breast cancer in a PPARγ-dependent manner. Follow-up *in vitro* studies on various organic solvents, including alcohols, suggested that ethanol and ethylene glycol inhibit PPARγ activation and induce estrogen biosynthesis.[21,22] The majority of breast cancers are estrogen receptor positive, meaning that the cancer cells grow in response to the hormone estrogen.[23] Exogenous chemicals can act as endocrine disruptors and promote breast cancer development by interfering with the function of the endocrine system.[24] The mechanisms by which many of these xenobiotics elicit their carcinogenic effects remains to be elucidated. Studying environmental and occupational chemicals for potentially carcinogenic effects is crucial for breast cancer prevention. However, it is difficult to obtain epidemiological evidence for the carcinogenic effects of exposure to individual chemicals since exposure often is a mixture of chemicals. Another limitation is the lack of information about important potential confounders. It is therefore important to complement epidemiological studies with mechanistic studies *in vitro* and *in vivo*.

Main objective

The main objective is to identify potential breast carcinogens that increase estrogen biosynthesis in the adipose tissue by inducing aromatase transcription through a PPARγ-dependent mechanism.

It is hypothesized that PPARγ antagonists can be identified among exogenous chemicals and that exposure to these antagonists results in increased estrogen production in the adipose tissue by inducing aromatase transcription via a mechanism involving PPARγ.

Specific aims

1) Identify environmental and occupational chemicals as PPARγ antagonists.
   Hypothesis: *In silico* tools facilitate identification of PPARγ antagonists among environmental chemicals.
2) Determine the effect of PPARγ antagonism on aromatase expression and estrogen production.
   Hypothesis: PPARγ antagonists increase aromatase expression and estrogen production in adipose tissue culture.
3) Investigate the impact of ethanol and ethylene glycol exposure on aromatase expression *in vivo* and *in vitro*, and assess whether effects are mediated by PPARγ.
   Hypothesis: Exposure to ethanol and ethylene glycol increases aromatase expression via inhibition of PPARγ.

Each hypothesis was addressed in a separate manuscript, with some degree of interconnection and shared contributions. The thesis begins with a detailed description of PPARγ and its role in adipose tissue function, cancer, metabolic disease, and steroid synthesis. Next, the scientific methods used in the project are considered and discussed. Then the three manuscripts are presented, and finally the thesis is concluded with a discussion of the findings.

Background

PPARγ structure and function

The peroxisome proliferator-activated receptors (PPARs) belong to the nuclear receptor superfamily of transcription factors and intracellular receptors.[25] Like other nuclear receptors, PPARs contain the following functional domains: an N-terminal domain containing a ligand-independent activation region (AF-1), a DNA-binding domain (DBD), a flexible hinge region, and a C-terminal ligand-binding domain (LBD) containing a ligand-dependent activation region (AF-2).[26] PPARs heterodimerize with retinoid X receptors (RXRs), and together they bind as a complex to peroxisome proliferator response elements (PPREs) in the promoter region of target genes.[26] PPARs regulate the expression of genes involved in processes such as cellular metabolism, differentiation, and development.[27] PPARs are nutrient sensors, and endogenous ligands include fatty acids and their derivatives, such as eicosanoids.[28] The three main forms of PPARs are PPARα, PPARγ, and PPARδ, which are transcribed from separate genes and differ in their tissue distribution patterns and ligand specificities.[29,30]

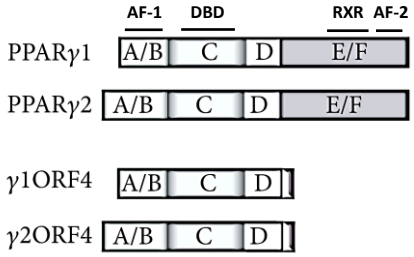

Figure 1. **Structure of PPARγ variants**. The figure shows a comparison of PPARγ1 and PPARγ2, as well as two dominant negative isoforms. Different domains and interaction regions are indicated. Adapted from Aprile M et al (2014).[31]

The most extensively studied member of the PPARs is PPARγ, which is a common target for therapeutic intervention.[32] There are two canonical PPARγ isoforms, PPARγ1 and PPARγ2, which consist of 475 and 505 amino acids, respectively, and arise from different *PPARG* transcript variants. In addition, there are dominant negative isoforms of PPARγ, which lack the LBD and impair the function of the canonical PPARγ isoforms (Figure 1).[31,33,34] The function of PPARγ is modified by structural changes in the LBD induced by ligand binding and recruitment of transcriptional coregulators.[35] PPARγ is also regulated by post-translational modifications, especially phosphorylation.[26,36]

Synthetic PPARγ agonists have been developed for the treatment of type 2 diabetes.[37] Some of these are now also in clinical trials for their tumor-suppressing effects,[28,37,38] since there appears to be a link between diabetes and some cancers.[15] Thiazolidinediones (TZDs) are a class of potent PPARγ activators and include rosiglitazone, troglitazone, pioglitazone, and ciglitazone.[37] Synthetic non-thiazolidinedione PPARγ agonists have also been developed, for instance L-764406, GW0072, and GW7845.[37] In addition, a multitude of PPARγ-activating natural products have been identified, including flavonoids, isoflavones, and amorfrutins.[39] Lastly, various environmental contaminants, such as the antagonist bisphenol A diglycidyl ether (BADGE), can also affect PPARγ activity,[37] and may have adverse effects.

PPARγ is mainly expressed in adipose tissue and is indispensable for adipogenesis.[40] This is evident from several knockout studies *in vitro* and *in vivo*. Knockout of *Pparg* in mouse embryonic fibroblasts inhibits differentiation into adipocytes.[41] Ablation of only the PPARγ2 variant in mouse embryonic fibroblasts also dramatically reduced the capacity for adipogenesis compared with wild-type cells.[42]

In mice, knockout of *Pparg* is embryonic lethal. However, epiblast-restricted knockout of *Pparg* rescued embryonic lethality and resulted in severe lipodystrophy and insulin resistance.[43] Dominant-negative missense mutations in *PPARG* also led to lipodystrophy.[44] Adipocyte-specific homozygous knockout of PPARγ in mice caused a dramatic loss of adipose tissue, severe insulin resistance, and massive fatty livers, while heterozygous knockout mice exhibited no significant phenotypic difference from the control mice.[45] A study also shows that PPARγ is essential for the *in vivo* survival of mature adipocytes as inducible adipocyte-specific knockout of *Pparg* causes adipocytes to die within a few days, eventually being replaced by newly formed PPARγ-positive

adipocytes.[46] Death of the PPARγ-deficient adipocytes triggered an inflammatory reaction resulting in deposition of collagen.[46]

There are also a number of studies that specifically investigated the effect of PPARγ2 ablation *in vivo*. Lack of PPARγ2 in mice caused a reduction in adipose tissue mass and lipid accumulation, a decrease in the expression of adipogenic genes, and a male-specific reduction in insulin sensitivity.[42] In a second study, lack of PPARγ2 impaired lipid storage rate in mouse adipose tissue, and this chronic metabolic inflexibility of the adipose tissue led to insulin resistance with age.[47] A third study showed that ablation of *Pparg2* had little effect in mice, except for a significant reduction in plasma adiponectin.[48] However, in obese hyperphagic leptin-deficient mice, lack of PPARγ2 resulted in lower fat mass and larger adipocytes, suggesting impaired potential for adipocyte recruitment.[48] Furthermore, the PPARγ2-deficient mice had lower plasma level of adiponectin and higher levels of glucose, free fatty acids, and triglycerides.[48] These studies indicate an important role of the PPARγ2 variant in adipose tissue.

A missense single-nucleotide polymorphism (SNP) in the first coding exon of *PPARG* (rs1801282) results in a substitution of proline with alanine at position 12 in the amino acid sequence. This Pro12Ala variant is specific to PPARγ2. There is significant variation in allelic frequencies across different ethnic groups,[49] with frequencies ranging from about 1% to 10%.[50,51] It has been shown that PPARγ Pro12Ala is associated with decreased receptor activity,[52,53] reduced adipogenic function,[53,54] and lower adiponectin secretion.[54] It has also been suggested that the metabolic impact of the Pro12Ala variant strongly depends on gene-environment interactions.[55]

Tumor suppressing effect of PPARγ

PPARγ ligands have, in some studies, been shown to potentiate tumorigenesis and in other studies been shown to attenuate tumorigenesis.[56] There is a larger body of evidence supporting that PPARγ and its ligands inhibit carcinogenesis, particularly in the breast, however the mechanisms are still unclear. In rodent cancer models, chemical carcinogens are widely used to mimic cancer development through the phases of initiation, promotion, and progression.[57] Particularly, 7,12-dimethylbenzanthracene (DMBA) and *N*-methyl-*N*-nitrosourea (NMU) consistently induce mammary cancer and are therefore commonly used to study breast cancer.[58,59] PPARγ has repeatedly been shown to act as a tumor suppressor in this kind of model, as described next.

Heterozygous knockout of *Pparg* increased the number of DMBA-induced tumors in female mice and decreased their survival rate.[60] Particularly, malignant tumors of the skin, ovary, and mammary gland were increased.[60] Adipocyte-specific *Pparg* deletion also increased the DMBA-induced malignant mammary tumor incidence and multiplicity in female mice.[61] In addition, mammary adenocarcinoma incidence and multiplicity were accelerated in mice with mammary gland-directed expression of the dominant-negative transgene, Pax8PPARγ.[62]

Several studies describe that ligands of PPARγ also affect carcinogenesis *in vivo*, *ex vivo*, and *in vitro*. The potent non-thiazolidinedione PPARγ agonist, GW7845, decreased NMU-induced mammary tumor incidence, number, and size in female rats.[63] Furthermore, DMBA-induced mammary tumor incidence was delayed in female mice treated with GW7845.[62] Conversely, treatment with the PPARγ antagonist GW9662 accelerated medroxy-progesterone- and DMBA-induced tumorigenesis in mice.[64] In mouse mammary gland organ culture, the PPARγ agonist, troglitazone, inhibited the growth of DMBA-induced preneoplastic lesions.[65] The RXR-specific ligand LG10068 had no effect by itself but enhanced the effect of troglitazone.[65] In accordance with this, GW7845 inhibited the development of DMBA-induced precancerous mammary alveolar lesions in mouse mammary gland organ culture.[66] Surprisingly, GW9662 also inhibited DMBA-induced lesions, but at a 100-fold greater concentration, indicating that GW9662 action may have been independent of association with PPARγ.[66] At such high concentration, GW9662 has been shown to also modulate the activity of PPARα and PPARδ,[67] both of which influence mammary carcinogenesis.[37,68,69] Consistent with rodent and organ culture studies, an *in vitro* study showed that thiazolidinedione treatment of cultured breast cancer cells caused lipid accumulation and reduced proliferation, and exhibited a less malignant gene expression pattern.[70]

In mice, GW9662 treatment,[64] Pax8PPARγ expression,[62] and adipocyte-specific *Pparg* knockout[61] increased the expression of estrogen receptor alpha (ERα) in mammary adenocarcinomas; cultured primary mammary

epithelial or adenocarcinoma cells; and mammary ductal adenocarcinomas, respectively. The stronger ERα expression in response to ablation of PPARγ suggests that inhibition of PPARγ signaling may promote estrogen-dependent carcinogenesis. Consistent with this, the mechanism by which PPARγ affects breast cancer has been proposed to involve regulation of the estrogen-producing enzyme aromatase (encoded by *CYP19A1*),[16,17] which increases the supply of estrogen to nearby breast epithelial cells.

PPARγ as a target of xenobiotics

PPARγ function can be modulated by a variety of environmental and occupational chemicals, which may lead to endocrine and metabolic disruption.[13] It is important to study the potential health effects of substances in the environment, since they have been linked to a long range of adverse outcomes such as reduced fertility, immune dysfunction, endometriosis, obesity, and cancer.[71] The importance of lifestyle and environmental factors on cancer is emphasized in a recent population-based cohort study, which found that the risk of breast, colorectal, and lung cancer was higher in women born in Nordic countries than in women born in non-Western countries, and that immigration to Nordic countries increased cancer incidence and mortality with duration of residence.[72]

PPARγ is a major target of certain chemical compounds called obesogens. Obesogens are environmental chemicals that promote obesity by interfering with metabolic homeostasis and the action of hormones.[73] Many obesogens are endocrine-disrupting chemicals that can alter appetite regulation, lipid metabolism, adipocyte differentiation, or inflammatory responses.[73,74] Modulation of PPARγ activity by obesogens can inappropriately stimulate adipogenesis and increase lipid storage.[75] Obesogens may also act through interference with steroid hormone receptors as they too influence lipid storage and fat deposition.[75] Some examples of obesogens are organotins, phthalates, organophosphates, organobromines, polyfluoroalkyl substances (PFASs), and heavy metals.[73]

Organotins, such as tributyltin or triphenyltin, can act as potent agonists of both RXRs and PPARγ,[7,76–82] inducing adipogenesis.[7,77–80,83,84] Interestingly, tributyltin appears to promote development of a phenotypically distinct adipocyte,[85–87] which may be dysfunctional. Phthalate monoesters, such as mono-(2-ethylhexyl)-phthalate (MEHP), have also been shown to increase PPARγ activity.[79,88–92] MEHP is highly relevant as it is the major metabolite of the common phthalate, di-(2-ethylhexyl)-phthalate (DEHP), which does not activate PPARγ itself.[88,91] Instead, DEHP antagonizes PPARγ, according to one study.[93]

Bisphenols have recently been shown to act as PPARγ antagonists, inhibiting PPARγ activity and adipogenesis at low, environmentally relevant concentrations.[94] However, the literature on bisphenol effects on PPARγ is inconsistent. Some studies show that bisphenols activate PPARγ[95] or induce adipogenesis[95–100] while others show that they do not.[92,101] However, halogenated analogs of bisphenol A, such as tetrabromobisphenol A (TBBPA) and tetrachlorobisphenol A (TCBPA), have consistently been shown to activate PPARγ.[92,102]

An *in vitro* screening of 200 pesticides showed that none of them could activate PPARγ in CV-1 monkey kidney cells,[103] but these pesticides were not tested for antagonistic effects. Another study identified both PPARγ agonists and antagonists among a selection of pesticides.[104] The observed effects on PPARγ transcriptional activity in COS-7 cells were consistent with effects on adipogenesis in 3T3-L1 cells.[104] Multiple other studies have found effects of various pesticides on adipogenesis.[105,106]

Agonistic and antagonistic effects on PPARγ have also been reported in response to compounds of various other chemical classes, such as ketones, benzaldehydes, and organochlorines.[93,107] In addition, many xenobiotics alter the activity of multiple nuclear receptors rather than just a single receptor,[76–78,81,88–91,93,108] and in many cases chemicals affect other cellular targets too.[5,109,110] The complexity is further increased as humans are exposed to complex mixtures of chemicals instead of single compounds. A few studies have investigated the effect of chemical mixtures on PPARγ activity. For example, one study showed that extracts from various food contact materials increased PPARγ activity in a reporter gene assay in agonist mode. However, not all extracts activated PPARγ, and it is unknown whether some extracts might inhibit PPARγ as the study did not include an assay in antagonist mode.[111]

Another study has shown that exposure to mixtures of persistent organic pollutants (POPs) or POP metabolites, composed according to the concentrations found in polar bear adipose tissue, suppressed the activity of PPARγ and inhibited adipocyte differentiation in 3T3-L1 cells.[107] Oppositely, contaminant extracts from polar bear liver and adipose tissue induced adipogenesis,[107] which is likely due to the presence of additional contaminants in the extracts compared to the synthetic mixtures. Alternatively, endogenous PPARγ ligands present in the extracts could in part have been responsible for the adipogenic effect.

A third study tested 23 commonly used unconventional oil and gas chemicals (UOG), at environmentally relevant concentrations, for effects on PPARγ activity and adipogenesis using 3T3-L1 cells.[112] The UOG mixture included alcohols such as 2-ethylhexanol, diethanolamine, ethylene glycol, and propylene glycol. Treatment with the UOG mixture during adipogenesis promoted lipid accumulation, but an agonist-mode reporter assay revealed no impact on PPARγ activity, demonstrating that the effect was PPARγ-independent. This was supported by antagonist reporter assays showing that the UOG mixture decreased activities of estrogen receptor alpha (ERα), androgen receptor (AR), progesterone receptor B (PR-B), glucocorticoid receptor (GR), and thyroid receptor beta (TRβ), some of which can influence adipogenesis. A PPARγ assay in antagonist-mode was not performed.[112]

The same study also showed that treatment with 5 out of 9 wastewater-impacted water samples increased adipogenesis, and 4 of these also increased PPARγ activity. Agonist and antagonist assays were performed for the other mentioned nuclear receptors and showed highest levels of overall antagonism in response to the 4 PPARγ-activating samples, indicating that PPARγ-independent mechanisms may have contributed to some extent to the induced adipogenesis.[112] The individual chemicals in the UOG mixture and wastewater samples were not studied for effects on PPARγ activity.[112] However, other studies have reported decreases in PPARγ activity in response to the two alcohols, ethanol and ethylene glycol, using reporter assays.[21,22] Consistent with this, ethanol has also been shown to impair adipogenesis in human adipose stromal cells (ASCs).

Adipose tissue as an endocrine organ

The function of the adipose tissue multi-depot organ is primarily to serve as an energy storing reservoir and to secrete hormones important for whole-body energy homeostasis.[113] Adipose tissue also acts as a thermal insulator and a cushion to protect vital organs.[114] It is composed of different cell types including adipocytes, fibroblast-like stromal cells, and immune cells, as well as an extracellular matrix.[115,116] The stromal cells can differentiate into adipocytes as part of adipose tissue maintenance and expansion.[117] Some specialized adipocytes within the adipose tissue have alternative functions. In contrast to the unilocular white adipocytes, brown and beige adipocytes are smaller, have multiple lipid droplets, and produce heat by a process called thermogenesis.[118]

White adipose tissue can be found in two different main anatomical locations: the subcutaneous adipose tissue residing underneath the skin and the visceral adipose tissue (intra-abdominal adipose tissue) surrounding the internal organs inside the abdominal cavity.[119] Ectopic fat accumulation is the storage of lipids outside of the adipose tissue, which is associated with inflammation and insulin resistance.[120] Lipids preferentially accumulate in the subcutaneous adipose tissue, which is the largest depot, but when the storage capacity has reached its limit, excess lipids accumulate in the visceral adipose tissue and ectopic tissues.[120] Subcutaneous adipose tissue has a higher adipogenic capacity than visceral adipose tissue, which is reflected by a greater response to PPARγ agonists.[121] Adipose tissue function and plasticity is compromised by PPARγ dysregulation, leading to a dysmetabolic state characterized by ectopic fat accretion and lipotoxicity as well as peripheral insulin resistance.[121–123]

The adipose tissue can expand via hyperplasia and hypertrophy (Figure 2). Hyperplasia is the generation of new adipocytes via adipogenesis, and hypertrophy is the increase in volume of existing adipocytes.[124] Hypertrophy is predominant especially in visceral depots and leads to a proinflammatory profile and insulin resistance.[124] The subcutaneous to visceral adipose tissue ratio is important for the risk of metabolic and cardiovascular disease.[119] Men tend to accumulate more visceral fat than women due to lower estrogen levels.[125] Similarly, after

menopause, the subcutaneous to visceral fat ratio decreases, and this is primarily because of reduced estrogen levels.[125]

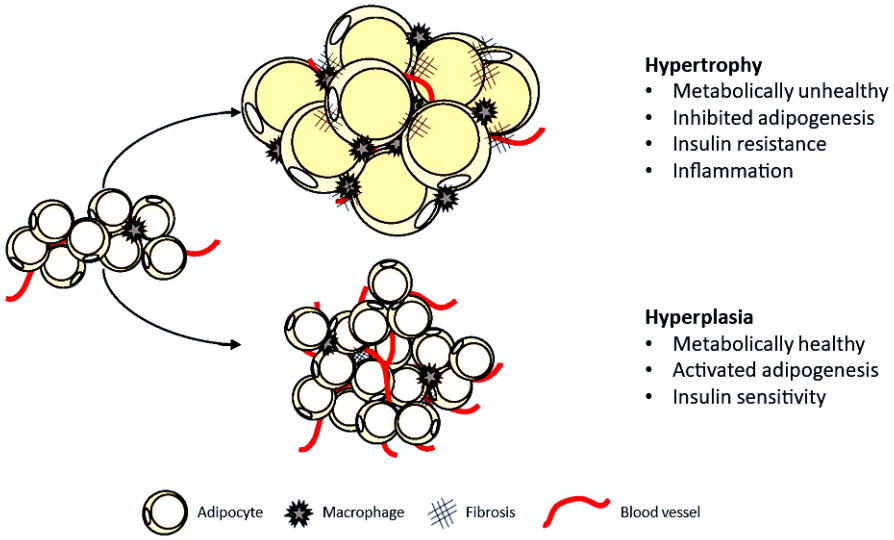

Figure 2: **Adipose tissue expansion**. In response to increased nutrient availability, adipose tissue expands via hypertrophy and hyperplasia. Hypertrophy is considered metabolically unhealthy and is associated with inflammation and insulin resistance, while hyperplasia is more metabolically healthy and is associated with insulin sensitivity. Adapted from Steiner BM et al (2022).[119]

Adipose tissue constitutes the majority of the breast[126] and is a significant site of estrogen synthesis, especially in men and postmenopausal women.[127] It is a major supplier of estrogen to the breast tissue, and its close proximity to the breast epithelial cells may impact carcinogenesis substantially.[128] In the adipose tissue of obese individuals, aromatase expression is elevated, contributing to the development of estrogen receptor-positive breast cancer in postmenopausal women.[129]

The role of PPARγ in steroidogenesis

Steroidogenesis is the process of steroid hormone biosynthesis by various enzymes and cofactors (Figure 3).[130] *De novo* biosynthesis of steroids is the conversion of the main precursor steroid, cholesterol, into its steroid hormone derivatives.[131] Classical steroidogenic tissues include the adrenal gland and the gonads, and these can synthesize steroid hormones *de novo*.[131] Adipose tissue is well-established as a conversion site for steroid precursors that are taken up from the circulation.[131] It is a major reservoir for steroid hormones, constitutes an important site for steroid biosynthesis and metabolism, and regulates local homeostasis through paracrine and autocrine signaling.[131] It has been shown that adipose tissue is also capable of *de novo* steroidogenesis, although its physiological relevance is still unknown.[131] Estrogen synthesized by aromatase in the adipose tissue can reach high concentrations and act locally in a paracrine manner without significantly affecting circulating levels.[132]

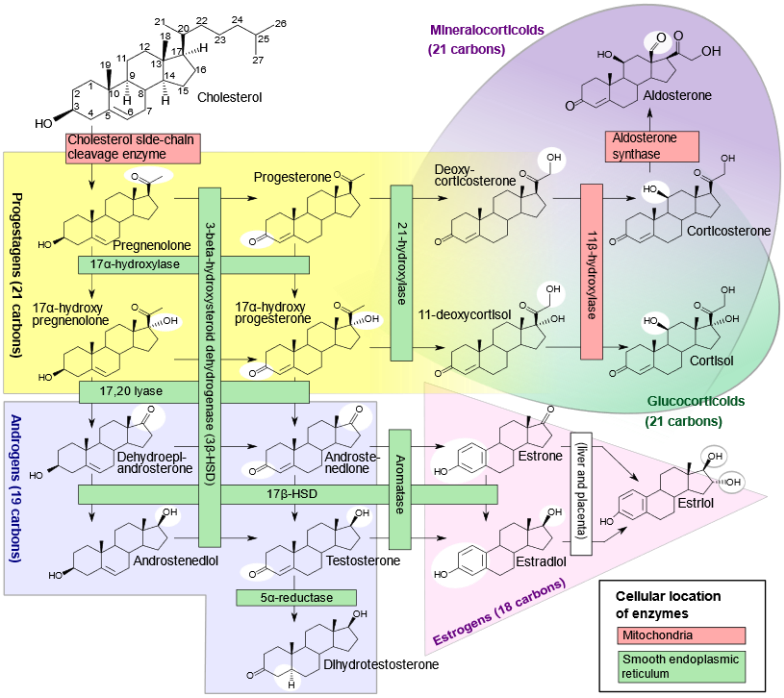

Figure 3: **Steroidogenesis pathways**. Steroid hormones and enzymes. Reproduced from Häggström M & Richfield D (2014).[133]

The involvement of PPARγ in steroid hormone synthesis has been demonstrated in numerous studies. PPARγ and its agonists have been shown to suppress *CYP11B2* expression and aldosterone production in H295R cells.[134] PPARγ agonist pioglitazone has also been shown to inhibit expression of *CYP17A1* and *HSD3B2* in H295R cells in part via a PPARγ-independent pathway.[135] In addition, PPARγ and its agonists inhibit aromatase expression in KGN cells[136] and suppress aromatase expression in rat ovarian granulosa cells.[137] *In vivo*, aromatase mRNA abundance was decreased in granulosa cells of cattle injected intrafollicularly with troglitazone for 24 h.[138] Anoter *in vivo* study showed that prenatal exposure to PPARγ agonist for 60 days reduced aromatase expression and increased PPARγ target gene *Fabp4* expression in the visceral adipose tissue of female sheep.[139]

It has been demonstrated that treatment with the potential PPARγ antagonist, ethanol, increases aromatase expression in the MCF-7 human breast cancer cell line,[140] and that chronic ethanol ingestion increases plasma estradiol in rats.[141] A study in male rats revealed an increase in adipose tissue aromatase expression in response to ethanol consumption.[142] Only a limited number of studies have explored the effects of ethylene glycol, another potential PPARγ antagonist. Both ethanol and ethylene glycol have been reported to increase estrogen production in a human adrenocortical cell line.[21,22] In addition, ethylene glycol exhibited estrogenic activity in rainbow trout.[143] However, it has not been determined how ethylene glycol affects aromatase expression in adipose tissue. Also, the mechanism of induced estrogen synthesis in response to ethanol and ethylene glycol is still unknown.

Transcriptional control of aromatase

Aromatase is the rate-limiting enzyme in estrogen biosynthesis and is encoded by the *CYP19A1* gene. The *CYP19A1* gene contains 10 exons, of which 9 are coding. There are 11 transcript variants, differing only in the untranslated first exon and each regulated by separate upstream cognate promoters. In the adipose tissue, aromatase expression is driven mainly by the three promoters, PI.4, PI.3, and PII.[144] Binding of the transcription factor Sp1 is essential for promoter I.4 stimulation.[144] Promoter I.4 is also regulated by the AP-1 transcription factor, type I cytokines, and glucocorticoid receptor.[144]

Promoters I.3 and II are located within 215 bp from each other and therefore share some *cis*-regulatory elements.[144] These include cAMP-responsive elements, an AP-1 site, CCAAT/enhancer binding protein (C/EBP) elements, and a SF-1 binding site.[144] The cAMP-responsive elements are bound by CREB1 in response to activation by protein kinase A (PKA).[144] Leptin or adiponectin can affect the activity of these elements by

increasing or decreasing CREB-regulated transcriptional coactivator binding, respectively.[145] Protein kinase C (PKC) has an effect similar to leptin.[144] For the study of aromatase regulation, a combination of PKA and PKC activation using forskolin and phorbol-12-myristate-13-acetate (PMA), respectively, is often used to strongly induce aromatase expression. The C/EBP and SF-1 binding sites are activated by C/EBPβ and LRH-1, respectively.[144] Furthermore, SF-1 mediates the action of follicle stimulating hormone (FSH),[144] which is secreted by the pituitary gland.[146]

NF-κB has been shown to upregulate aromatase via promoter II activation.[147] PPARγ inhibits aromatase promoter II activation by interfering with the promoter interaction of NF-κB.[147] Also, it has been shown that PPARγ does not bind the promoter I.3/II of aromatase,[17] indicating that the mechanism that PPARγ regulates aromatase via this promoter is indirect.

Methodological considerations

Throughout the project, different biological models and experimental methods have been applied. Female rats were used, as well as cell and tissue models including human and mouse pre-adipocyte cell lines, a human adrenocortical cell line, a human embryonic kidney cell line, human primary adipose stromal cells, and breast adipose tissue explants. Methods include luciferase reporter assay, cytotoxicity assay, immunoblotting, RT-qPCR, transient transfection, confocal microscopy, and adipogenesis assays.

The studied chemicals were selected from the Tox21 PPARγ antagonist assay based on inhibition of PPARγ by at least 25%, no agonist activity, and commercial availability. To increase the occupational relevance of the selected chemicals, known drugs were not included, and pesticides were selected only if approved for use in the EU.

PPARγ transcriptional activity assay in HEK293 cells

The human embryonic kidney 293 (HEK293) cell line was isolated from the kidney of a human embryo and exhibits epithelial morphology.[148] It is widely used due to its rapid growth rate and propensity for transfection.[149] To study transcriptional activation of PPARγ in response to selected chemicals, a PPARγ LBD-driven GAL4 luciferase reporter HEK293 stable cell line (SL-3002, Signosis) was utilized. It overexpresses a chimeric protein containing the LBD of PPARγ fused to the DBD of the yeast GAL4 transcription factor (Figure 4), which does not have an ortholog in mammalian genomes.[150] The reporter gene is the coding region of firefly luciferase, which is joined to the GAL4 upstream activation sequence (UAS). When luciferase is expressed, it produces bioluminescence (light emission) through an enzymatic reaction with its luminogenic substrate luciferin. The enzymatic activity of luciferase correlates with the activation of the GAL4 UAS and is used as a measure of transcriptional activity.

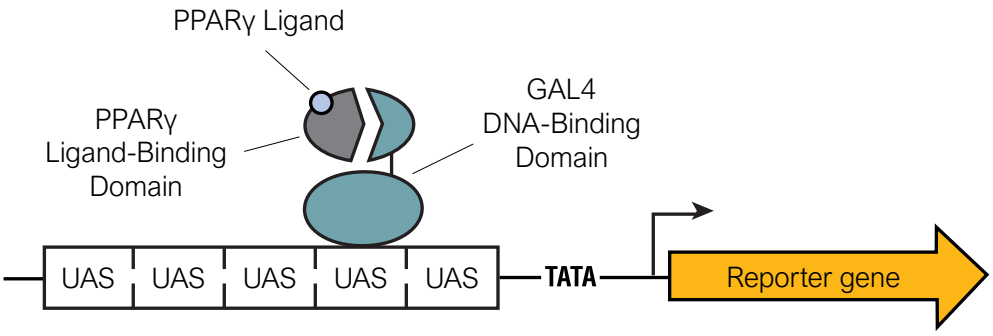

Figure 4: **The PPARγ reporter system**. The LBD of PPARγ is fused to the DBD of GAL4. Binding of ligands to the PPARγ LBD activates the PPARγ-GAL4 fusion protein, releasing co-repressors bound to the LBD. The transcriptional machinery is recruited to the luciferase reporter gene by co-activators, resulting in luciferase expression. Figure adapted from Reporter Genes and their Applications, Promega.[151]

An advantage of this reporter system is that luminescence offers a greater sensitivity (signal to background ratio) than fluorescence due to lower background interference (emission from compounds, media, and cells).[152,153] However, firefly luciferase produces luminescence intensity that fades over several minutes, which can cause artifacts as luminescence is measured in each well at a different time point. Therefore, the data in this project was corrected for signal decay.

Many test chemicals can interfere with reporter assays and produce artifacts. While compound fluorescence can be an issue when using a fluorescent-based reporter system, luciferase inhibitory activity of compounds can cause interference too. Luciferase inhibition is twice as common as compound fluorescence (blue or green wavelength) according to interference assays of the Tox21 chemical library.[154]

The HEK293 cell line with the stably transfected reporter system from Signosis was easy to work with since it was not necessary to perform transient transfections. This also meant that there was no need for a transfection control reporter, such as constitutively expressed renilla luciferase. However, a limitation was that there was no

convenient way to normalize to the cell number in the wells. It was therefore assumed that all wells contained equal numbers of cells, and each treatment was performed in technical triplicates to reduce variation.

Cytotoxicity was assessed using a colorimetric lactate dehydrogenase (LDH) release assay, which measures the amount of LDH released into the culture medium upon damage to the plasma membrane. An advantage of using this method was that cytotoxicity could be quantified from the same cells for which reporter signal was measured, as the medium just needed to be collected before cell lysis. An important disadvantage was that the assay can detect cell death only when the cell membranes rupture, as in necrotic cell death, however it can not detect apoptosis where cell membranes remain intact.[155]

The GAL4-UAS system is a powerful technique for studying ligand effects on nuclear receptor transcriptional activity. An advantage is that only the receptor LBD is present and therefore any observed effects are most likely caused by an interaction between ligand and LBD. Expression of GAL4 chimeric receptors is also usually nontoxic to the cells because of the heterologous DBD.[156] Additional advantages include the high specificity and sensitivity of this reporter system, and that effects of endogenous receptor activation does not interfere with the assay, because it can not bind to the UAS. The main disadvantage of the GAL4-UAS system is the lack of interactions with the other domains of PPARγ as well as PPARγ binding partners, such as RXRs, which would take place in normal conditions.[150]

The signal for basal transcriptional activity is very low in the PPARγ reporter cell line (Figure 5A). Antagonism of the basal PPARγ activity could therefore not be studied. However, PPARγ activity could be increased by treatment with rosiglitazone, and the effect of PPARγ antagonists on rosiglitazone-induced activation could then be studied.

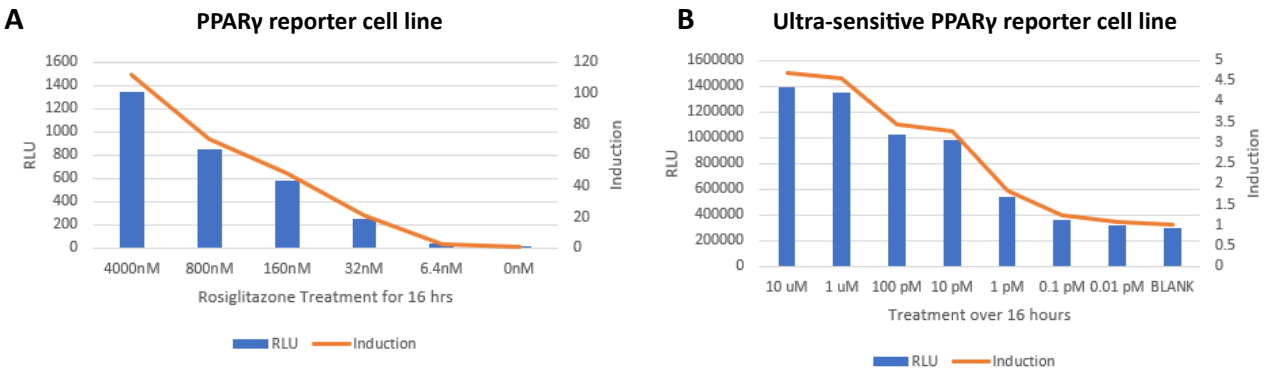

Figure 5: **PPARγ transcriptional activity in response to different concentrations of rosiglitazone in cell lines from Signosis**. (**A**) The PPARγ LBD-driven GAL4 luciferase reporter HEK293 stable cell line. (**B**) The ultra-sensitive PPARγ LBD-driven GAL4 luciferase reporter HEK293 stable cell line. Figures adapted from the product pages on the Signosis website.[157,158]

Signosis has recently generated an ultra-sensitive version of the reporter cell line (SL-3002-HS, Signosis), which uses an optimized promoter upstream of the luciferase gene to maximize signal output. This gives a much greater luminescent signal (Figure 5B), resulting in a more sensitive assay. In addition, the basal signal is enhanced, possibly making it suitable for detecting antagonist-induced decreases in activity in the absence of an activator. Theoretically, an antagonist should be able to reduce even endogenous activity, but Signosis state that they did not test this, and it probably depends on the level of endogenous activity if there is any.

Reporter assay results from Manuscript I indicate that the signal for basal PPARγ activity was too low to detect significant decreases in activity, but the effect of chemicals on the basal activity of PPARγ could be studied to determine if any chemicals displayed agonist activity. Before performing reporter assays, a single test experiment was performed to compare the luminescent signal at different cell densities (Appendix I).

In vitro adipogenesis and hormone assays

Pre-adipocyte cell lines were employed to study adipogenesis and aromatase expression. The human hTERT A41hWAT-SVF cell line (CRL-3386, ATCC) was established from the subcutaneous neck adipose tissue from a 56-year-old man.[159] This cell line was used for studying the effect of short-term chemical treatments (24 h) on aromatase expression in both undifferentiated and differentiated cells. It was also applied to study the effects

of chemical exposure on aromatase expression during adipocyte differentiation for 12 days. The A41 cell line is ideal for studying adipose tissue browning and thermogenesis, and it can also be used to adipogenesis and other adipocyte functions. However, it would have been better to use a cell line from breast adipose tissue in this study.

The C3H10T1/2 cell line (CCL-226, ATCC) was established in 1973 from C3H mouse embryos.[160] In the project, it was used for studying adipocyte differentiation in the presence or absence of selected chemicals. Mouse PPARγ1 and PPARγ2 have similar lengths as the human orthologs, and sequences are 98.3% and 96.2% identical, respectively. Mouse and human PPARγ proteins have been shown to be activated by ligands in a nearly similar way.[88–90] In Manuscript II, the C3H10T1/2 cells were differentiated according to the protocol (Appendix II), but in Manuscript III the cells were differentiated using one fifth of the shown concentrations. The reason for this was that inhibition of adipogenesis only occurred at high PPARγ antagonist concentrations using the standard protocol (Manuscript II). Inducing differentiation less strongly would therefore better reveal the effects of a potential antagonist (as seen in Manuscript II, Figure 1).

The human Simpson-Golabi-Behmel syndrome (SGBS) preadipocyte cell strain was derived from the subcutaneous adipose tissue of a 3-month-old male infant.[161] It was only used for some test experiments, as it was more difficult to work with, primarily because of its slow growth rate, high contact inhibition, and use of different culture medium.

The human H295R adrenocarcinoma cell line was isolated from the adrenal gland of a 48-year-old woman in 1980.[162] It expresses genes for all the key enzymes in steroidogenesis, making it a great tool for studying the effect of xenobiotic exposure on steroid hormone levels.[163] It has been shown to respond to PPARγ ligands, suggesting that it is suitable for studying PPARγ-mediated effects.[134]

Human primary cells and explants were collected from the adipose tissue of persons undergoing mastectomy, abdominoplasty, or mammoplasty. Primary cells are considered more physiologically relevant than cell lines as they originate from fresh tissue and have not been immortalized, and therefore better recapitulate *in vivo* features. In addition, experiments can be performed in biological replicates, displaying donor-specific differences, which is not possible using cell lines. The main disadvantage is the low number of cells due to limited adipose tissue availability, slow proliferation, and limited proliferative capacity. Adipose tissue explants have the same advantages as primary cells, and the disadvantages are limited availability and high variability among experiments. The latter can be avoided by including more technical replicates.

The differentiation protocols for pre-adipocyte cell lines are shown in Appendix II. Induction of aromatase in response to forskolin and PMA co-treatment in primary human adipose stromal cells was tested using different primer pairs (Appendix III). Two of the primer sets were designed for this project using Primer-BLAST[164] and one was a primer set commonly used in the aromatase field.[165] The primer set selected for further studies was shown to specifically amplify aromatase in A41 cells (Appendix IV).

***In vivo* study**

The animal study was carried out using 24 female Wistar rats. It was investigated if acute exposure to GW9662, ethanol, or ethylene glycol would increase the expression of aromatase in the adipose tissue. The rats were treated for 48 h via a hazelnut chocolate cream vehicle (GW9662)[166,167] or via the drinking water (ethanol and ethylene glycol). The dietary energy intake of the four experimental groups (control, GW9662, ethanol, ethylene glycol) was not isocaloric, because the dietary energy content in ethanol was not compensated for in the other groups. However, this likely had little impact due to the short time frame of the experiment.

The PPARγ expression pattern is similar in humans and rodents, suggesting that function is well-conserved.[168] Rat PPARγ1 and PPARγ2 have similar lengths as the human orthologs, and the sequences are only 98.1% and 95.8% identical, respectively. It has previously been reported that aromatase is not expressed in rodent adipose tissue.[169] However, other studies demonstrate that aromatase is expressed in adipose tissue of both male and female rats at the mRNA and protein level.[142,170–172] The promoter region of aromatase is dissimilar in rodents

and humans, and aromatase is therefore regulated differently,[144,169] which possibly leads to a low basal expression in rat adipose tissue. Still, rodent models have previously been used for studying aromatase expression in adipose tissue in response to oral treatment.[142,173,174] One study investigated the effect of red wine or ethanol exposure on aromatase expression in the adipose tissue.[142] That study was used for statistical power calculation to determine the number of animals needed per group.

Laboratories and contributions

Reporter assay experiments were performed at the National Research Centre for the Working Environment with support from Anne-Karin Asp. Experiments with human primary ASCs and explants were performed at Weill Cornell Medicine in the laboratory of Kristy A. Brown, and access to the human adipose tissue was facilitated by Jason A. Spector. Experiments with C3H10T1/2, A41, and SGBS cells, as well as immunoblotting, were performed at the Novo Nordisk Foundation Center for Basic Metabolic Research at the University of Copenhagen (UCPH) in the laboratory of Brice Emanuelli with support from Patricia S. S. Petersen. Development of PPARγ antagonist QSAR models based on Tox21 dataset were carried out by Ana C. V. E. Nissen, Eva Bay Wedebye, and Nikolai Georgiev Nikolov from National Food Institute at the Technical University of Denmark (DTU Food). Investigation of the binding of selected chemicals to the ligand-binding pocket of PPARγ using VirtualToxLab was done by Martin Smieško from the University of Basel. NMR spectroscopy was performed by Daniel Saar and Birthe B. Kragelund from the Department of Biology at UCPH. Animal study setup with the BioFacility at the Technical University of Denmark was organized by Sofie Christiansen, and animal dissection was performed together with Gitte Ravn-Haren, Niels Hadrup, Dorte Lykkegaard Korsbech, Heidi Broksø Letting, and Lillian Sztuk. Analysis of animal tissue and H295R cell culture were performed in the laboratory of Terje Svingen at DTU Food with support from Heidi Broksø Letting and Dorte Lykkegaard Korsbech, respectively. Analysis of H295R cell-secreted hormones by LC-MS/MS was performed by Maud Bering Andersen and Mikael Pedersen from DTU Food.

Table 1 shows a summary of the main assays and techniques used in the project. It includes *in silico* studies predicting molecular interactions, multiple cell-based and cell-free *in vitro* studies, an *ex vivo* study using human breast adipose tissue, and an *in vivo* study using female Wistar rats.

Discipline	Study type	Material	Material description	Assay type	Technique	Outcome
Cheminformatics	*in silico*	Biological data	Molecular descriptors	Computational	QSAR	PPARγ antagonist predictions
Cheminformatics	*in silico*	Structural data	Molecular structures	Computational	Molecular docking	PPARγ affinity predictions
Biophysics	*in vitro*	Purified protein	PPARγ LBD	Ligand binding	NMR spectroscopy	PPARγ ligand interactions
Cell biology	*in vitro*	Cell line	HEK293 cells	Transactivation	Reporter system	PPARγ activity
Cell biology	*in vitro*	Cell line	H295R cells	Steroidogenesis	LC-MS/MS	Steroid production
Cell biology	*in vitro*	Cell line	A41 cells	Gene expression	RT-qPCR	Aromatase mRNA levels
Cell biology	*in vitro*	Cell line	C3H10T1/2 cells	Adipogenesis	RT-qPCR	Adipogenic activity
Cell biology	*in vitro*	Primary cells	Adipose stromal cells	Adipogenesis	Lipid staining	Adipogenic activity
Physiology	*ex vivo*	Tissue explants	Human adipose tissue	Gene expression	RT-qPCR	Aromatase mRNA levels
Physiology	*in vivo*	Animal model	Wistar rats	Gene expression	RT-qPCR	Aromatase mRNA levels

Table 1: **Overview of methods used in the project**. The work performed by collaborators is highlighted in gray.

Manuscript I

Orthogonal Assay and QSAR Modeling of Tox21 PPARγ Antagonist In Vitro High-Throughput Screening Assay

Jacob Ardenkjær-Skinnerup, Ana Caroline Vasconcelos Engedal Nissen, Nikolai Georgiev Nikolov, Martin Smieško, Niels Hadrup, Gitte Ravn-Haren, Eva Bay Wedebye, Ulla Vogel

In this manuscript, a selection of chemicals from a high-throughput screening study of PPARγ antagonists from the Tox21 Program were used in an orthogonal assay with the aim of assessing the reproducibility of the Tox21 results. Subsequent construction of a quantitative structure-activity relationship (QSAR) model for PPARγ antagonism allowed identification of additional PPARγ antagonists in the environment. The manuscript has been submitted to Environmental Toxicology and Pharmacology and is under review.

Orthogonal Assay and QSAR Modeling of Tox21 PPARγ Antagonist *In Vitro* High-Throughput Screening Assay

Jacob Ardenkjær-Skinnerup[a,b], Ana Caroline Vasconcelos Engedal Nissen[a], Nikolai Georgiev Nikolov[a], Martin Smieško[c], Niels Hadrup[a,b], Gitte Ravn-Haren[a], Eva Bay Wedebye[a], Ulla Vogel[a,b,*]

[a] The National Food Institute, Technical University of Denmark, Kemitorvet 202, 2800 Kongens Lyngby, Denmark
[b] The National Research Centre for the Working Environment, Lersø Parkallé 105, 2100 Copenhagen Ø, Denmark
[c] Department of Pharmaceutical Sciences, University of Basel, Klingelbergstrasse 50, 4056 Basel, Switzerland

* Correspondence: Ulla Vogel (ubv@nfa.dk; +4540406386), Lersø Parkallé 105, 2100 Copenhagen Ø, Denmark

Highlights

- Tox21 PPARγ antagonist qHTS data was confirmed in orthogonal assay
- A QSAR model for PPARγ antagonism was developed
- Five chemicals predicted by the QSAR model were tested *in vitro*
- PPARγ binding affinity was predicted by flexible docking-based simulation

Abstract

Disruption of signaling mediated by the nuclear receptor peroxisome proliferator-activated receptor gamma (PPARγ) is associated with risk of cancer, metabolic diseases, and endocrine disruption. The purpose of this study was to identify environmental chemicals acting as PPARγ antagonists. Data from the Tox21 PPARγ antagonism assay were replicated using a reporter system in HEK293 cells. Two quantitative structure-activity relationship (QSAR) models were developed, and five REACH-registered substances predicted positive were tested in vitro. Reporter assay results were consistent with Tox21 data since all conflicting results could be explained by assay interference. QSAR models showed good predictive performance, and follow-up experiments revealed two PPARγ antagonists out of three non-interfering chemicals. Finally, molecular docking simulation generally supported binding of the chemicals to the ligand-binding pocket of PPARγ. In conclusion, the developed QSAR models and follow-up experiments are important steps in the discovery of potential endocrine- and metabolism-disrupting chemicals.

Keywords: PPARγ; Tox21; endocrine disruption; metabolic disruption; QSAR; breast cancer

1. Introduction

Exposure to chemicals in foods, household products, medicine, and in the working environment may contribute to various adverse health effects. The nuclear receptor peroxisome proliferator-activated receptor gamma (PPARγ) is an inadvertent target of various environmental chemicals and pharmaceutical agents that disrupt its function.[1–3] Dysregulation of PPARγ signaling is associated with a variety of adverse outcomes, including cancer, type 2 diabetes, and obesity.[4]

PPARγ is a ligand-activated transcription factor that regulates metabolism, development, and adipogenesis. In the nucleus, PPARγ forms obligate heterodimers with retinoid X receptor (RXR),[5] and controls target gene transcription through binding to PPAR-responsive regulatory elements (PPREs) and/or PPAR-associated conserved motifs (PACMs) in target gene promoters.[6] Like other nuclear receptors, PPARγ consists of three major functional domains: an N-terminal ligand-independent transactivation domain (AF1), a highly conserved DNA-binding domain (DBD), and a C-terminal ligand-binding domain (LBD) containing a ligand-dependent transactivation function (AF2).[4,7] PPARγ signaling is modulated by numerous naturally occurring phenols, including flavonoids and cannabinoids, as well as other natural lipophilic ligands such as unsaturated fatty acids and their derivatives, particularly oxidized fatty acids, nitrated fatty acids, and eicosanoids. In addition, some drugs exhibit high affinity towards PPARγ, such as the antidiabetic class of thiazolidinediones, which includes rosiglitazone.[8]

Loss of PPARγ has been studied in a variety of rodent models. Selective disruption of PPARγ2 in mice decreased adipogenic mRNA level and reduced white adipose tissue mass and adipocyte lipid accumulation. In addition, it impaired insulin sensitivity in males.[9] Targeted deletion of PPARγ in mouse adipose tissue (aP2-expressing cells) reduced adipose tissue mass and increased the level of free fatty acids in plasma. It caused adipocyte hypocellularity and hypertrophy accompanied by macrophage infiltration and fibrosis. Adipocyte-specific PPARγ knockout mice also developed hepatic insulin resistance and steatosis.[10] In humans, heterozygous loss-of-function and dominant-negative mutations in the *PPARG* gene leads to development of familial partial lipodystrophy subtype 3 (FPLD3), often accompanied by insulin resistance and other metabolic disturbances as a result from accumulation of ectopic fat.[11]

The role of PPARγ in carcinogenesis has been controversial and depends on many factors. However, growing evidence suggests that PPARγ functions as a tumor suppressor, for example in cancers of the breast, prostate, and lung.[4,12] Activation of PPARγ in cultured adipose stromal cells inhibits estrogen biosynthesis by indirect repression of aromatase expression and activity, suggesting a protective function of PPARγ against breast carcinoma.[13,14] Other proposed mechanisms of mammary tumor suppression by PPARγ include induction of BRCA1 expression[15] and reduction in production of inflammatory mediators.[16] Gene-environment interactions have been reported for polymorphisms in PPARγ,[17] including an interaction between the P12A polymorphism and alcohol consumption indicating resistance to alcohol-related breast cancer by the A12 variant of PPARγ.[18,19]

Experimental testing of chemical substances to identify PPARγ agonists and antagonists have for example been conducted in the U.S. Toxicology in the 21st Century (Tox21) collaborative program.[20,21] In this program, a library of around ten thousand environmental chemicals was screened using cell-based quantitative high-throughput nuclear receptor transcriptional activity assays. One of the objectives of Tox21 is the development of new computational approaches for predictive toxicology. Quantitative structure-activity relationships (QSARs) are mathematical models that predict physicochemical, biological, or environment fate properties of compounds based on their chemical structure descriptors.[22,23] With an established model, it is possible to generate QSAR predictions for big inventories of substances in a short time, making the models good tools for screening and priority setting purposes, for assessment of chemical substances in Integrated Approaches to Testing and Assessments (IATA), and for hypothesis development for read-across.

In the present study, the effects of various environmental chemicals on PPARγ transcriptional activity were investigated with the aim of discovering PPARγ antagonists that may act as metabolic and endocrine disrupters to promote diseases such as breast cancer. A PPARγ antagonist reporter assay in human embryonic kidney (HEK293) cells was performed to corroborate the findings of the Tox21 assay, in this case using a luciferase reporter instead of the β-lactamase reporter. Based on data from Tox21, and after removal of chemicals that interfere with the Tox21 assay scoring by compound fluorescence, QSAR models were

developed for prediction of additional environmental and occupational PPARγ antagonist compounds. Computational QSAR models based on Tox21 experimental results, as well as based on other data sets, have been developed for PPARγ antagonism.[24–27] Contrary to earlier QSAR models developed for PPARγ antagonism, the QSAR training and validation sets in this study were made by applying a newly developed comprehensive data curation procedure to choose only the most robust positive and negative results and with use of absolute potency cut-offs.[28] Also, the models developed in this study will be made freely available for real-time predictions of user-defined structures and screening through pre-calculated predictions for 650,000 substances (https://qsar.food.dtu.dk). Furthermore, 11,092 EU REACH-registered chemical substances were QSAR-predicted and five of the predicted compounds were subsequently assayed *in vitro*. In addition, flexible docking-based simulation was used to evaluate the plausibility of ligand binding for the studied chemicals.

2. Materials and methods

2.1 Cell culture

A PPARγ LBD-driven GAL4 reporter HEK293 stable cell line (Signosis, SL-3002) was cultured in Dulbecco's Modified Eagle Medium (DMEM; Thermo Fisher Scientific, 11995-065) containing 10% heat-inactivated fetal bovine serum (FBS; Biological Industries, 04-007-1A), 1% penicillin-streptomycin solution (Biological Industries, 03-031-1B), and 100 µg/mL hygromycin B (Sigma-Aldrich, H3274) in humidified incubators at 37°C and 5% CO_2. Culture medium was changed every 2 or 3 days, and cell culturing experiments were performed in independent triplicates with at least replicates of three within each plate.

Cells were subcultured into white-walled 96-well plates (Greiner Bio-One, 655098) with 10^5 cells per well in 100 µL phenol red-free DMEM (Thermo Fisher Scientific, 31053-028) containing 0.1% FBS. The plates were incubated overnight followed by addition of 100 µL medium with serially diluted chemical to each well resulting in six different concentrations in the range 0.1 nM to 100 µM (varied between chemicals). Cells were incubated for 18 h until medium collection and cell lysis. Chemicals used for cell exposure were dissolved in DMSO (Supelco, 102931) and are listed in Table S1 (in the Supplemental Material). The final concentration of DMSO vehicle during chemical treatment was between 0.0001% and 0.1001%.

The chemicals were primarily pesticides, dyes, and additives. They were selected with the criterion of PPARγ inhibition by at least 25% at non-cytotoxic concentrations in the Tox21 PPARγ antagonist assay. Additionally, they were selected to cover a large range of potency levels and to not be active in the Tox21 PPARγ agonist assay. Known drugs were not included, except for the positive control GW9662. For pesticides, only those approved for use in the EU were selected. Experiments were performed either in the presence or absence of 50 nM rosiglitazone.

2.2 Cytotoxicity assay

A colorimetric lactate dehydrogenase (LDH) release assay was applied for measuring cytotoxicity. From each well, 100 µL supernatant was transferred into corresponding wells of an optically clear 96-well microplate (Thermo Fisher Scientific, 243656). LDH activity in the supernatants was determined using LDH Cytotoxicity Detection Kit (F. Hoffmann-La Roche, 11644793001) by addition of 100 µL freshly prepared reaction mixture to each well and incubation for 10-15 min protected from light and at room temperature. Finally, 50 µL 1 M HCl stop solution (Sigma-Aldrich, 30721) was added to each well, and absorbance was measured in a microplate reader (Wallac 1420 VICTOR2 MultiLabel Counter, PerkinElmer) for 1 s at 490 nm. Background signal from cell-free wells was subtracted from the values, which were then normalized to the sum of values within the experiment. The signal for vehicle-treated cells was set to 100%, and the signal from cells treated with 2% Triton X (Millipore, 1086031000) was set to 0%.

2.3 Transcriptional activity assay

Transcriptional activity of PPARγ was measured using a luciferase reporter system. Remaining culture medium was removed from the wells, and 20 µL 1X Firefly Luciferase Lysis Buffer (Signosis, LS-001) was added to each well. Cells were incubated at room temperature for 20 min with gentle agitation. Then 100 µL Firefly Luciferase Substrate (Signosis, LUC100) was added to each well, and luminescence was immediately measured in the plate reader twice at 10 seconds integration. Signal decay correction was applied by normalization of

the two consecutive measurements to the same time point using linear regression. Cell-free background signal was subtracted from the values, which were normalized to the sum of values within the experiment. The response of 100% was defined as vehicle-treated cells co-treated with 50 nM rosiglitazone.

Subsequently, fluorescence was measured with 485 nm excitation and 535 nm emission filters for 0.1 s to determine if chemicals emit light that overlaps with the fluorophore spectrum used in the Tox21 assay. Cell-free wells were used to subtract background signal from the values.

2.4 Statistical analysis

One-way ANOVA with Dunnett's test for multiple comparisons was applied to compare the solvent control with each individual exposure concentration. Concentration-response curves were fitted using the four-parameter logistic regression model with slope constraints of -1.5 to 0 and with starting response set to 100% for cytotoxicity curves and rosiglitazone co-treatment curves. Logistic regression assumes monotonic relationship between response and concentration, and therefore monotonicity was determined using Spearman's rank-order correlation. For non-monotonic relationships (Spearman's test, $p \geq 0.005$) with a significant extremum (Dunnett's test, $p \leq 0.05$), all data at greater concentrations than the extremum were excluded from the curve fitting and analysis.

After exclusion of data, re-analysis with one-way ANOVA was performed to test for overall differences in response between exposure concentrations. Based on this, and Tox21 assay data for compound fluorescence and luciferase inhibition, chemicals were categorized as either antagonists, partial agonists, full agonists, inconclusive, or not ligands. Antagonists were defined by a decrease in rosiglitazone-induced PPARγ activity with no increase in basal activity; partial agonists decrease rosiglitazone-induced activity and increase basal activity; full agonists increase basal activity without changing rosiglitazone-induced activation; chemicals that decreased PPARγ activity only when cytotoxicity was ≥20% were labeled inconclusive; luciferase inhibitors were labeled inconclusive; and chemicals resulting in no response were categorized as not being ligands.

2.5 Data and structure curation for QSAR modeling

A newly developed comprehensive in-house data curation procedure[28] was applied to the Tox21 PPARγ antagonism assay data downloaded from the NIH Tox21 Gateway.[29] The procedure is presented in Figure S1 (in the Supplemental Material) and includes selection of substances tested in highest purity, best quality of experimental curve fittings for positive and negative substances, user-defined settings for required magnitude of absolute (abs.) activity at a maximum concentration, actives required to show activity at non-cytotoxic concentrations, negatives required tested up to high concentrations without cytotoxicity, exclusion of substances which might show wrong results due to relevant assay signal interference (artifacts). Details are presented in Nikolov NG et al. (2023).[28]

Data were prepared to develop two models: One based on potent antagonists (minimum 25% absolute antagonism at maximum 10 µM concentration) and another based on all antagonists (minimum 25 % absolute antagonism with no concentration threshold: no upper limit, NUL).

Briefly, the following were chosen (see details in Nikolov et al. 2023):[28]

- Only the most robust positives with the best Hill curve fitting, Tox21 curve classes -1.1, -1.2, -2.1 or -2.2 (i.e. having inflection, p-value < 0.05 and efficacy > 3 standard deviations of control), exhibiting 'absolute' activity (here, IC_{25}) at or below the defined concentration cut-off (10 µM or NUL, respectively), and requiring non-cytotoxicity at effect concentration defined as minimum 80% of cells being alive.
- Only the most robust negatives with Tox21 curve class 4 and tested up to high concentration (here, 50 µM) without cytotoxicity.
- Only positives and negatives tested in high purity (at least 90%), i.e. Tox21 purity class A, to have higher certainty that correlations are made to the correct chemical structures.

As the applied Tox21 data were generated by a β-lactamase-based assay with fluorescence read-out, substances identified in Tox21 in HEK293 cells or cell-free cultures as showing auto-fluorescence at the background wavelength (channel 1, green), possibly leading to false-positive results, and substances showing

auto-fluorescence at the signal wavelength (channel 2, blue), possibly leading to false-negative results, were removed.

The Tox21 PPARγ antagonism assay works with 18 hours incubation after adding the test substance. As volatile and lipophilic substances tend to dissipate out of solution, possibly leading to false negative results, log K_{aw} and log K_{ow} thresholds were defined for acceptable negative *in vitro* results.[30–34] Based on previous research,[34] all inactive substances with log K_{ow} > 4 or log K_{aw} > -3 (as predicted by EPI WSKOW v1.42 and KOAWIN v1.10) were taken out of the training and validation sets.

2.6 Training and validation of QSAR models

After the data and structure curation, the data were divided by random into sets for training of initial models (80% of positives and 80% of negatives, however with a maximum of 10 negative substances per 1 positive substance) and validation (20% of positives and at least 20% of negatives).

Then, initial models were developed with the commercial software Leadscope® Predictive Data Miner (LPDM), part of Leadscope Enterprise Server version 3.5 (Leadscope Inc., an Instem company). Because of the imbalanced nature of the training sets with many more negatives than positives, a single model on the full training set may underperform, tending to predict the larger class too often. For this reason, LPDM offers composite models where the smaller class (positives) is reused against different portions of the bigger class (negatives) in several sub-models. A final averaging predictive model is thus obtained, generating predictions based on the predictions from the sub-models.[35] A further refinement of this approach by some of the authors was used,[36,37] where a model made on the full training set is combined with the 10 composite sub-models (for the case of 10 µM threshold) or with the 7 composite sub-models (for the NUL). Details on the modeling are available under 'cocktail modeling approach' in previous publications.[28,36–38]

Applicability domains of the QSAR models were generically defined before model development. Details on the applicability domain definition are presented in Nikolov NG et al. (2023),[28] however briefly described here: For a substance to be in the applicability domain, we required that: 1) it is inside the model's structural domain as defined in LPDM; and 2) a positive prediction should have a LPDM positive prediction probability ≥ 0.7, while a negative prediction should have a LPDM positive prediction probability ≤ 0.3.

After the initial models' development was complete, they underwent external validations with the left-out validation sets and were subjected to 10 times 5-fold external cross-validation procedures previously described.[28] Subsequently, the validation sets were integrated into the respective training sets and final expanded models were developed using the same modeling approach. Cooper statistics[39,40] were calculated by counting the true positives (TP – predicted positive and tested positive), false positives (FP – predicted positive and tested negative), true negatives (TN – predicted negative and tested negative) and false negatives (FN – predicted negative and tested positive) and using these to calculate sensitivity (TP / (TP + FN)), specificity (TN / (TN + FP)), balanced accuracy (BA, (sensitivity + specificity) / 2), and coverage (the ratio of the number of test substances in the applicability domain to the total number of substances in a test set, (TP + TN + FP + FN) / N for a given test set of size N). Only predictions inside the applicability domains were included. For external validations, 95% confidence intervals (CIs) for sensitivity and specificity were calculated according to the exact Clopper-Pearson method,[41] and for external cross-validations standard deviations were calculated. During the whole process, there was no exclusion of outliers.

2.7 Screening of REACH-registered substances and selection for *in vitro* testing

As an example of follow-up testing to a QSAR screening exercise, we used the 10 µM final model to predict 11,092 REACH-registered substances and selected 5 substances predicted positive for PPARγ antagonism for experimental testing. The follow-up testing was not meant to be an external validation of the models as they had already undergone external validation and 5 substances would be too few to obtain external validation results associated with acceptable confidence. The 5 substances were manually chosen by considering the positive prediction probability from LPDM, by representing different identified positive alerts, i.e. not overlapping too much in chemical structure, and lastly by considering the availability of test substance from suppliers. Information about the 5 substances is shown in Table S1 in the Supplemental Material together with rosiglitazone and the 25 substances selected from Tox21.

2.8 Molecular docking

The VirtualToxLab is an *in silico* platform which combines automated, flexible docking with multi-dimensional QSAR.[42,43] The predictive model for PPARγ is based on the agonist conformation of receptor protein co-crystallized with rosiglitazone.

Missing isomers were added to compounds featuring chiral centers to evaluate all isomers, as the tested compounds may be racemic mixtures. If one of the isomers of a compound bound to the receptor better than the others, the highest binding affinity value was chosen.

3. Results

3.1 PPARγ transcriptional activity assay

A selection of 25 chemicals from the Tox21 chemical library was used to test the reproducibility of the results from the Tox21 PPARγ antagonist assay. A transcriptional activity assay was performed in HEK293 cells in response to the selected chemicals using a GAL4/UAS reporter system. The cells were treated with nine concentrations of the PPARγ agonist rosiglitazone in the range of 0.1 nM to 50 µM to determine the proper concentration for subsequent co-treatment with chemicals of interest (Figure S2 in the Supplemental Material). No cytotoxicity was observed, and the half-maximal activity concentration (AC_{50}) was 12.4 nM. The concentration of 50 nM resulted in an almost maximal response and was therefore applied in the following experiments.

Two of the selected chemicals were fluorescent at the wavelength used for measuring background signal in fluorescence-based Tox21 assays, causing assay interference. The increased background signal caused a decrease in the signal to background ratio even though there were no changes in the reporter signal for PPARγ activity. To confirm that increased background signal was caused by fluorescence interference of the Tox21 assay and not variations in β-lactamase substrate concentration, fluorescence at 485/535 nm was measured after luminescence measurements (Figure S3 in the Supplemental Material). For comparison, fluorescence was measured for seven other chemicals. It was revealed that fluorescein and 1-nitropyrene were fluorescent at this wavelength, and no other chemicals displayed fluorescence. This indicates that fluorescein and 1-nitropyrene are not antagonists in the Tox21 assay, and they were therefore used as negative controls in the present study.

Cells were exposed individually to the 25 chemicals of interest in the presence or absence of 50 nM rosiglitazone (Figure 1). Out of the 25 chemicals, the two negative controls (fluorescein and 1-nitropyrene) were confirmed to not affect PPARγ activity and the remaining 23 chemicals had varying effects on PPARγ activity. The effect of heptylparaben was inconclusive because of cytotoxicity. Assay interference by luciferase inhibition was assessed by applying data from the Tox21 assay for luciferase inhibition. Four chemicals (Solvent Yellow 3, Solvent Yellow 7, Michler's ketone, and piperine) inhibited luciferase by at least 30% at 10 µM. Three other chemicals (butylparaben, heptylparaben, and 4,4'-biphenol) inhibited luciferase by at least 30% at concentrations higher than 10 µM, and these chemicals modulated PPARγ activity only at this concentration or above. Therefore, the seven luciferase inhibitors were categorized as inconclusive with regards to effects on PPARγ activity in the present study due to assay interference or cytotoxicity.

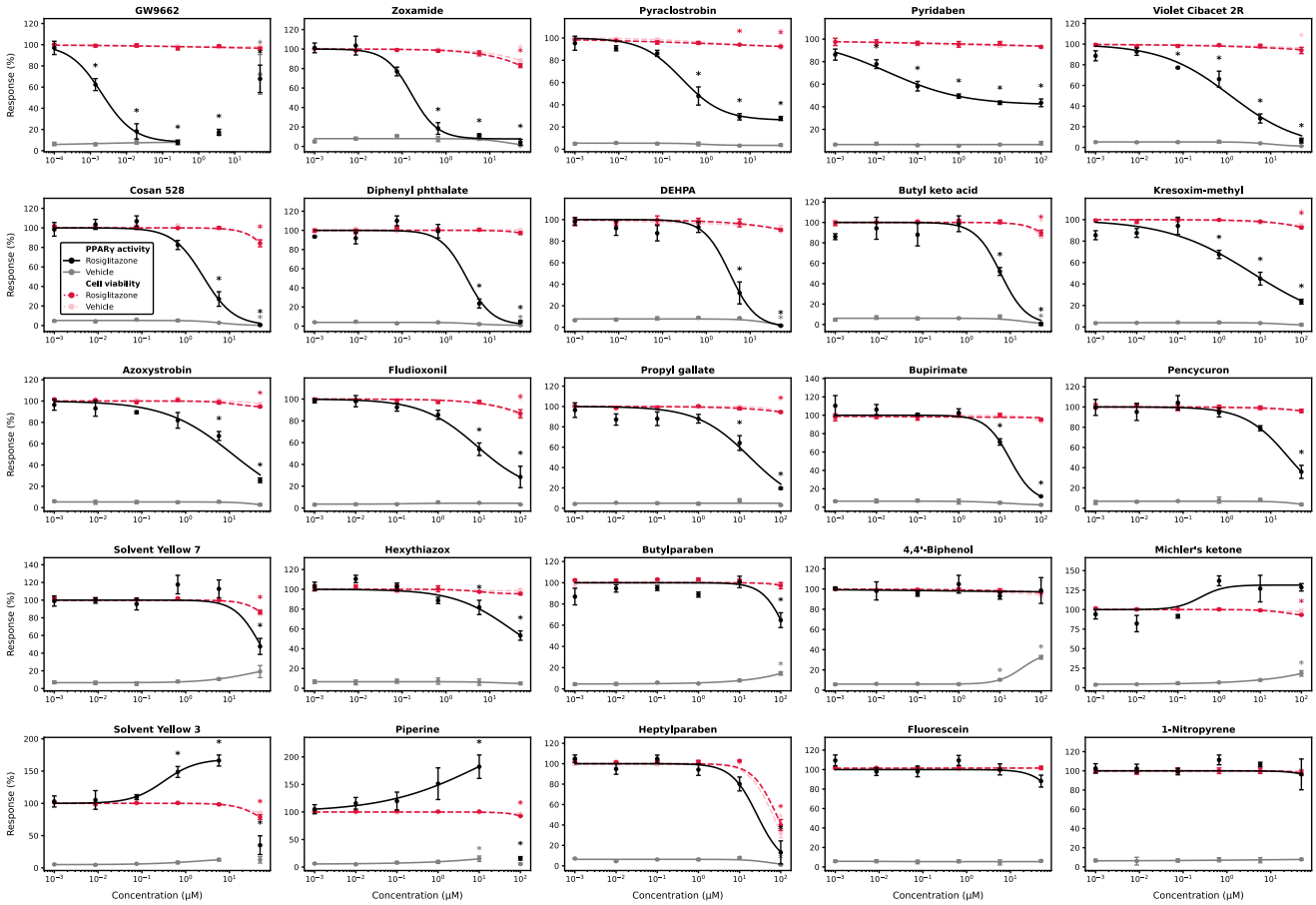

Figure 1: PPARγ activity in HEK293 cells in response to 18 h chemical exposure together with 50 nM rosiglitazone (black) or vehicle (gray). Viability is shown as dashed lines for rosiglitazone- (red) and vehicle-treated cells (pink). Means and SEM are shown; *n* = 3. The response to each concentration is compared with the vehicle control for all four assays. Statistical significance is indicated with an asterisk; * $p < 0.05$.

The remaining 16 chemicals antagonized the effect of rosiglitazone on PPARγ activity without increasing basal PPARγ activity. A summary of the results regarding assay interference, ligand potency, maximal response, and ligand type of chemicals are shown in Table S2 (in the Supplemental Material).

3.2 Data and structure curation for QSAR modeling of PPARγ antagonism

Training and validation sets for two QSAR models for PPARγ antagonism were made based on data from the Tox21 PPARγ antagonist assay after removal of chemicals causing assay interference. For one of the QSAR models, positives with an absolute IC_{25} threshold of 10 µM were used and for the other all positives with an absolute IC_{25} were used, i.e. no upper concentration limit was applied.

Results from all the intermediate steps done during the data and structure curation are presented in Table S3 (in the Supplemental Material). This table also presents results from the split made for obtaining the training and validation sets for initial models.

3.3 Training and validation sets for QSAR modeling of PPARγ antagonism

Two QSAR models for PPARγ antagonism were developed, each by first developing a so-called initial model on a reduced training set followed by development of final models based on all the positives and as many as possible of the negatives. The two initial models presented good performance in both external validation and external cross-validation with balanced accuracies (BAs) between around 83-87 % as presented in Table 1. The two final models, which were developed based on integration of the initial training sets and validation sets, showed as good performance as the initial models by external cross-validation. Standard deviations (SDs) decreased somewhat for the final models, indicating that the robustness improved compared to the initial smaller models. In Table 1 the number of true positive (TP), true negative (TN), false positive (FP), and false negative (FN) predictions are also presented.

Table 1: External validation of the PPARγ antagonism QSAR model

Model validation		Sens (%)[a]	Spec (%)[a]	BA (%)[a]	TP	TN	FP	FN	Coverage (%)[a]
10 µM	Initial model cross-validation	79.7 ± 15.2	94.2 ± 2.8	87.0 ± 7.6	341	5,422	331	85	72.0 ± 3.4
	Initial model validation	72.7 (39.0 - 94.0)	92.8 (90.7 - 94.7)	82.8	8	645	50	3	74.2
	Final model cross-validation	79.5 ± 11.1	93.8 ± 2.2	86.6 ± 5.5	434	6,686	443	112	71.2 ± 3.0
	Final model validation	-	93.4 (91.0 - 95.3)	-	-	508	36	-	74.4
NUL	Initial model cross-validation	79.8 ± 7.4	92.5 ± 2.1	86.2 ± 3.6	940	8,969	721	238	69.4 ± 2.7
	Initial model validation	73.7 (56.8 - 86.6)	91.4 (87.1 - 94.6)	82.5	28	222	21	10	71.9
	Final model cross-validation	80.7 ± 5.9	92.6 ± 1.9	86.6 ± 3.2	1,237	11,131	890	296	69.2 ± 2.5

[a] For external cross-validation, SDs are included for sensitivity (Sens), specificity (Spec), BA, and coverage, and for external validation, 95% CIs are included for sensitivity and specificity

3.4 *In vitro* testing of substances predicted positive by QSAR model for PPARγ antagonism

From the 11,092 REACH-registered substances screened with the final 10 µM QSAR model, 40.6% of the substances were in the applicability domain, of which 454 were predicted positive and 4,051 predicted negative. Five substances predicted positive for PPARγ antagonism by the final 10 µM QSAR model were selected for experimental *in vitro* testing in the PPARγ reporter assay (Figure 2). The effect of zuclopenthixol on PPARγ activity was inconclusive because of cytotoxicity. There was a 38% decrease in cell viability at 50 µM which was the only concentration at which an effect on PPARγ activity was observed. A chemoinformatic model for luciferase inhibition was used to predict if chemicals were luciferase inhibitors.[44] It was predicted that 2-methoxyphenothiazine was likely to exhibit luciferase inhibitory activity, and 2-methoxyphenothiazine was consequently categorized as inconclusive in this study. Diclofenac chloroacetyl impurity had high potency and efficiency as an antagonist. Dasatinib dichloro impurity was also a potent antagonist, but the efficiency was low and microscopy pictures revealed that the cells changed appearance at the concentrations that caused a response in PPARγ activity (Figure S4 in the Supplemental Material). This suggests that the observed decrease in PPARγ activity could be caused by an indirect effect on the reporter system, independent of PPARγ. Finally, trimebutine had no statistically significant effect on PPARγ activity. Assay interference, ligand potency, maximal response, and ligand type of the chemicals are summarized in Table S4 (in the Supplemental Material). In addition, Table S5 in the Supplemental Material presents the chemical structures of all chemicals applied in the *in vitro* assays, including the 25 chemicals selected from Tox21, the 5 QSAR-predicted chemicals, and rosiglitazone.

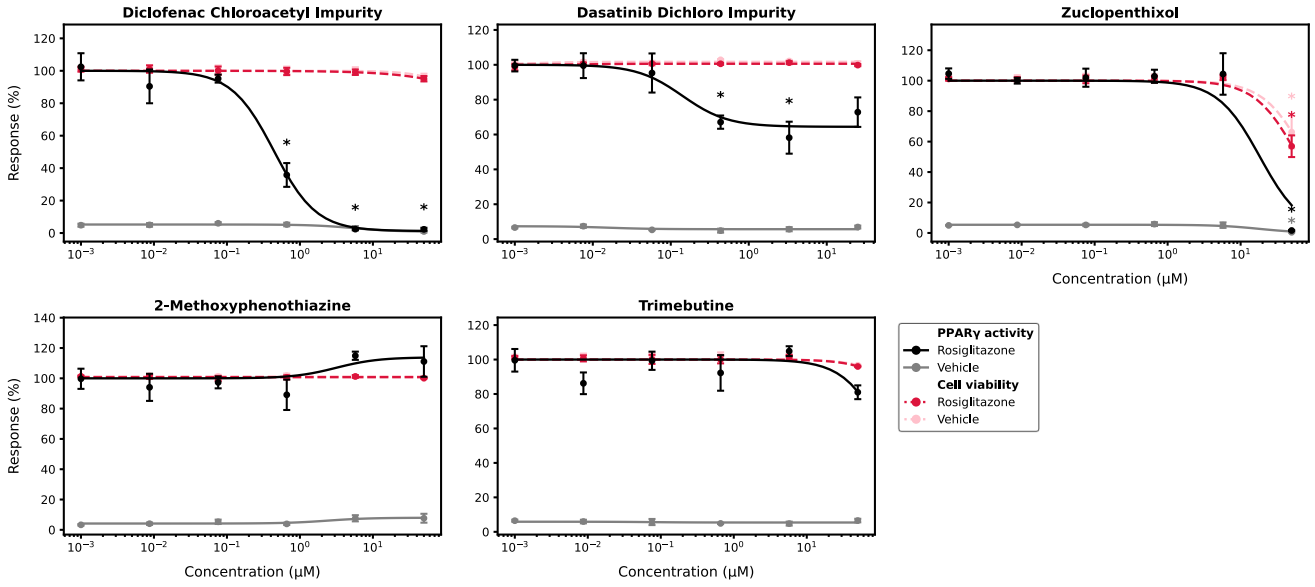

Figure 2: PPARγ activity in HEK293 cells in response to 18 h exposure to chemicals predicted to be PPARγ antagonists by the QSAR model. Chemical treatment was performed together with 50 nM rosiglitazone (black) or vehicle (gray). Viability is shown as dashed lines for rosiglitazone- (red) and vehicle-treated cells (pink). Means and SEM are shown; $n = 3$. The response to each concentration is compared with the vehicle control for all four assays. Statistical significance is indicated with an asterisk; * $p < 0.05$.

3.5 Flexible ligand docking

The VirtualToxLab is an *in silico* technology that can simulate and quantify the binding of small molecules to the ligand binding pocket of PPARγ LBD. The chemicals used in the present study were distributed into six groups according to the inhibitory constant (K_i) predicted by VirtualToxLab (Table S5 in the Supplemental Material).

The relationships between the K_i values predicted by VirtualToxLab and the relative IC_{50} values from the PPARγ assay in the present study or the corresponding half-maximal activity concentration (AC_{50}) values in the Tox21 PPARγ antagonist assay were assessed (Figure 3). In addition, the IC_{50} and Tox21 AC_{50} values were also compared. Chemicals without an IC_{50} or K_i were excluded as well as chemicals that are cytotoxic, luciferase inhibitors, or known to covalently bind to PPARγ. Linear regression was applied for the logarithmically transformed variables.

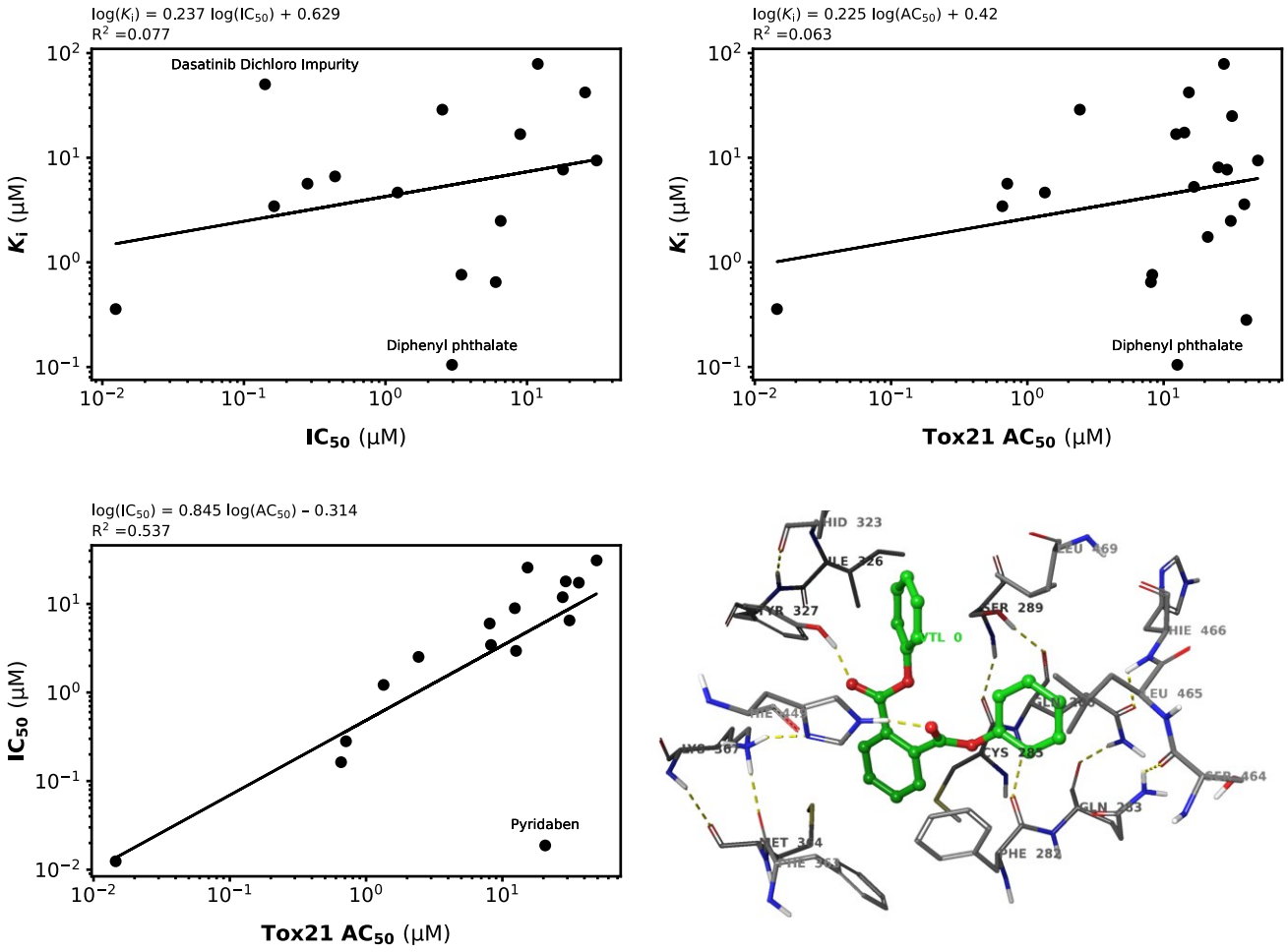

Figure 3: Scatter plots comparing K_i values predicted using VirtualToxLab with the relative IC_{50} values from the PPARγ antagonist assay in present study or with AC_{50} values from the Tox21 PPARγ antagonist assay. IC_{50} and AC_{50} values were also compared with each other. The equation and R^2 from the regression analysis are shown in each plot. A 3D figure shows the binding mode of diphenyl phthalate with H-bonding interactions indicated by yellow dashed lines to amino acid side chains in the binding site of PPARγ.

There was good correlation (R^2 = 0.537) between IC_{50} values calculated in this study and the AC_{50} values reported in the Tox21 data. When removing pyridaben, for which the IC_{50} and AC_{50} values were clearly not consistent between the two studies, the overall correlation increased dramatically (R^2 = 0.928). The correlation between IC_{50} values and predicted K_i values and between Tox21 AC_{50} values and predicted K_i values were similar, and R^2-values were relatively low. In Figure 3, the binding mode is shown for diphenyl phthalate, which was predicted to have the lowest K_i, and for which the corresponding IC_{50} and AC_{50} values were 28 and 120 times higher, respectively. In contrast, dasatinib dichloro impurity was predicted to have one of the highest K_i values, but the IC_{50} was determined to be one of the lowest.

4. Discussion

In the present study, PPARγ antagonists identified in the Tox21 PPARγ antagonist assay were confirmed in an orthogonal assay and applied for development of QSAR models for PPARγ antagonism to discover novel PPARγ antagonist candidates. Inhibition of PPARγ by antagonist may be associated with various physiological effects and cause adverse outcomes including increased risk of breast cancer.

4.1 Assay interference

Initially, the 25 PPARγ antagonist compounds selected from the Tox21 study were not analyzed for assay interference, although they were retrospectively analyzed for compound fluorescence and luciferase inhibition using fluorescence measurements and Tox21 luciferase inhibitor assay, respectively. This changed the interpretation of results markedly and led to a significantly higher consistency between assays from Tox21 and the present study. This highlights the importance of identifying compounds that interfere with assay readout.

Fluorescein and 1-nitropyrene were antagonists in the Tox21 PPARγ antagonist assay based on the background-normalized reporter signal. However, the reporter signal itself was unaffected by these chemicals, and the background signal increased, suggesting interference by compound fluorescence at the green wavelength of the background signal. The green fluorescence was confirmed in the present study, and the two chemicals were therefore categorized as inactive as PPARγ antagonists.

The PPARγ reporter assay in the present study was luciferase-based, and therefore the tested compounds were analyzed for luciferase inhibition using the Tox21 luciferase inhibitor assay. This indicated that 27% (8/30) of the tested compounds were luciferase inhibitors. Surprisingly, all of those chemicals, except the cytotoxic heptylparaben, caused either a statistically significant increase or a tendency to an increase in basal or rosiglitazone-induced reporter output. This was unexpected because luciferase inhibitors reduce luciferase activity in biochemical assays, such as the Tox21 luciferase inhibitor assay. However, in cell-based assays, luciferase inhibitors can stabilize ectopically expressed luciferase enzyme, extending the half-life and leading to an increased bioluminescent signal.[45] Similarly, the tested compounds may have other off-target activities interfering with the reporter system. For example, the pesticides azoxystrobin, pyraclostrobin, and pyridaben are known to inhibit mitochondrial respiration by blocking the electron transport chain, which could hypothetically increase production of reactive oxygen species and result in assay artifacts.

4.2 Orthogonal assay for validation of Tox21 PPARγ data

The application of orthogonal activity assays to high-throughput screening studies minimizes false positives and increases the evidence for the compounds which produce similar results, because complementary assays are susceptible to different types of interference.

In this study, a PPARγ transcriptional activity reporter assay in HEK293 cells using the GAL4/UAS system was used to assess chemical-induced effects on PPARγ activity. The same system was used in the Tox21 PPARγ assays, except that in the present study, the measurement system was luciferase-based and the Tox21 assays were based on measurements of β-lactamase activity. A limitation to this reporter system is that only the ligand-binding domain of PPARγ is contained within the PPARγ/GAL4 fusion protein. Consequently, interaction with RXR, and possibly other co-regulators, does not occur. The response to chemical treatment in this system may therefore, in some cases, differ from physiological conditions in which the full-length PPARγ is expressed and heterodimerizes with RXR.

The reporter assay in the present study showed responses similar to those observed in the Tox21 PPARγ antagonist assay for the 16 chemicals expected to inhibit PPARγ activity and for which no assay interference was found. The two assays were also consistent for the two negative controls. Likewise, the present study was in agreement with the Tox21 PPARγ agonist assay, showing no effects of any of the non-interfering chemicals or negative controls on PPARγ activity in cells not co-treated with rosiglitazone. In general, the calculated IC_{50} values were lower than the Tox21 AC_{50} values. This could be explained by the sorption of compounds to polystyrene walls,[30] which is expected to be higher in the Tox21 assay compared with the present assay, because of the more than three times higher surface area to volume ratio in the 1536-well plates of the Tox21 study than in the 96-well plates used in the current study.

An orthogonal assay to the Tox21 PPARγ assay in CV-1 cells was recently reported to be in 59% (16/27) agreement with the Tox21 PPARγ antagonist assay, excluding chemicals with an inconclusive response.[46] The study did not, however, consider assay interference in the analysis of the orthogonal assay nor in the analysis of Tox21 data. For example, the compound 3-aminofluoranthene is fluorescent at the green wavelength, and the decreased PPARγ activity in response to this chemical is most likely an artifact caused by a concentration-dependent increase in background fluorescence. In contrast, the authors observe increased activity of PPARγ in the orthogonal assay, which is also very likely to be an artifact, in this case explained by inhibition of luciferase activity by the chemical. The chemical is therefore inconclusive and may possibly be inactive as a ligand for PPARγ. Greater consistency between Tox21 and orthogonal assay would have been found if assay interference had been explored in the study, which would allow exclusion of chemicals from the analysis.

4.3 Environmental chemicals and modulation of PPARγ activity

PPARγ activity has previously been shown to be modulated by chemicals in the environment, resulting in disturbances in adipogenesis.[47] Some of the chemicals investigated in the present study have been studied by other research groups for effects on PPARγ activity. For example, propyl gallate inhibits PPARγ activity in HEK293 cells, consistent with the present results. It also inhibits adipogenesis as well as expression of PPARγ and adipocyte markers in human adipose tissue-derived mesenchymal stem cells.[48] In contrast to the Tox21 study, butylparaben activated PPARγ, promoted adipogenesis, and increased PPARγ and adipogenic gene expression in both 3T3-L1 cells[49] and C3H10T1/2 cells.[50] Zoxamide, pyridaben, pyraclostrobin, and fludioxonil have been shown to either increase PPARγ activity or have no effect,[51] however in another study pyraclostrobin downregulated PPARγ and PPARγ target genes in 3T3-L1 cells, disturbing normal adipogenesis.[52] Finally, piperine has previously been described as an agonist in some studies[53,54] and as an antagonist in other studies.[55,56] This suggests that PPARγ ligands may have different effects depending on the cell type or model system used.

The solvents ethanol and ethylene glycol were previously demonstrated to inhibit PPARγ transcriptional activation.[19,57] These chemicals are much smaller than the typical nuclear receptor ligand and elicit their effects at concentrations more than a thousand times higher. They may therefore affect PPARγ activity through indirect mechanisms, post-translational modifications, or disruption of co-regulator interactions instead of through interaction with the ligand binding pocket to cause conformational changes.

4.4 QSAR modeling of PPARγ antagonism

QSAR and SAR models of PPARγ antagonism based on Tox21 data have been developed previously.[24–27] The models developed in this work showed very good BAs of 83% by external validation of initial models and 87% by 10 times 5-fold external cross-validation of the final models.

The potent and efficient PPARγ antagonist diclofenac chloroacetyl impurity was discovered by predicting EU REACH-registered substances with one of the final QSAR models (positives with 25% inhibition at maximum 10 µM). There are no published data on the effect of this chemical on PPARγ activity or expression. However, the structurally similar diclofenac was shown to be a PPARγ antagonist in a PPARγ2-CALUX® cell line,[2] and diclofenac sodium was a PPARγ antagonist in the Tox21 PPARγ antagonist assay.

4.5 Molecular docking

Chemicals may inhibit PPARγ activity by post-translational modifications, such as by phosphorylation of PPARγ at S273, instead of binding as ligands. It has been shown before that rosiglitazone-induced PPARγ activity is inhibited by S273 phosphorylation in a GAL4/UAS reporter system in HEK293 cells.[58] Biophysical techniques can be used in addition to reporter assay to exclude false positive PPARγ ligands.[59] Alternatively, molecular docking is a useful technique to simulate the binding of ligand to the binding pocket of PPARγ.

The PPARγ predictive model is based on docking to the agonist form of the receptor. Predicted affinities therefore correspond to agonist behavior of the compound. However, high affinity could indicate either agonism or antagonism, because some compounds bound to the agonist form of the protein might antagonize the activity of the PPARγ by blocking the orthosteric binding site, thus rendering it unavailable for natural ligands. The true antagonism, caused typically by larger, voluminous ligands leading to substantial rearrangement of helices, which, in turn, prevents interaction with activators and/or oligomerization,[60] is not

simulated by this method. GW9662 covalently binds to one of the cysteine residues (C285) in the binding site of the PPARγ receptor.[61] This means that its binding affinity cannot be compared to the *in silico* scoring, as the covalent inhibition affects apparent K_i and as the methods are not able to simulate covalent effects.

Cell-based assays entail several confounding factors like metabolism or potential efflux of the compound from the cell, so the results from idealized *in silico* simulations do not translate perfectly to experimental observations. In addition, differences between predicted binding affinities and the experimental potencies could be explained by the application of the PPARγ agonist form for docking, which may not in all cases be a good substitute for the antagonist form. Nevertheless, most of the predictions match the *in vitro* binding. Exceptions include fluorescein and 1-nitropyrene, which did not affect PPARγ activity in reporter assays, but were predicted to have K_i values below 5 and 50 µM, respectively. Furthermore, the PPARγ inhibitors bupirimate and pyridaben were predicted to not bind PPARγ, which raises the question if they could have produced a response in the reporter assay in a PPARγ-independent manner. Similarly, dasatinib dichloro impurity was predicted to have one of the lowest affinities for PPARγ among the studied compounds. This compound drastically changed the appearance of the cells at the concentrations that produced a response, suggesting that the response may not have been a result of binding to the LBD of PPARγ but could instead be caused by an indirect mechanism.

4.6 Perspectives

The results in the current study enable further studies on the mechanisms through which exposure to environmental and occupational PPARγ antagonists may lead to metabolic disturbances or non-genotoxic carcinogenesis. This could ultimately help to discover and subsequently prevent exposure to potentially harmful chemicals.

5. Conclusion

In the present study, Tox21 data on PPARγ antagonism were replicated in a similar model system, and the Tox21 data were used to build a QSAR model for PPARγ antagonism after removal of false positive chemicals. *In vitro* testing of QSAR model predictions showed cases where the QSAR model successfully predicted PPARγ antagonists. Thus, the study highlights the importance of investigating assay interference in cell-based systems.

Acknowledgements

We thank Anne-Karin Asp for excellent technical assistance with the *in vitro* studies.

Competing interests

The authors declare that they have no competing interests.

Funding

This work was supported by FFIKA, Focused Research Effort on Chemicals in the Working Environment, from the Danish Government. The funding source was not involved in the conduct of the research or preparation of the article.

Availability of data and materials

The developed QSAR models have been applied to predict > 650.000 organic substances, including 13.406 REACH-registered substances, and the predictions are available in the free online Danish (Q)SAR database (https://qsar.food.dtu.dk). Furthermore, the two final models documented in the QSAR Model Reporting Format (QMRF) have been published in the free online Danish (Q)SAR Models website for real-time prediction of user-submitted structures and download of the detailed results in the QSAR Prediction Reporting Format (QPRF) (https://qsarmodels.food.dtu.dk).

Authors' contributions

Jacob Ardenkjær-Skinnerup: Conceptualization, Methodology, Investigation, Formal analysis, Visualization, Writing - Original Draft, Writing - Review & Editing.

Ana Caroline Vasconcelos Engedal Nissen: Methodology, Software, Data Curation, Formal analysis, Visualization, Writing - Review & Editing.

Nikolai Georgiev Nikolov: Methodology, Software, Data Curation, Formal analysis, Visualization, Writing - Review & Editing.

Martin Smieško: Methodology, Software, Formal analysis, Visualization, Writing - Review & Editing.

Niels Hadrup: Conceptualization, Methodology, Supervision, Writing - Review & Editing.

Gitte Ravn-Haren: Conceptualization, Methodology, Supervision, Writing - Review & Editing.

Eva Bay Wedebye: Methodology, Software, Data Curation, Formal analysis, Visualization, Writing - Review & Editing.

Ulla Vogel: Conceptualization, Methodology, Supervision, Resources, Project administration, Funding acquisition, Writing - Review & Editing.

References

1. Schaffert A, Krieg L, Weiner J, et al. Alternatives for the worse: Molecular insights into adverse effects of bisphenol a and substitutes during human adipocyte differentiation. *Environ Int*. 2021;156.
2. Dusserre C, Mollergues J, Lo Piparo E, et al. Using bisphenol A and its analogs to address the feasibility and usefulness of the CALUX-PPARγ assay to identify chemicals with obesogenic potential. *Toxicol In Vitro*. 2018;53:208-221.
3. Fang M, Webster TF, Ferguson PL, Stapleton HM. Characterizing the peroxisome proliferator-activated receptor (PPARγ) ligand binding potential of several major flame retardants, their metabolites, and chemical mixtures in house dust. *Environ Health Perspect*. 2015;123(2):166-172.
4. Hernandez-Quiles M, Broekema MF, Kalkhoven E. PPARgamma in Metabolism, Immunity, and Cancer: Unified and Diverse Mechanisms of Action. *Front Endocrinol (Lausanne)*. 2021;12.
5. Sauer S. Ligands for the Nuclear Peroxisome Proliferator-Activated Receptor Gamma. *Trends Pharmacol Sci*. 2015;36(10):688-704.
6. Lemay DG, Hwang DH. Genome-wide identification of peroxisome proliferator response elements using integrated computational genomics. *J Lipid Res*. 2006;47(7):1583-1587.
7. Chandra V, Huang P, Hamuro Y, et al. Structure of the intact PPAR-gamma-RXR- nuclear receptor complex on DNA. *Nature*. 2008;456(7220):350-356.
8. Marion-Letellier R, Savoye G, Ghosh S. Fatty acids, eicosanoids and PPAR gamma. *Eur J Pharmacol*. 2016;785:44-49.
9. Zhang J, Fu M, Cui T, et al. Selective disruption of PPARgamma 2 impairs the development of adipose tissue and insulin sensitivity. *Proc Natl Acad Sci U S A*. 2004;101(29):10703-10708.

10. He W, Barak Y, Hevener A, et al. Adipose-specific peroxisome proliferator-activated receptor gamma knockout causes insulin resistance in fat and liver but not in muscle. *Proc Natl Acad Sci U S A*. 2003;100(26):15712-15717.

11. Broekema MF, Savage DB, Monajemi H, Kalkhoven E. Gene-gene and gene-environment interactions in lipodystrophy: Lessons learned from natural PPARγ mutants. *Biochim Biophys acta Mol cell Biol lipids*. 2019;1864(5):715-732.

12. Augimeri G, Giordano C, Gelsomino L, et al. The Role of PPARγ Ligands in Breast Cancer: From Basic Research to Clinical Studies. *Cancers (Basel)*. 2020;12(9):1-28.

13. Rubin GL, Zhao Y, Kalus AM, Simpson ER. Peroxisome proliferator-activated receptor gamma ligands inhibit estrogen biosynthesis in human breast adipose tissue: possible implications for breast cancer therapy. *Cancer Res*. 2000;60(6):1604-1608.

14. Rubin GL, Duong JH, Clyne CD, et al. Ligands for the peroxisomal proliferator-activated receptor gamma and the retinoid X receptor inhibit aromatase cytochrome P450 (CYP19) expression mediated by promoter II in human breast adipose. *Endocrinology*. 2002;143(8):2863-2871.

15. Skelhorne-gross G, Reid AL, Apostoli AJ, et al. Stromal adipocyte PPARγ protects against breast tumorigenesis. *Carcinogenesis*. 2012;33(7):1412-1420.

16. Gionfriddo G, Plastina P, Augimeri G, et al. Modulating Tumor-Associated Macrophage Polarization by Synthetic and Natural PPARγ Ligands as a Potential Target in Breast Cancer. *Cells*. 2020;9(1).

17. Zeinomar N, Oskar S, Kehm RD, Sahebzeda S, Terry MB. Environmental exposures and breast cancer risk in the context of underlying susceptibility: A systematic review of the epidemiological literature. *Environ Res*. 2020;187.

18. Vogel U, Christensen J, Nexø BA, Wallin H, Friis S, Tjønneland A. Peroxisome proliferator-activated receptor-gamma2 Pro12Ala, interaction with alcohol intake and NSAID use, in relation to risk of breast cancer in a prospective study of Danes. *Carcinogenesis*. 2007;28(2):427-434.

19. Petersen RK, Larsen SB, Jensen DM, et al. PPARgamma-PGC-1alpha activity is determinant of alcohol related breast cancer. *Cancer Lett*. 2012;315(1):59-68.

20. Huang R, Xia M, Cho MH, et al. Chemical genomics profiling of environmental chemical modulation of human nuclear receptors. *Environ Health Perspect*. 2011;119(8):1142-1148.

21. Richard AM, Huang R, Waidyanatha S, et al. The Tox21 10K Compound Library: Collaborative Chemistry Advancing Toxicology. *Chem Res Toxicol*. 2021;34(2):189-216.

22. OECD. ENV/JM/MONO(2007)2 - Guidance Document on the Validation of (Quantitative) Structure-Activity Relationship [(Q)SAR] Models. 2007;154.

23. ECHA. Chapter R.6: QSARs and grouping of chemicals, Guid. Inf. Requir. Chem. Saf. Assess. 2008;134.

24. Koh DH, Song WS, Kim E young. Multi-step structure-activity relationship screening efficiently predicts diverse PPARγ antagonists. *Chemosphere*. 2022;286(Pt 1).

25. Kurosaki K, Wu R, Uesawa Y. A Toxicity Prediction Tool for Potential Agonist/Antagonist Activities in Molecular Initiating Events Based on Chemical Structures. *Int J Mol Sci*. 2020;21(21):1-20.

26. Seo M, Chae CH, Lee Y, Kim HR, Kim J. Novel QSAR Models for Molecular Initiating Event Modeling in Two Intersecting Adverse Outcome Pathways Based Pulmonary Fibrosis Prediction for Biocidal Mixtures. *Toxics*. 2021;9(3).

27. Sivamani Y, Shanmugarajan D, Durai Ananda Kumar T, et al. A promising in silico protocol to develop novel PPARγ antagonists as potential anticancer agents: Design, synthesis and experimental validation via PPARγ protein activity and competitive binding assay. *Comput Biol Chem*. 2021;95.

28. Nikolov NG, Nissen ACVE, Wedebye EB. A method for in vitro data and structure curation to optimize

for QSAR modelling of minimum absolute potency levels and a comparative use case. *Environ Toxicol Pharmacol*. 2023;98:104069.

29. PPAR-gamma-BLA HEK 293H Cell-based Assay / tox21-pparg-bla-antagonist-p1. Downloaded from https://tripod.nih.gov/tox/.

30. Schreiber R, Altenburger R, Paschke A, Küster E. How to deal with lipophilic and volatile organic substances in microtiter plate assays. *Environ Toxicol Chem*. 2008;27(8):1.

31. Kramer NI, Busser FJM, Oosterwijk MTT, Schirmer K, Escher BI, Hermens JLM. Development of a partition-controlled dosing system for cell assays. *Chem Res Toxicol*. 2010;23(11):1806-1814.

32. Stalter D, Dutt M, Escher BI. Headspace-free setup of in vitro bioassays for the evaluation of volatile disinfection by-products. *Chem Res Toxicol*. 2013;26(11):1605-1614.

33. Groothuis FA, Heringa MB, Nicol B, Hermens JLM, Blaauboer BJ, Kramer NI. Dose metric considerations in in vitro assays to improve quantitative in vitro-in vivo dose extrapolations. *Toxicology*. 2015;332:30-40.

34. Birch H, Kramer NI, Mayer P. Time-Resolved Freely Dissolved Concentrations of Semivolatile and Hydrophobic Test Chemicals in In Vitro Assays-Measuring High Losses and Crossover by Headspace Solid-Phase Microextraction. *Chem Res Toxicol*. 2019;32(9):1780-1790.

35. Leadscope Inc. Leadscope Model Applier Manual 3.1. 2021:106.

36. Rosenberg SA, Watt ED, Judson RS, et al. QSAR models for thyroperoxidase inhibition and screening of U.S. and EU chemical inventories. *Comput Toxicol*. 2017;4:11-21.

37. Chinen KK, Klimenko K, Taxvig C, Nikolov NG, Wedebye EB. QSAR modeling of different minimum potency levels for in vitro human CAR activation and inhibition and screening of 80,086 REACH and 54,971 U.S. substances. *Comput Toxicol*. 2020;14:100121.

38. Klimenko K, Rosenberg SA, Dybdahl M, Wedebye EB, Nikolov NG. QSAR modelling of a large imbalanced aryl hydrocarbon activation dataset by rational and random sampling and screening of 80,086 REACH pre-registered and/or registered substances. *PLoS One*. 2019;14(3).

39. Yerushalmy J. Statistical problems in assessing methods of medical diagnosis, with special reference to X-ray techniques. *Public Heal reports (Washington, DC 1896)*. 1947;62(40):1432-1449.

40. Cooper JA 2nd, Saracci R, Cole P. Describing the validity of carcinogen screening tests. *Br J Cancer*. 1979;39(1):87-89.

41. Newcombe RG. Two-sided confidence intervals for the single proportion: comparison of seven methods. *Stat Med*. 1998;17(8):857-872.

42. Vedani A, Dobler M, Smieško M. VirtualToxLab - a platform for estimating the toxic potential of drugs, chemicals and natural products. *Toxicol Appl Pharmacol*. 2012;261(2):142-153.

43. Vedani A, Dobler M, Hu Z, Smieško M. OpenVirtualToxLab--a platform for generating and exchanging in silico toxicity data. *Toxicol Lett*. 2015;232(2):519-532.

44. Ghosh D, Koch U, Hadian K, Sattler M, Tetko I V. Luciferase Advisor: High-Accuracy Model To Flag False Positive Hits in Luciferase HTS Assays. *J Chem Inf Model*. 2018;58(5):933-942.

45. Auld DS, Southall NT, Jadhav A, et al. Characterization of chemical libraries for luciferase inhibitory activity. *J Med Chem*. 2008;51(8):2372-2386.

46. Song WS, Koh DH, Kim EY. Orthogonal assay for validation of Tox21 PPARγ data and applicability to in silico prediction model. *Toxicol In Vitro*. 2022;84.

47. Routti H, Lille-Langoy R, Berg MK, et al. Environmental Chemicals Modulate Polar Bear (Ursus maritimus) Peroxisome Proliferator-Activated Receptor Gamma (PPARG) and Adipogenesis in Vitro.

Environ Sci Technol. 2016;50(19):10708-10720.

48. Lee JE, Kim JM, Jang HJ, et al. Propyl gallate inhibits adipogenesis by stimulating extracellular signal-related kinases in human adipose tissue-derived mesenchymal stem cells. *Mol Cells*. 2015;38(4):336-342.

49. Hu P, Chen X, Whitener RJ, et al. Effects of parabens on adipocyte differentiation. *Toxicol Sci*. 2013;131(1):56-70.

50. Hu P, Overby H, Heal E, et al. Methylparaben and butylparaben alter multipotent mesenchymal stem cell fates towards adipocyte lineage. *Toxicol Appl Pharmacol*. 2017;329:48-57.

51. Janesick AS, Dimastrogiovanni G, Vanek L, et al. On the Utility of ToxCast™ and ToxPi as Methods for Identifying New Obesogens. *Environ Health Perspect*. 2016;124(8):1214-1226.

52. Luz AL, Kassotis CD, Stapleton HM, Meyer JN. The high-production volume fungicide pyraclostrobin induces triglyceride accumulation associated with mitochondrial dysfunction, and promotes adipocyte differentiation independent of PPARγ activation, in 3T3-L1 cells. *Toxicology*. 2018;393:150-159.

53. Ma ZG, Yuan YP, Zhang X, Xu SC, Wang SS, Tang QZ. Piperine Attenuates Pathological Cardiac Fibrosis Via PPAR-γ/AKT Pathways. *EBioMedicine*. 2017;18:179-187.

54. Kharbanda C, Alam MS, Hamid H, et al. Novel Piperine Derivatives with Antidiabetic Effect as PPAR-γ Agonists. *Chem Biol Drug Des*. 2016;88(3):354-362.

55. Oruganti L, Reddy Sankaran K, Dinnupati HG, Kotakadi VS, Meriga B. Anti-adipogenic and lipid-lowering activity of piperine and epigallocatechin gallate in 3T3-L1 adipocytes. *Arch Physiol Biochem*. 2021.

56. Park UH, Jeong HS, Jo EY, et al. Piperine, a component of black pepper, inhibits adipogenesis by antagonizing PPARγ activity in 3T3-L1 cells. *J Agric Food Chem*. 2012;60(15):3853-3860.

57. Kopp TI, Lundqvist J, Petersen RK, et al. In vitro screening of inhibition of PPAR-gamma activity as a first step in identification of potential breast carcinogens. *Hum Exp Toxicol*. 2015;34(11):1106-1118.

58. Dias MMG, Batista FAH, Tittanegro TH, et al. PPARγ S273 Phosphorylation Modifies the Dynamics of Coregulator Proteins Recruitment. *Front Endocrinol (Lausanne)*. 2020;11.

59. Videira NB, Batista FAH, Torres Cordeiro A, Figueira ACM. Cellular and Biophysical Pipeline for the Screening of Peroxisome Proliferator-Activated Receptor Beta/Delta Agonists: Avoiding False Positives. *PPAR Res*. 2018;2018.

60. Frkic RL, Marshall AC, Blayo AL, et al. PPARγ in Complex with an Antagonist and Inverse Agonist: a Tumble and Trap Mechanism of the Activation Helix. *iScience*. 2018;5:69-79.

61. Leesnitzer LM, Parks DJ, Bledsoe RK, et al. Functional consequences of cysteine modification in the ligand binding sites of peroxisome proliferator activated receptors by GW9662. *Biochemistry*. 2002;41(21):6640-6650.

Supplemental Material for Orthogonal Assay and QSAR Modeling of Tox21 PPARγ Antagonist *In Vitro* High-Throughput Screening Assay

Jacob Ardenkjær-Skinnerup[1,2], Ana Caroline Vasconcelos Engedal Nissen[1], Nikolai Georgiev Nikolov[1], Martin Smieško[3], Niels Hadrup[1,2], Gitte Ravn-Haren[1], Eva Bay Wedebye[1], Ulla Vogel[1,2]

[1] The National Food Institute, Technical University of Denmark, Kongens Lyngby, Denmark
[2] The National Research Centre for the Working Environment, Copenhagen Ø, Denmark
[3] Department of Pharmaceutical Sciences, University of Basel, Basel, Switzerland

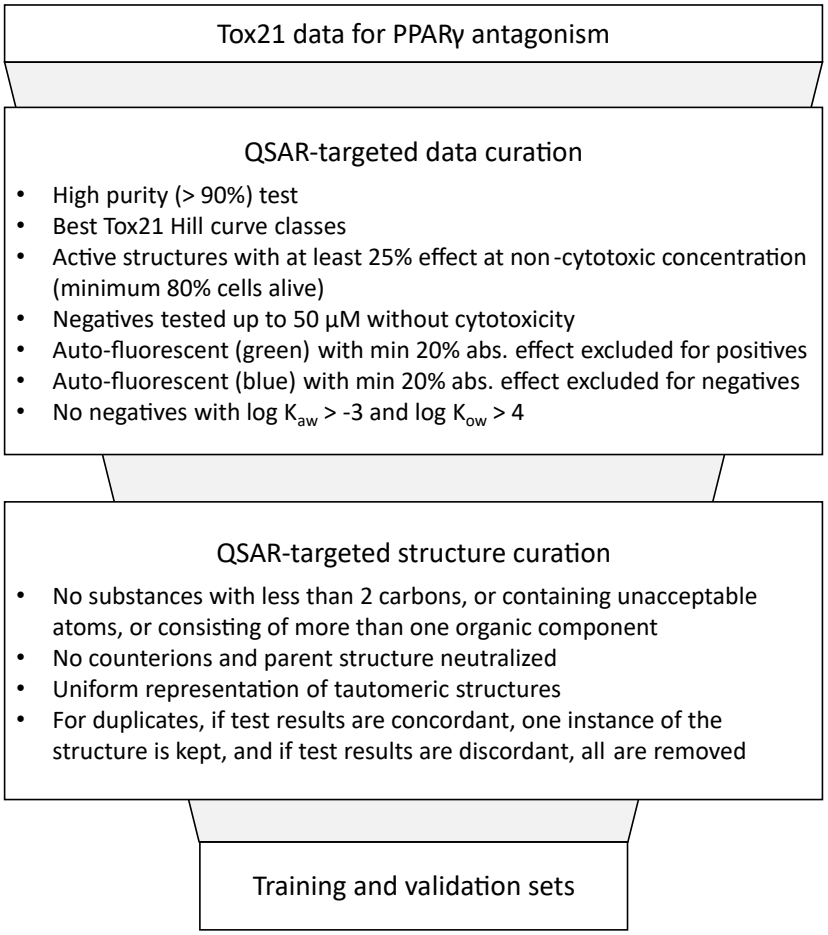

Figure S1: Summary of the data and structure curation for QSAR training and validation sets.

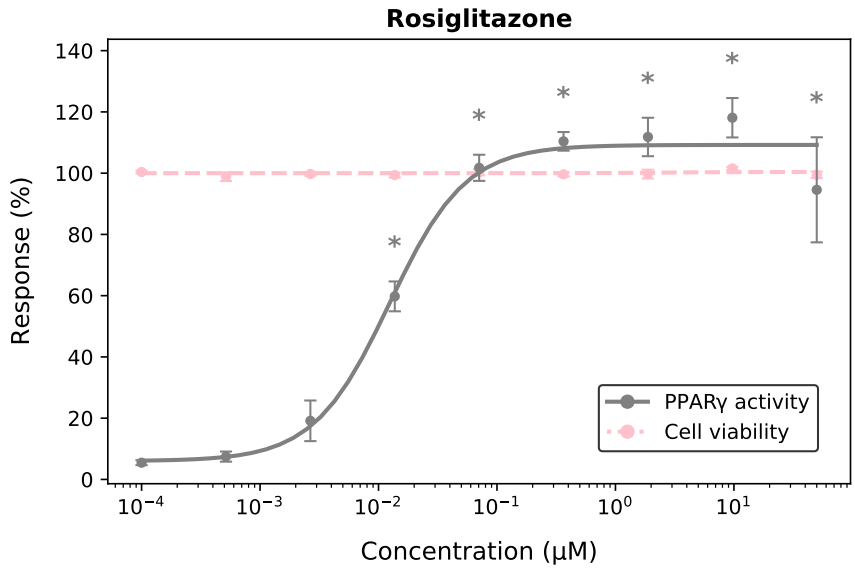

Figure S2: Activity of PPARγ LBD in response to 18 h rosiglitazone treatment of HEK293 cells (gray). Cell viability was measured using an LDH release assay in which 100% indicates no cell death and 0% indicates all cells dead (dashed line in red). Means and SEM are shown; $n = 3$. The response to each concentration was compared with the vehicle control for each assay. Statistical significance is indicated with an asterisk; * $p < 0.05$.

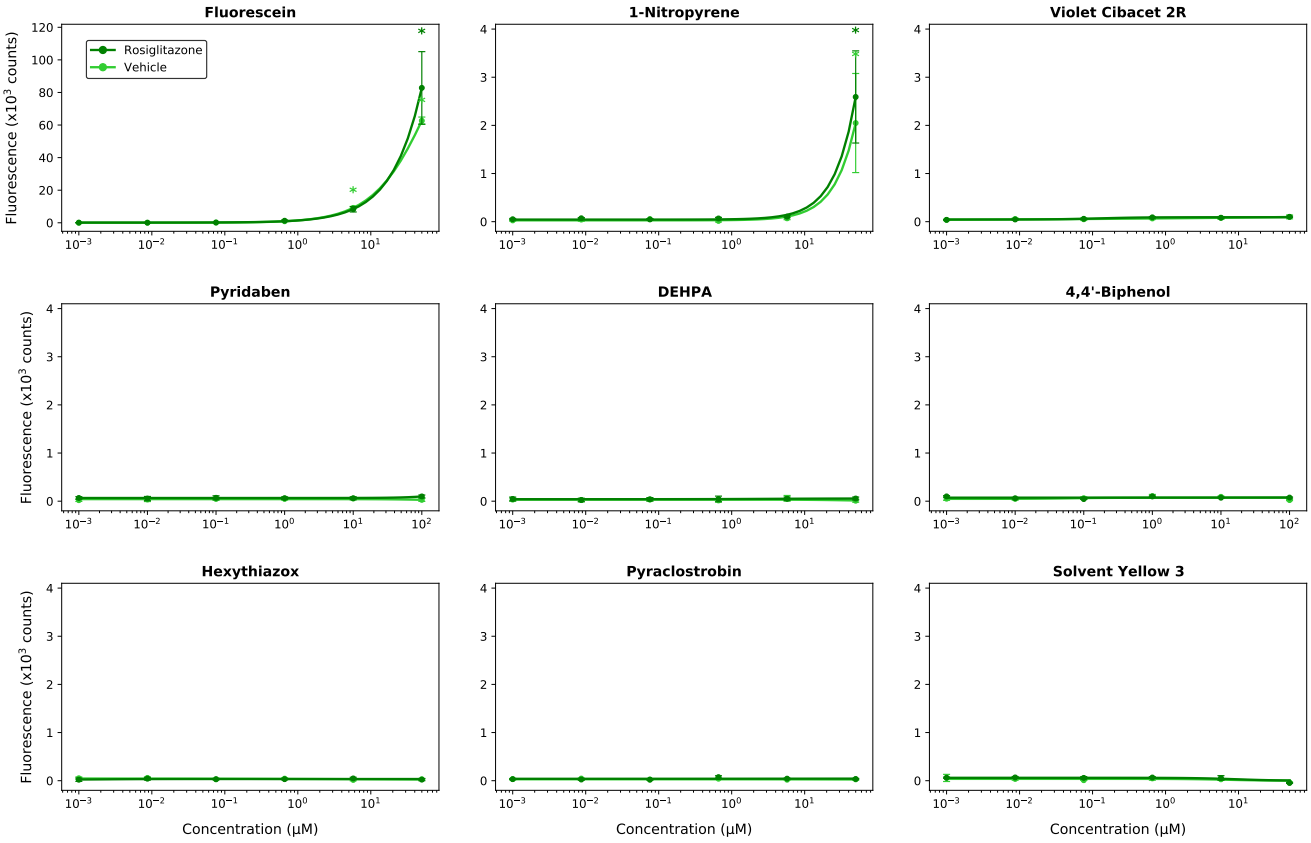

Figure S3: Fluorescence at 485/535 nm in response to 18 h chemical treatment of HEK293 cells with either 50 nM rosiglitazone (dark green) or vehicle (light green). Examples of measurements from seven chemical treatments are shown in addition to the chemicals, fluorescein and 1-nitropyrene, suspected to be fluorescent. Means and SEM are shown; $n = 3$. The response to each concentration is compared with the vehicle control. Statistical significance is indicated with an asterisk; * $p < 0.05$.

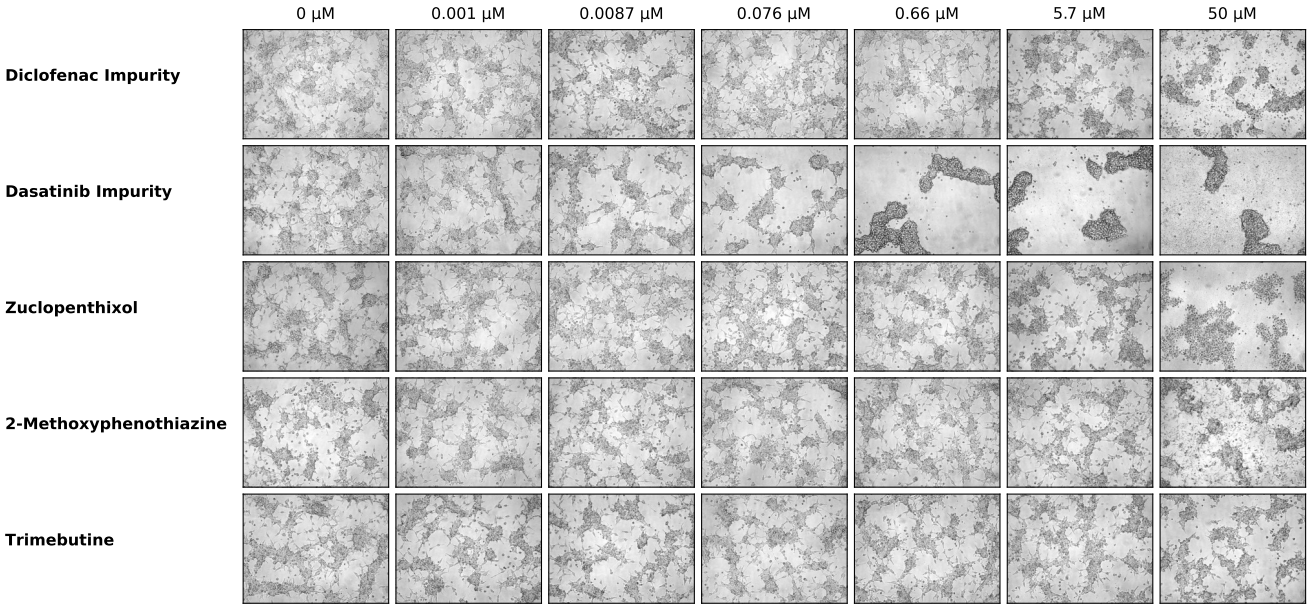

Figure S4: Microscopy pictures of HEK293 cells treated with different concentrations of chemicals for 18 h.

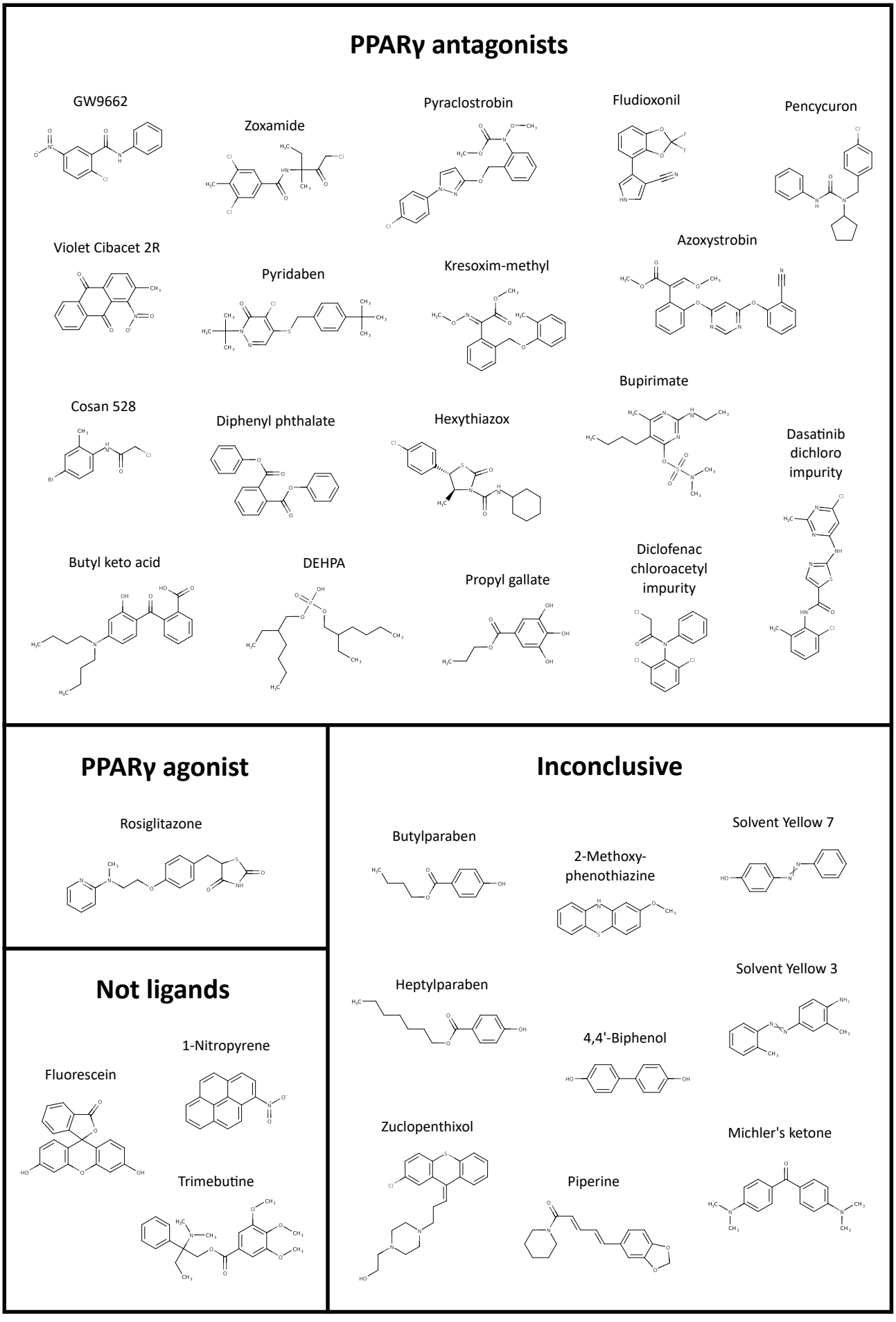

Figure S5: Chemical structures grouped according to their effects on PPARγ activity. The chemicals include 25 selected from Tox21, 5 predicted from the QSAR model, and rosiglitazone.

Table S1: List of chemicals included in this study

Short name	CAS	Company	Catalog #	Purity[a]
1-Nitropyrene	5522-43-0	Sigma-Aldrich	N22959	99.50 %
2-Methoxyphenothiazine	1771-18-2	Apollo Scientific Ltd	OR52313	97.70 %
4,4'-Biphenol	92-88-6	Sigma-Aldrich	168734	99.90 %
Azoxystrobin	131860-33-8	Supelco	31697	99.30 %
Bupirimate	41483-43-6	Supelco	31510	99.70 %
Butyl keto acid	54574-82-2	Sigma-Aldrich	402400	99.80 %
Butylparaben	94-26-8	Sigma-Aldrich	54680	100.00 %
Cosan 528	96686-51-0	Sigma-Aldrich	S878456	N/A
Dasatinib dichloro impurity	302964-08-5	BLD Pharmatech Ltd.	BD164165	95.00 %
DEHPA	298-07-7	Sigma-Aldrich	237825	100.00 %
Diclofenac chloroacetyl impurity	15308-01-7	BLD Pharmatech Ltd.	BD73713	97.72 %
Diphenyl phthalate	84-62-8	Sigma-Aldrich	105880	99.90 %
Fludioxonil	131341-86-1	Supelco	46102	99.90 %
Fluorescein	2321-07-5	EDQM	Y0000796	99.20 %
GW9662	22978-25-2	Sigma-Aldrich	M6191	98.80 %
Heptylparaben	1085-12-7	Sigma-Aldrich	CDS001278	N/A
Hexythiazox	78587-05-0	Supelco	33365	98.60 %
Kresoxim-methyl	143390-89-0	Supelco	37899	98.50 %
Michler's ketone	90-94-8	Supelco	56614	98.40 %
Pencycuron	66063-05-6	Supelco	31118	99.70 %
Piperine	94-62-2	Supelco	75047	97.00 %
Propyl gallate	121-79-9	Sigma-Aldrich	P3130	100.00 %
Pyraclostrobin	175013-18-0	Supelco	33696	99.90 %
Pyridaben	96489-71-3	Supelco	46047	99.30 %
Rosiglitazone	122320-73-4	Sigma-Aldrich	R2408	99.20 %
Solvent Yellow 3	97-56-3	Sigma-Aldrich	121568	99.00 %
Solvent Yellow 7	1689-82-3	Sigma-Aldrich	131083	99.00 %
Trimebutine	39133-31-8	Supelco	T6159	100.00 %
Violet Cibacet 2R	129-15-7	Sigma-Aldrich	S363650	N/A
Zoxamide	156052-68-5	Supelco	32501	99.60 %
Zuclopenthixol	53772-83-1	Targetmol Chemicals Inc.	T4117	99.96 %

[a] For some chemicals, information about purity was not available (N/A).

Table S2: Summary of orthogonal assay results for 25 selected chemicals

	Assay interference[a]		EC_{50} (μM)[b]		E_{max} (%)[c]			Ligand type
	Fluoresc	FLuc inhib	Absolute	Relative	Basal	Rosi	Viability	
GW9662	Negative	Negative	0.002	0.002		8.1	97.2	Antagonist
Zoxamide	Negative	Negative	0.183	0.163		4.3	85.6	Antagonist
Pyraclostrobin	Negative	Negative	0.610	0.281		27.6	92.4	Antagonist
Pyridaben	Negative	Negative	0.810	0.019		43.5	93.2	Antagonist
Violet Cibacet 2R	Negative	Negative	1.218	1.218		6.4	94.7	Antagonist
Cosan 528	Negative	Negative	2.522	2.522		0.7	84.8	Antagonist
Diphenyl phthalate	Negative	Negative	2.995	2.950		4.7	98.4	Antagonist
DEHPA	Negative	Negative	3.439	3.439		1.4	90.8	Antagonist
Butyl keto acid	Negative	Negative	6.010	6.010		0.7	88.4	Antagonist
Kresoxim-methyl	Negative	Negative	6.512	6.512		23.5	93.6	Antagonist
Azoxystrobin	Negative	Negative	11.91	11.91		25.7	95.9	Antagonist
Fludioxonil	Negative	Negative	14.33	8.947		28.5	85.8	Antagonist
Propyl gallate	Negative	Negative	17.95	17.95		19.7	94.4	Antagonist
Bupirimate	Negative	Negative	18.72	17.36		11.8	94.5	Antagonist
Pencycuron	Negative	Negative	25.71	25.71		35.9	96.0	Antagonist
Solvent Yellow 7	Negative	Positive	50.08	50.08		47.6	86.3	Inconclusive[d]
Hexythiazox	Negative	Negative	65.42	31.01		53.2	97.4	Antagonist
Butylparaben	Negative	Positive	150.6	150.6	14.6	64.7	98.2	Inconclusive[d]
4,4'-Biphenol	Negative	Positive			32.5		95.4	Inconclusive[d]
Michler's ketone	Negative	Positive		0.353	18.3	128.5	95.5	Inconclusive[d]
Solvent Yellow 3	Negative	Positive		0.319	12.7	166.3	81.9	Inconclusive[d]
Piperine	Negative	Positive		10.65	15.1	182.3	94.7	Inconclusive[d]
Heptylparaben	Negative	Positive	26.50	26.50		13.1	35.9	Inconclusive[d,e]
Fluorescein	Positive	Negative					101.4	Not ligand[f]
1-Nitropyrene	Positive	Negative					98.8	Not ligand[f]

[a] Assay interference by compound fluorescence (Fluoresc) and luciferase inhibition (FLuc inhib)

[b] Ligand potency calculated as absolute and relative half maximal effective concentrations (EC_{50}) for the PPARγ luciferase reporter assay co-treated with rosiglitazone

[c] Response at the highest used concentration (E_{max}) for PPARγ transcriptional activity assay in vehicle- (basal) or rosiglitazone-treated (rosi) cells as well as for the cytotoxicity assay for which viability is taken as the average between the vehicle- or rosiglitazone-treated cells

[d] Inconclusive due to luciferase inhibition

[e] Inconclusive due to cytotoxicity

[f] Inactive as PPARγ antagonist in Tox21 (antagonism was an artifact resulting from compound fluorescence)

Table S3: Data curation and division into training and validation sets

Data treatment	10 µM		NUL	
	Positives	Negatives	Positives	Negatives
Initial substances (SIDs)	9,315		9,315	
SIDs with purity at least 90%	6,283		6,283	
SIDs with DTU interpretations of positives and negatives	239	4,344	658	4,344
SIDs after cytotoxicity filter	165	4,313	400	4,313
SIDs after excluding auto-fluorescent substances	112	4,198	291	4,198
CASs after excluding when SIDs have conflicting data	105	2,568	256	2,568
CASs with QSAR-acceptable structures (organic mono-constituent etc.)	99	2,478	248	2,478
CASs after excluding volatile or lipophilic negatives	99	1,787	248	1,787
Structures after duplicates removal at structure level	98	1,711	245	1,711
Structures random split 80% (training set) : 20% (ext. validation set) for initial models[a]	78 : 20	780 : 931	196 : 49	1,369 : 342
Structures for training set and validation sets for final models	98 : 0	980 : 731	245 : 0	1711 : 0

[a] Maximum 10 times as many negatives as positives in training set

Table S4: Summary of experimental validation of 5 predicted PPARγ antagonists

	Assay interference[a]		EC_{50} (µM)[b]		E_{max} (%)[c]			Ligand type
	Fluoresc	FLuc inhib	Absolute	Relative	Basal	Rosi	Viability	
Diclofenac chloroacetyl impurity		Negative	0.448	0.440		2.3	95.7	Antagonist
Dasatinib dichloro impurity		Negative		0.141		72.8	100.3	Antagonist
Zuclopenthixol		Negative	18.36	18.36		1.6	61.6	Inconclusive[e]
2-Methoxyphenothiazine		Positive					100.1	Inconclusive[d]
Trimebutine		Negative					96.3	Not ligand

[a] Assay interference by compound fluorescence (Fluoresc) and luciferase inhibition (FLuc inhib)

[b] Ligand potency calculated as absolute and relative half maximal effective concentrations (EC_{50}) for the PPARγ luciferase reporter assay co-treated with rosiglitazone

[c] Response at the highest used concentration (E_{max}) for PPARγ transcriptional activity assay in vehicle- (basal) or rosiglitazone-treated (rosi) cells as well as for the cytotoxicity assay for which viability is taken as the average between the vehicle- and rosiglitazone-treated cells

[d] Inconclusive due to luciferase inhibition

[e] Inconclusive due to cytotoxicity

Table S5: Chemicals grouped by the inhibitory constant predicted by VirtualToxLab

Inhibitory constant, K_i (µM)					
0 – 0.5	0.5 – 1	1 – 5	5 – 10	10 – 50	50+
Diphenyl phthalate	Butyl keto acid	Michler's ketone	Solvent Yellow 3	2-Methoxyphenothiazine	Dasatinib Impurity
Piperine	DEHPA	Kresoxim-methyl	Pyraclostrobin	Fludioxonil	Azoxystrobin
Rosiglitazone		Fluorescein	Diclofenac Impurity	4,4'-Biphenol	Bupirimate
		Zoxamide	Trimebutine	GW9662	Pyridaben
		Heptylparaben	Propyl gallate	Butylparaben	
		Violet Cibacet 2R	Solvent Yellow 7	Cosan 528	
		Zuclopenthixol	Hexythiazox	1-Nitropyrene	
				Pencycuron	

Manuscript II

PPARγ Antagonists Induce Aromatase Transcription in Adipose Tissue Cultures

Jacob Ardenkjær-Skinnerup, Daniel Saar, Patricia S. S. Petersen, Mikael Pedersen, Terje Svingen, Birthe B. Kragelund, Niels Hadrup, Gitte Ravn-Haren, Brice Emanuelli, Kristy A. Brown, Ulla B. Vogel

In this manuscript, it was investigated if previously identified PPARγ antagonists could affect aromatase expression in adipose tissue cells and explants. This manuscript has not yet been submitted for publication.

PPARγ Antagonists Induce Aromatase Transcription in Adipose Tissue Cultures

Jacob Ardenkjær-Skinnerup[1-4], Daniel Saar[5], Patricia S. S. Petersen[1], Mikael Pedersen[2], Terje Svingen[2], Birthe B. Kragelund[5], Niels Hadrup[2,3], Gitte Ravn-Haren[2], Brice Emanuelli[1], Kristy A. Brown[4,6,*], Ulla B. Vogel[2,3,*]

[1] The Novo Nordisk Foundation Center for Basic Metabolic Research, University of Copenhagen, Copenhagen N, Denmark
[2] The National Food Institute, Technical University of Denmark, Kongens Lyngby, Denmark
[3] The National Research Centre for the Working Environment, Copenhagen Ø, Denmark
[4] Department of Medicine, Weill Cornell Medicine, New York, NY, USA
[5] REPIN and Structural Biology and NMR Laboratory, Department of Biology, University of Copenhagen, Copenhagen N, Denmark
[6] Department of Cell Biology and Physiology, University of Kansas Medical Center, Kansas City, KS, USA

* Corresponding authors at: Department of Cell Biology and Physiology, University of Kansas Medical Center, Kansas City, KS, USA (Kristy A. Brown) and the National Research Centre for the Working Environment, Copenhagen Ø, Denmark (Ulla B. Vogel).

E-mail addresses: kbrown46@kumc.edu (Kristy A. Brown), ubv@nfa.dk (Ulla B. Vogel)

Abstract

Aromatase is the rate-limiting enzyme in the biosynthesis of estrogens and a key risk factor for hormone receptor-positive breast cancer. In postmenopausal women, estrogens synthesized in adipose tissue promotes the growth of estrogen receptor positive breast cancers. Activation of peroxisome proliferator-activated receptor gamma (PPARγ) in adipose stromal cells (ASCs) leads to decreased expression of aromatase and differentiation of ASCs into adipocytes. Environmental chemicals can act as antagonists of PPARγ and disrupt its function. This study aimed to test the hypothesis that PPARγ antagonists can promote breast cancer by stimulating aromatase expression in human adipose tissue.

Primary cells and explants from human adipose tissue as well as A41hWAT, C3H10T1/2, and H295R cell lines were used to investigate PPARγ antagonist-stimulated effects on adipogenesis, aromatase expression, and estrogen synthesis. Selected antagonists inhibited adipocyte differentiation, preventing the adipogenesis-associated downregulation of aromatase. NMR spectroscopy confirmed direct interaction between the potent antagonist DEHPA and PPARγ, inhibiting agonist binding. Short-term exposure of ASCs to PPARγ antagonists upregulated aromatase only in differentiated cells, and a similar effect could be observed in human breast adipose tissue explants. Overexpression of *PPARG* with or without agonist treatment reduced aromatase expression in ASCs.

The data suggest that environmental PPARγ antagonists regulate aromatase expression in adipose tissue through two mechanisms. The first is indirect and involves inhibition of adipogenesis. The second mechanism occurs more acutely and is unrelated to adipocyte differentiation.

Keywords: PPARγ, aromatase, adipogenesis, adipose tissue, breast cancer, endocrine disruption, metabolic disruption

Abbreviations

9cRA	9-*cis*-retinoic acid
ANOVA	analysis of variance
ASC	adipose stromal cell
AU	arbitrary units
BMI	body mass index
cDNA	complementary DNA
DEHPA	di(2-ethylhexyl)phosphoric acid
DHEA	dehydroepiandrosterone
DHT	dihydrotestosterone
DMEM	Dulbecco's modified Eagle medium
DPhP	diphenyl phthalate
DSS	4,4-dimethyl-4-silapentane-1-sulfonic acid
ESI	electrospray ionization
EV	empty vector
FBS	fetal bovine serum
FSK	forskolin
IBMX	3-isobutyl-1-methylxanthine
LBD	ligand-binding domain
LOD	limit of detection
LOQ	limit of quantification
ND	not detected
NMR	nuclear magnetic resonance
PBS	phosphate-buffered saline
PMA	phorbol 12-myristate 13-acetate
PPARγ	peroxisome proliferator-activated receptor gamma
RT-qPCR	quantitative reverse transcription PCR
RXR	retinoid X receptor
SEM	standard error of the mean
SNP	single nucleotide polymorphism
T_3	triiodothyronine

Introduction

Breast cancer is the most commonly diagnosed cancer worldwide.[1] In women, the systemic levels of steroid hormones, not least estrogens, are major risk factors for breast cancer,[2] and exposure to endocrine disrupting chemical may contribute to breast cancer risk.[3,4] The nuclear receptor peroxisome proliferator-activated receptor gamma (PPARγ) has been suggested to be a protective factor in breast cancer development,[5] with a proposed mechanism being negative regulation of aromatase (encoded by *CYP19A1*),[6,7] the rate-limiting enzyme in the biosynthesis of estrogens. Notably, most studies investigating this link have focused on the effect of PPARγ activation on aromatase, with inactivation of PPARγ being less explored.

Numerous environmental and occupational compounds can target PPARγ by binding as agonists or antagonists in the binding pocket of the ligand-binding domain (LBD) (Ardenkjær-Skinnerup et al, submitted).[8] PPARγ is highly expressed in adipose tissue, which is an important site of xenobiotic bioaccumulation and metabolic disruption.[9] Adipose tissue is also an endocrine organ that plays important roles in the development and function of mammary epithelial cells, but it also contributes to development and progression of breast cancer.[10] Environmental PPARγ antagonists may potentially promote breast cancer development by inhibiting PPARγ function, leading to a derepression of aromatase expression and, consequently, increased production of estrogens acting locally on adjacent breast epithelial cells.

PPARγ is essential for adipogenesis.[11] It exists as two isomers, PPARγ1 and PPARγ2, transcribed from different promoters of the *PPARG* gene. The PPARγ2 is almost exclusively expressed in the adipose tissue[12] and encompasses 30 additional N-terminal amino acids compared to PPARγ1. A common missense single nucleotide polymorphism (SNP) of PPARγ2, Pro12Ala (rs1801282), is associated with modified breast cancer risk in postmenopausal women,[13,14] as well as impaired adipogenesis.[15] However, its impact on metabolism is highly dependent on gene-environment interactions.[16]

Since exposure to environmental chemicals may contribute to breast cancer development,[17] it is important to fully understand the underlying mechanisms in order to identify potential interventions. The role of aromatase in promoting breast cancer development and progression is well established,[18] however it is still unknown whether exposure to PPARγ antagonists affects aromatase expression in human adipose tissue cells. It is therefore hypothesized that PPARγ antagonism induces aromatase expression in the adipose tissue.

In this study, human adipose stromal cells (ASCs) were differentiated in the presence of previously identified PPARγ antagonists (Ardenkjær-Skinnerup et al, submitted) to address the inhibitory effect of selected chemicals on PPARγ and to study the effect of impaired adipogenesis on aromatase expression. In addition, interactions between PPARγ and selected chemicals, alone or in combination, were determined using NMR spectroscopy. Finally, a more acute effect of PPARγ ligands on aromatase expression was studied by treating ASCs, differentiated ASCs, or adipose tissue explants with PPARγ antagonists.

Methods

Isolation of primary cells and explants

Primary cells were isolated from adipose tissue obtained from patients undergoing mastectomy, abdominoplasty, or reduction mammoplasty at Weill Cornell Medicine under IRB-approved protocol #20-01021391. Adipose tissue was finely minced, and 20-25 mL tissue was placed in a 50 mL centrifuge tube, which was filled with pre-warmed F-12 medium (10-080-CV, Corning) containing 10% fetal bovine serum (FBS; 35-010-CV, Corning) and 1% penicillin-streptomycin solution (15140122, Gibco). The tissue was incubated with 1 mg/mL collagenase (C0130, Sigma-Aldrich) and 0.01 mg/mL hyaluronidase (H3506, Sigma-Aldrich) for 1 h at 37 °C while rotating, followed by centrifugation at 500 × g for 15 min. The oil layer at the top was removed, and adipocytes were collected from the layer below. The cell pellet was resuspended in 20 mL culture medium and passed through 100 µm and 40 µm filters. The filtrate was centrifuged at 500 × g for 5 min, and the supernatant was removed. The cell pellet was resuspended in 1 mL Red Blood Cell Lysis Buffer (11814389001, Roche) and inverted periodically for 10 min. The tube was centrifuged at 500 × g for 5 min, supernatant was

discarded, and the pellet was resuspended in culture medium or collected for lysis. The cell suspension was transferred to tissue culture flasks and incubated at 37 °C and 5% CO_2 for 1 h before the medium was renewed. Information on the study participants is shown in Table 1.

#	Surgery	Sex	Age	BMI
1	Mastectomy	Female	37	35.51
2	Mastectomy	Female	46	28.70
3	Mastectomy	Female	40	26.20
4	Mastectomy	Female	56	27.20
5	Mastectomy	Female	65	19.49
6	Mastectomy	Female	45	30.70
7	Abdominoplasty	Female	55	36.28
8	Abdominoplasty	Female	39	38.37
9	Mammoplasty	Female	57	31.85
10	Mammoplasty	Male	18	23.95
11	Mammoplasty	Female	45	24.70
12	Mammoplasty	Female	35	32.34
13	Mammoplasty	Female	40	29.60

Table 1: Participant number (#), surgery type, sex, age, and body mass index (BMI).

Adipose tissue explants were obtained by cutting 2-5 mm^3 sections of adipose tissue and incubating multiple pieces per well in the F-12 culture medium in 12-well plates at 37 °C. After a few hours, the medium was changed.

Primary adipocytes and ASCs collected for lysis were washed by adding phosphate-buffered saline (PBS) and inverting several times. ASCs were subsequently centrifuged for 5 min at 500 g. Adipocytes and ASCs were then frozen in liquid nitrogen and kept at -80 °C until gene expression analysis.

Cell culture and treatment

The human A41 ASCs cell line (hTERT A41hWAT-SVF, passage 8-19)[19] and the mouse C3H10T1/2 mesenchymal stem cell line (CCL-226, ATCC, passage 6-11) were cultured in Dulbecco's Modified Eagle Medium (DMEM; 41965-039, Gibco) containing 10% FBS (F7524, Sigma-Aldrich) and 1% penicillin-streptomycin solution (15070063, Gibco). The human NCI-H295R adrenocortical carcinoma cell line (CRL-2128, ATCC, passage 10-13) was cultured in DMEM/F-12 (11039, Thermo Fisher Scientific) supplemented with 2.5% Nu-Serum (355100, Corning) and 1% ITS+ (354352, Corning). All cells were cultured in humidified incubators at 37 °C and 5% CO_2. Culture medium was changed every 2 or 3 days. Cells and explants were stimulated with the chemicals listed in Table 2. Solvent volumes were equal across all conditions for each experiment.

Compound	CAS	Company	Catalog #
9-*cis*-Retinoic acid	5300-03-8	Sigma-Aldrich	R4643
Cosan 528	96686-51-0	Sigma-Aldrich	S878456
DEHPA	298-07-7	Sigma-Aldrich	237825
Diphenyl phthalate	84-62-8	Sigma-Aldrich	105880
Forskolin	66575-29-9	Sigma-Aldrich	F3917
GW9662	22978-25-2	Sigma-Aldrich	M6191
Kresoxim-methyl	143390-89-0	Supelco	37899
PMA	16561-29-8	Sigma-Aldrich	P8139
Prochloraz	67747-09-5	Supelco	45631
Pyraclostrobin	175013-18-0	Supelco	33696
Pyridaben	96489-71-3	Supelco	46047
Rosiglitazone	122320-73-4	Sigma-Aldrich	R2408
Violet Cibacet 2R	129-15-7	Sigma-Aldrich	S363650
Zoxamide	156052-68-5	Supelco	32501

Table 2: The chemicals used for treatment of cells.

Adipose tissue explants were treated with chemicals for 48 h, then washed in PBS and lysed with QIAzol (Qiagen). For each biological explant sample, multiple technical replicate samples were collected for analysis. Undifferentiated or 12-day differentiated A41 cells in basal culture medium were treated for 24 h, while, in other experiments, primary ASCs, C3H10T1/2 cells, and A41 cells were treated throughout differentiation. Concentrations were selected based on previous reporter assay experiments (Ardenkjær-Skinnerup et al, submitted). Cells were washed in PBS and lysed with Buffer RLT (Qiagen) containing 1% β-mercaptoethanol.

H295R cells were subcultured at approximately 50-60% confluency (3 x 10^5 cells) into 24-well plates and left overnight. Next day, culture medium was removed by aspiration and replaced with medium containing each chemical of interest. The plates were incubated at 37 °C and 5% CO_2 for 48 h. Finally, medium was transferred to new 24-well plates and frozen at -80 °C until further processing to analyze hormone concentrations. Cells were washed with PBS and frozen at -80 °C for subsequent protein analysis. The experiment was performed in triplicates and repeated three times independently.

Adipocyte differentiation

Primary human ASCs were subcultured at high density to reach 100% confluence. The cells were then washed twice with PBS and induced to differentiate by changing basal culture medium to serum-free adipogenic medium containing 0.1 or 2 µM rosiglitazone (day 0-4), 0.25 µM dexamethasone (day 0-6), 500 µM IBMX (day 0-6), 20 nM insulin, 0.2 nM T_3, 33 µM biotin, 17 µM pantothenic acid, 0.1 µM transferrin, and 10 µg/mL cortisol (all from Sigma-Aldrich). The cells were kept in adipogenic medium for 12 days and the medium was changed every 2 days.

A41 and C3H10T1/2 cells were grown to confluence, and differentiation was induced in serum-containing medium. For differentiation of A41 cells, the culture medium was supplemented with 1 µM rosiglitazone, 0.1 µM dexamethasone, 500 µM IBMX, 500 nM insulin, 2 nM T_3, 33 µM biotin, and 17 µM pantothenic acid. Differentiation of C3H10T1/2 cells was induced by supplementing the culture medium with 0.5 µM rosiglitazone, 1 µM dexamethasone (day 0-2), 500 µM IBMX (day 0-2), and 20 nM insulin (day 0-4). The adipogenic medium was changed every 2 or 3 days for C3H10T1/2 and A41 cells, respectively.

In experiments where cells were exposed to additional chemicals (Table 2) during differentiation, these chemicals were added together with the adipogenic factors every time the medium was replenished. Mature A41 cells used for acute chemical treatment were differentiated for 12 days and returned to regular growth medium for 2 days before 24 h treatment with chemical.

Lipid staining and quantification

Transparent 96-well plates were used for staining with Oil Red O. Cells were washed in PBS and fixed with 4% formaldehyde (252549, Sigma-Aldrich) in PBS for 30 min at room temperature. The cells were then washed twice with water and incubated with 60% isopropanol for 5 min. Afterwards, cells were incubated with sterile filtered 60% Oil Red O (O0625, Sigma-Aldrich) solution for 20 min. Cells were washed 3 times with water and then viewed under the microscope. For quantification, cells were washed 3 times with 60% isopropanol for 5 min. Oil Red O was then extracted with 50 µL 100% isopropanol for 20 min. Finally, 40 µL of the extracted Oil Red O was transferred to a 384 well plate. Absorbance was read at 518 nm in a Varioskan LUX Multimode Microplate Reader (Thermo Scientific), and 100% isopropanol was used as a background control.

Fluorescent staining was carried out in black-walled 96-well plates. Cells were washed in PBS and fixed with 4% formaldehyde in PBS for 30 min at room temperature. The cells were then washed with PBS and incubated another 30 min with LipidTOX (H34477, Invitrogen; 1:5000 dilution) and Hoechst 33342 (sc-495790, Santa Cruz; 1:10000 dilution). Cells were washed in PBS, and confocal imaging was performed using a Zeiss LSM 880 AxioObserver. Images were taken in random regions of each well to avoid selection bias. Image analysis was performed to determine nucleus and lipid droplet number as well as lipid droplet diameter using Imaris 9.9.0 (Oxford Instruments). For quantification, batch analysis of images was carried out in a blinded and automated manner. In addition, LipidTOX and Hoechst were quantified in the plate reader by measuring fluorescence at 637/655 nm and 350/461 nm, respectively. Cell-free wells were subtracted as background.

Transient transfection

Human A41 cells were transiently transfected with pcDNA3.1 or pcDNA3.1 PPARg2 (donated by Karsten Kristiansen, University of Copenhagen, Denmark) at about 80-95% confluence in 6-well plates. For each well, 2 µg plasmid DNA and 6 µL TransIT-X2 (MIR6000, Mirus Bio) were added to 200 µL Opti-MEM (31985070, Gibco). The mixture was incubated for 15-30 min and added to cell culture wells. The cells were incubated at 37 °C for 24 h, and then the medium was replaced with culture medium containing rosiglitazone or solvent. After an additional 24 h incubation, cells were lysed.

For reverse transfection, 200 µL of the mixture with TransIT-X2:DNA complexes were added to the culture wells and incubated for 25 min. Cell suspension was then transferred to the wells. Incubation, treatment, and lysis were performed as described above.

Gene expression analysis

RNA from cultured cells or adipose tissue explants was extracted using RNeasy Kit (Qiagen) and RNeasy Lipid Tissue Mini Kit (Qiagen), respectively. Complementary DNA (cDNA) was synthesized from 1 µg RNA using iScript cDNA Synthesis Kit (1708891, Bio-Rad) for cell lines or from 1 µg, 0.2 µg, or 0.5 µg RNA using qScript cDNA Synthesis Kit (95047, Quantabio) for adipose tissue explants, directly isolated cells, and primary cell cultures, respectively. Quantitative reverse transcription PCR (RT-qPCR) was performed using Brilliant III Ultra-Fast SYBR Green qPCR Master Mix (600882, Agilent) and the CFX384 Real-Time PCR Detection System (Bio-Rad); Fast SYBR Green Master Mix (4385612, Applied Biosystems) and the 7500 Fast Real-Time PCR System (Applied Biosystems); or TaqMan Fast Advanced Master Mix (4444557, Applied Biosystems) and the QuantStudio 7 Flex Real-Time PCR System (Applied Biosystems). Each biological sample was measured in technical triplicates and the $2^{-\Delta\Delta Ct}$ method was used for relative quantification. Primers were purchased from TAG Copenhagen and are shown in Table 3. In addition, TaqMan assays (4331182, Applied Biosystems) were used for mouse *Cyp19a1* (Assay ID: Mm00484049_m1) and *Rps18* (Assay ID: Mm02601777_g1). The criteria for exclusion of outliers in the technical replicates was a standard deviation above 0.3 and a two-fold difference in the distance to the median.

Gene	**Species**	**Sequence** (forward)	**Sequence** (reverse)
RPL32	Human	CAGGGTTCGTAGAAGATTCAAGGG	CTTGGAGGAAACATTGTGAGCGATC
CYP19A1	Human	TTGACCCTTCTGCGTCGTGT	AGGAGAGCTTGCCATGCATCA
PPARG	Human	AGAAAGCGATTCCTTCACTGAT	AGAATGGCATCTCTGTGTCAAC
ADIPOQ	Human	GCAGTCTGTGGTTCTGATTCC	CATGACCGGGCAGAGCTAAT
FASN	Human	TACAACATCGACACCAGCTC	CGTCTTCCACACTATGCTCA
Rn18s	Mouse	AGTCCCTGCCCTTTGTACACA	GATCCGAGGGCCTCACTAAAC
Pparg	Mouse	GCATGGTGCCTTCGCTGA	TGGCATCTCTGTGTCAACCATG
Adipoq	Mouse	GATGGCACTCCTGGAGAGAA	TCTCCAGGCTCTCCTTTCCT
Fabp4	Mouse	CTGGGCGTGGAATTCGAT	GCTCTTCACCTTCCTGTCGTCT
Slc2a4	Mouse	GTGACTGGAACACTGGTCCTA	CCAGCCACGTTGCATTGTAG

Table 3: Primers used for RT-qPCR.

Protein immunoblotting

Cells were washed with PBS and lysed using RIPA buffer (89900, Thermo Scientific) containing protease inhibitors (S8820, Sigma-Aldrich). The lysates from wells of similarly treated cells were pooled. Lysates were then centrifuged for 10 min at 4 °C and 16,100 × g, supernatant was collected, and protein concentrations were determined using bicinchoninic acid assay. Samples were diluted in lysis buffer to obtain equal protein concentrations. Afterwards, Laemmli sample buffer was added, and samples were heated at 95 °C for 5 min. Proteins were separated by SDS-PAGE and transferred onto a PVDF membrane. Immunostaining was performed using PPARγ (sc-7273, Santa Cruz) and vinculin (13901, Cell Signaling) primary antibodies and HRP-conjugated secondary antibodies (1706515 and 1706516, Bio-Rad). Chemiluminescent imaging was performed using the ChemiDoc XRS+ System (Bio-Rad).

Hormone analysis

Steroid hormone levels were analyzed by LC-MS/MS as previously described.[20] Deuterated internal standards were added to the cell culture supernatants, which were then centrifuged at 15,000 g for 10 min. Steroid hormones were separated, detected, and quantified by online SPE-LC-MS/MS using a Waters Oasis HLB column (186002035, UVISON Technologies; 2.1 x 20 mm, 15 µm) for online SPE. For 17β-estradiol and estrone analysis, a Kinetex C18 column (00D-4462-AN, Phenomenex; 2.1 x 100 mm, 2.6 µm) was used with an injection volume of 100 mL, measuring with negative electrospray ionization (ESI) and using methanol and 0.2 mM ammoniumfluoride in water as the mobile phases (gradient flow rate was 0.4 mL/min). For the other hormones, an Ascentis Express C8 column (SU-53832-U, Supelco; 2.1 x 100 mm, 2.7 µm) was used with an injection volume of 100 mL, measuring with negative and positive ESI with acetonitrile and 0.1% formic acid in water as the mobile phases (gradient flow rate was 0.25 mL/min). The following steroid hormones were measured: androstenedione, corticosterone, cortisol, dehydroepiandrosterone (DHEA), 11-deoxycortisol, dihydrotestosterone (DHT), epitestosterone, 17β-estradiol, estrone, 18-hydroxycortisol, 17α-hydroxyprogesterone, pregnenolone, progesterone, and testosterone. The limit of quantification (LOQ) was 1.0 ng/mL for pregnenolone; 0.25 ng/mL for 11-deoxycortisol; 0.1 ng/mL for cortisol, DHEA, and DHT; 0.05 ng/mL for epitestosterone and hydroxyprogesterone; 0.02 ng/mL for androstenedione, corticosterone, 17β-estradiol, and testosterone; and 0.01 ng/mL for estrone, 18-hydroxycortisol, and progesterone. For quantification, external calibration standards were run before and after the samples at levels of 0.05, 0.1, 0.2, 0.5, 1.0, 2.0, 10.0 and 20 ng/mL, with 4.0 ng/mL internal standards (testosterone-d2, methyltestosterone-d3, progesterone-c2 and estradiol-d3 from EURL Wageningen and cortisol-d4 and deoxycortisol-d8 from LGC Standards). For cortisol, deoxycortisol, estradiol, progesterone, and testosterone, dedicated internal standards were used. Furthermore, cortisol-d4 was used for hydroxyprogesterone; deoxycortisol-d8 was used for corticosterone; progesterone-c2 was used for pregnenolone; and estradiol-d3 was used for estrone. The limit of detection (LOD) and LOQ were estimated as the concentrations corresponding to three and ten times the signal-to-noise, respectively. The mass spectrometer was an EVOQ ELITE Triple Quadrupole instrument from Bruker (Bremen, Germany) and the UHPLC system was an UltiMate 3000 System with a DGP-3600RS dual-gradient pump. Data handling was done using the software MS Workstation version 8.2.1.

Protein production

Human PPARγ2 cDNA (residues 231 to 505, corresponding to the PPARγ LBD) was cloned into a modified pET24a vector, encoding it with an N-terminal hexahistidine- and SUMO-tag (H_6-SUMO). The protein was produced in *E. coli* BL21(-DE3) cells (New England BioLabs, Frankfurt, Germany) in auto-induction minimal medium,[21] using $^{15}NH_4Cl$ as a nitrogen source for isotope labeling. Production was induced at OD_{600} of 0.8 by changing the temperature from 37 °C to 18 °C and allowing to proceed for 24 h. Cells were harvested by centrifugation at 5.000 × g for 20 min and resuspended in lysis buffer (20 mM imidazole, 50 mM Tris pH 8, 200 mM NaCl, 10% (v/v) glycerol). All buffers contained 5 mM β-mercaptoethanol. Cells were lysed using a cell disrupter (Constant Systems Ltd., Daventry, UK) at 25 kpsi and the lysate was cleared by centrifugation at 20.000 × g for 45 min. The supernatant was passed two times over 5 mL Ni-NTA resin (Qiagen, Hilden, Germany), pre-equilibrated with lysis buffer. Three wash steps were done first with lysis buffer, then with lysis buffer containing 1 M NaCl and then with lysis buffer again, and the bound proteins finally eluted with elution buffer (lysis buffer with 500 mM imidazole). The protein was cleaved in 40 mM Tris, pH 8, 10% (w/v) glycerol, 200 mM NaCl and 5 mM β-mercaptoethanol overnight at 4 °C with ULP1-protease (in-house production, produced and purified as described in Reverter and Lima 2009).[22] The His_6-SUMO tag and ULP1 were removed by reverse Ni-NTA purification. The protein was further purified by ion exchange chromatography using a HiTrap QFF 5 mL column (Cytiva) and size exclusion chromatography using a Superdex 200 Increase 10/300 GL (Sigma-Aldrich). Ion exchange buffers were 25 mM bis-Tris pH 7.4, with the elution buffer containing additionally 1 M NaCl. The size exclusion buffer contained 40 mM Tris pH 8 and 500 mM NaCl.

Nuclear magnetic resonance (NMR) spectroscopy

NMR samples containing 80 µM ^{15}N PPARγ LBD were changed into PBS buffer (pH 7.3, 137 mM NaCl, 10% D_2O, room temperature), and 0.7 mM 4,4-dimethyl-4-silapentane-1-sulfonic acid (DSS) was added as reference.

Rosiglitazone, GW9662, and DEHPA were added at concentrations of 320 µM, 240 µM, and 1 mM, respectively. All NMR spectra were acquired at 298 K on a Bruker AVANCE III 750-MHz (^{1}H) spectrometer equipped with a cryogenic probe. Free induction decays were transformed and visualized in TopSpin (Bruker BioSpin), and subsequently analyzed using the CcpNmr Analysis software.[23] Proton chemical shifts were internally referenced to DSS at 0.00 ppm, with heteronuclei referenced by relative gyromagnetic ratios. Assignments of PPARγ LBD were exported from BMRB entry 17975, as published by Hughes et al. 2012, and transferred to the spectra without ambiquities.[24] For each spectrum, intensities were normalized to the NMR peak of E235, which was the most intense peak in every condition.

DNA sequence analysis

Cells were washed in PBS and DNA isolation was performed using QIAamp DNA Mini Kit (51304, Qiagen). A *PPARG* sequence containing the position of the rs1801282 SNP was amplified in a C1000 Touch Thermal Cycler (Bio-Rad) using Q5 Hot Start High-Fidelity 2X Master Mix (M0494S, New England Biolabs), forward primer (5'-GCCAATTCAAGCCCAGTCCT3'-) and reverse primer (5'-TTACATAAATGCCCCCACGTCC-3'). The PCR products were run on an agarose gel to confirm that the amplicon size was correct. The QIAquick PCR Purification Kit (28104, Qiagen) was applied for isolation of the PCR products. The samples were sent to GENEWIZ (Azenta Life Sciences) for Sanger sequencing using the primers for PCR.

Statistical analysis

Statistical significance was tested using the two-tailed (unpaired) Student's t-test, Dunnett's multiple comparison test, or one- or two-way analysis of variance (ANOVA), depending on the number of samples and variables. When there were more than two levels within a variable of the two-way ANOVA, Dunnett's test for multiple comparisons was applied for the levels of that variable. Dunnett's test was also performed following one-way ANOVA. When all values in a group were below the detection limit, a two sample Z test for proportions followed by Bonferroni correction for multiple comparisons was performed to compare the number of quantifiable values, including all technical replicates, in each group. For calculation of half-maximal inhibitory concentrations (IC_{50}), concentration-response curves were fitted using the four-parameter logistic regression model with slope constraints of -1.5 to 0 and with starting response set to 1. Logistic regression could not be performed when there was a non-monotonic relationship between response and concentration. Data was normalized to the sum of values within each experiment, and the control group was set to 1. Differences between groups were considered significant if $p \leq 0.05$, and data were presented as means and standard errors of the mean (SEM).

Results

Environmental PPARγ antagonists, previously identified by the Tox21 Program and verified in an orthogonal HEK293 cell-based reporter assay (Ardenkjær-Skinnerup et al, submitted), were used in the present study to investigate PPARγ-mediated effects on the transcription of aromatase in ASCs, adipocytes, and adipose tissue explants.

Effect of putative PPARγ antagonists on adipogenesis

Human ASCs were differentiated in the presence of seven different PPARγ antagonists, including the PPARγ antagonist GW9662 that served as a positive control for inhibition of adipogenesis. Lipid staining with Oil Red O revealed that all seven chemicals inhibited lipid accumulation in the studied concentration ranges (Figure 1). The IC_{50} and maximal inhibition for each chemical are shown in Table 4. The inhibitory effect of GW9662, zoxamide, Cosan 528, and DEHPA was greater when cells were differentiated using the lower concentration of rosiglitazone (0.1 µM) compared with the higher concentration (2 µM).

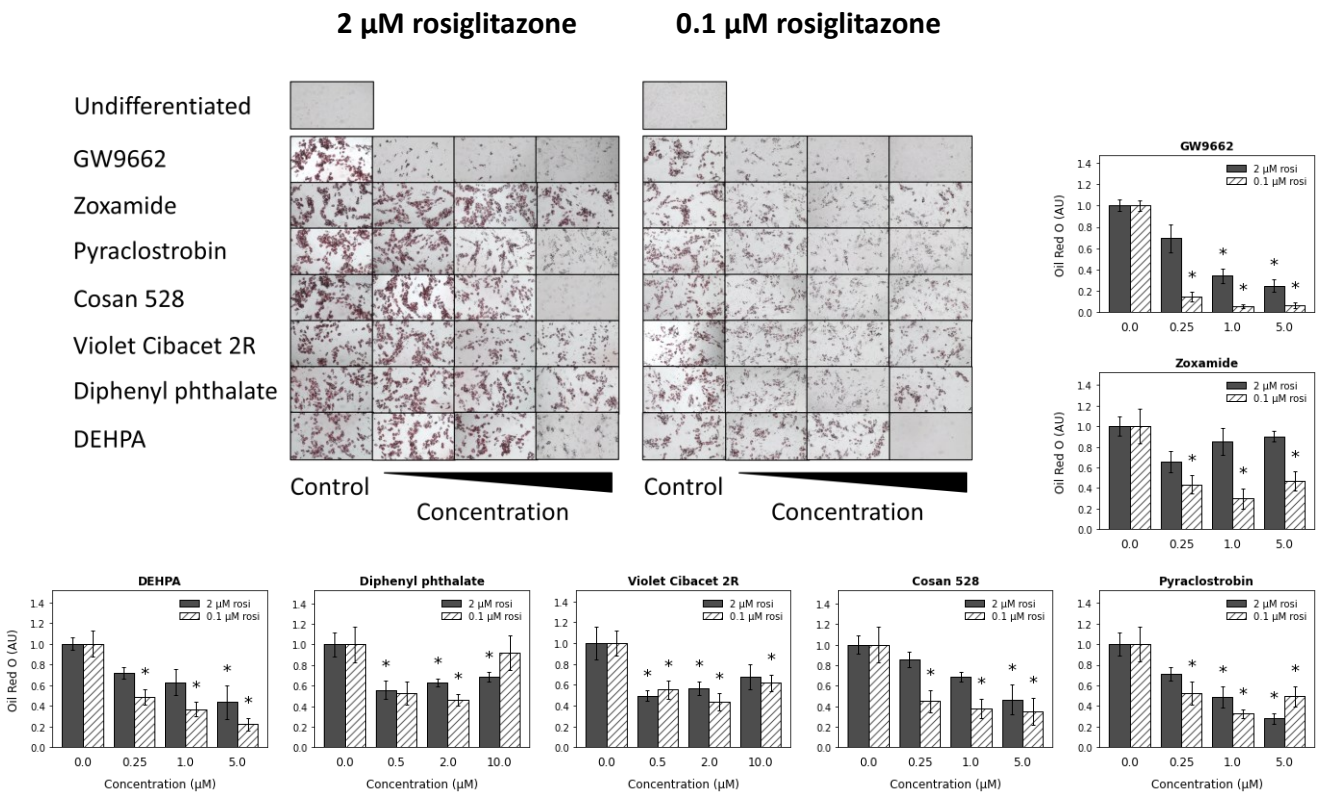

Figure 1. **Lipid accumulation in human ASCs exposed to putative PPARγ antagonists during adipogenesis**. Differentiation of human ASCs was induced with either high (2 µM) or low (0.1 µM) concentrations of rosiglitazone in the adipogenic medium. During differentiation, cells were treated with different environmental chemicals previously found to be PPARγ antagonists at concentrations of 0.25 to 5 µM or 0.5 to 10 µM. Lipids were stained with Oil Red O at day 12 of differentiation. Microscopy pictures show lipid accumulation in undifferentiated control cells and in differentiated cells treated with different concentrations of putative PPARγ antagonists or solvent control (0 to 0.01% DMSO). Lipid staining was quantified and presented in graphs showing means ± SEM (n = 4-6). Asterisks (*) indicate statistically significant differences compared to control cells using Dunnett's test ($p < 0.05$).

	IC_{50} (µM)		I_{max}	
Rosiglitazone	**2**	**0.1**	**2**	**0.1**
GW9662	0.49	0.06	75%	94%
Zoxamide	-	0.15	34%	70%
Pyraclostrobin	0.93	0.27	72%	67%
Cosan 528	3.77	0.14	53%	65%
Violet Cibacet 2R	-	-	50%	56%
Diphenyl phthalate	-	-	44%	54%
DEHPA	2.90	0.23	56%	78%

Table 4: Absolute half-maximal inhibitory concentration (IC_{50}) and maximal relative inhibition at any concentration (I_{max}) are shown for lipid accumulation by Oil Red O for each chemical.

Confocal microscopy was performed to analyze differences in lipid droplet number and size in response to PPARγ antagonist treatment during differentiation (2 µM rosiglitazone) of primary ASCs (Figure 2A). Lipids and nuclei were stained with LipidTOX and Hoechst, respectively. Image analysis showed that treatment with GW9662, pyraclostrobin, Cosan 528, and DEHPA decreased the average number of lipid droplets per cell significantly (Figure 2B), and pyraclostrobin treatment also reduced lipid droplet size (Figure 2C). There was considerable variation between cells from the different study participants (Figure 2B-2C). Fluorescence intensities of LipidTOX and Hoechst were measured in a plate reader, and the LipidTOX/Hoechst ratios were determined (Figure 2D). Lipid accumulation normalized to cell number was decreased by treatment with all tested PPARγ antagonists.

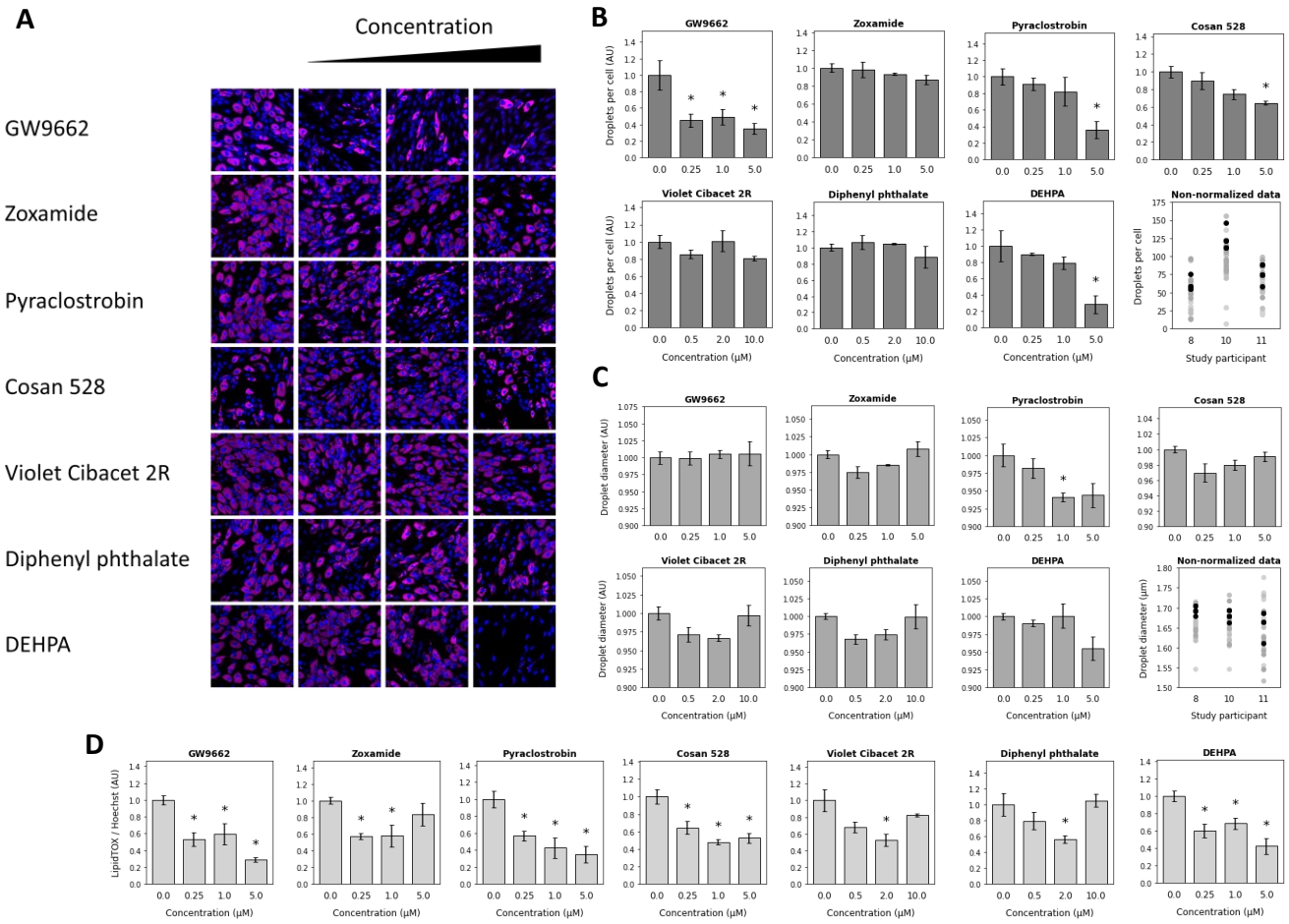

Figure 2. **Lipid droplet size and number in human ASCs exposed to putative PPARγ antagonists during adipogenesis**. Differentiation of human ASCs was induced with adipogenic medium containing 2 µM rosiglitazone. During differentiation, cells were treated with previously identified PPARγ antagonists or solvent control (0 to 0.01% DMSO). At day 12 of differentiation, lipids and nuclei were stained with LipidTOX and Hoechst, respectively. (**A**) Confocal microscopy pictures show lipids in pink and nuclei in blue. (**B**) Average lipid droplets per cell and (**C**) average lipid droplet diameter quantified by image analysis. Non-normalized data for all chemicals are shown for each study participant in **B** and **C**, where black is vehicle control and lighter shades of gray are higher concentrations of chemical. (**D**) Quantification of fluorescent stains using a plate reader and presented as LipidTOX normalized to Hoechst. Data are shown in graphs as means ± SEM (*n* = 3). Asterisks (*) indicate statistically significant differences compared to control cells using Dunnett's test ($p < 0.05$).

Aromatase expression during adipogenesis

To determine the influence of differentiation stage on aromatase expression, aromatase mRNA abundance was measured in ASCs and mature adipocytes. The adipocyte markers, *PPARG* and *FASN*, were used to confirm difference in cell types. Isolated human ASCs expressed higher levels of aromatase and lower levels of the adipocyte markers compared to mature adipocytes (Figure 3A). Similarly, cultured undifferentiated A41 cells expressed higher level of aromatase and lower level of *PPARG* than fully differentiated A41 cells (Figure 3B).

The effect of interruption of adipogenesis on aromatase expression was examined in A41 cells by removal of the adipogenic medium. On day 6 of differentiation, the adipogenic medium was renewed or changed to basal culture medium for 2 days. Removal of the adipogenic medium resulted in a 9-fold increase in aromatase, and a corresponding decrease in *PPARG* expression (Figure 3C). When A41 cells were differentiated for either 6 or 12 days in the presence of the PPARγ antagonist GW9662, expression of aromatase increased, and expression of the adipocyte markers, *PPARG*, *ADIPOQ*, and *FASN*, decreased, compared to the solvent control (Figure 3D-3E).

Exposure of human ASCs to PPARγ antagonists GW9662, pyraclostrobin, or Cosan 528 during 12 days of differentiation increased aromatase expression by 1.6- to 4.0-fold, while aromatase was slightly downregulated by zoxamide exposure (Figure 3F). The antagonist-stimulated increase in aromatase mRNA

was associated with decreased lipid accumulation (Figure 3G), however there was no clear correlation between the extent of adipogenesis inhibition and the aromatase mRNA level.

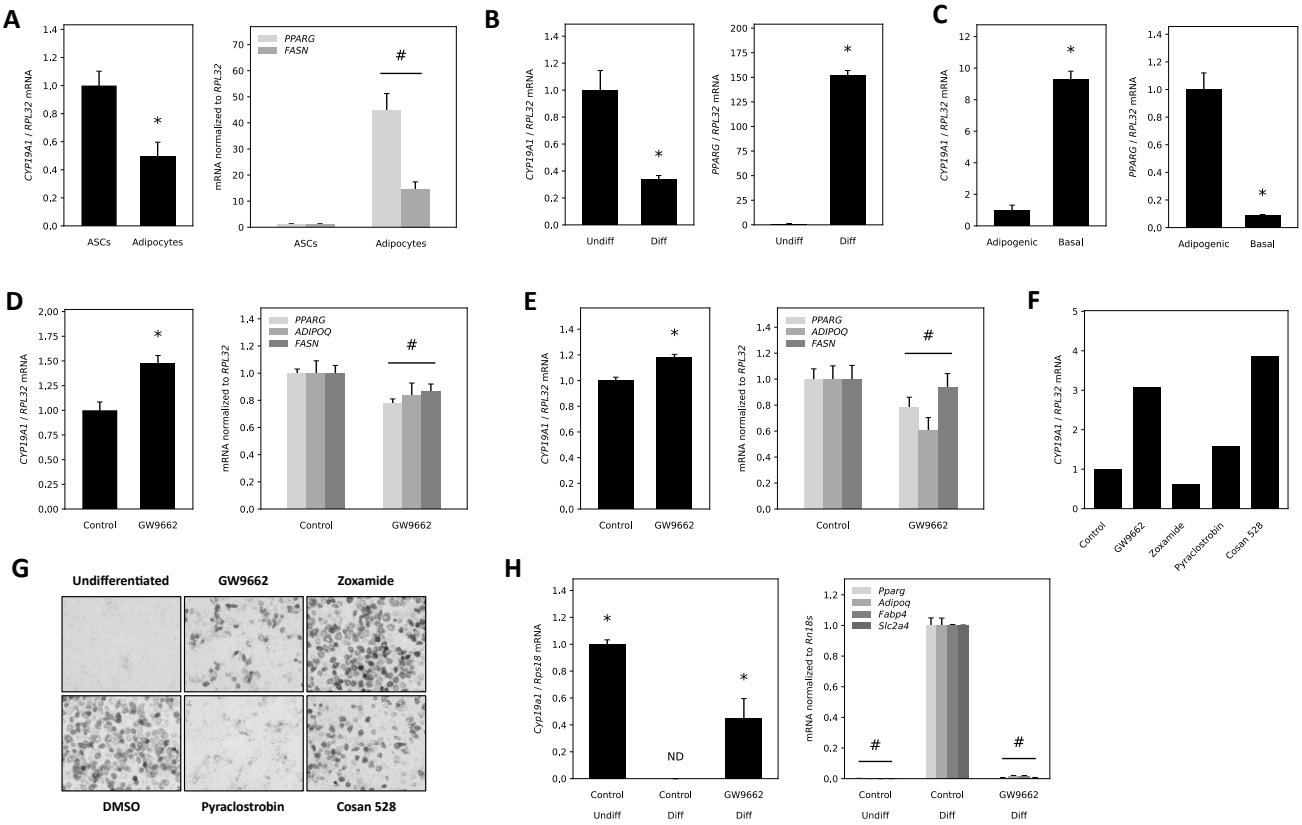

Figure 3. **Level of aromatase and adipocyte marker mRNA in response to inhibition of adipogenesis by PPARγ antagonists**. Gene expression analysis of aromatase (*CYP19A1*) and adipocyte markers (*PPARG*, *ADIPOQ*, *FASN*) by RT-qPCR. (**A**) Humans ASCs and adipocytes were directly isolated from human adipose tissue (n = 7). (**B**) A41 pre-adipocytes were undifferentiated or differentiated for 12 days (n = 8-10). (**C**) A41 cells at day 6 of differentiation were either returned to basal medium or kept in adipogenic medium for 2 days (n = 4). (**D**) A41 cells at day 6 (n = 3-4) or (**E**) at day 12 (n = 4) of differentiation were treated with 5 µM or 1 µM GW9662, respectively, during differentiation, and compared with a solvent control group (0.01% DMSO). (**F**) Primary human ASCs were differentiated for 12 days (with 2 µM rosiglitazone) in the presence or absence of 5 µM PPARγ antagonist (n = 1). (**G**) Bright-field microscopy pictures taken before lysis show clearly visible lipid droplets which indicate the level of adipogenesis. (**H**) Mouse C3H10T1/2 cells were differentiated for 6 days in the presence or absence of 10 µM GW9662 or left undifferentiated. Gene expression analysis by RT-qPCR was performed for aromatase (*Cyp19a1*) using TaqMan assay and adipocyte markers (*Pparg*, *Adipoq*, *Fabp4*, and *Slc2a4*) using SYBR Green assay (n = 3). The graphs present means ± SEM. Asterisk (*) and hash (#) indicate statistically significant differences compared to control cells using t test or two-way ANOVA, respectively ($p < 0.05$). For C3H10T1/2 cells, asterisk indicates statistically significant difference compared to differentiated control cells using two sample proportion test with Bonferroni correction ($p < 0.05$). ND: not detected.

The effect of PPARγ inhibition on aromatase mRNA expression in mouse cells was also examined (Figure 3H). Aromatase was very weakly expressed in mouse adipose tissue, and TaqMan assay was therefore applied to avoid nonspecific amplification. In C3H10T1/2 cells differentiated for 6 days, aromatase transcripts were not detected, while in undifferentiated cells and cells exposed to GW9662 during differentiation there were detectable aromatase transcript levels. The adipocyte markers, *Pparg*, *Adipoq*, *Fabp4*, and *Slc2a4*, were strongly upregulated in response to 6 days of differentiation, an effect that was absent in response to GW9662 treatment during differentiation.

Direct interaction between PPARγ and ligands

NMR spectroscopy was used to address any direct interaction of PPARγ with ligands tested in this study. First, multiple controls were established by recording ^{15}N-HSQCs of the ^{15}N-labeled PPARγ LBD bound to known agonist rosiglitazone and known antagonist GW9662, as well as monitoring the effect of DMSO presence, the solvent of the small molecule ligands (Figure 4A-4C). These spectra were used as comparison controls for the activity state of PPARγ LBD in the presence of DEHPA (Figure 4A-4E). It was observed that the apo-state and the GW9662-bound state of the PPARγ LBD only featured 109 annotatable peaks in the NMR spectra

corresponding to only roughly ~40% of the residues of the protein (Figure 4F). The rosiglitazone-bound PPARγ LBD featured 208 peaks that all could be assigned to the sequence, corresponding to ~75% of the residues in the LBD (an 88% increase compared to solvent control). These additional peaks were mainly found lining the binding pocket of the LBD as well as in helix 12 (Figure 4G). The spectrum of rosiglitazone-bound PPARγ LBD in the presence of DEHPA featured only ~132 peaks assignable (~47% of all LBD-residues) and was similar to the GW9662-bound state and the free state (Figure 4F). The NMR peak intensity profiles of the different spectra, plotted as a function of sequence, are shown in Figure 3B-3E. GW9662-bound, inactive PPARγ LBD, had a similar profile as free PPARγ LBD (Figure 4B). Also, rosiglitazone-bound PPARγ LBD to which GW9662 or DEHPA was added, showed a nearly identical profile to the GW9662-bound PPARγ LBD (Figure 4D-4E). Thus, adding DEPHA to the agonist-bound PPARγ LBD reversed the protein to the inactive state by direct interaction, outcompeting the effect of rosiglitazone.

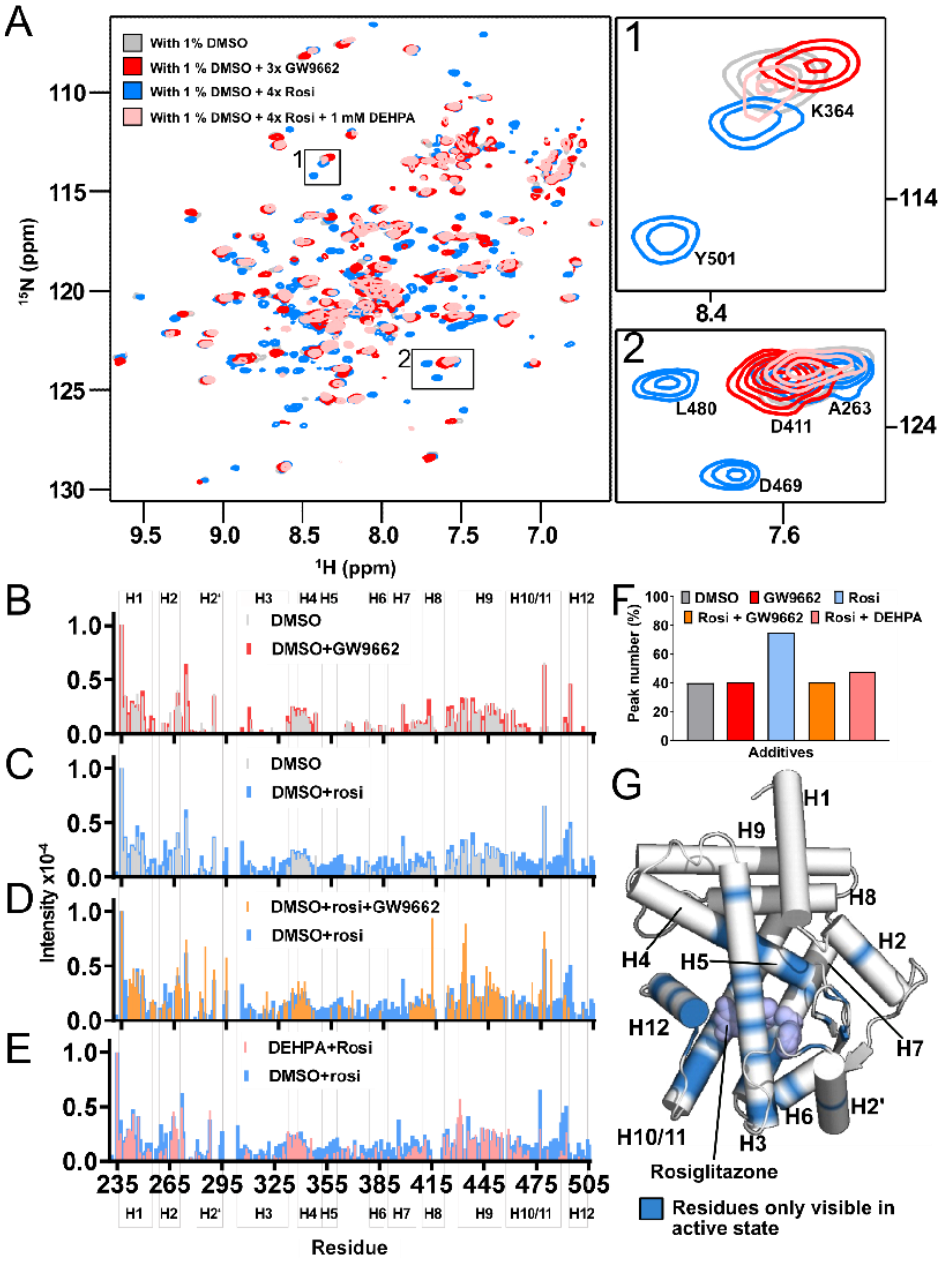

Figure 4. **Direct interaction between DEHPA and PPARγ**. (**A**) ^{15}N-HSQCs of the PPARγ LBD with added chemical compounds. (**B**) Peak intensity profile of the rosiglitazone-bound PPARγ LBD compared to free PPARγ LBD in solvent (1% DMSO). (**C**) Peak intensity profile of the GW9662-bound PPARγ LBD compared to free PPARγ LBD in solvent (1% DMSO). (**D**) Peak intensity profile of the rosiglitazone-bound PPARγ LBD compared to rosiglitazone-bound PPARγ LBD after GW9662 addition. (**E**) Peak intensity profile of the rosiglitazone-bound PPARγ LBD compared to rosiglitazone-bound PPARγ LBD after DEHPA addition. (**F**) Percentage of peaks visible and assignable depending on additives. (**G**) Cartoon representation of the crystal structure of PPARγ LBD bound to rosiglitazone (PDB: 1FM6). Rosiglitazone is shown as spheres in the binding pocket. Residues that are visible in the ^{15}N-HSQCs when only rosiglitazone is bound are shown in blue.

Short-term regulation of aromatase by PPARγ

A more acute effect of PPARγ on aromatase expression was studied by treatment of undifferentiated (Figure 5A) or differentiated (Figure 5B) A41 cells with PPARγ ligands for 24 h. Stimulation of cells with rosiglitazone reduced aromatase expression in both undifferentiated and differentiated cells. Treatment with the PPARγ antagonists, GW9662, diphenyl phthalate, pyraclostrobin, DEHPA, or kresoxim-methyl, had no effect on aromatase expression in undifferentiated A41 cells (Figure 5A). However, in mature adipocytes, treatment with every antagonist increased aromatase mRNA, except for diphenyl phthalate, which had no effect (Figure 5B). The effects were not as strong as that of forskolin (FSK) and phorbol 12-myristate 13-acetate (PMA) co-treatment, which was used as a positive control for aromatase induction and which appeared to downregulate *PPARG* and the PPARγ target genes, *ADIPOQ* and *FASN* (Figure 5C). Since PPARγ forms obligate heterodimers with retinoid X receptors (RXRs), it was studied if the RXR agonist 9-*cis*-retinoic acid (9cRA) affected aromatase expression like rosiglitazone. Treatment of A41 cells with 9cRA caused a decrease in aromatase expression in undifferentiated cells (Figure 5D) but had no effect on aromatase in mature A41 adipocytes (Figure 5E).

It was tested if the PPARγ ligands rosiglitazone and GW9662 also influenced aromatase expression in human breast adipose tissue explants (Figure 5F). Aromatase expression was significantly reduced in response to 48 h exposure to rosiglitazone, whereas there was a tendency (p = 0.076) to increased aromatase expression in response to GW9662.

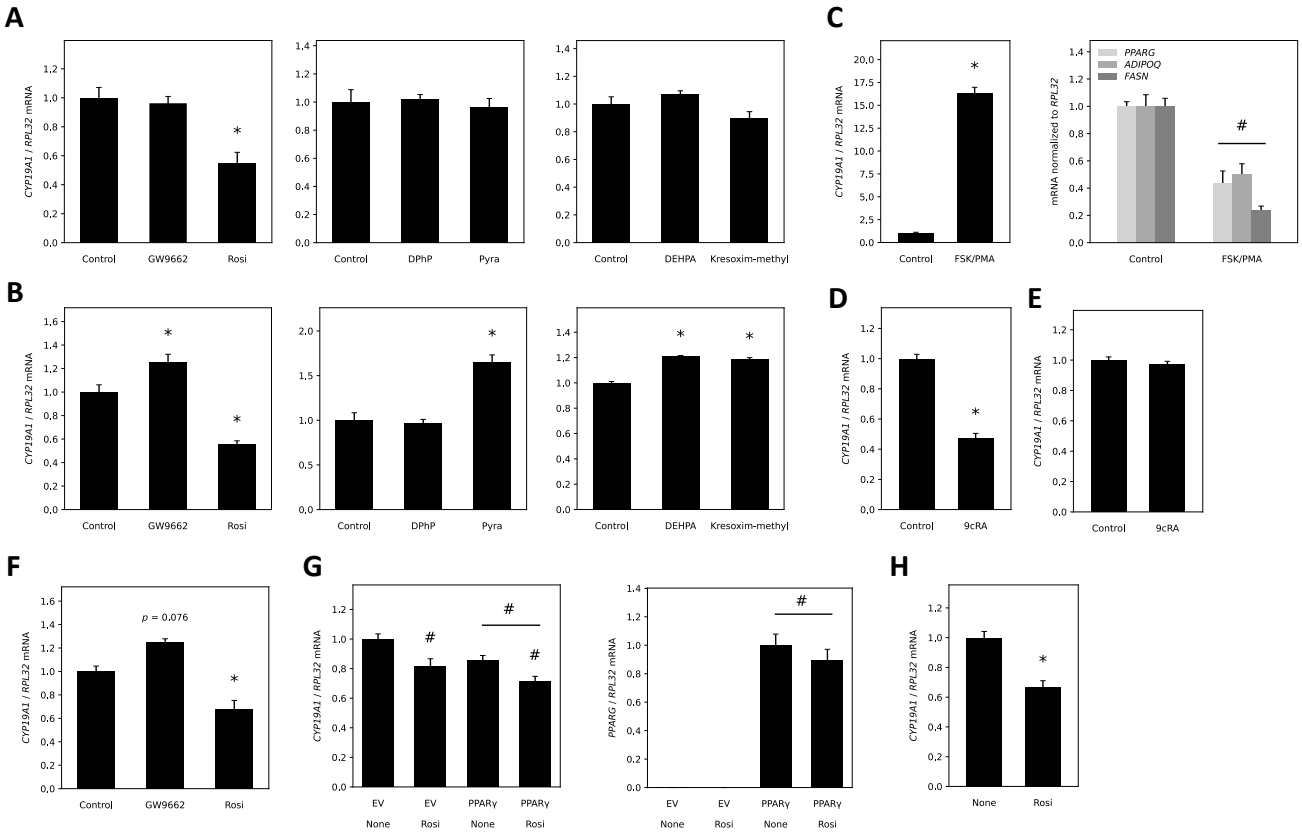

Figure 5. **Aromatase mRNA level in response to chemical exposure or PPARγ2 overexpression**. Gene expression analysis of aromatase (*CYP19A1*) and adipocyte markers (*PPARG*, *ADIPOQ*, *FASN*) by RT-qPCR. (**A**) Undifferentiated (n = 3) or (**B**) differentiated (n = 3-5) A41 cells were treated for 24 h with 5 µM of rosiglitazone, GW9662, diphenyl phthalate (DPhP), pyraclostrobin, or DEHPA, or with 10 µM kresoxim-methyl. (**C**) Differentiated A41 cells were treated for 24 h with 2.5 µM forskolin (FSK) and 4 nM PMA (n = 3-5). (**D**) Undifferentiated or (**E**) differentiated A41 cells were treated with 1 µM of 9-*cis*-retinoic acid (9cRA) for 24 h (n = 3). (**F**) Breast adipose tissue explants were treated with 5 µM GW9662 or rosiglitazone for 48 h (n = 2). (**G**) Undifferentiated A41 cells were transiently transfected with pcDNA3.1 empty vector (EV) or pcDNA3.1 *PPARG2* vector, and were treated with 5 µM rosiglitazone or solvent (0.02% DMSO) for 24 h (n = 3). (**H**) Differentiated A41 adipocytes were reverse transfected with pcDNA3.1 *PPARG2* and treated for 24 h with 5 µM rosiglitazone or solvent (n = 3). The graphs present means ± SEM. Asterisk (*) indicates statistically significant difference compared to control group using t test, Dunnett's test, or two-way ANOVA (p < 0.05). Hash (#) indicates statistically significant differences compared to control groups (solvent controls or EV controls) using two-way ANOVA (p < 0.05).

To explore how the PPARγ protein level affects aromatase expression, *PPARG* was overexpressed in undifferentiated A41 cells in combination with rosiglitazone or solvent treatment (Figure 5G). Overexpression of *PPARG* or treatment with rosiglitazone reduced aromatase expression and had an additive effect in combination. In mature adipocytes overexpressing *PPARG*, rosiglitazone decreased aromatase expression (Figure 5H) to a similar extent as in non-transfected mature A41 adipocytes (Figure 5B).

The human H295R adrenocarcinoma cell line was used to measure estrogen levels in response to PPARγ antagonist treatment (Figure 6A). FSK and prochloraz were used as controls for increased and decreased estrogen levels, respectively. Rosiglitazone and GW9662 were used as controls for PPARγ-mediated effects. The PPARγ control ligands had no effects on steroidogenesis, which also was the case for the PPARγ antagonists in general, except for pyridaben and pyraclostrobin, both of which decreased the levels of many steroid hormones, including estrone. In addition, diphenyl phthalate slightly increased the levels of some steroids. To evaluate aromatase activity, the ratios of estrogens to their androgen substrates were calculated, but this did not reveal any effects of PPARγ ligands (Figure 6B). The PPARγ protein level in the H295R cells was measured by immunoblotting, which clearly showed lower levels in the H295R cells compared to differentiated A41 cells (Figure 6C).

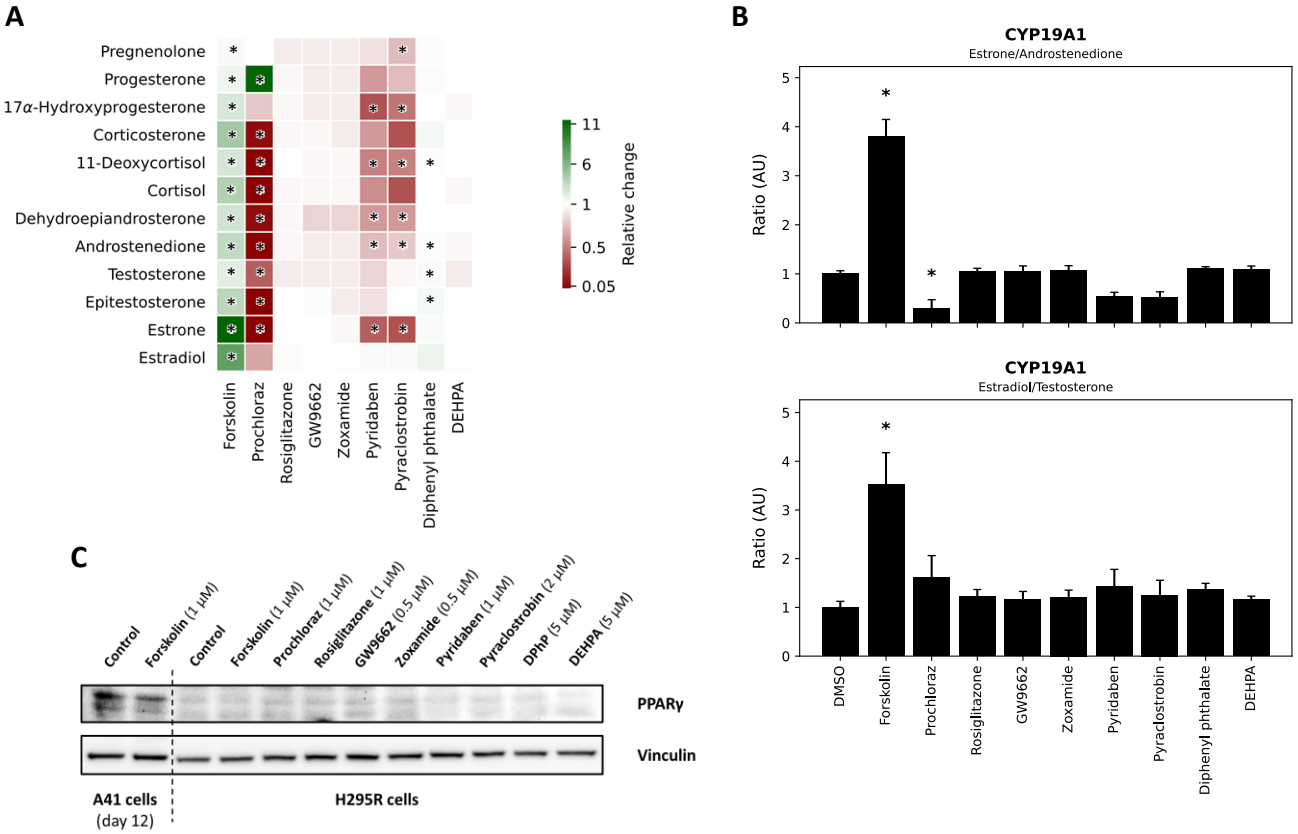

Figure 6. **Steroid hormone levels in response to PPARγ agonist or antagonist exposure**. Hormone levels for a subset of steroids were measured in the culture medium of H295R cells using LC-MS/MS in response to treatment with 0.5 µM of GW9662 or zoxamide; 1 µM of forskolin, prochloraz, rosiglitazone, or pyridaben; 2 µM of pyraclostrobin; 5 µM of diphenyl phthalate or DEHPA; or solvent (0.005% DMSO) for 48 h. (**A**) A heatmap shows the chemical-induced changes in the concentration of hormones secreted by H295R cells (n = 3). (**B**) Ratios of estrogens to androgens are shown in bar plots. (**C**) Immunoblots show PPARγ protein levels in H295R cells compared to differentiated A41 adipocytes with vinculin as a reference protein. Data are presented as means ± SEM. Asterisk (*) indicates statistically significant difference compared to control cells using Dunnett's test ($p < 0.05$).

Effect of *PPARG* Pro12Ala polymorphism

Due to the potential effect of PPARγ Pro12Ala on the response to chemical treatment, the first coding exon of *PPARG* in the human primary ASCs was genotyped. Two of the study participants were heterozygous for the SNP (Figure 7). However, cells from those persons did not appear to respond differently to treatments.

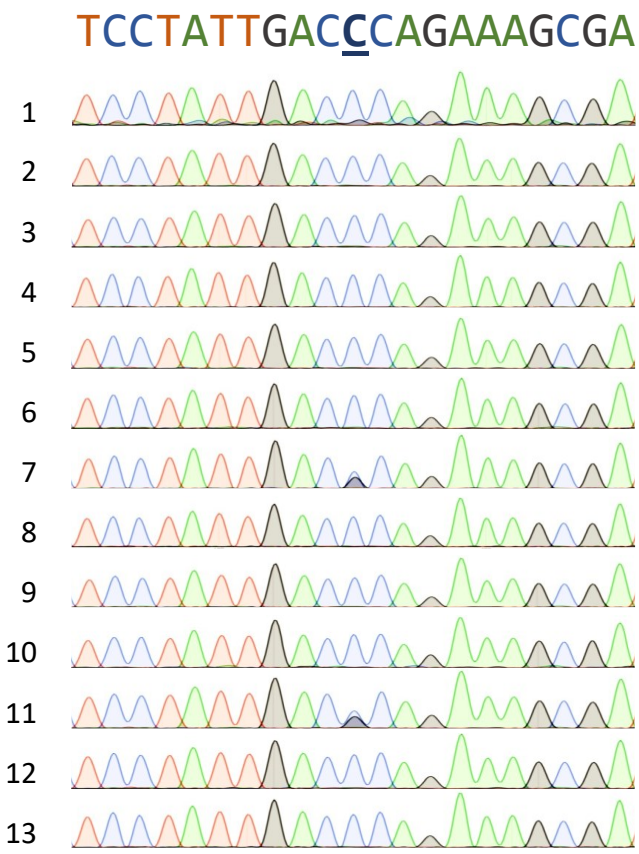

Figure 7. **Sequencing of the *PPARG* gene in cells collected from human adipose tissue**. The DNA sequencing chromatogram for nucleotides 24-44 of *PPARG2* is shown for each study participant.

Discussion

This study demonstrated that previously identified PPARγ antagonists had an inhibitory effect on human adipocyte differentiation. The impaired adipogenesis resulted in an upregulation of aromatase expression, consistent with aromatase expression being higher in ASCs compared to mature adipocytes. In addition, a more acute negative effect of PPARγ activation on aromatase expression was demonstrated in mature adipocytes and adipose tissue explants.

PPARγ antagonism and adipogenesis

Adipogenesis in primary human ASCs during exposure to different putative PPARγ antagonists was studied to determine if the environmental chemicals would act as antagonists in adipocytes. The non-monotonic concentration-response relationships for some of the PPARγ antagonists indicate that at high concentrations these chemicals likely targeted other pathways related to adipogenesis, abrogating the inhibitory effect on differentiation. Despite this, there was generally a greater inhibitory effect of PPARγ antagonists on adipogenesis at low rosiglitazone concentration (only statistically significant for GW9662, zoxamide, Cosan 528, and DEHPA), indicating competitive binding of antagonists and rosiglitazone to the ligand binding pocket of PPARγ. However, it cannot be excluded that PPARγ-independent mechanisms contributed to adipogenesis inhibition. Interestingly, the data suggest that the mechanisms affecting lipid content may be different across compounds, as some have more pronounced effects on either lipid droplet number or size, while others still have effects on both. Overall, the data support previous results in HEK293 cells showing that these PPARγ antagonists inhibit rosiglitazone-induced activity of human PPARγ (Ardenkjær-Skinnerup et al, submitted).

Higher aromatase expression in undifferentiated cells compared to mature adipocytes was observed in cells directly isolated from adipose tissue as well as in the A41 and C3H10T1/2 cell lines. Consistent with this, aromatase expression was previously reported to be higher in undifferentiated ASCs than in adipocytes.[25,26]

Therefore, blocking adipogenesis by removal of PPARγ-inducing and -activating factors produced a strong elevation in aromatase mRNA. Likewise, inhibition of adipogenesis by PPARγ antagonists led to increased expression of aromatase. PPARγ antagonist treatment of differentiating human primary ASCs revealed increased aromatase mRNA only for the three antagonists that visibly decreased lipid accumulation in microscopy pictures. Zoxamide did not increase aromatase expression and has previously been reported to activate mouse PPARγ in COS-7 cells and induce adipogenesis in 3T3-L1 cells,[27] while having no effect on adipogenesis in human ASCs.[28] The discordance between studies may be explained by the different model systems and protocols for differentiation.

These results suggest that impaired adipogenesis in response to PPARγ antagonists may promote breast carcinogenesis by increasing the ratio of ASCs to adipocytes and thereby increasing the tissue expression of aromatase.

Direct interaction of antagonists with PPARγ LDB

Based on functional similarity to GW9662, DEHPA was selected for analysis by NMR spectroscopy to confirm direct interaction. To explore the interaction with PPARγ, the binding of DEHPA to rosiglitazone-bound PPARγ LBD was compared to the binding of GW9662. NMR studies on the isolated PPARγ LBD have described that activating ligands, such as rosiglitazone, stabilize the LBD in the active state, homogenizing the ensemble of states resulting in more discernable peaks in the NMR spectra.[29] This was also observed here, and especially residues in helix 12 became visible in the rosiglitazone-bound state. Helix 12 is strongly connected to PPARγ activity, where it is solvent exposed in the active state, while buried in the repressive state.[30] In addition, peaks originating from helix 3, helices 5 to 7, and the loops between them, as well as the C-terminal half of helix 10/11, became resolved. All these areas of PPARγ LBD outline the ligand binding pocket and would be affected by helix 12 moving in or out. As the NMR peak intensity profile lacked peaks corresponding to helix 12, and the structural elements forming the binding pocket, the NMR data confirmed direct inactivation of the rosiglitazone-bound PPARγ LBD by DEHPA, as observed for GW9662. The NMR peak profile looked very similar to the ligand-free or GW9662-bound states, which are both repressive states of PPARγ LBD. This underscores the hypothesis that the observed aromatase induction follows a direct repression of PPARγ activity by DEHPA. It would be highly relevant to apply NMR spectroscopy to investigate the interaction between the PPARγ LBD and chemicals that were predicted to be PPARγ antagonists in a recently developed PPARγ antagonism QSAR model (Ardenkjær-Skinnerup et al, submitted).

Short-term regulation of aromatase by PPARγ

In addition to the effect occurring through inhibition of adipogenesis, a short-term effect of PPARγ on aromatase expression was demonstrated. Reduced aromatase expression has been observed in response to thiazolidinediones in human ASCs[6,7] and other human cell types such as ovarian granulosa cells[31] and endometrial stromal cells.[32] In the present study, effect of PPARγ antagonists was adipocyte-specific, supporting the hypothesis that it is mediated by PPARγ, as adipocytes express much higher levels of PPARγ than ASCs. It has been demonstrated that the antagonist GW9662 reverses rosiglitazone-induced aromatase repression in rat granulosa cells,[33] consistent with the present results. Treatment of breast adipose explants with rosiglitazone and GW9662 resembled the effects observed in A41 adipocytes more closely than those in A41 pre-adipocytes, even though the GW9662-stimulated aromatase induction was not statistically significant. This is in accordance with the high expression level of *PPARG* in adipose tissue as well as most of the adipose tissue consisting of fully developed adipocytes.

Since PPARγ is a heterodimeric partner with RXR, the effect of the RXR agonist 9cRA on aromatase expression was expected. Activation of RXR was previously shown to repress aromatase expression or activity, both alone and in combination with PPARγ activation.[31,33–35] In the current study, treatment with 9cRA had a similar effect as rosiglitazone in undifferentiated cells but had no effect in differentiated cells, suggesting involvement of a PPARγ-independent mechanism. The combined treatment of ASCs with FSK and PMA has been shown to induce aromatase expression and activity in human breast ASCs.[7,26] This treatment also resulted in decreased *PPARG* mRNA level, suggesting that FSK/PMA treatment may exert its effect on aromatase partially through

downregulation of *PPARG*. This would also explain the strong repressive effect of troglitazone on FSK/PMA-induced aromatase expression observed previously.[7]

Overexpression of *PPARG2* resulted in reduced aromatase expression, consistent with a study in which *PPARG* overexpression decreased FSH-induced aromatase expression in KGN cells.[36] Surprisingly, there was no synergy between *PPARG2* overexpression and rosiglitazone treatment. This could suggest that the effect of rosiglitazone is independent of PPARγ or, more likely, that the limit of aromatase repression via PPARγ-dependent pathway was reached. This was supported by the observation that rosiglitazone treatment in *PPARG*-overexpressing A41 adipocytes reduced aromatase expression by less than 50%, suggesting that aromatase transcription cannot be further reduced through alteration of the PPARγ level or activity.

The human H295R adrenocarcinoma cell line has been used previously to study effects of PPARγ ligands on steroidogenesis,[37] however this cell model was not suitable for studying PPARγ-mediated effects due to the low expression level of *PPARG*, which most likely explains the lack of response to rosiglitazone and GW9662.

Relevance of the findings to adverse health effects

The influence of the Pro12Ala variant of PPARγ on the response to PPARγ antagonists was difficult to assess because of the low number of study participants carrying the minor allele as well as the large biological variation between cells isolated from different persons. In relation to breast cancer, PPARγ Pro12Ala has been reported to modify the effect of alcohol intake such that only homozygous major allele carriers were at increased risk of breast cancer when drinking alcohol, while variant allele carriers were not at increased risk.[13,14]

Studies of PPARγ antagonists as endocrine and metabolic disruptors may provide new insights into potential health risks presented by various environmental and occupational exposures. Dysregulation of PPARγ signaling is connected to various adverse outcomes such as type 2 diabetes, obesity, and cancer.[38,39] This study associates lowered PPARγ activity with increased aromatase transcription in adipose tissue, and thereby supports that PPARγ antagonists may act as breast carcinogens. In addition, PPARγ antagonists inhibit adipocyte differentiation, an effect that may lead to hypertrophy and ectopic fat deposition, resulting in local inflammation and insulin resistance.

Conclusion

The present study indicates that environmental chemicals acting as PPARγ antagonists, such as DEHPA, may increase breast cancer risk by elevating aromatase expression in the adipose tissue. In addition, the study indicates that this occurs both indirectly via inhibition of adipogenesis and via a more direct, yet to be defined, mechanism.

Acknowledgements

We thank the laboratory technicians at the National Food Institute, Maud Bering Andersen and Dorte Lykkegaard Korsbech, for their work and technical assistance, and Jason A. Spector, Department of Surgery at Weill Cornell Medicine, for facilitating access to reduction mammoplasty tissue. Studies were conducted with the support provided by the Center for Translational Pathology at Weill Cornell Medicine.

This work was supported by FFIKA, Focused Research Effort on Chemicals in the Working Environment, from the Danish Government and by the Novo Nordisk Foundation Center for Basic Metabolic Research, an independent research center at the University of Copenhagen partially funded by an unrestricted donation from the Novo Nordisk Foundation. KAB was supported by the National Cancer Institute of the National Institutes of Health grant 1R01CA215797, the Anne Moore Breast Cancer Research Fund, and the Emilie Lippmann and Janice Jacobs McCarthy Research Scholar Award in Breast Cancer. JAS was supported by Idella Foundation, William Demant Foundation, and Christian and Ottilia Brorson Travel Grant. DS was supported by Studienstiftung des Deutschen Volkes. BBK was supported by the Novo Nordisk Foundation Challenge Center

REPIN (NNF18OC0033926). NMR data were recorded at cOpenNMR, an infrastructure supported by the Novo Nordisk Foundation (NNF18OC0032996).

Author contributions

Jacob Ardenkjær-Skinnerup: Conceptualization, Methodology, Investigation, Formal analysis, Visualization, Writing - Original Draft, Writing - Review & Editing.

Daniel Saar: Methodology, Investigation, Formal analysis, Visualization, Writing - Review & Editing.

Patricia S. S. Petersen: Investigation, Writing - Review & Editing.

Mikael Pedersen: Resources, Methodology, Writing - Review & Editing.

Terje Svingen: Resources, Methodology, Writing - Review & Editing.

Birthe B. Kragelund: Supervision, Resources, Methodology, Writing - Review & Editing.

Niels Hadrup: Conceptualization, Supervision, Writing - Review & Editing.

Gitte Ravn-Haren: Conceptualization, Supervision, Writing - Review & Editing.

Brice Emanuelli: Supervision, Resources, Methodology, Writing - Review & Editing.

Kristy A. Brown: Supervision, Resources, Methodology, Investigation, Writing - Review & Editing.

Ulla B. Vogel: Conceptualization, Supervision, Project administration, Funding acquisition, Writing - Review & Editing.

References

1. Sung H, Ferlay J, Siegel RL, et al. Global Cancer Statistics 2020: GLOBOCAN Estimates of Incidence and Mortality Worldwide for 36 Cancers in 185 Countries. *CA Cancer J Clin*. 2021;71(3):209-249. doi:10.3322/caac.21660

2. Drummond AE, Swain CTV, Brown KA, et al. Linking Physical Activity to Breast Cancer via Sex Steroid Hormones, Part 2: The Effect of Sex Steroid Hormones on Breast Cancer Risk. *Cancer Epidemiol Biomarkers Prev*. 2022;31(1):28-37. doi:10.1158/1055-9965.EPI-21-0438

3. Eve L, Fervers B, Romancer M Le, Etienne-Selloum N. Exposure to endocrine disrupting chemicals and risk of breast cancer. *Int J Mol Sci*. 2020;21(23):1-43. doi:10.3390/ijms21239139

4. du Plessis M, Fourie C, Stone W, Engelbrecht AM. The impact of endocrine disrupting compounds and carcinogens in wastewater: Implications for breast cancer. *Biochimie*. 2023;209:103-115. doi:10.1016/j.biochi.2023.02.006

5. Augimeri G, Giordano C, Gelsomino L, et al. The Role of PPARγ Ligands in Breast Cancer: From Basic Research to Clinical Studies. *Cancers (Basel)*. 2020;12(9):1-28. doi:10.3390/CANCERS12092623

6. Rubin GL, Zhao Y, Kalus AM, Simpson ER. Peroxisome proliferator-activated receptor gamma ligands inhibit estrogen biosynthesis in human breast adipose tissue: possible implications for breast cancer therapy. *Cancer Res*. 2000;60(6):1604-1608.

7. Rubin GL, Duong JH, Clyne CD, et al. Ligands for the peroxisomal proliferator-activated receptor gamma and the retinoid X receptor inhibit aromatase cytochrome P450 (CYP19) expression mediated by promoter II in human breast adipose. *Endocrinology*. 2002;143(8):2863-2871. doi:10.1210/ENDO.143.8.8932

8. Huang R, Xia M, Cho MH, et al. Chemical genomics profiling of environmental chemical modulation of human nuclear receptors. *Environ Health Perspect*. 2011;119(8):1142-1148. doi:10.1289/EHP.1002952

9. Regnier SM, Sargis RM. Adipocytes under assault: Environmental disruption of adipose physiology. *Biochim Biophys Acta Mol Basis Dis*. 2014;1842(3):520-533. doi:10.1016/j.bbadis.2013.05.028

10. Brown KA, Scherer PE. Update on Adipose Tissue and Cancer. *Endocr Rev*. 2023;(May):1-14. doi:10.1210/endrev/bnad015

11. Lefterova MI, Haakonsson AK, Lazar MA, Mandrup S. PPARγ and the global map of adipogenesis and beyond. *Trends in Endocrinology and Metabolism*. 2014;25(6):293-302. doi:10.1016/j.tem.2014.04.001

12. Shi HB, Zhao WS, Luo J, et al. Peroxisome proliferator-activated receptor γ1 and γ2 isoforms alter lipogenic gene networks in goat mammary epithelial cells to different extents. *J Dairy Sci*. 2014;97(9):5437-5447. doi:10.3168/jds.2013-7863

13. Petersen RK, Larsen SB, Jensen DM, et al. PPARgamma-PGC-1alpha activity is determinant of alcohol related breast cancer. *Cancer Lett*. 2012;315(1):59-68. doi:10.1016/j.canlet.2011.10.009

14. Vogel U, Christensen J, Nexø BA, Wallin H, Friis S, Tjønneland A. Peroxisome proliferator-activated receptor-gamma2 Pro12Ala, interaction with alcohol intake and NSAID use, in relation to risk of breast cancer in a prospective study of Danes. *Carcinogenesis*. 2007;28(2):427-434. doi:10.1093/CARCIN/BGL170

15. Wan R, Ding Z, Xia S, Zheng L, Lu J. Effects of pparγ2 pro12ala variant on adipocyte phenotype dependent of dha. *Diabetes, Metabolic Syndrome and Obesity*. 2019;12:2273-2279. doi:10.2147/DMSO.S214526

16. Heikkinen S, Argmann C, Feige JN, et al. The Pro12Ala PPARγ2 Variant Determines Metabolism at the Gene-Environment Interface. *Cell Metab*. 2009;9(1):88-98. doi:10.1016/j.cmet.2008.11.007

17. Rodgers KM, Udesky JO, Rudel RA, Brody JG. Environmental chemicals and breast cancer: An updated review of epidemiological literature informed by biological mechanisms. *Environ Res*. 2018;160(April 2017):152-182. doi:10.1016/j.envres.2017.08.045

18. Rubinstein MM, Brown KA, Iyengar NM. Targeting obesity-related dysfunction in hormonally driven cancers. *Br J Cancer*. 2021;125(4):495-509. doi:10.1038/s41416-021-01393-y

19. Xue R, Lynes MD, Dreyfuss JM, et al. Clonal analyses and gene profiling identify genetic biomarkers of the thermogenic potential of human brown and white preadipocytes. *Nat Med*. 2015;21(7):760-768. doi:10.1038/nm.3881

20. Draskau MK, Boberg J, Taxvig C, et al. In vitro and in vivo endocrine disrupting effects of the azole fungicides triticonazole and flusilazole. *Environmental Pollution*. 2019;255. doi:10.1016/j.envpol.2019.113309

21. Studier FW. Protein production by auto-induction in high density shaking cultures. *Protein Expr Purif*. 2005;41(1):207-234. doi:10.1016/J.PEP.2005.01.016

22. Reverter D, Lima CD. Preparation of SUMO proteases and kinetic analysis using endogenous substrates. *Methods Mol Biol*. 2009;497:225-239. doi:10.1007/978-1-59745-566-4_15

23. Vranken WF, Boucher W, Stevens TJ, et al. The CCPN data model for NMR spectroscopy: development of a software pipeline. *Proteins*. 2005;59(4):687-696. doi:10.1002/PROT.20449

24. Hughes TS, Chalmers MJ, Novick S, et al. Ligand and receptor dynamics contribute to the mechanism of graded PPARγ agonism. *Structure*. 2012;20(1):139-150. doi:10.1016/J.STR.2011.10.018

25. Price TM, O'brien SN. Determination of estrogen receptor messenger ribonucleic acid (mRNA) and cytochrome P450 aromatase mRNA levels in adipocytes and adipose stromal cells by competitive polymerase chain reaction amplification. *Journal of Clinical Endocrinology and Metabolism*. 1993;77(4):1041-1045. doi:10.1210/jcem.77.4.8408452

26. McInnes KJ, Brown KA, Knower KC, Chand AL, Clyne CD, Simpson ER. Characterisation of aromatase expression in the human adipocyte cell line SGBS. *Breast Cancer Res Treat*. 2008;112(3):429-435. doi:10.1007/s10549-007-9883-2

27. Janesick AS, Dimastrogiovanni G, Vanek L, et al. On the Utility of ToxCast™ and ToxPi as Methods for Identifying New Obesogens. *Environ Health Perspect*. 2016;124(8):1214-1226. doi:10.1289/EHP.1510352

28. Foley B, Doheny DL, Black MB, et al. Screening ToxCast prioritized chemicals for PPARG function in a human adipose-derived stem cell model of adipogenesis. *Toxicological Sciences*. 2017;155(1):85-100. doi:10.1093/toxsci/kfw186

29. Johnson BA, Wilson EM, Li Y, Moller DE, Smith RG, Zhou G. Ligand-induced stabilization of PPARgamma monitored by NMR spectroscopy: implications for nuclear receptor activation. *J Mol Biol*. 2000;298(2):187-194. doi:10.1006/JMBI.2000.3636

30. Shang J, Mosure SA, Zheng J, et al. A molecular switch regulating transcriptional repression and activation of PPARγ. *Nature Communications 2020 11:1*. 2020;11(1):1-14. doi:10.1038/s41467-020-14750-x

31. Mu YM, Yanase T, Nishi Y, et al. Insulin sensitizer, troglitazone, directly inhibits aromatase activity in human ovarian granulosa cells. 2000;713:710-713. doi:10.1006/bbrc.2000.2701

32. Chang HJ, Lee JH, Hwang KJ, Kim MR, Yoo JH. Peroxisome proliferator-activated receptor γ agonist suppresses human telomerase reverse transcriptase expression and aromatase activity in eutopic endometrial stromal cells from endometriosis. *Clin Exp Reprod Med*. 2013;40(2):67-75. doi:10.5653/cerm.2013.40.2.67

33. Lovekamp-Swan T, Jetten AM, Davis BJ. Dual activation of PPARα and PPARγ by mono-(2-ethylhexyl) phthalate in rat ovarian granulosa cells. *Mol Cell Endocrinol*. 2003;201(1-2):133-141. doi:10.1016/S0303-7207(02)00423-9

34. Mu YM, Yanase T, Nishi Y, Takayanagi R. Combined treatment with specific ligands for PPARgamma:RXR nuclear receptor system markedly inhibits the expression of cytochrome P450arom in human granulosa cancer cells. 2001;181:239-248.

35. Fan W, Yanase T, Morinaga H, Mu YM, Nomura M, Okabe T. Activation of peroxisome proliferator-activated receptor-gamma and retinoid X receptor inhibits aromatase transcription via nuclear factor-kappaB. 2005;146(1):85-92. doi:10.1210/en.2004-1046

36. Kwintkiewicz J, Nishi Y, Yanase T, Giudice LC. Peroxisome proliferator-activated receptor-γ mediates bisphenol A inhibition of FSH-stimulated IGF-1, aromatase, and estradiol in human granulosa cells. *Environ Health Perspect*. 2010;118(3):400-406. doi:10.1289/ehp.0901161

37. Uruno A, Matsuda K, Noguchi N, et al. Peroxisome proliferator-activated receptor-{gamma} suppresses CYP11B2 expression and aldosterone production. *J Mol Endocrinol*. 2011;46(1):37-49. doi:10.1677/JME-10-0088

38. Corrales P, Vidal-Puig A, Medina-Gómez G. PPARS and metabolic disorders associated with challenged adipose tissue plasticity. *Int J Mol Sci*. 2018;19(7). doi:10.3390/ijms19072124

39. Hernandez-Quiles M, Broekema MF, Kalkhoven E. PPARgamma in Metabolism, Immunity, and Cancer: Unified and Diverse Mechanisms of Action. *Front Endocrinol (Lausanne)*. 2021;12. doi:10.3389/FENDO.2021.624112

Manuscript III

PPARγ-mediated effect of ethanol and ethylene glycol on aromatase expression in adipose tissue

Jacob Ardenkjær-Skinnerup, Daniel Saar, Sofie Christiansen, Terje Svingen, Niels Hadrup, Kristy A. Brown, Brice Emanuelli, Birthe B. Kragelund, Gitte Ravn-Haren, Ulla B. Vogel

In this manuscript, it was studied if the organic solvents ethanol and ethylene glycol directly interacted with PPARγ LBD. It was also investigated if exposure to these solvents increased aromatase expression in adipose tissue cells and in rat adipose tissue. This manuscript has not yet been submitted for publication.

PPARγ-mediated effect of ethanol and ethylene glycol on aromatase expression in adipose tissue

Jacob Ardenkjær-Skinnerup[1-4], Daniel Saar[5], Sofie Christiansen[1], Terje Svingen[1], Niels Hadrup[1,2], Kristy A. Brown[3,6], Brice Emanuelli[4], Birthe B. Kragelund[5], Gitte Ravn-Haren[1,*], Ulla B. Vogel[1,2,*]

[1] The National Food Institute, Technical University of Denmark, Kongens Lyngby, Denmark
[2] The National Research Centre for the Working Environment, Copenhagen Ø, Denmark
[3] Department of Medicine, Weill Cornell Medicine, New York, NY, USA
[4] The Novo Nordisk Foundation Center for Basic Metabolic Research, University of Copenhagen, Copenhagen N, Denmark
[5] REPIN and Structural Biology and NMR Laboratory, Department of Biology, University of Copenhagen, Copenhagen N, Denmark
[6] Department of Cell Biology and Physiology, University of Kansas Medical Center, Kansas City, KS, USA

* co-corresponding authors

Abstract

The estrogen-synthesizing enzyme aromatase is expressed in adipose tissue where it controls the local concentration of estrogen. It has been suggested that the organic solvents ethanol and ethylene glycol can induce estrogen synthesis by inhibiting PPARγ activity. Since elevated estrogen levels in adipose tissue is a risk factor for breast cancer development, it is of interest to further characterize the mechanisms regulating estrogen levels. Here, we explored the mechanisms by which ethanol and ethylene glycol modulate aromatase expression and ultimately convert androgens to estrogens.

NMR spectroscopy revealed that ethanol and ethylene glycol influence the active state of PPARγ, and that the binding mechanism is different from most other PPARγ ligands. An inhibitory effect on PPARγ was confirmed by adipogenesis assays and short-term treatment of adipocytes, showing reduced mRNA levels of PPARγ target genes. However, only ethanol increased aromatase mRNA in differentiated human pre-adipocytes. In contrast, ethylene glycol downregulated aromatase, most likely in a PPARγ-independent manner, as the effect also occurred in undifferentiated PPARγ-deficient pre-adipocytes.

An animal study using female rats was conducted to assess the acute effects of ethanol and ethylene glycol on aromatase expression in adipose tissue within a physiological context. The PPARγ antagonist GW9662 was used as a control for PPARγ-dependent effects. No changes in aromatase or PPARγ target gene (*Adipoq* and *Fabp4*) levels were observed in adipose tissue or ovary in response to treatment, suggesting an absence of acute PPARγ-mediated effects in these organs.

The results suggest that ethanol and ethylene glycol are weak PPARγ antagonists. Both compounds can affect adipocyte aromatase expression *in vitro*, but no acute effects on aromatase expression or PPARγ activity were observed in adipose tissue or ovary in rats.

Introduction

Breast cancer remains a significant global health concern with continued rise in incidence rates. Common risk factors include increasing age, hormone therapy, obesity, and sedentary behavior.[1] Extensive research efforts have been dedicated to explaining the interplay between environmental factors, hormonal imbalances, and breast cancer development.[2] Among the environmental influences, alcohol consumption stands out as a major risk factor. Specifically, ethanol has been associated with increased development of estrogen receptor-positive tumors, potentially mediated by an increase in estrogen levels.[3] Thus, one drink per day (10 g alcohol) was associated with 4.2% (95% CI: 2.7-5.8%) increased risk of breast cancer in the EPIC cohort.[4]

Like exposure to ethanol, occupational exposure to other organic solvents has been linked to an increased risk of breast cancer.[5] Although there is consistent evidence linking breast cancer to alcohol consumption, the mechanism-of-action for carcinogenesis induced by ethanol, as well as other organic solvents, is not fully understood. Ethanol and its metabolite acetaldehyde are both group 1 carcinogens,[6] but it has been suggested that it is ethanol rather than acetaldehyde that is the carcinogenic substance in postmenopausal breast cancer.[7] Another highly relevant alcohol is ethylene glycol, a high-production-volume industrial compound present in numerous consumer products.[8] Studies suggest that ethanol and ethylene glycol may affect breast cancer risk via a mechanism involving the nuclear receptor peroxisome proliferator-activated receptor gamma (PPARγ).[9,10] Both alcohols have been reported to inhibit PPARγ activity in H293 cells[9,10] and expression in rodent kidney[11,12] or adipose tissue.[13,14]

PPARγ is a ligand-activated transcription factor abundantly expressed in adipose tissue where it regulates adipogenesis, lipid metabolism, and insulin sensitivity.[15] There are two main isoforms, PPARγ1 and PPARγ2, the latter being a stronger inducer of adipogenesis.[16] *In vitro* studies suggest that PPARγ activation protects against breast cancer via repression of aromatase (*CYP19A1*).[17,18] In contrast, PPARγ can be inhibited by environmental antagonists (Ardenkjær-Skinnerup et al, submitted), which leads to upregulation of aromatase in human adipose tissue culture (Ardenkjær-Skinnerup et al). Since ethanol and ethylene glycol have been demonstrated to inhibit PPARγ signaling, they may promote breast carcinogenesis through a mechanism involving upregulation of aromatase in adipose tissue.

This study aims to elucidate the impact of ethanol and ethylene glycol on aromatase expression in adipose tissue by employing *in vitro* and *in vivo* methods. First, interaction of the solvents with PPARγ was studied to uncover whether observed effects were directly or indirectly related to PPARγ activity. Effects on adipogenesis and acute aromatase regulation were then studied in mouse and human adipose stromal cell (ASC) lines, respectively. Finally, the expression of aromatase and aromatase-associated cytokines was investigated in rat adipose tissue in response to short-term treatment with ethanol and ethylene glycol, using GW9662 as a control antagonist of PPARγ.

Methods

Animal study

Twenty-four female Wistar (Han) rats (purchased by Charles River, Germany; distributed by SCANBUR, Denmark) with mean body weight of 180 g were maintained at 22°C under 12 h light/dark cycles. The animals were fed Altromin 1314 diet (soy and alfalfa-free, Altromin GmbH, Lage, Germany) and provided water *ad libitum*.

The animals were randomized into four groups of six animals that were subjected to different treatments. One group served as a control for the other three groups that received either GW9662 (M6191, Sigma-Aldrich), ethanol (Navimer Alcohol Pur 96%), or ethylene glycol (324558, Sigma-Aldrich). Rats were administered ethanol or ethylene glycol at concentrations of 10% or 0.75%, respectively, via drinking water, while GW9662 (2 mg/day) was delivered in a semi-solid vehicle consisting of 1 g hazelnut cream (Nutella) on a 0.8 g Marie biscuit (Salling Group). A single control group was sufficient because all groups received the vehicle (with or

without GW9662). Rats were housed in pairs and temporarily relocated to separate cages during delivery of vehicle.

Before treatment, rats received the vehicle (without treatment) for five days, followed by a two-day break. Then rats were treated with chemicals for two days, and finally euthanized on the tenth day. Ethanol and ethylene glycol were accessible up until euthanasia. Ovaries, trimmed from the fat pad, as well as subcutaneous and visceral adipose tissue were collected and immediately immersed in RNA*later* (AM7021, Invitrogen).

The animal experiment was conducted at the National Food Institute, Technical University of Denmark (DTU Food, Lyngby). Ethical approval was obtained from the Danish Animal Experiments Inspectorate (Council for Animal Experimentation, authorization number 2020-15-0201-00570), and the experiment was monitored by the Animal Welfare Committee of the National Food Institute.

Cell culture

Primary cells were isolated from adipose tissue and cultured as described previously (Ardenkjær-Skinnerup et al). The cells were isolated from adipose tissue obtained from patients undergoing mastectomy, abdominoplasty, or reduction mammoplasty at Weill Cornell Medicine (under IRB-approved protocol #20-01021391). Primary cells were cultured in F-12 medium (10-080-CV, Corning) containing 10% fetal bovine serum (FBS; 35-010-CV, Corning) and 1% penicillin-streptomycin solution (15140122, Gibco). The human A41 ASC line (hTERT A41hWAT-SVF)[19] and the mouse C3H10T1/2 mesenchymal stem cell line (CCL-226, ATCC) were cultured in Dulbecco's Modified Eagle Medium (DMEM; 41965-039, Gibco) containing 10% FBS (F7524, Sigma-Aldrich) and 1% penicillin-streptomycin solution (15070063, Gibco). All cells were cultured in humidified incubators at 37°C and 5% CO_2. Culture medium was changed every 2 or 3 days.

Cells were stimulated with ethylene glycol (99.8% purity) or absolute ethanol (≥99.5% purity). Undifferentiated or 12-day differentiated A41 cells in basal culture medium were treated for 24 h. In the differentiation experiments, primary ASCs, C3H10T1/2 cells, or A41 cells were treated throughout differentiation.

Adipocyte differentiation

Cells were induced to differentiate when they were 100% confluent. Primary human ASCs were washed twice with phosphate-buffered saline (PBS) and differentiated for 12 days using serum-free culture medium containing 0.1 or 2 µM rosiglitazone (day 0-4), 0.25 µM dexamethasone (day 0-6), 500 µM IBMX (day 0-6), 20 nM insulin, 0.2 nM triiodothyronine (T_3), 33 µM biotin, 17 µM pantothenic acid, 0.1 µM transferrin, and 10 µg/mL cortisol (all from Sigma-Aldrich).

A41 cells were differentiated in serum-containing culture medium supplemented with 1 µM rosiglitazone, 0.1 µM dexamethasone, 500 µM IBMX, 500 nM insulin, 2 nM T_3, 33 µM biotin, and 17 µM pantothenic acid. C3H10T1/2 cells were differentiated by adding 0.1 µM rosiglitazone, 0.2 µM dexamethasone (day 0-2), 100 µM IBMX (day 0-2), and 4 nM insulin (day 0-4) to the serum-containing culture medium. Adipogenic medium was changed every 2, 2, or 3 days for primary ASCs, C3H10T1/2, and A41 cells, respectively.

In experiments where cells were exposed to chemicals during differentiation, the chemicals were added every time differentiation medium was renewed. Mature A41 cells, used for acute chemical treatment, were differentiated for 12 days and returned to regular growth medium for 2 days before 24 h treatment with chemicals.

Lipid staining and quantification

The cells were differentiated in transparent 96-well plates, and on day 12 of differentiation, they were washed in PBS and fixed with 4% formaldehyde (252549, Sigma-Aldrich) in PBS for 30 min at room temperature. Then cells were washed twice with water and incubated with 60% isopropanol for 5 min, followed by further incubation with sterile filtered 60% Oil Red O (O0625, Sigma-Aldrich) solution for 20 min. Cells were washed 3

times with water and then viewed under the microscope. Stained lipids were quantified by washing 3 times with 60% isopropanol for 5 min, and then extracting the Oil Red O stain with 50 µL 100% isopropanol for 20 min. Finally, 40 µL of the extracted Oil Red O was transferred to a 384 well plate. Absorbance was read at 518 nm, and 100% isopropanol was used as a background control.

Gene expression analysis

Cells were washed in PBS before lysis. Cultured cells and ovaries were lysed with Buffer RLT (Qiagen) containing 1% β-mercaptoethanol, and RNA was extracted using RNeasy Kit (Qiagen). Adipose tissue samples were lysed with QIAzol (Qiagen), and RNA was isolated RNeasy Lipid Tissue Mini Kit (Qiagen). For cell lines, cDNA synthesis from 1 µg RNA was performed using iScript cDNA Synthesis Kit (1708891, Bio-Rad), and quantitative reverse transcription polymerase chain reaction (RT-qPCR) was performed using Brilliant III Ultra-Fast SYBR Green qPCR Master Mix (600882, Agilent) and the CFX384 Real-Time PCR Detection System (Bio-Rad). Primers were purchased from TAG Copenhagen and are shown in Table 1. For tissue samples, Omniscript RT Kit (205113, Qiagen), SUPERase-In RNase Inhibitor (AM2694, Invitrogen), and Random Primer Mix (S1330, New England Biolabs) were used for cDNA synthesis from 2 µg RNA. TaqMan Fast Advanced Master Mix (4444557, Applied Biosystems) and the QuantStudio 7 Flex Real-Time PCR System (Applied Biosystems) were applied for qPCR. TaqMan assays (4331182, Applied Biosystems) were used for rat *Rps18* (Rn01428913_gH), *Cyp19a1* (Rn00567222_m1), *Pparg*, (Rn00440945_m1), *Fabp4* (Rn04219585_m1), *Adipoq* (Rn00595250_m1), *Lep* (Rn00565158_m1), and *Il6* (Rn01410330_m1). Each biological sample was measured in technical triplicates, and the $2^{-\Delta\Delta Ct}$ method was used for relative quantification.

Gene	**Species**	**Sequence** (forward)	**Sequence** (reverse)
RPL32	Human	CAGGGTTCGTAGAAGATTCAAGGG	CTTGGAGGAAACATTGTGAGCGATC
CYP19A1	Human	TTGACCCTTCTGCGTCGTGT	AGGAGAGCTTGCCATGCATCA
ADIPOQ	Human	GCAGTCTGTGGTTCTGATTCC	CATGACCGGGCAGAGCTAAT
FASN	Human	TACAACATCGACACCAGCTC	CGTCTTCCACACTATGCTCA
Cyp19a1	Rat	CGCAGAGTATCCGGAGGTGG	CTGATACCGCAGGCTCTCGT
Rn18s	Mouse	AGTCCCTGCCCTTTGTACACA	GATCCGAGGGCCTCACTAAAC
Pparg	Mouse	GCATGGTGCCTTCGCTGA	TGGCATCTCTGTGTCAACCATG
Adipoq	Mouse	GATGGCACTCCTGGAGAGAA	TCTCCAGGCTCTCCTTTCCT
Fabp4	Mouse	CTGGGCGTGGAATTCGAT	GCTCTTCACCTTCCTGTCGTCT
Slc2a4	Mouse	GTGACTGGAACACTGGTCCTA	CCAGCCACGTTGCATTGTAG

Table 1: Primers used for RT-qPCR using SYBR Green.

Protein production

Human PPARγ ligand binding domain (LBD) cDNA (residues 231 to 505) with an N-terminal hexahistidine- and SUMO-tag (H_6-SUMO) was cloned into a modified pET24a vector. Protein production was performed in *E. coli* BL21(-DE3) cells (New England BioLabs, Frankfurt, Germany) in auto-induction minimal medium,[20] with ^{15}N NH_4Cl as a nitrogen source for isotope labeling. Temperature was changed at OD_{600} of 0.8 from 37 °C to 18 °C, and protein production was allowed to proceed for 24 h. Cells were harvested by centrifugation at 5.000 x g for 20 min. For purification, pellets were resuspended in lysis buffer (20 mM imidazole, 50 mM Tris pH 8, 200 mM NaCl, 10 % (v/v) glycerol). All purification buffers contained 5 mM β-mercaptoethanol. Cells were lysed with a cell disrupter (Constant Systems Ltd., Daventry, UK) at 25 kpsi and the lysate was cleared by centrifugation at 20,000 x g for 45 min. The supernatant, pre-equilibrated with lysis buffer, was twice passed over 5 mL Ni-NTA resin (Qiagen, Hilden, Germany). The three wash steps were done with lysis buffer first, then with lysis buffer containing 1 M NaCl, and finally with lysis buffer again. For elution of bound proteins, lysis buffer with 500 mM imidazole was used. The protein was cleaved overnight at 4 °C using ULP1-protease (in-house production) under dialysis into 40 mM Tris, pH 8, 10 % glycerol, 200 mM NaCl, and 5 mM β-mercaptoethanol. The His_6-SUMO tag was removed by passing again over the Ni-NTA column. Purification continued by ion exchange chromatography using a HiTrap QFF 5 mL column (Cytiva) and an ÄKTA pure 25 chromatography system (GE Healthcare, Munich, Germany) and size exclusion chromatography using a Superdex 200 Increase 10/300 GL (Sigma-Aldrich). Ion exchange buffers were 25 mM bis-Tris pH 7.4, with the

elution buffer containing 1 M NaCl in addition. The buffer for size exclusion contained 40 mM Tris pH 8 and 500 mM NaCl.

Nuclear magnetic resonance (NMR) spectroscopy

NMR samples were kept at room temperature and contained 80 µM ^{15}N PPARγ LBD in PBS buffer, pH 7.3, 137 mM NaCl. As a reference, 10% D_2O (v/v) and 0.7 mM 4,4-dimethyl-4-silapentane-1-sulfonic acid (DSS) were added. Ethanol or ethylene glycol was added to a final concentration of 3%. NMR spectra were recorded at 298 K on a Bruker AVANCE III 750-MHz (^{1}H) spectrometer equipped with a cryogenic probe. Free induction decays were transformed and visualized in Topspin (Bruker Biospin), and subsequently analyzed using the CcpNmr Analysis software.[21] Proton chemical shifts were internally referenced to DSS at 0.00 ppm with heteronuclei referenced by relative gyromagnetic ratios. Assignments of nitrogen peaks of PPARγ LBD were exported from BMRB[22] and transferred from an assignment by Hughes at al. 2012.[23] Intensities were internally normalized to the E235 peak of each spectrum, which was the most intense peak in every condition.

Statistical analysis

Statistical significance was tested using Dunnett's multiple comparison test or two-way analysis of variance (ANOVA), depending on the number of variables. When there were more than two levels within a variable of the two-way ANOVA, Dunnett's test for multiple comparisons was applied for the levels of that variable. Data was normalized to the sum of values within each experiment, and the control group was set to 1. Differences between groups were considered significant if $p \leq 0.05$, and data were presented as means and standard errors of the mean (SEM).

Results

Direct interaction of ethanol and ethylene glycol with PPARγ LBD

NMR spectroscopy was used to verify previously reported inactivation of PPARγ by ethanol and ethylene glycol.[9,10] An activity control was established in a previous study by recording ^{15}N-HSQCs of PPARγ LBD bound to known agonist rosiglitazone in the presence or absence of antagonist GW9662 (Ardenkjær-Skinnerup et al). These spectra were used as negative and positive controls for activity states of PPARγ LBD, respectively (Figure 1A, 1B) (Ardenkjær-Skinnerup et al). The number and NMR peak intensity of annotatable signals, especially around the ligand-binding pocket and in helix 12, were used as an indication for activity (Figure 1F). The rosiglitazone-bound active state featured 208 peaks that could be assigned, corresponding to ~75 % of the residues in the LBD (Figure 1E) (Ardenkjær-Skinnerup et al). Addition of GW9662 to rosiglitazone-bound PPARγ LBD reverted the number of assignable peaks to ~40 % of the possible NMR signals of the LBD (Figure 1B, 1E) (Ardenkjær-Skinnerup et al). Adding ethanol and ethylene glycol to rosiglitazone-bound PPARγ LBD led to some chemical shifts and NMR peak intensity changes (Figure 1A, 1C, 1D), but not nearly as much as for GW9662, resulting in ~74 % and ~75 % of the residues being accounted for, respectively (Figure 1E). These peaks were in general less intense than without ethanol and ethylene glycol. In contrast, ethanol or ethylene glycol had no effect on the basal state of PPARγ LBD (Supplemental Figure S1). This suggests that ethanol and ethylene glycol to some extent influence the active state of PPARγ LBD, however the degree and the mechanisms cannot be elucidated from these data.

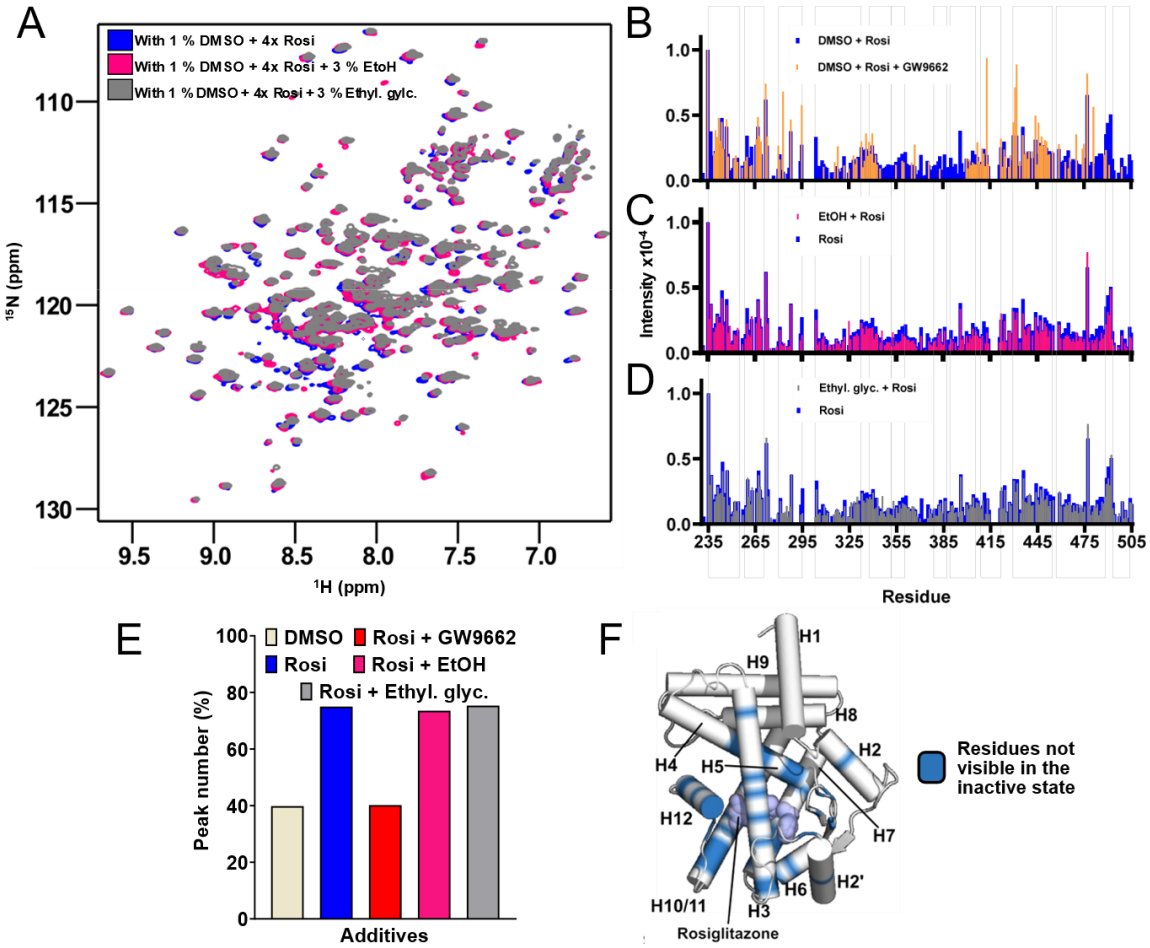

Figure 1. **Direct interactions of ethanol and ethylene glycol with PPARγ LBD in the presence of rosiglitazone**. NMR spectroscopy was performed using PPARγ LBD and different chemical compounds. The data for rosiglitazone treatment alone or together with GW9662 were previously published (Ardenkjær-Skinnerup J et al). (**A**) ^{15}N-HSQCs of the PPARγ LBD together with rosiglitazone and either ethanol or ethylene glycol. (**B**-**D**) Peak intensity profile of the rosiglitazone-bound PPARγ LBD compared to rosiglitazone-bound PPARγ LBD after addition of (**B**) GW9662, (**C**) ethanol, or (**D**) ethylene glycol. (**E**) Percentages of the number of visible and assignable peaks depending on bound chemical. (**F**) Crystal structure of PPARγ LBD bound to rosiglitazone in cartoon representation (PDB: 1FM6). Rosiglitazone is shown as spheres in the binding pocket, and residues only visible in the active state are shown in blue.

Effect of ethanol and ethylene glycol on adipogenesis

To determine if ethanol or ethylene glycol influenced adipogenesis, mouse C3H10T1/2 cells were treated during differentiation and mRNA levels of four adipocyte markers (*Pparg*, *Adipoq*, *Fabp4*, and *Slc2a4*) were measured. Treatment with 0.3 or 1% ethanol during differentiation induced a modest, concentration-dependent reduction in adipocyte marker mRNA abundance (Figure 2A). The effect was greater for ethylene glycol, which reduced mRNA markers by about 50% at a concentration of 1% (Figure 2B).

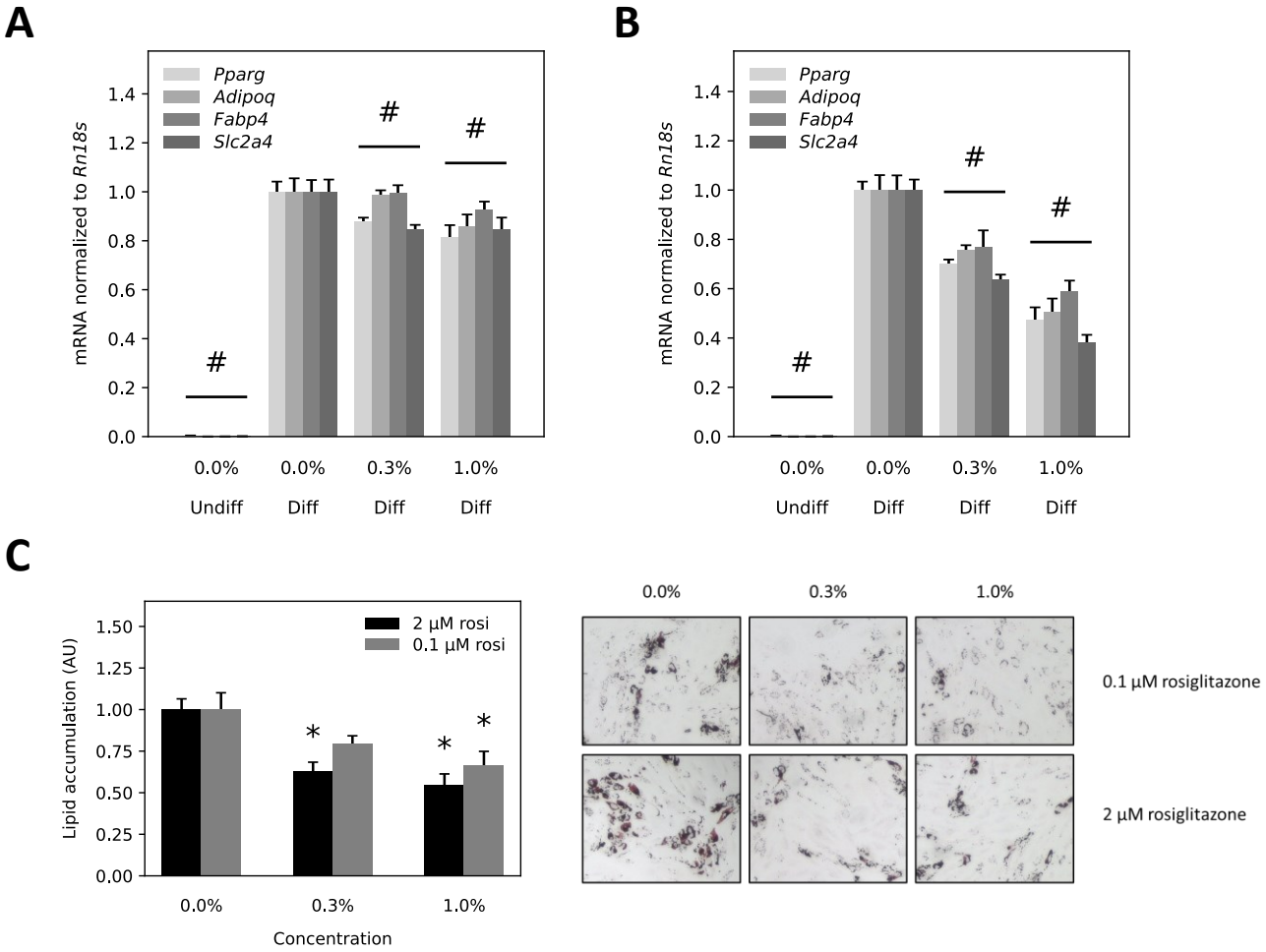

Figure 2. **Lipid accumulation and adipogenic marker mRNA in response to adipocyte differentiation during chemical exposure**. C3H10T1/2 cells were differentiated for 6 days in the presence of 0, 0.3, or 1% (**A**) ethanol or (**B**) ethylene glycol. Cells were compared to an undifferentiated control. Gene expression analysis by RT-qPCR was performed for adipocyte markers (*Pparg*, *Adipoq*, *Fabp4*, *Slc2a4*) using SYBR Green assay (n = 4). (**C**) Differentiation of human ASCs was induced with either high (2 µM) or low (0.1 µM) concentrations of rosiglitazone in the adipogenic medium. During differentiation, cells were treated with 0, 0.3, or 1% ethanol. Lipids were stained with Oil Red O at day 12 of differentiation, visualized by microscopy, and quantified (n = 4). The graphs show means ± SEM. Asterisk (*) and hash (#) indicate statistically significant differences compared to control cells using Dunnett's test or two-way ANOVA, respectively ($p < 0.05$).

Primary human ASCs were differentiated in the presence of 0.3 or 1% ethanol, using 0.1 µM or 2 µM rosiglitazone in the adipogenic medium, to determine if the effect observed in mouse cells could also be found in human cells (Figure 2C). Lipid staining by Oil Red O showed a decrease in lipid accumulation in response to ethanol at both concentrations of rosiglitazone. Furthermore, the effect was independent of rosiglitazone as there was no statistically significant difference between the two concentrations used (two-way ANOVA, $p > 0.05$).

Short-term regulation of aromatase *in vitro* by ethanol and ethylene glycol

To determine a potential acute effect of exposure to ethanol or ethylene glycol, human A41 pre-adipocytes or adipocytes were treated for 24 h at concentrations of 1% (Figure 3). Ethanol had no effect in pre-adipocytes, while ethylene glycol decreased aromatase mRNA levels (Figure 3A). In mature adipocytes, ethanol treatment increased aromatase expression, and ethylene glycol treatment again resulted in a downregulation of aromatase mRNA (Figure 3B). Treatment with either ethanol or ethylene glycol caused lowered mRNA levels of the two PPARγ target genes, *ADIPOQ* and *FASN*, which were used as measures of PPARγ activity. Repeating the treatment in A41 adipocytes in serum-free conditions produced a similar effect on aromatase expression as in conditions with serum (Supplemental Figure 2).

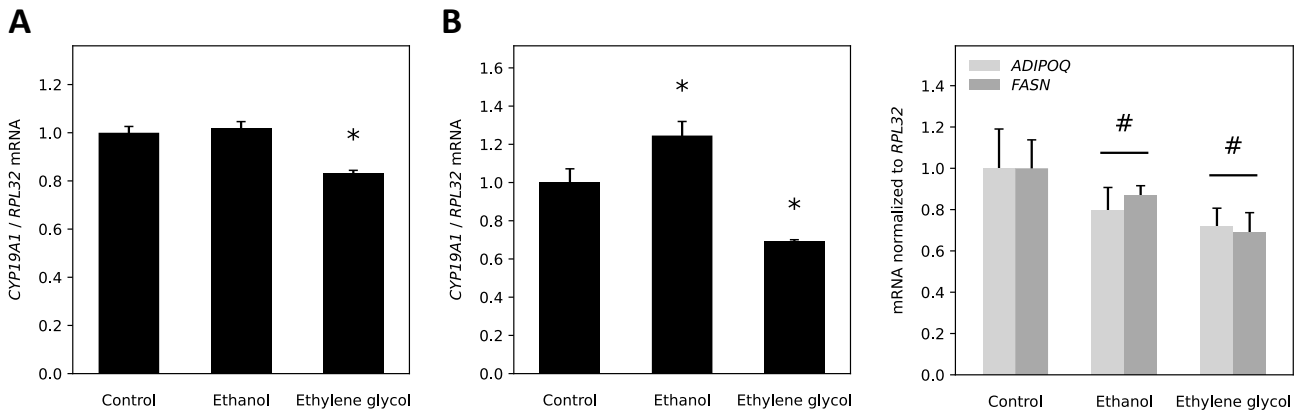

Figure 3. **Aromatase mRNA level in response to chemical exposure**. Gene expression analysis of aromatase (*CYP19A1*) and adipocyte markers (*ADIPOQ* and *FASN*) was performed by RT-qPCR. (**A**) Undifferentiated or (**B**) differentiated A41 cells were treated for 24 h with 1% ethanol or ethylene glycol. The graphs present means ± SEM (n = 3). The graphs show means ± SEM. Asterisk (*) and hash (#) indicate statistically significant differences compared to control cells using Dunnett's test or two-way ANOVA, respectively ($p < 0.05$).

Regulation of aromatase by ethanol and ethylene glycol in rats

The acute effects of ethanol and ethylene glycol were further explored *in vivo* by a two-day oral exposure in female rats, using the PPARγ antagonist GW9662 as a positive control for PPARγ-mediated effects. Ethanol and ethylene glycol were dosed in the drinking water at 10% and 0.75%, respectively, and GW9662 was administered through a vehicle consisting of hazelnut cream on biscuit. The daily intake of GW9662, ethanol, and ethylene glycol corresponded to 10 mg/kg bw, 14 g/kg bw/day, and 1.3 g/kg bw, respectively. The vehicle was delivered to all experimental groups. There were no significant differences in fluid intake and weight gain between the experimental groups (Supplemental Figure S3).

Subcutaneous white adipose tissue (sWAT), visceral white adipose tissue (vWAT), and ovaries were collected for gene expression analysis by RT-qPCR (Figure 4). Expression levels of aromatase (*Cyp19a1*), PPARγ (*Pparg*), fatty acid binding protein 4 (*Fabp4*), adiponectin (*Adipoq*), leptin (*Lep*), and interleukin 6 (*Il6*) were measured. Treatments had no effect on the expression of these genes, apart from an increase in leptin expression in sWAT in response to ethylene glycol treatment. Aromatase was very weakly expressed in rat adipose tissue, indicated by a lack of amplification in a significant number of the technical replicates. However, specific *Cyp19a1* amplification in sWAT samples was confirmed in the TaqMan assay by agarose gel electrophoresis of the PCR product (Supplemental Figure S4). In contrast, amplification of *Cyp19a1* using SYBR Green produced both *Cyp19a1* and non-specific amplicons.

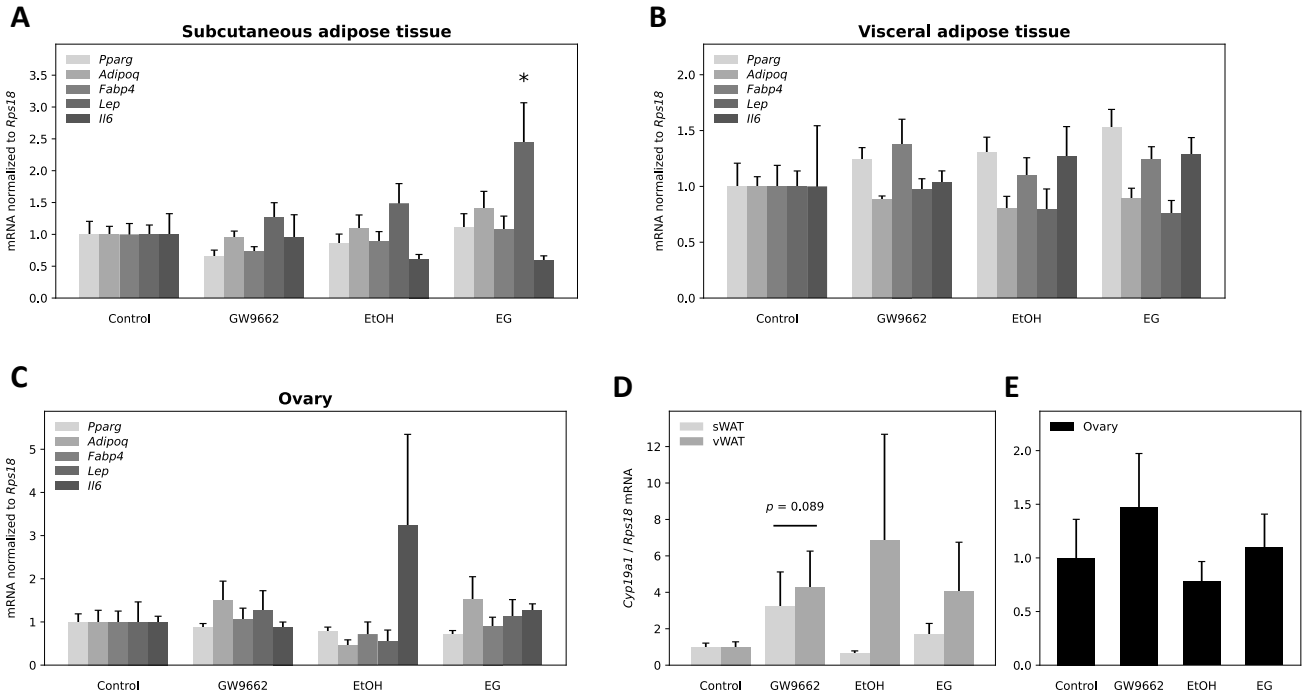

Figure 4. **Gene expression in rat tissues in response to short-term oral chemical exposure**. Wistar rats were exposed to GW9662, ethanol, or ethylene glycol for 2 days before euthanasia. Gene expression analysis of *Cyp19a1*, *Pparg*, *Fabp4*, *Adipoq*, *Lep*, and *Il6* in (**A**,**D**) subcutaneous adipose tissue, (**B**,**D**) visceral adipose tissue, and (**C**,**E**) ovaries was performed by RT-qPCR. The graphs present means ± SEM (n = 6; n = 4-6 for *Cyp19a1* in adipose tissue). Asterisk (*) and p value indicate statistically significant differences compared to control rats using Dunnett's test or two-way ANOVA, respectively ($p < 0.05$).

Discussion

We have shown that ethanol and ethylene glycol can, to some degree, influence the active state of PPARγ despite their structures being different from canonical PPARγ ligands. Further, both chemicals display some limiting effect on adipogenesis. Short-term stimulation of human adipocytes with ethanol increased aromatase expression, however this was not the case for ethylene glycol. Female rats exposed orally for two days did not exhibit altered gene expression of aromatase or PPARγ target genes in adipose tissue.

Interaction of ethanol and ethylene glycol with PPARγ

Activating ligands, such as rosiglitazone, stabilize the PPARγ LBD in the active state, leading to more visible peaks in 2D NMR spectra (Ardenkjær-Skinnerup et al).[24] The same was observed in the unpublished control experiments (Ardenkjær-Skinnerup et al), where especially helix 12 became visible in the rosiglitazone-bound state, which has been described to be solvent exposed in the active state and buried in the ligand binding pocket in the repressive state.[25] Along with helix 12, peaks belonging to residues outlining the ligand binding pocket (helix 3, helices 5 to 7, C-terminal half of helix 10/11) also appeared (Ardenkjær-Skinnerup et al). These peaks were lost when PPARγ LBD was forced into the repressive state by the addition of repressors such as GW9662 or DEHPA (Ardenkjær-Skinnerup et al). In contrast, addition of ethanol or ethylene glycol to PPARγ LBD did not seem to completely destabilize the rosiglitazone-bound active state. Peaks from helix 12 and the residues of the ligand binding pocket remained visible. In the case of ethanol, these peaks lost intensity, maybe suggesting repression. It has been suggested that significant changes in the function of a protein may occur in response to ethanol if binding occurs in regions of a protein that are involved in binding of other molecules.[26] It may therefore be that the observed differences result from a modulation of rosiglitazone's activating effect. But this is less clear for the addition of ethylene glycol, where many peaks remain of similar intensity. The data do not give obvious indications of a repression of PPARγ as observed for other known repressors. Repression may therefore be less strong or occur through a different or LBD-independent

mechanism. Furthermore, it should be noted that metabolites of ethanol and ethylene glycol may also affect PPARγ function.

Effect of ethanol and ethylene glycol on adipogenesis

The effect of ethanol and ethylene glycol on adipogenesis was studied since a link between PPARγ antagonist-induced loss of adipogenic capacity and elevated aromatase expression was recently demonstrated in human ASCs (Ardenkjær-Skinnerup et al). The impaired adipogenesis in response to ethanol and ethylene glycol supports the reported inhibitory effect of these chemicals on PPARγ[9,10] and implies that a stimulation of aromatase expression may follow from this. Ethanol has been demonstrated to inhibit adipogenesis in human ASCs at a concentration of 50 mM, corresponding to 0.3%, which is consistent with the present results.[27] In contrast, 100 mM ethanol has been shown to induce adipocyte differentiation of the mouse OP9 cell line.[28] These inconsistencies might result from differential expression and activity of ethanol-metabolizing enzymes, which have been shown to be present in adipocytes.[27]

Ethanol has numerous biological effects and is believed to act on many different proteins making it difficult to identify its direct targets.[29] For example, ethanol may affect adipogenesis through its inhibitory effect on insulin action.[30] The inhibition of adipogenesis by ethanol in primary human ASCs occurred independently of the rosiglitazone concentration, which is in contrast to the effects of other studied PPARγ inhibitors, such as GW9662, Cosan 528, and DEHPA (Ardenkjær-Skinnerup et al). This could indicate that PPARγ-independent mechanisms of ethanol contribute to the impaired adipogenesis.

Short-term regulation of aromatase by ethanol and ethylene glycol *in vitro*

An acute effect of PPARγ antagonists on aromatase expression has previously been reported (Ardenkjær-Skinnerup et al), and it was therefore investigated if a similar effect would occur in response to ethanol or ethylene glycol. Like other PPARγ antagonists, ethanol increased aromatase mRNA in *PPARG*-expressing A41 adipocytes, but not in A41 pre-adipocytes, suggesting that the effect was mediated by PPARγ. Consistent with this, a study has demonstrated that ethanol treatment increases aromatase expression in the MCF-7 human breast cancer cell line.[31] Surprisingly, ethylene glycol reduced aromatase mRNA in the A41 adipocytes, despite inhibiting PPARγ activity. The corresponding decrease in aromatase mRNA at the pre-adipocyte stage, where *PPARG* is lowly expressed, suggests that the ethylene glycol-induced effects on aromatase were PPARγ-independent.

***In vivo* regulation of aromatase by ethanol and ethylene glycol**

Acute exposure of rats to GW9662, ethanol, or ethylene glycol did not result in any apparent effects on mRNA levels of aromatase or aromatase-associated cytokines,[32] nor on *Pparg* or PPARγ target genes. Aromatase expression was expected to increase in response to PPARγ antagonist treatment as previously demonstrated in cultured adipocytes (Ardenkjær-Skinnerup et al). *In vivo* studies have reported that ethanol consumption downregulates *Pparg*, *Fabp4*, and *Adipoq* and upregulates *Cyp19a1* and *Il6* in male rodent adipose tissue,[13,14,28,33,34] while ethylene glycol downregulates renal *Pparg* and increases serum IL-6.[11]

Upregulation of aromatase in response to ethanol was at the protein level, and the effect occurred after 8 weeks of *ad libitum* access to 13% ethanol in form of red wine or ethanol.[34] Because treatment was chronic, the upregulation of aromatase may be a result of impaired adipogenesis, which is consistent with the negative correlation between aromatase protein levels and body weight gain as well as the reduced body weight of rats treated with red wine or ethanol compared with the control group.

The lack of effects in the current study may be explained by the short duration of exposure. In most rodent studies on these chemicals, exposure was performed for weeks.[11–14,34] However, acute exposures have been shown to affect gene expression when administered intraperitoneally. For instance, treatment with 2 mg/kg GW9662 for 26 h or 3.5 g/kg ethanol for 3 h increased *Il6* expression in rodent hippocampus.[35,36] The reason that PPARγ activity was unaffected by treatment, as observed by the unchanged PPARγ target gene

expression, may have to do with fluctuations in adipose tissue PPARγ expression over the course of estrous cycle.[37,38] This could also affect the expression of other measured genes, such as *Cyp19a1*.

In addition, the aromatase mRNA level was very low in rat adipose tissue, which has also been observed in mouse adipose tissue cells (Ardenkjær-Skinnerup et al) and tissue,[39] causing large variation within experimental groups. A transgenic humanized aromatase mouse model has been generated to mimic human tissue-specific patterns of aromatase expression and estrogen production, and this would be an ideal model for studying effects on aromatase mRNA in adipose tissue.[39]

Conclusion

Our results suggest that ethanol and ethylene glycol can inhibit PPARγ activity, likely through a direct interaction with PPARγ. Short-term ethanol treatment increased aromatase expression in adipocytes, whereas ethylene glycol treatment decreased aromatase expression, most likely by a PPARγ-independent mechanism. There were no acute effects of GW9662, ethanol, or ethylene glycol on aromatase *in vivo*.

Acknowledgements

We thank the laboratory technicians at the National Food Institute, Heidi Broksø Letting, Dorte Lykkegaard Korsbech, and Lillian Sztuk, for assisting with the rat study, and Jason A. Spector, Department of Surgery at Weill Cornell Medicine, for facilitating access to reduction mammoplasty tissue. We also acknowledge the personnel in the Bio Facility at the National Food Institute. Studies were conducted with the support and facilities provided by the Microscopy and Image Analysis Core Facility and Center for Translational Pathology at Weill Cornell Medicine.

This work was supported by FFIKA, Focused Research Effort on Chemicals in the Working Environment, from the Danish Government and by the Novo Nordisk Foundation Center for Basic Metabolic Research, an independent research center at the University of Copenhagen partially funded by an unrestricted donation from the Novo Nordisk Foundation. JAS was supported by Idella Foundation, William Demant Foundation, and Christian and Ottilia Brorson Travel Grant. KAB was supported by the National Cancer Institute of the National Institutes of Health grant 1R01CA215797, the Anne Moore Breast Cancer Research Fund, and the Emilie Lippmann and Janice Jacobs McCarthy Research Scholar Award in Breast Cancer. BBK and DS were supported by Studienstiftung des Deutschen Volkes (DS) and the Novo Nordisk Foundation Challenge Center REPIN (BBK; NNF18OC0033926). NMR data were recorded at cOpenNMR, an infrastructure supported by the Novo Nordisk Foundation (NNF18OC0032996).

Author contributions

Jacob Ardenkjær-Skinnerup: Conceptualization, Methodology, Investigation, Formal analysis, Visualization, Writing - Original Draft, Writing - Review & Editing.

Daniel Saar: Methodology, Investigation, Formal analysis, Visualization, Writing - Review & Editing.

Sofie Christiansen: Methodology, Resources, Writing - Review & Editing.

Terje Svingen: Resources, Writing - Review & Editing.

Niels Hadrup: Conceptualization, Supervision, Methodology, Investigation, Writing - Review & Editing.

Kristy A. Brown: Supervision, Resources, Methodology, Writing - Review & Editing.

Brice Emanuelli: Supervision, Resources, Methodology, Writing - Review & Editing.

Birthe B. Kragelund: Supervision, Resources, Methodology, Writing - Review & Editing.

Gitte Ravn-Haren: Conceptualization, Supervision, Methodology, Investigation, Writing - Review & Editing.

Ulla B. Vogel: Conceptualization, Supervision, Project administration, Funding acquisition, Writing - Review & Editing.

References

1. Admoun C, Mayrovitz HN. The Etiology of Breast Cancer. *Breast Cancer*. Published online August 4, 2022:21-30. doi:10.36255/EXON-PUBLICATIONS-BREAST-CANCER-ETIOLOGY

2. Rodgers KM, Udesky JO, Rudel RA, Brody JG. Environmental chemicals and breast cancer: An updated review of epidemiological literature informed by biological mechanisms. *Environ Res*. 2018;160(April 2017):152-182. doi:10.1016/j.envres.2017.08.045

3. Starek-Świechowicz B, Budziszewska B, Starek A. Alcohol and breast cancer. *Pharmacological Reports*. 2023;75(1):69-84. doi:10.1007/s43440-022-00426-4

4. Romieu I, Scoccianti C, Chajès V, et al. Alcohol intake and breast cancer in the European prospective investigation into cancer and nutrition. *Int J Cancer*. 2015;137(8):1921-1930. doi:10.1002/IJC.29469

5. Pedersen JE, Strandberg-Larsen K, Andersson M, Hansen J. Risk of breast cancer in Danish women occupationally exposed to organic solvents, including ethanol. *Am J Ind Med*. 2022;65(8):660-668. doi:10.1002/ajim.23397

6. International Agency for Research on Cancer. *Personal Habits and Indoor Combustions. IARC Monographs on the Evaluation of Carcinogenic Risks to Humans*. Vol 100E. IARC; 2012.

7. Benzon Larsen S, Vogel U, Christensen J, et al. Interaction between ADH1C Arg(272)Gln and alcohol intake in relation to breast cancer risk suggests that ethanol is the causal factor in alcohol related breast cancer. *Cancer Lett*. 2010;295(2):191-197. doi:10.1016/J.CANLET.2010.02.023

8. Yue H, Zhao Y, Ma X, Gong J. Ethylene glycol: properties, synthesis, and applications. *Chem Soc Rev*. 2012;41(11):4218-4244. doi:10.1039/C2CS15359A

9. Petersen RK, Larsen SB, Jensen DM, et al. PPARgamma-PGC-1alpha activity is determinant of alcohol related breast cancer. *Cancer Lett*. 2012;315(1):59-68. doi:10.1016/j.canlet.2011.10.009

10. Kopp TI, Lundqvist J, Petersen RK, et al. In vitro screening of inhibition of PPAR-gamma activity as a first step in identification of potential breast carcinogens. *Hum Exp Toxicol*. 2015;34(11):1106-1118. doi:10.1177/0960327115569811

11. Yuan H, Zhang J, Yin X, et al. The protective role of corilagin on renal calcium oxalate crystal-induced oxidative stress, inflammatory response, and apoptosis via PPAR-γ and PI3K/Akt pathway in rats. *Biotechnol Appl Biochem*. 2021;68(6):1323-1331. doi:10.1002/bab.2054

12. Su M, Sang S, Liang T, Li H. PPARG: A Novel Target for Yellow Tea in Kidney Stone Prevention. *Int J Mol Sci*. 2023;24(15). doi:10.3390/IJMS241511955

13. Sun X, Tang Y, Tan X, et al. Activation of peroxisome proliferator-activated receptor-γ by rosiglitazone improves lipid homeostasis at the adipose tissue-liver axis in ethanol-fed mice. *Am J Physiol Gastrointest Liver Physiol*. 2012;302(5):548-557. doi:10.1152/ajpgi.00342.2011

14. Tian C, Jin X, Ye X, et al. Long term intake of 0.1% ethanol decreases serum adiponectin by suppressing PPARγ expression via p38 MAPK pathway. *Food and Chemical Toxicology*. 2014;65:329-334. doi:10.1016/j.fct.2014.01.007

15. Corrales P, Vidal-Puig A, Medina-Gómez G. PPARS and metabolic disorders associated with challenged adipose tissue plasticity. *Int J Mol Sci*. 2018;19(7). doi:10.3390/ijms19072124

16. Mueller E, Drori S, Aiyer A, et al. Genetic analysis of adipogenesis through peroxisome proliferator-activated receptor gamma isoforms. *J Biol Chem*. 2002;277(44):41925-41930. doi:10.1074/JBC.M206950200

17. Rubin GL, Zhao Y, Kalus AM, Simpson ER. Peroxisome proliferator-activated receptor gamma ligands inhibit estrogen biosynthesis in human breast adipose tissue: possible implications for breast cancer therapy. *Cancer Res*. 2000;60(6):1604-1608.

18. Rubin GL, Duong JH, Clyne CD, et al. Ligands for the peroxisomal proliferator-activated receptor gamma and the retinoid X receptor inhibit aromatase cytochrome P450 (CYP19) expression mediated by promoter II in human breast adipose. *Endocrinology*. 2002;143(8):2863-2871. doi:10.1210/ENDO.143.8.8932

19. Xue R, Lynes MD, Dreyfuss JM, et al. Clonal analyses and gene profiling identify genetic biomarkers of the thermogenic potential of human brown and white preadipocytes. *Nat Med*. 2015;21(7):760-768. doi:10.1038/nm.3881

20. Studier FW. Protein production by auto-induction in high density shaking cultures. *Protein Expr Purif*. 2005;41(1):207-234. doi:10.1016/J.PEP.2005.01.016

21. Vranken WF, Boucher W, Stevens TJ, et al. The CCPN data model for NMR spectroscopy: development of a software pipeline. *Proteins*. 2005;59(4):687-696. doi:10.1002/PROT.20449

22. Hoch JC, Baskaran K, Burr H, et al. Biological Magnetic Resonance Data Bank. *Nucleic Acids Res*. 2023;51(D1):D368-D376. doi:10.1093/NAR/GKAC1050

23. Hughes TS, Chalmers MJ, Novick S, et al. Ligand and receptor dynamics contribute to the mechanism of graded PPARγ agonism. *Structure*. 2012;20(1):139-150. doi:10.1016/J.STR.2011.10.018

24. Johnson BA, Wilson EM, Li Y, Moller DE, Smith RG, Zhou G. Ligand-induced stabilization of PPARgamma monitored by NMR spectroscopy: implications for nuclear receptor activation. *J Mol Biol*. 2000;298(2):187-194. doi:10.1006/JMBI.2000.3636

25. Shang J, Mosure SA, Zheng J, et al. A molecular switch regulating transcriptional repression and activation of PPARγ. *Nature Communications 2020 11:1*. 2020;11(1):1-14. doi:10.1038/s41467-020-14750-x

26. Khrustalev VV, Khrustaleva TA, Lelevich SV. Ethanol binding sites on proteins. *J Mol Graph Model*. 2017;78:187-194. doi:10.1016/j.jmgm.2017.10.017

27. Crabb DW, Zeng Y, Liangpunsakul S, Jones RM, Considine R. Ethanol impairs differentiation of human adipocyte stromal cells in culture. *Alcohol Clin Exp Res*. 2011;35(9):1584-1592. doi:10.1111/j.1530-0277.2011.01504.x

28. He Z, Li M, Zheng D, Chen Q, Liu W, Feng L. Adipose tissue hypoxia and low-grade inflammation: A possible mechanism for ethanol-related glucose intolerance? *British Journal of Nutrition*. 2015;113(9):1355-1364. doi:10.1017/S000711451500077X

29. Harris RA, Trudell JR, Mihic SJ. Ethanol's molecular targets. *Sci Signal*. 2008;1(28). doi:10.1126/scisignal.128re7

30. Yi SJ, Jhun BH. Ethanol impairs insulin's actions through phosphatidylinositol 3-kinase. *J Med Food*. 2004;7(1):24-30. doi:10.1089/109662004322984662

31. Etique N, Chardard D, Chesnel A, Merlin JL, Flament S, Grillier-Vuissoz I. Ethanol stimulates proliferation, ERalpha and aromatase expression in MCF-7 human breast cancer cells. *Int J Mol Med*. 2004;13(1):149-155. doi:10.3892/ijmm.13.1.149

32. Brown KA, Scherer PE. Update on Adipose Tissue and Cancer. *Endocr Rev*. 2023;(May):1-14. doi:10.1210/endrev/bnad015

33. Kang L, Sebastian BM, Pritchard MT, Pratt BT, Previs SF, Nagy LE. Chronic ethanol-induced insulin resistance is associated with macrophage infiltration into adipose tissue and altered expression of adipocytokines. *Alcohol Clin Exp Res*. 2007;31(9):1581-1588. doi:10.1111/J.1530-0277.2007.00452.X

34. Monteiro R, Soares R, Guerreiro S, Pestana D, Calhau C, Azevedo I. Red wine increases adipose tissue aromatase expression and regulates body weight and adipocyte size. *Nutrition*. 2009;25(6):699-705. doi:10.1016/j.nut.2009.01.001

35. Barney TM, Vore AS, Deak T. Acute Ethanol Challenge Differentially Regulates Expression of Growth Factors and miRNA Expression Profile of Whole Tissue of the Dorsal Hippocampus. *Front Neurosci*. 2022;16. doi:10.3389/FNINS.2022.884197

36. Liao L, Zhang XD, Li J, et al. Pioglitazone attenuates lipopolysaccharide-induced depression-like behaviors, modulates NF-κB/IL-6/STAT3, CREB/BDNF pathways and central serotonergic neurotransmission in mice. *Int Immunopharmacol*. 2017;49:178-186. doi:10.1016/J.INTIMP.2017.05.036

37. Gui Y, Cai Z, Silha J V., Murphy LJ. Variations in parametrial white adipose tissue mass during the mouse estrous cycle: relationship with the expression of peroxisome proliferator-activated receptor-gamma and retinoic acid receptor-alpha. *Can J Physiol Pharmacol*. 2006;84(8-9):887-892. doi:10.1139/Y06-032

38. Kadowaki K, Fukino K, Negishi E, Ueno K. Sex differences in PPARgamma expressions in rat adipose tissues. *Biol Pharm Bull*. 2007;30(4):818-820. doi:10.1248/BPB.30.818

39. Zhao H, Pearson EK, Brooks DC, et al. A humanized pattern of aromatase expression is associated with mammary hyperplasia in mice. *Endocrinology*. 2012;153(6):2701-2713. doi:10.1210/en.2011-1761

Supplemental Figures

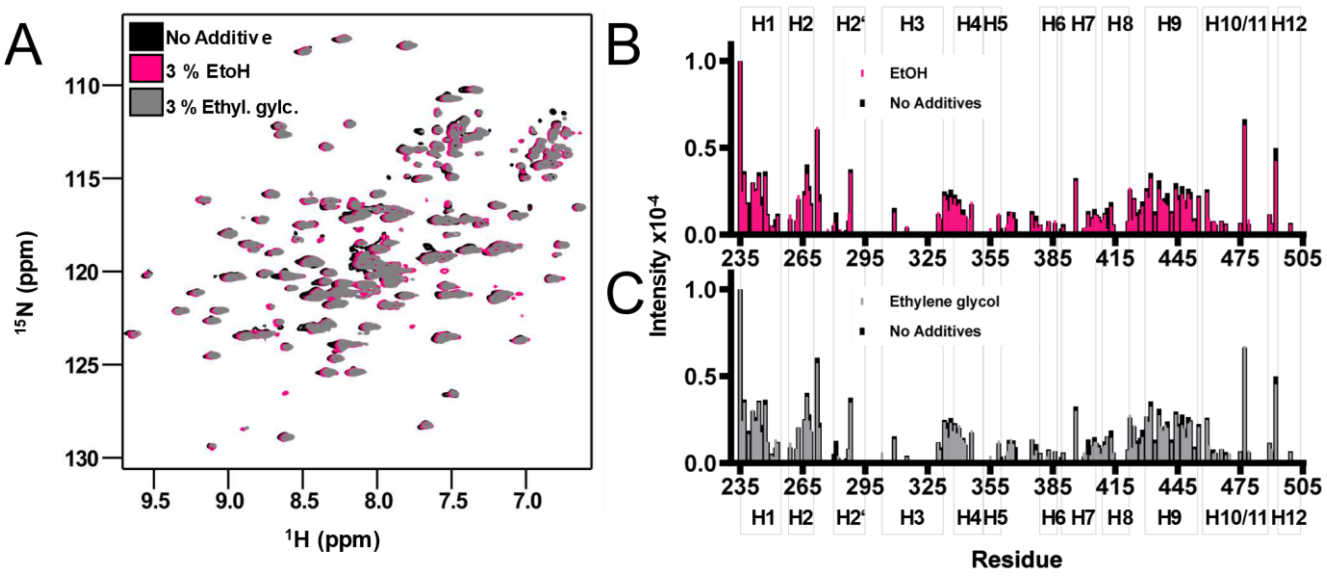

Supplemental Figure S1. **Direct interactions of ethanol and ethylene glycol with PPARγ LBD**. NMR spectroscopy was performed using PPARγ LBD and either ethanol or ethylene glycol. (**A**) ^{15}N-HSQCs of the PPARγ LBD together with ethanol or ethylene glycol. (**B**-**C**) Peak intensity profile of the free PPARγ LBD compared to PPARγ LBD with added (**B**) ethanol or (**C**) ethylene glycol.

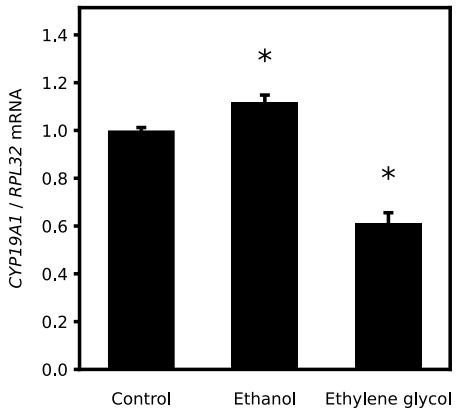

Supplemental Figure S2. **Aromatase mRNA level in response to chemical exposure in serum-free conditions**. Gene expression analysis of aromatase (*CYP19A1*) was performed by RT-qPCR. Differentiated A41 cells were treated for 24 h with 1% ethanol or ethylene glycol. The graphs present means ± SEM (n = 3). Asterisk (*) indicates statistically significant difference compared to control cells using Dunnett's test ($p < 0.05$).

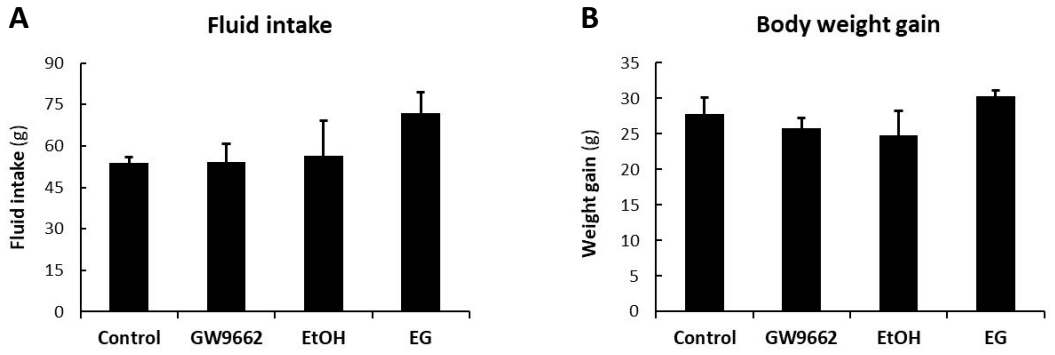

Supplemental Figure S3. **Average daily fluid intake and 12-day body weight gain**. (**A**) Average fluid intake per cage per day during the two experimental days (n = 3). (**B**) Average body weight gain over the period of 12 days that the animals were in the facility, including the 2 experimental days (n = 5-6). The graphs present means ± SEM. Dunnett's test revealed no statistically significant differences compared to control rats ($p < 0.05$).

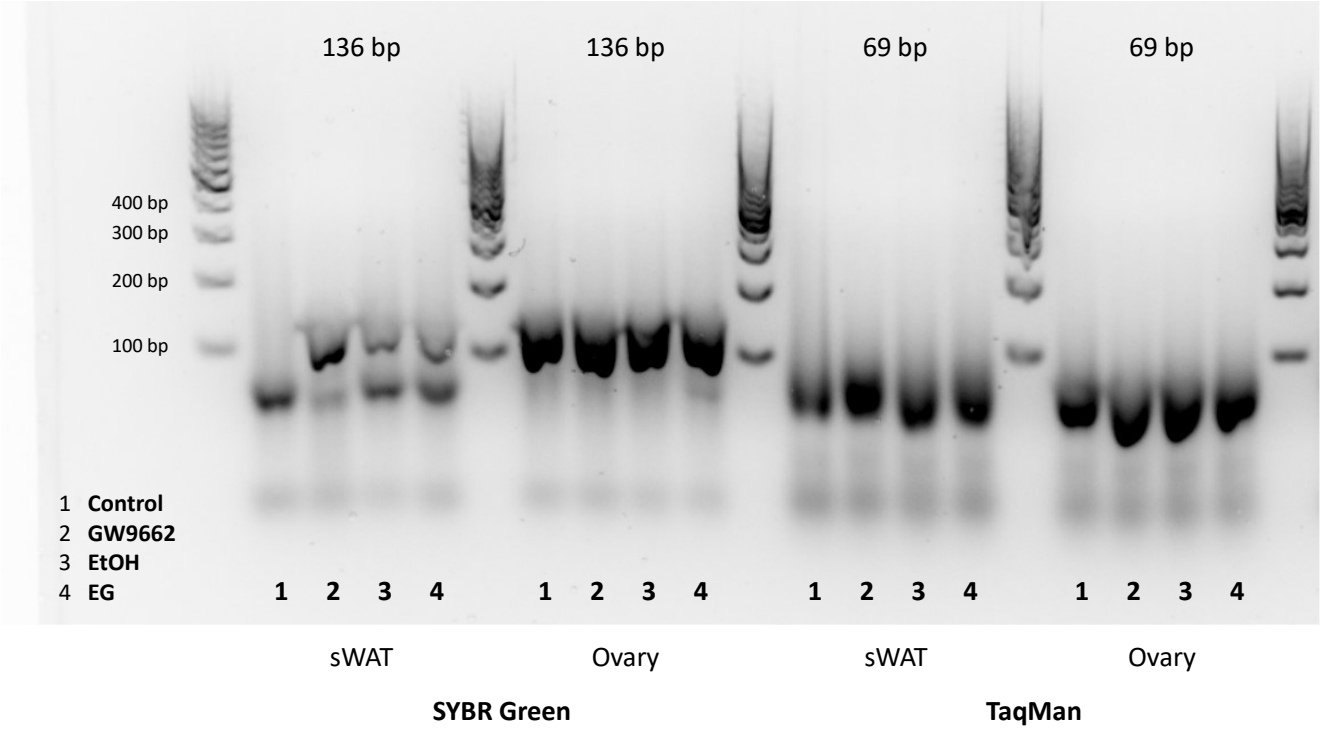

Supplemental Figure S4. **Specificity of aromatase cDNA amplification**. Agarose gel electrophoresis of *Cyp19a1* qPCR products from subcutaneous adipose tissue and ovary of a rat from each experimental group. SYBR Green or TaqMan methods were used for amplification.

Discussion

Identification of PPARγ antagonists among exogenous chemicals

The first aim of this project was assessed mostly in Manuscript I. It was hypothesized that various environmental and occupational chemicals could be identified as PPARγ antagonists. The Tox21 project has screened a large number of chemicals in HEK293 cells for effects on PPARγ activity, and many PPARγ agonists and antagonists were identified in these high-throughput screening assays. Almost twice as many chemicals were found to be antagonists of PPARγ than agonists.[5] Nevertheless, it is important to perform orthogonal assays using different reporters in the same cell line to determine if the tested compounds are showing PPARγ-mediated activity and exclude that observed effects are caused by assay interference. Additionally, it is critical to measure cytotoxicity in antagonist assays to avoid false positive results due to lower cell number or non-specific downregulation of the proteins involved in the reporter system. During selection of PPARγ antagonists for orthogonal reporter assay, the Tox21 cytotoxicity counterscreen was taken into consideration to avoid false positives. In contrast, interference by compound fluorescence and luciferase inhibition were not investigated prospectively. Two of the selected chemicals (fluorescein and 1-nitropyrene), which were expected to be PPARγ antagonists, were later discovered to be false positives due to compound fluorescence and instead served as negative controls. Regrettably, luciferase inhibitory activity of several chemicals led to inconclusive results in the orthogonal assay. This could have been avoided if luciferase inhibition had been considered during chemical prioritization and different chemicals could have been selected. Apparently, the importance of considering assay interference in reporter assays was also overlooked in another recent study on PPARγ antagonists.[175]

The orthogonal assay was performed using HEK293 cells, and the results were highly consistent with the results of the Tox21 PPARγ antagonist reporter assay. Generally, there was reasonable correlation between the AC_{50} values from the Tox21 assay and the IC_{50} values from the experiment in the present study. However, this was only the case after exclusion of chemicals that interfered with the assay based on a retrospective analysis for compound fluorescence and luciferase inhibition. An LDH cytotoxicity assay was performed in parallel to the reporter assay but, in some cases, it did not detect what looked like cell death in the microscope. For example, dasatinib dichloro impurity was not cytotoxic in the LDH assay, despite microscopy clearly showing detachment and aggregation of cells exposed to concentrations higher than 0.5 µM (Manuscript I, Supplemental Figure S4). Out of the 30 tested PPARγ antagonists, 8 were luciferase inhibitors, 2 were fluorescent at 485/535 nm, and 2 were cytotoxic. The number of luciferase inhibitors was surprisingly high considering that the frequency of luciferase inhibitors has been reported to be only about 3%.[176] An explanation could be that there are some common structural characteristics between them and PPARγ antagonists causing an enrichment of luciferase inhibitors among the selected PPARγ antagonists.

In the reporter assay, PPARγ activity was induced by rosiglitazone to allow detection of antagonistic effects, as there was almost no basal activation of PPARγ. Another way to activate PPARγ could be using endogenous ligands, such as fatty acids or prostaglandins, as done in other studies.[177] This would be a more physiologically relevant approach to study effects of xenobiotics on activated PPARγ. Also, if the ultra-sensitive PPARγ reporter cell line from Signosis had been used, antagonistic effects on the basal PPARγ activity could possibly have been detected. Alternatively, it could be useful to test chemicals in a reporter assay using PPREs and the full-length PPARγ rather than the PPARγ-GAL4 fusion protein. This was previously done in a screening of organic solvents for effects on PPARγ activity in transiently transfected HEK293 cells,[22] but it can also be done in stably transfected cells. For example, a stable human PPRE-driven reporter system has been developed based on the T24/83 human bladder carcinoma cell line.[177] This cell line expresses sufficient levels of endogenous PPARγ and RXRα, and therefore reflects the natural conditions in cells.[177] Instead of firefly luciferase, the expressed reporter is NanoLuc, which is superior in terms of sensitivity and stability.[178]

A similar reporter cell model was generated using the human primary ASCs from Manuscript II. The cells were transduced with a PPRE lentiviral reporter vector (pGreenFire1-PPRE, TR101VA-P, System Biosciences) to study PPARγ activity in response to chemical treatment in adipocytes. ASCs from six study participants (1, 2, 8, 9, 11, and 12) were successfully transduced and cryopreserved. However, reporter studies were never conducted

because of limited time in the laboratory of Kristy A. Brown and because the cells were difficult to transduce and required extensive optimization and puromycin selection. In these cells, both luciferase and green fluorescent protein (GFP) are expressed as reporters, enabling luciferase reporter assays as well as fluorescence microscopy. Figure 6 shows the intensity of GFP in untransduced ASCs, transduced ASCs, and transduced ASCs on day two of differentiation.

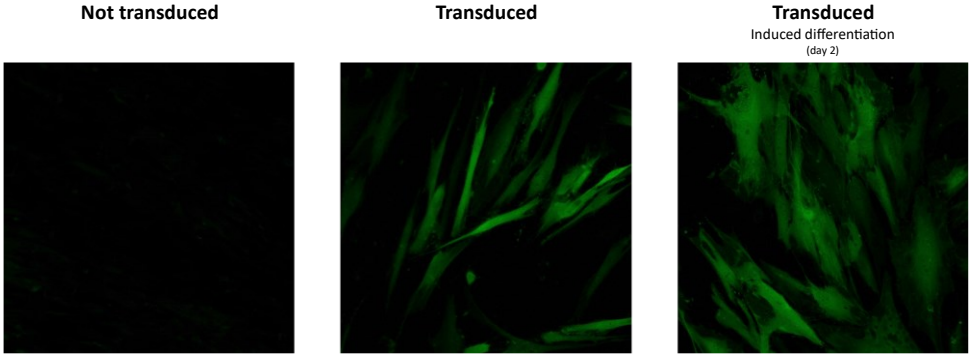

Figure 6: **Primary human ASCs transduced with a PPRE reporter system**. Confocal microscopy images show green fluorescent protein (GFP) intensity in green for untransduced cells, transduced cells, and transduced cells that were induced to differentiate for two days.

An advantage of using the full-length PPARγ for reporter assays is that it also allows study of the Pro12Ala variant, which potentially alters the effects of ligands binding. In the primary ASCs, cells from study participant 11 (Pro12Ala heterozygote) could be compared to the homozygous major allele carriers. Alternatively, wildtype PPARγ could be changed to PPARγ Pro12Ala using site-directed mutagenesis before transfection of cells, or the Pro12Ala mutation could be introduced in the *PPARG* gene of cells using the CRISPR/Cas9 technology.

There are many inconsistencies in the literature regarding the effect of PPARγ ligands on PPARγ transcriptional activity. These inconsistencies may arise from, for example, the use of different cell lines or different reporter systems. In contrast to the Tox21 PPARγ reporter assay, which shows that piperine, butylparaben, and zoxamide inhibit PPARγ activity in HEK293 cells, other studies have shown these chemicals activate PPARγ in mouse cardiac fibroblasts,[179] human osteosarcoma U-2 OS cells,[80] and monkey kidney COS7 cells,[104] respectively. This necessitates assessment of chemical interactions with PPARγ using other methods to support reporter assay studies. Examples include thermal shift assay (TSA),[180] 8-anilino-1-naphthalenesulfonic acid (ANS) fluorescence quenching assay,[180] fluorescence anisotropy assay,[81] isothermal titration calorimetry (ITC),[181,182] surface plasmon resonance (SPR) analysis,[94,181,182] X-ray crystallography,[182–184] and NMR spectroscopy.[182,184] Complementing cell-based reporter assays with one or more of these biophysical techniques will help confirm that observed effects on transcriptional activity are caused by direct binding, rather than indirect mechanisms. Some of the techniques have high-throughput capability, while others can provide additional information, such as details about the binding mode or affinity.

Using NMR spectroscopy, Daniel Saar and Birthe B. Kragelund from UCPH showed that the control PPARγ antagonist GW9662 and the industrial chemical DEHPA directly interact with PPARγ and inhibit its activity in a similar manner. DEHPA was interesting because it is a high-production volume chemical,[185] it was the only nonaromatic compound among the chemicals studied in this project, and it was functionally similar to GW9662 in the *in vitro* assays of Manuscript II (discussed later). Another method applied to corroborate the findings of the PPARγ reporter assay was a computational procedure called molecular docking, which can predict the affinity of ligands to the binding pocket of PPARγ. All of the 30 antagonists were, together with rosiglitazone, examined in molecular docking simulations (using VirtualToxLab) performed by Martin Smieško from the University of Basel to investigate if the compounds were likely to bind to the ligand-binding pocket of PPARγ. This revealed that only two of the antagonists (bupirimate and pyridaben) were predicted unlikely to be ligands of PPARγ, while the rest were predicted to bind with different affinities (Manuscript I, Supplemental Table S5). The three chemicals that were inactive as PPARγ ligands in reporter assays (fluorescein, trimebutine, and 1-nitropyrene), were among the chemicals predicted to bind the PPARγ ligand-binding pocket, indicating that there was some uncertainty associated with the molecular docking predictions. It would have been better if the molecular

docking simulations had been performed using the antagonist conformation of PPARγ rather than the agonist conformation. The successor of the VirtualToxLab tool is called PanScreen (https://www.panscreen.ch/) and is currently under development. It will support all potential modes of action in the protein ensemble for PPARγ.

The good accordance between the Tox21 PPARγ antagonist assay and the reporter assay in the present study suggests that the Tox21 assay results are reproducible and that the tested compounds show PPARγ-mediated activity. Therefore, the dataset from the Tox21 PPARγ antagonist study was used by Eva Bay Wedebye, Ana C. V. E. Nissen, and Nikolai Georgiev Nikolov from DTU Food to construct quantitative structure-activity relationship (QSAR) models for prediction of additional PPARγ antagonists. The model with potency cut-off at 10 µM predicted thousands of active PPARγ antagonists, which can be selected based on annual tonnage and/or biopersistence and subsequently screened with a tool, such as PanScreen, to predict PPARγ affinities and binding modes. Finally, chemicals can be selected for *in vitro* or *in vivo* studies.

Some of the compounds that were shown to be antagonists in both Tox21 and Manuscript I reporter assays, as well as ligands in the molecular docking simulations, were tested in Manuscript II in an adipogenesis assay to determine their effect on PPARγ in ASCs. All tested chemicals (GW9662, zoxamide, pyraclostrobin, Cosan 528, Violet Cibacet 2R, diphenyl phthalate, and DEHPA) to some degree blocked adipogenesis, indicating inhibition of PPARγ, which was consistent with reporter assays and molecular docking. Furthermore, the chemicals had different effects on lipid droplet number per cell and lipid droplet size, indicating that the interactions of the chemicals with PPARγ differed to some extent and/or the chemicals exhibited different off-target effects influencing adipogenesis in various ways.

The *in vitro* studies assessing effects of exogenous chemicals on PPARγ activity were all performed in the presence of the PPARγ activator, rosiglitazone. Reporter assays, adipogenesis assays, and NMR spectroscopy showed inhibitory effects on rosiglitazone-stimulated PPARγ activity or adipogenesis, indicating competition for the PPARγ binding pocket. However, common environmental and occupational chemical mixtures have not been studied in this project. The effects of chemical mixtures on PPARγ activity and adipogenesis have been investigated before,[105,107,111,112] and could be highly relevant to study in adipose tissue to investigate the effect on aromatase expression.

In conclusion, the results suggest that there are numerous PPARγ antagonists present in the environment, including the working environment, and that these can be identified using a combination of *in silico* and *in vitro* methods. The developed PPARγ antagonist QSAR model can predict potential PPARγ antagonists, which can then be tested *in vitro* for PPARγ antagonism and potential adverse effects.

Influence of PPARγ antagonism on aromatase expression and estrogen production

In Manuscript II, the second aim of the project was assessed. Here, it was hypothesized that exposure to PPARγ antagonists upregulates aromatase expression and thereby increases the synthesis of estrogen. It has been demonstrated previously that undifferentiated ASCs express more aromatase than differentiated ASCs,[186] which was also shown in Manuscript II.

As previously mentioned, all seven chemicals tested in the adipogenesis assay inhibited adipogenesis in human primary ASCs. The impaired adipogenesis was subsequently shown to be associated with elevated aromatase expression, suggesting that as a mechanism through which PPARγ antagonists can induce aromatase. Supporting this, removal of the adipogenic medium during differentiation also resulted in higher aromatase expression compared with cells that were kept in adipogenic medium. This suggested that the adipogenic agents, including rosiglitazone, caused a repression of aromatase throughout adipogenesis.

It could be interesting to study PPARγ antagonist effects during adipogenesis induced by typical dietary fatty acids,[187] instead of rosiglitazone, as well as lower concentrations of other adipogenic factors.[188] A recently study proposed that superphysiological concentrations of the components of the adipogenic medium may have detrimental effects on adipocyte function.[188] A more physiologically relevant induction of adipocyte differentiation may also allow for better detection of both inducers and inhibitors of adipogenesis. Strongly

inducing adipogenesis using a high rosiglitazone concentration will usually result in identification of inhibitory effects,[94] while leaving rosiglitazone out of the differentiation medium will more easily reveal activators of adipogenesis.[189]

The adipogenesis protocol for the A41 and C3H10T1/2 cell lines in Manuscript II may have been too strong to properly detect PPARγ inhibition, as GW9662 treatment minimally affected adipogenesis in these cell lines. In A41 cells, adipogenesis could be inhibited enough to observe increased aromatase expression, whereas in C3H10T1/2 cells there was no effect of GW9662 at concentrations lower than 10 µM. While GW9662 is relatively specific to PPARγ, other tested chemicals may exhibit off-target effects or cytotoxicity at this concentration. Therefore, it is probably better to optimize the differentiation protocol to be more sensitive to treatment than expose cells to excessive concentrations of test chemicals.

Improvements that could be made to better detect PPARγ antagonist effects on adipogenesis include starting antagonist treatment before induction of adipogenesis rather than concurrently, using a less strong and more physiologically relevant adipogenesis protocol (as already discussed), replacing the culture medium with for example low-glucose or serum-free medium, and renewing medium with test chemical more often. For instance, the half-life of GW9662 in cell culture is less than 10% of the half-life of rosiglitazone,[7] and changing medium more often during adipogenesis may therefore enhance the anti-adipogenic effect of GW9662.

It was investigated if the PPARγ antagonists could affect aromatase expression in A41 cells by short-term treatment which does not influence the degree of differentiation. FSK/PMA was used as a positive control for aromatase induction in A41 adipocytes. Rosiglitazone treatment downregulated aromatase expression in A41 ASCs, which is consistent with previous results showing that troglitazone downregulates FSK/PMA-induced aromatase expression in human primary ASCs.[17] An experiment without replicates was performed to reproduce the finding that aromatase upregulation by FSK/PMA could be reversed by 24 h thiazolidinedione treatment in human primary ASCs (Figure 7).

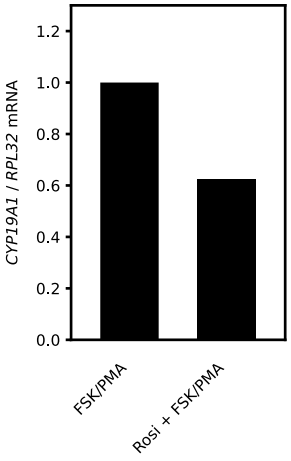

Figure 7: **Aromatase expression in FSK/PMA-stimulated human primary ASCs co-treated with vehicle or rosiglitazone**. Cells were treated for 24 h in serum-free conditions, and the chemical concentrations were with 1 µM forskolin (FSK), 4 nM PMA, and 10 µM rosiglitazone.

PPARγ antagonists had no effect on aromatase in ASCs, most likely because of the low PPARγ expression in this cell type (as shown in figure 3 in Manuscript II). In contrast, there was an upregulation of aromatase expression when treating mature PPARγ-expressing A41 adipocytes with antagonists except in response to diphenyl phthalate. A single experiment was also performed in SGBS adipocytes which were treated for 24 h with 5 µM GW9662 and compared with vehicle-treated control cells (Figure 8). Consistent with the results in A41 cells, there seemed to be an increase in aromatase expression in response to GW9662. There was no effect on *PPARG*, but a decrease in the PPARγ target gene *ADIPOQ*, suggesting that PPARγ activity but not expression was inhibited.

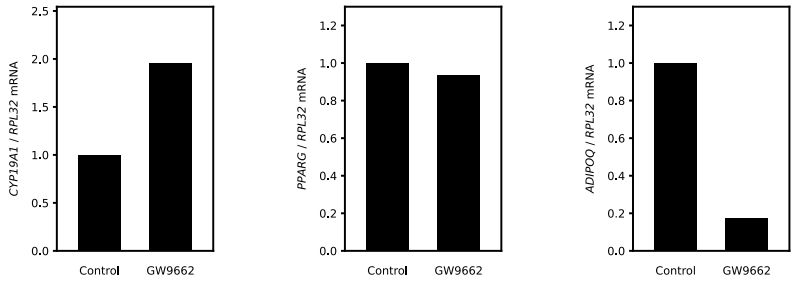

Figure 8: **Acute treatment of differentiated SGBS cells with GW9662**. Mature SGBS adipocytes were treated for 24 h with 5 µM GW9662 or vehicle (DMSO). Gene expression analysis of *CYP19A1*, *PPARG*, and *ADIPOQ* was performed by RT-qPCR (n = 1).

The reason why a PPARγ agonist and not an antagonist has an effect in the PPARγ-lacking ASCs is likely because agonists stimulate the expression and activity of PPARγ whereas antagonists do not have any effect due to the

already low PPARγ expression and activity. This is supported by a study showing increased expression of the PPARγ target gene *Fabp4* in response to 24 h rosiglitazone treatment in 3T3-L1 pre-adipocytes.[190] Although adipocytes constitute more than 90% of the adipose tissue volume, less than 15% of the cells are adipocytes.[191] In breast adipose tissue explants, which consist of various cell types including ASCs and adipocytes, the effect of rosiglitazone treatment on aromatase expression resembled the rosiglitazone-stimulated effects observed in ASCs and adipocytes. In response to GW9662 treatment, there was a tendency to increased aromatase expression, but it was statistically insignificant, likely due to the low number of biological replicates.

Activation of RXR was stimulated with 9-*cis*-retinoic acid to test if this heterodimeric partner of PPARγ was involved in the regulation of aromatase. As expected, the effect was similar to the effect of rosiglitazone in A41 pre-adipocytes. However, in mature A41 adipocytes, there was no effect. RXR heterodimerizes with other nuclear receptors than PPARγ, such as RAR. Activation of the RAR:RXR complex has been shown to induce aromatase expression.[192,193] It has been shown that specifically RARα upregulates aromatase via the retinoic acid response element 2 (RARE2) in the aromatase promoter I.4 region.[194] An increase in RARα expression after differentiation has been observed,[195] suggesting a greater effect at that stage. Retinoic acid treatment also downregulates PPARγ in 3T3-L1 cells, both at the protein[196,197] and mRNA level,[198] which is expected to have a greater effect at the mature adipocyte stage than in the pre-adipocytes. This may explain the lack of effect in adipocytes. It could have been interesting to investigate the combined treatment of rosiglitazone and retinoic acid to determine if there were synergistic effects.

Diphenyl phthalate was the only tested PPARγ antagonist that did not acutely upregulate aromatase in A41 adipocytes. Diphenyl phthalate has been shown to exhibit weak estrogenic activity[199,200] and may repress aromatase like other xenoestrogens, including phytoestrogens.[136,201,202] It may thus be involved in the regulation of aromatase through both PPARγ-dependent and -independent mechanisms. Pyraclostrobin was the antagonist causing the greatest induction of aromatase. Previous studies on this pesticide show conflicting results in relation to the effect on PPARγ. Pyraclostrobin has been shown to have no effect on mouse PPARγ LBD activity,[104] but a tendency to decreased basal human PPARγ LBD activity in HEK293 cells (Manuscript I).[5,203] Furthermore, pyraclostrobin has been found to downregulate *Pparg* and PPARγ target genes in differentiating 3T3-L1 cells,[203] which maintained a fibroblast-like morphology, increased lipid accumulation,[105,106] and altered lipid droplet morphology after differentiation.[203] In the adipogenesis assay of Manuscript II, pyraclostrobin reduced lipid accumulation in primary human ASCs via both decreased lipid droplet number and size. However, whether PPARγ-independent mechanisms contributed to this effect is unknown.

The use of multiple known PPARγ agonists and antagonists, ideally from different chemical classes, as controls for increased and decreased PPARγ activity would confirm that effects on aromatase are PPARγ-mediated. In addition to rosiglitazone, the synthetic agonist GW7845[182] or the endogenous agonist 15-deoxy-$\Delta^{12,14}$-prostaglandin J_2 (15d-PGJ2),[181] could be used to activate PPARγ. Additional antagonists could include SR1664[184] or SR11023.[183] It could also be interesting to study if biologically relevant concentrations of endogenous and dietary PPARγ agonists, such as fatty acids, repress aromatase expression. Co-treatment of cells with a PPARγ antagonist could address how aromatase expression is affected by disruption of a physiological activity level of PPARγ. In cell culture, addition of FBS provides only a very small fraction of the fatty acids available to cells in the body.[204]

Apart from using diverse PPARγ ligands, knockdown or overexpression of *PPARG* can be performed to determine if observed effects are dependent on PPARγ. Knockdown of PPARγ was attempted in A41 adipocytes by forward or reverse transfection with *PPARG*-targeting siRNA (s10888, Invitrogen), but neither worked despite being performed in parallel with successful *PPARG* overexpression and despite other studies showing positive results with this siRNA.[205,206] As an alternative to siRNA-mediated knockdown, overexpression of a dominant-negative PPARγ variant could have been applied as a method to inhibit PPARγ function.[34] The results from *PPARG* overexpression in A41 pre-adipocytes showed that upregulation of *PPARG* reduced aromatase expression, either with or without subsequent rosiglitazone treatment, suggesting that PPARγ is involved in the regulation of aromatase. Therefore, the effects observed by PPARγ antagonist treatment are also likely PPARγ-dependent.

In addition, the previously mentioned NMR spectroscopy by collaborators confirmed binding of DEHPA to the ligand-binding pocket of PPARγ, inhibiting its function in a manner similar to GW9662. The inhibitory effect of DEHPA on PPARγ is supported by rodent studies showing that oral exposure to DEHPA decreased body weight gain and serum alanine aminotransferase (ALT).[185] Similar effects have been reported in response to GW9662.[207,208] In addition, DEHPA treatment decreased serum levels of luteinizing hormone (LH) and follicle-stimulating hormone (FSH) in males,[185] which has also been shown to occur in response to pituitary-specific deletion of *Pparg*, although the effect on LH was not statistically significant.[209] Finally, a tendency to increased serum estradiol appeared in response to DEHPA exposure (not significant),[185] which is consistent with increased adipose tissue aromatase expression in response to PPARγ antagonists (Manuscript II), including ethanol (Manuscript III).[142]

The effect of xenobiotics on aromatase may not always occur via direct PPARγ interaction. Aromatase can potentially be regulated indirectly by effects on PPARγ endogenous ligand production or expression, or by effects on PPARγ turnover. Chemical treatment may also indirectly induce post-translational modifications, which can influence PPARγ function. In addition, PPARγ-independent effects may contribute to the regulation of aromatase. It is possible that some chemicals act through a combination of such effects.

It was challenging to assess the influence of PPARγ Pro12Ala on the response to PPARγ antagonists due to the limited number of study participants with the minor allele and the substantial biological variation among cells isolated from different individuals. The use of cells from different subcutaneous adipose depots probably increased variation further. Chemical-induced effects were observed both in cells with the common Pro12 variant and in cells heterozygous for the Ala12 variant. Creation of a human pre-adipocyte cell line with the PPARγ Pro12Ala variant using CRISPR/Cas9 gene editing could be interesting as it would allow direct comparison of adipogenic capacity and aromatase expression to the wildtype cells, both in the basal state and in response to various environmental and occupational chemicals as well as chemical mixtures. Such a cell line has not been generated before and would be a useful tool for studying this common PPARγ SNP.

A disadvantage of the experiments in this project is that all aromatase measurements are at the mRNA level. It would have been better to also study aromatase at the protein level. Three different aromatase antibodies were tested in immunoblotting of pre-adipocyte and adipocyte lysates, but the antibodies produced many unspecific bands. An advantage of using RT-qPCR to measure aromatase expression is that the abundance of separate transcript variants can be measured using different primer pairs to get insight into the mechanism of aromatase regulation. All 11 aromatase transcript variants encode the same aromatase protein.

Several research groups have demonstrated a good correlation between protein and mRNA levels of aromatase and estrogen production. In SGBS cells, aromatase mRNA and protein levels, as well as the level of secreted estrogen, have been shown to be comparable in response to different treatments.[210] Aromatase mRNA and protein levels were also similarly affected by treatments in primary mouse preadipocytes isolated from the inguinal mammary gland.[210] Furthermore, it has been shown in human primary adipose stromal cells that PPARγ agonist-induced repression of aromatase mRNA is associated with reduced aromatase activity,[17] suggesting that changes in aromatase mRNA can be anticipated to lead to equivalent changes in local estrogen production. Also, the mRNA expression pattern of aromatase across breast cancer cell lines correlates well with the aromatase activity levels.[211]

The human H295R adrenocarcinoma cell line was used to investigate the effect of PPARγ antagonism on estrogen production. The steroid hormones secreted into the medium were analyzed by Mikael Pedersen from DTU Food. The positive control forskolin increased the levels of all measured steroid hormones, including estrone and estradiol, while the negative control prochloraz decreased the levels of most hormones, including estrone. However, as PPARγ control ligands rosiglitazone and GW9662 had no effects on steroidogenesis, the results suggest that the altered hormone levels in response to pyridaben, pyraclostrobin, and diphenyl phthalate were PPARγ-independent. The protein level of PPARγ was low in this cell line, which could explain the lack of effects in response to rosiglitazone and GW9662. Thus, the H295R cell line was not a good model for studying effects of PPARγ ligands. Instead, estrogen production by ASCs or adipocytes could be measured in response to PPARγ

ligands, although this would likely require supplementation of the androgenic steroid substrate, either androstenedione or testosterone.

In summary, the results show that the PPARγ antagonists GW9662, zoxamide, pyraclostrobin, Cosan 528, Violet Cibacet 2R, diphenyl phthalate, and DEHPA inhibit adipogenesis in human primary ASCs, which was associated with increased aromatase expression. In addition, short-term treatment with GW9662, pyraclostrobin, DEHPA, and kresoxim-methyl caused an induction of aromatase mRNA. Together, these data demonstrate that inhibition of PPARγ activity by environmental chemicals elevates aromatase transcription through impaired adipogenesis and through a short-term mechanism, which is consistent with PPARγ being a repressor of aromatase.

Impact of ethanol and ethylene glycol on PPARγ activity and aromatase expression

Manuscript III addressed the final aim of the project. The hypothesis was that exposure to the chemicals, ethanol and ethylene glycol, leads to increased aromatase expression by inhibiting PPARγ. Ethanol has a wide range of uses across many industries and is the primary psychoactive component of alcoholic beverages. Ethylene glycol is a high-production-volume alcohol that is also used in various industrial applications. Previous studies suggest that exposure to these chemicals can inhibit PPARγ activity[21,22] or expression.[212–214]

In this study, it was first investigated if and how ethanol and ethylene glycol interact with the ligand-binding domain of PPARγ. These alcohols are significantly smaller than the typical PPARγ ligand. It has been suggested that ethanol binding to some proteins is better characterized by an interaction region that can accommodate multiple molecules of ethanol.[215] As the ligand binding pocket of PPARγ is one of the largest among the nuclear receptors,[216] it allows for promiscuous binding of various low-affinity ligands.[36] Using NMR spectroscopy, Daniel Saar and Birthe B. Kragelund from UCPH showed that ethanol and ethylene glycol had no effect on the basal PPARγ state. When added in combination with rosiglitazone, the results showed a slightly altered activity, most likely a direct inhibitory effect on the rosiglitazone-induced PPARγ activation. The effect was weak, and therefore it is difficult to know whether it is biologically significant.

Ethanol exposure is known to affect a great number of functions in the body,[217–220] suggesting that PPARγ may be one of many molecular targets. This makes it difficult to distinguish between potential PPARγ-dependent and -independent mechanisms. Complicating things further, ethanol and ethylene glycol are oxidized into aldehydes by alcohol dehydrogenase (ADH) and further oxidized into carboxylic acids by aldehyde dehydrogenase (ALDH). These metabolites may also affect functions in the body. For example, acetaldehyde is the primary metabolite of ethanol and is highly reactive.[221,222] It has a range of health effects, although its contribution to the effects of alcohol consumption is still unknown.

In relation to breast cancer, PPARγ Pro12Ala was reported to modify the effect of alcohol intake such that only homozygous major allele carriers were at increased risk of breast cancer when drinking alcohol, while variant allele carriers were not at increased risk.[20,21] The observed interaction between alcohol intake and the PPARγ polymorphism Pro12Ala strongly suggests that PPARγ and alcohol intake are part of the same biological mechanism-of-action of alcohol-related breast cancer.[20,21]

Multiple *in vivo* studies have shown that PPARγ plays a role in mammary cancer. Inhibition of PPARγ signaling by GW9662 ingestion,[64] heterozygous *Pparg* knockout,[60] adipocyte-specific *Pparg* knockout,[61] or mammary gland-directed expression of dominant-negative Pax8PPARγ fusion protein[62] accelerates DMBA-induced mammary tumorigenesis in mice. The exact mechanism is not known, but it is hypothesized that impaired PPARγ function causes a derepression of aromatase, leading to increased estrogen biosynthesis and risk of breast cancer. Here, the aim was to investigate the effects of ethanol and ethylene glycol on adipogenesis and aromatase expression in adipose tissue culture and rat adipose tissue.

An adipogenesis assay was performed in Manuscript III by measuring *Pparg* and other adipocyte markers in C3H10T1/2 cells. The results revealed that adipogenesis was inhibited in response to both ethanol and ethylene glycol. The degree of inhibition observed in response to ethanol was lower than that of ethylene glycol. The concentrations and choice of the adipogenic induction chemicals have been shown to greatly influence the

extent of differentiation,[188] and in Manuscript II the concentration of rosiglitazone also influenced the response to some chemical treatments. In C3H10T1/2 cells, it was found that a high concentration (10 µM) of GW9662 was necessary to see any effect on adipogenesis. However, when reducing the concentrations of prodifferentiative agents used in the adipogenic medium to one fifth, the effect of GW9662 treatment on adipogenic markers significantly increased. Therefore, when testing the anti-adipogenic effect of the alcohols in Manuscript III, the concentrations of prodifferentiative agents used in the adipogenic medium were one fifth of those in the standard protocol. If treatments had been started 2 days before induction of adipogenesis, as reported before,[223] they may have had an even greater impact on adipogenesis. When lipid accumulation in response to ethanol was measured in primary human ASCs after 12 days of differentiation, ethanol treatment appeared to have a stronger inhibitory effect on adipogenesis than in the C3H10T1/2 cells. However, the lack of effect of rosiglitazone concentration suggests that a PPARγ-independent mechanism of ethanol contributed to the impaired adipogenesis.

Together, the experiments indicate that ethanol and ethylene glycol inhibit PPARγ activity or expression, possibly through a direct interaction with PPARγ, resulting in impaired adipogenesis. Indirect effects may contribute to the anti-adipogenic effect. For example, ethanol has been shown to inhibit insulin action,[224] which can affect adipogenesis because insulin is an activator of C/EBP-β and -δ in the initial stages of adipogenesis, inducing the transcription of PPARγ.[41] In Manuscript II, inhibition of adipogenesis was linked to increased aromatase expression, suggesting that ethanol and ethylene glycol may induce aromatase via the mechanism of impaired adipogenesis.

The acute effects of ethanol and ethylene glycol on adipose aromatase expression *in vivo* and *in vitro* were investigated next. *In vitro*, *ADIPOQ* and *FASN* were used as measures of PPARγ activity. The effect of ethanol on aromatase expression was similar to the effect of the control antagonist of PPARγ, GW9662. This indicates that the induction of aromatase in response to ethanol was mediated by PPARγ. Ethylene glycol exposure, on the other hand, produced a decrease in aromatase expression, which was unexpected because ethylene glycol appeared to inhibit PPARγ activity to a greater extent than similar concentrations of ethanol, both when C3H10T1/2 cells were treated during adipogenesis and when A41 adipocytes were treated for 24 h. When the acute ethylene glycol treatment was repeated in serum-free conditions, to exclude that the effect was caused by interactions with the serum, similar effects were observed. There was also a decrease in aromatase mRNA at the pre-adipocyte stage, where *PPARG* is lowly expressed, suggesting that the observed effect of ethylene glycol on aromatase mRNA was PPARγ-independent. Since ethylene glycol functions as a PPARγ antagonist, it is still possible that it can elevate aromatase via PPARγ-mediated inhibition of adipocyte differentiation or acutely in response to lower and more physiologically relevant exposure concentrations. From the studies on ethanol and ethylene glycol, it can not be concluded whether the observed effects in response to these chemicals occur as a result of direct action on PPARγ or as a consequence of PPARγ being inhibited or downregulated via an indirect mechanism. However, the results suggest involvement of PPARγ as its expression or activity markers were inhibited in response to ethanol or ethylene glycol exposure.

The animal study showed that female rats exposed to GW9662, ethanol, or ethylene glycol orally for two days did not exhibit altered gene expression of aromatase- and PPARγ-related genes in adipose tissue, although there was a statistically insignificant tendency to increased aromatase expression in response to GW9662. GW9662 was used as a control for PPARγ inhibition, and it was therefore surprising that no significant effects were observed. It is unlikely that the lack of effects was because of a too low basal PPARγ activation that could not be lowered, as a hazelnut-chocolate vehicle was administered to all animals before and during treatment. This was expected to induce PPARγ activity to some extent, like a high-fat diet,[225] and might increase the sensitivity to potential chemical-induced inhibitory effects on PPARγ and aromatase. A study in mice on a high-fat diet showed that a low GW9662 dose (0.5 mg/kg/day) administered in the drinking water had effects on the adipose tissue.[226] These mice, however, were treated for 12 weeks. The lack of effects in the animal study in Manuscript III may therefore be due to the short exposure duration.

In most rodent studies involving these chemicals, the exposure duration was several weeks.[142,212–214,226–228] GW9662 and ethanol have also been shown to affect gene expression acutely, however in those studies the

chemical was injected rather than given orally, which may increase bioavailability dramatically. In one study, male mice were injected intraperitoneally with 2 mg/kg GW9662 for 26 h, which abrogated the hippocampal effects of PPARγ activation by pioglitazone (1 mg/kg), including a pioglitazone-induced decrease in IL-6 protein level.[229] In another study, intraperitoneal injection of 3.5 g/kg ethanol in male and female rats affected gene expression in the brain after 3 h, for example elevating the mRNA expression of *Il6* in hippocampus and amygdala.[230] A third study showed that mice administered 1.8 g/kg ethanol intraperitoneally had altered gene expression in the hippocampus after 4 hours.

GW9662 has been shown to be metabolized rapidly and has a biological half-life of 7 min following intravenous administration of 2.5 mg/kg in rats.[231] Moreover, it has been suggested that GW9662 is metabolized by intestinal microbiota.[231] This could explain why the short treatment period had no effect. Ethanol and ethylene glycol are also metabolized, primarily in the liver, although at a lower rate.[222,232,233] If effects had been observed in response to treatment with these solvents, it would be difficult to know if they resulted from the action of the parent compound or from one or more metabolites. For example, acetaldehyde treatment of adipose tissue explants or 3T3-L1 adipocytes has been shown to decrease the levels of PPARγ protein and protein products of PPARγ target genes.[234] Ethanol is insoluble in lipids and distributes into tissues in proportion to their relative water contents.[235] The water content in adipose tissue is only about 5-20% whereas in most other organs it is 60-80%.[236] This suggests that if effects of ethanol had been observed in adipose tissue it could potentially have been an indirect result of effects on other organs.

Furthermore, any potential impact on gene expression in response to treatment may have been concealed by estrous cycle-controlled variations in Cyp19a1 expression,[237,238] as the adipose tissue undergoes significant gene expression changes during the estrous cycle.[239] For example, PPARγ expression in the adipose tissue fluctuates over the course of estrous cycle.[240,241] Therefore, it would have been better if the rats had been ovariectomized, as it could have revealed statistically significant changes in gene expression. Aromatase was very weakly expressed in rat adipose tissue, indicated by a lack of amplification in a significant number of the technical replicates. This low expression level of aromatase in adipose tissue likely also increased variation, making it difficult to detect differences between experimental groups. In some animals, aromatase was completely undetectable in the adipose tissue.

The genes *Fabp4* and *Adipoq* were selected as markers of PPARγ activity, while *Lep* and *Il6* were selected because of their reported effects on aromatase. The cytokine adiponectin is associated with reduced aromatase expression, while leptin and IL-6 are associated with increased aromatase expression.[242] GW9662 treatment has previously been shown to reduce serum adiponectin in mice[226] and increase leptin expression in adipose tissue of rats.[228] In mice, *Pparg*, *Fabp4* and *Adipoq* were decreased more than 10-fold in response to 0.1% GW9662 in the diet for 25 weeks.[64] Assuming that the food consumption of the mice was 15% of their body weight,[243] this dose of GW9662 corresponds to 150 mg/kg bw/day, which is 15 times higher (relative to body weight) than the dose used in the rat experiment in Manuscript III. The duration of exposure was also 87 times longer in the mouse study. The high dose and duration of exposure may explain the dramatic effects on gene expression.

Ethanol consumption for multiple weeks has been demonstrated to downregulate *Pparg*, *Fabp4*, and *Adipoq* and upregulate *Tnfa* and *Il6* in rodent adipose tissue.[213,214,244,245] The ethanol-stimulated downregulation of *Pparg* and upregulation of *Tnfa* and *Il6* in mouse adipose tissue was reversed by rosiglitazone treatment,[213] suggesting that ethanol may act PPARγ-dependently. In addition, consumption of 13% ethanol in drinking water for 8 weeks resulted in increased aromatase protein level in male rats.[142] Ethylene glycol administered at 0.75% in drinking water for 4 weeks has been shown to downregulate renal *Pparg* and increase serum TNFα and IL-6 in male rats.[212]

In the rat study of Manuscript III, positive correlations were observed among ΔC_t values of *Cyp19a1*, *Pparg*, *Adipoq*, *Fabp4*, and *Lep* in adipose tissue (Figure 9). *Pparg* also correlated with *Il6*, but not as strongly. The positive correlations between *Pparg*, *Adipoq*, *Fabp4*, and *Lep* were particularly strong. PPARγ is known to induce *Adipoq* and *Fabp4*, consistent with that observation. It has previously been shown that mRNA levels of *PPARG* and *LEP* are positively correlated in human adipose tissue,[246] despite PPARγ being a negative regulator of

leptin.[228,247,248] In 3T3-L1 cells, it was reported that IL-6 repressed *Pparg*, and PPARγ repressed *Il6*,[249,250] and in mouse liposarcomas, *Pparg* and *Il6* mRNA correlated positively.[251] Overall, these correlations observed in the adipose tissue of the rats from Manuscript III are consistent with the literature. However, the moderate positive correlation between *Cyp19a1* and *Pparg* or PPARγ-regulated genes was unexpected but may result from upregulation of *Cyp19a1* and *Pparg* by FSH, which has been shown to occur in rodent adipose tissue and may overrule the effect of PPARγ on aromatase.[252]

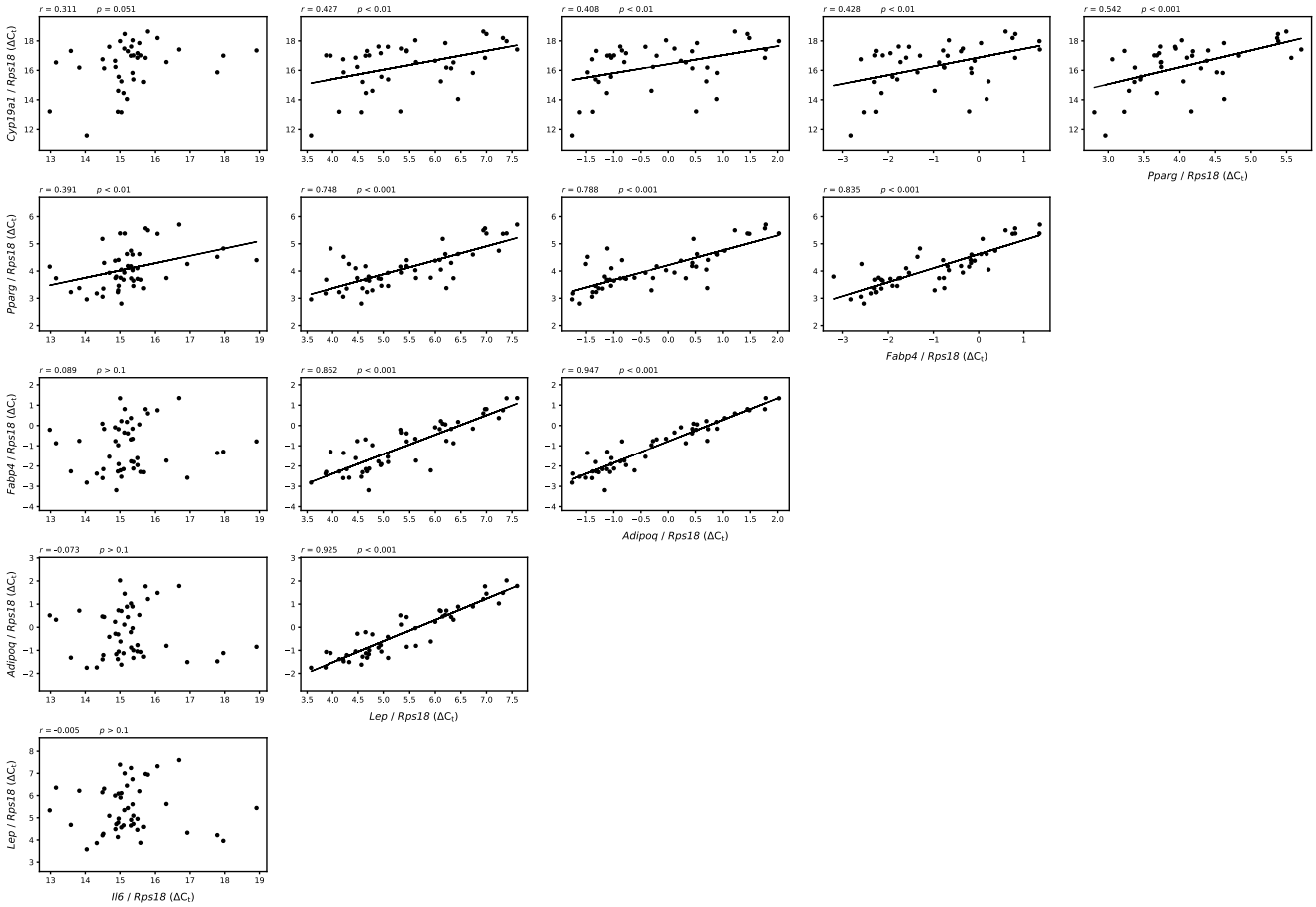

Figure 9: **Correlations between mRNA levels of different genes in WAT**. Scatter plots show correlations between the ΔC_t values for the measured mRNA's using Pearson correlation coefficient. Data from both subcutaneous and visceral adipose tissue are included. Linear regression lines are shown for significant correlations. Correlations were considered statistically significant when $p < 0.05$ and $r > 0.3$.

One animal in the ethanol group had an almost 5 times higher *Il6* expression in the ovary compared to the other animals, and the same animal expressed aromatase more than three-fold in visceral adipose tissue compared to the other animals. Although the visceral adipose tissue was not collected from the periovarian depot, the elevated adipose aromatase expression and ovarian *Il6* expression may still be related.

The female rats were not a good model for studying adipose tissue aromatase expression in response to PPARγ antagonists, because of potential interference from the estrous cycle and because rodents express very little aromatase in the adipose tissue. Ideally, male or ovariectomized female transgenic humanized aromatase mice would have been used.[253] The humanized mouse model mimics the human aromatase expression pattern and therefore expresses aromatase at a higher level in adipose tissue. [169]

In conclusion, ethanol and ethylene glycol appeared to inhibit PPARγ expression and activity *in vitro*, possibly via both direct and indirect mechanisms. In addition, both chemicals had anti-adipogenic activities. Ethanol induced aromatase expression in adipocytes acutely, which also have been observed for other PPARγ antagonists. Ethylene glycol reduced aromatase expression, and this was likely via a PPARγ-independent mechanism. The *in vivo* study showed no effects of the control chemical GW9662 or the organic solvents.

Conclusion

The primary objective in the project was to identify potential breast carcinogens that act by increasing estrogen biosynthesis in the adipose tissue through a PPARγ-mediated elevation of aromatase transcription.

PPARγ antagonist chemicals were selected from the Tox21 PPARγ antagonism assay and tested in an orthogonal reporter assay verifying inhibition of PPARγ. The importance of identifying assay interference was demonstrated since about a third of the tested chemicals caused some sort of interference with the assays. The reporter assay was supported by molecular docking simulations performed by a collaborator. Another group of collaborators developed a QSAR model for PPARγ antagonism, based on the Tox21 dataset, which can facilitate the discovery of novel PPARγ antagonists. Furthermore, a small selection of chemicals were shown to exhibit anti-adipogenic effects in human primary ASCs, corroborating reporter assay results. Chemicals were shown to bind PPARγ with different affinities and efficacies, and results also indicated that they may have different binding modes as lipid droplet size and number were affected differently across chemicals. Using NMR spectroscopy, a third group of collaborators showed that the PPARγ antagonist DEHPA directly interacts with the ligand-binding pocket of PPARγ and inhibits rosiglitazone-induced activity in a similar manner as GW9662. This indicates that functional assays and biophysical methods like these are important complementary techniques necessary to confirm ligand binding and define the type of interaction occurring between PPARγ and ligand. Furthermore, QSAR models are valuable *in silico* tools for screening large numbers of chemicals for potential inhibitory effects on PPARγ.

In vitro studies indicated that PPARγ antagonism causes a derepression of aromatase expression in adipose tissue via two mechanisms. The first mechanism involves impaired adipogenesis in response to PPARγ inhibition. Aromatase expression was shown to be greater in adipose stromal cells than in mature adipocytes, suggesting that adipogenesis downregulates aromatase. Accordingly, the adipogenesis-induced aromatase downregulation was inhibited by PPARγ antagonists, resulting in elevation of aromatase. The second mechanism through which antagonism of PPARγ increases aromatase expression was suggested to be independent of adipogenesis as effects were demonstrated after short-term treatment and in the absence of stimulation with adipogenic factors. Most of the tested antagonists induced expression of aromatase in mature adipocytes, where PPARγ is abundant. In contrast, this effect was absent in pre-adipocytes, which express far lower levels of PPARγ. Consistent with this, activation and/or exogenous overexpression of PPARγ repressed aromatase, suggesting a PPARγ-dependent mechanism. However, it is possible that the short-term effect of PPARγ on aromatase expression does not occur through direct binding to the aromatase promoter region. It is yet to be determined whether this is the case or if PPARγ exerts its effect via an indirect mechanism. Induced expression of aromatase is associated with a local increase in the adipose tissue estrogen level. However, an increased production of estrogen in response to PPARγ antagonism was not demonstrated due to application of an unsuitable model for studying PPARγ-mediated effects.

The solvents ethanol and ethylene glycol were among the studied chemicals. NMR spectroscopy suggested some degree of influence on the active state of PPARγ but did not give obvious indications of an inhibitory effect. While both ethanol and ethylene glycol impaired adipogenesis, only ethanol induced aromatase expression in adipocytes like the majority of the other studied PPARγ antagonists. Short-term oral exposure to ethanol and ethylene glycol, as well as the PPARγ control antagonist GW9662, did not affect aromatase expression in the adipose tissue of female rats. Aromatase appeared to be challenging to study in rat adipose tissue, since its regulation is markedly different in rodents than in humans, which was evident from the very low adipose tissue expression level of aromatase. Besides, the expression of genes, such as *Pparg* and cytokine genes, in adipose tissue and ovary were also not affected by treatment. The lack of effects may have been a result of interference from the estrous cycle but could also be due to short exposure duration and/or oral administration route. In summary, ethanol and ethylene glycol appeared to inhibit PPARγ *in vitro*, and ethanol induced aromatase expression in adipocytes. However, short-term treatment of rats with ethanol or ethylene glycol was ineffective.

Together, the results indicate that environmental and occupational PPARγ antagonists can be discovered using a combination of computational, biophysical, and cell-based methods. Antagonism of PPARγ was linked to induction of aromatase via an inhibitory effect on adipogenesis as well as a still undefined short-term

mechanism. It can not be excluded that PPARγ-independent effects of the studied chemicals contributed to or counteracted adipogenesis inhibition or aromatase induction to some extent. In conclusion, the findings in this project suggest that PPARγ antagonism may promote estrogen biosynthesis by inducing aromatase transcription in the adipose tissue, potentially increasing the risk of breast cancer.

Perspectives

The findings of this project have provided new insights into the molecular mechanisms linking PPARγ antagonism to the regulation of aromatase expression in adipose tissue. While this project has contributed to the understanding of the potential mechanisms involved, there are several important avenues for future research. First, multiple *in silico* tools could be utilized to prioritize various relevant environmental and occupational chemicals for subsequent *in vitro* screening by predicting their probability of binding to PPARγ. The PPARγ antagonists identified in reporter assays should be confirmed using high-throughput biophysical techniques and optimized adipogenesis assays to establish that direct interaction occurs with the ligand-binding pocket and to determine the functional significance of the chemicals as potential endocrine and metabolic disruptors. Second, more in-depth investigation is needed to understand the short-term mechanism through which PPARγ antagonism induces aromatase expression in mature adipocytes. This could be accomplished by measuring the abundance of separate PPARγ transcript variants in response to PPARγ antagonist treatment, which would give insight into regulation through specific promoters. It could also be addressed by determining PPARγ interactions with other proteins or with chromatin using immunoprecipitation. Third, *in vivo* studies with extended exposure durations may provide a better understanding of the long-term effects of PPARγ antagonists on aromatase expression. Adipose tissue aromatase levels and estrogen concentrations should be measured in response to long-term exposure of ovariectomized rodents to PPARγ antagonists using a humanized aromatase rodent model. In addition, hyperplastic effects on the mammary gland in response to PPARγ antagonist exposure could be examined to address whether there is a direct link between selected PPARγ antagonists and promotion of mammary carcinogenesis. This project provides a solid foundation for continued research into the effects of PPARγ antagonists on aromatase expression and adipogenesis, including the potential implications for human health. Addressing these perspectives will thus contribute to a further understanding of non-genotoxic carcinogens and the role of PPARγ in cancer biology.

References

1. Hernandez-Quiles M, Broekema MF, Kalkhoven E. PPARgamma in Metabolism, Immunity, and Cancer: Unified and Diverse Mechanisms of Action. *Front Endocrinol (Lausanne)*. 2021;12. doi:10.3389/FENDO.2021.624112

2. Chandra M, Miriyala S, Panchatcharam M. PPAR γ and Its Role in Cardiovascular Diseases. *PPAR Res*. 2017;2017. doi:10.1155/2017/6404638

3. Stienstra R, Duval C, Müller M, Kersten S. PPARs, Obesity, and Inflammation. *PPAR Res*. 2007;2007. doi:10.1155/2007/95974

4. Janesick A, Blumberg B. Minireview: PPARγ as the target of obesogens. *J Steroid Biochem Mol Biol*. 2011;127(1-2):4-8. doi:10.1016/J.JSBMB.2011.01.005

5. Huang R, Xia M, Sakamuru S, et al. Expanding biological space coverage enhances the prediction of drug adverse effects in human using in vitro activity profiles. *Scientific Reports 2018 8:1*. 2018;8(1):1-12. doi:10.1038/s41598-018-22046-w

6. Wei W, Wan Y. Thiazolidinediones on PPARγ: The Roles in Bone Remodeling. *PPAR Res*. 2011;2011. doi:10.1155/2011/867180

7. Li X, Ycaza J, Blumberg B. The environmental obesogen tributyltin chloride acts via peroxisome proliferator activated receptor gamma to induce adipogenesis in murine 3T3-L1 preadipocytes. *J Steroid Biochem Mol Biol*. 2011;127(1-2):9-15. doi:10.1016/J.JSBMB.2011.03.012

8. Choi SS, Park J, Choi JH. Revisiting PPARγ as a target for the treatment of metabolic disorders. *BMB Rep*. 2014;47(11):599-608. doi:10.5483/BMBREP.2014.47.11.174

9. Augimeri G, Bonofiglio D. PPARgamma: A Potential Intrinsic and Extrinsic Molecular Target for Breast Cancer Therapy. *Biomedicines*. 2021;9(5). doi:10.3390/BIOMEDICINES9050543

10. Lakatos HF, Thatcher TH, Kottmann RM, Garcia TM, Phipps RP, Sime PJ. The Role of PPARs in Lung Fibrosis. *PPAR Res*. 2007;2007. doi:10.1155/2007/71323

11. Jeong J, Choi J. Advancing the Adverse Outcome Pathway for PPARγ Inactivation Leading to Pulmonary Fibrosis Using Bradford-Hill Consideration and the Comparative Toxicogenomics Database. *Chem Res Toxicol*. 2022;35(2):233-243. doi:10.1021/ACS.CHEMRESTOX.1C00257

12. Heindel JJ, Blumberg B, Cave M, et al. Metabolism disrupting chemicals and metabolic disorders. *Reprod Toxicol*. 2017;68:3-33. doi:10.1016/J.REPROTOX.2016.10.001

13. Casals-Casas C, Feige JN, Desvergne B. Interference of pollutants with PPARs: endocrine disruption meets metabolism. *Int J Obes (Lond)*. 2008;32 Suppl 6:S53-S61. doi:10.1038/IJO.2008.207

14. Nappi F, Barrea L, Di Somma C, et al. Endocrine Aspects of Environmental “Obesogen” Pollutants. *Int J Environ Res Public Health*. 2016;13(8). doi:10.3390/IJERPH13080765

15. Giovannucci E, Harlan DM, Archer MC, et al. Diabetes and cancer: a consensus report. *CA Cancer J Clin*. 2010;60(4):207-221. doi:10.3322/CAAC.20078

16. Rubin GL, Zhao Y, Kalus AM, Simpson ER. Peroxisome proliferator-activated receptor gamma ligands inhibit estrogen biosynthesis in human breast adipose tissue: possible implications for breast cancer therapy. *Cancer Res*. 2000;60(6):1604-1608.

17. Rubin GL, Duong JH, Clyne CD, et al. Ligands for the peroxisomal proliferator-activated receptor gamma and the retinoid X receptor inhibit aromatase cytochrome P450 (CYP19) expression mediated by

promoter II in human breast adipose. *Endocrinology*. 2002;143(8):2863-2871. doi:10.1210/ENDO.143.8.8932

18. Newman L. Oncologic anthropology: Global variations in breast cancer risk, biology, and outcome. *J Surg Oncol*. Published online October 10, 2023. doi:10.1002/JSO.27459

19. Admoun C, Mayrovitz HN. The Etiology of Breast Cancer. *Breast Cancer*. Published online August 4, 2022:21-30. doi:10.36255/EXON-PUBLICATIONS-BREAST-CANCER-ETIOLOGY

20. Vogel U, Christensen J, Nexø BA, Wallin H, Friis S, Tjønneland A. Peroxisome proliferator-activated receptor-gamma2 Pro12Ala, interaction with alcohol intake and NSAID use, in relation to risk of breast cancer in a prospective study of Danes. *Carcinogenesis*. 2007;28(2):427-434. doi:10.1093/CARCIN/BGL170

21. Petersen RK, Larsen SB, Jensen DM, et al. PPARgamma-PGC-1alpha activity is determinant of alcohol related breast cancer. *Cancer Lett*. 2012;315(1):59-68. doi:10.1016/j.canlet.2011.10.009

22. Kopp TI, Lundqvist J, Petersen RK, et al. In vitro screening of inhibition of PPAR-gamma activity as a first step in identification of potential breast carcinogens. *Hum Exp Toxicol*. 2015;34(11):1106-1118. doi:10.1177/0960327115569811

23. Clusan L, Ferrière F, Flouriot G, Pakdel F. A Basic Review on Estrogen Receptor Signaling Pathways in Breast Cancer. *Int J Mol Sci*. 2023;24(7). doi:10.3390/IJMS24076834

24. Calaf GM, Ponce-Cusi R, Aguayo F, Muñoz JP, Bleak TC. Endocrine disruptors from the environment affecting breast cancer. *Oncol Lett*. 2020;20(1):19-32. doi:10.3892/OL.2020.11566

25. Weikum ER, Liu X, Ortlund EA. The nuclear receptor superfamily: A structural perspective. *Protein Sci*. 2018;27(11):1876-1892. doi:10.1002/PRO.3496

26. Burns KA, Vanden Heuvel JP. Modulation of PPAR activity via phosphorylation. *Biochim Biophys Acta*. 2007;1771(8):952-960. doi:10.1016/J.BBALIP.2007.04.018

27. Yessoufou A, Wahli W. Multifaceted roles of peroxisome proliferator-activated receptors (PPARs) at the cellular and whole organism levels. *Swiss Med Wkly*. 2010;140(September). doi:10.4414/SMW.2010.13071

28. Augimeri G, Giordano C, Gelsomino L, et al. The Role of PPARγ Ligands in Breast Cancer: From Basic Research to Clinical Studies. *Cancers (Basel)*. 2020;12(9):1-28. doi:10.3390/CANCERS12092623

29. Hong F, Pan S, Guo Y, Xu P, Zhai Y. PPARs as Nuclear Receptors for Nutrient and Energy Metabolism. *Molecules*. 2019;24(14). doi:10.3390/MOLECULES24142545

30. Azhar S. Peroxisome proliferator-activated receptors, metabolic syndrome and cardiovascular disease. *Future Cardiol*. 2010;6(5):657-691. doi:10.2217/FCA.10.86

31. Aprile M, Ambrosio MR, D'Esposito V, et al. PPARG in Human Adipogenesis: Differential Contribution of Canonical Transcripts and Dominant Negative Isoforms. *PPAR Res*. 2014;2014. doi:10.1155/2014/537865

32. Christofides A, Konstantinidou E, Jani C, Boussiotis VA. The role of peroxisome proliferator-activated receptors (PPAR) in immune responses. *Metabolism*. 2021;114. doi:10.1016/J.METABOL.2020.154338

33. Chao Y, Jiang Y, Zhong M, et al. Regulatory roles and mechanisms of alternative RNA splicing in adipogenesis and human metabolic health. *Cell Biosci*. 2021;11(1). doi:10.1186/S13578-021-00581-W

34. Aprile M, Cataldi S, Ambrosio MR, et al. PPARγΔ5, a Naturally Occurring Dominant-Negative Splice Isoform, Impairs PPARγ Function and Adipocyte Differentiation. *Cell Rep*. 2018;25(6):1577-1592.e6. doi:10.1016/J.CELREP.2018.10.035

35. Yu S, Reddy JK. Transcription coactivators for peroxisome proliferator-activated receptors. *Biochim Biophys Acta*. 2007;1771(8):936-951. doi:10.1016/J.BBALIP.2007.01.008

36. Kroker AJ, Bruning JB. Review of the Structural and Dynamic Mechanisms of PPARγ Partial Agonism. *PPAR Res*. 2015;2015. doi:10.1155/2015/816856

37. Zhao B, Xin Z, Ren P, Wu H. The Role of PPARs in Breast Cancer. *Cells*. 2022;12(1). doi:10.3390/CELLS12010130

38. Cheng HS, Tan WR, Low ZS, Marvalim C, Lee JYH, Tan NS. Exploration and Development of PPAR Modulators in Health and Disease: An Update of Clinical Evidence. *Int J Mol Sci*. 2019;20(20). doi:10.3390/IJMS20205055

39. Wang L, Waltenberger B, Pferschy-Wenzig EM, et al. Natural product agonists of peroxisome proliferator-activated receptor gamma (PPARγ): a review. *Biochem Pharmacol*. 2014;92(1):73-89. doi:10.1016/J.BCP.2014.07.018

40. Gross B, Pawlak M, Lefebvre P, Staels B. PPARs in obesity-induced T2DM, dyslipidaemia and NAFLD. *Nat Rev Endocrinol*. 2017;13(1):36-49. doi:10.1038/NRENDO.2016.135

41. Rosen ED, Hsu CH, Wang X, et al. C/EBPalpha induces adipogenesis through PPARgamma: a unified pathway. *Genes Dev*. 2002;16(1):22-26. doi:10.1101/GAD.948702

42. Zhang J, Fu M, Cui T, et al. Selective disruption of PPARgamma 2 impairs the development of adipose tissue and insulin sensitivity. *Proc Natl Acad Sci U S A*. 2004;101(29):10703-10708. doi:10.1073/PNAS.0403652101

43. Duan SZ, Ivashchenko CY, Whitesall SE, et al. Hypotension, lipodystrophy, and insulin resistance in generalized PPARgamma-deficient mice rescued from embryonic lethality. *J Clin Invest*. 2007;117(3):812-822. doi:10.1172/JCI28859

44. Barak Y, Kim S. Genetic manipulations of PPARs: effects on obesity and metabolic disease. *PPAR Res*. 2007;2007. doi:10.1155/2007/12781

45. Wang F, Mullican SE, DiSpirito JR, Peed LC, Lazar MA. Lipoatrophy and severe metabolic disturbance in mice with fat-specific deletion of PPARγ. *Proc Natl Acad Sci U S A*. 2013;110(46):18656-18661. doi:10.1073/PNAS.1314863110

46. Imai T, Takakuwa R, Marchand S, et al. Peroxisome proliferator-activated receptor gamma is required in mature white and brown adipocytes for their survival in the mouse. *Proc Natl Acad Sci U S A*. 2004;101(13):4543-4547. doi:10.1073/PNAS.0400356101

47. Virtue S, Petkevicius K, Moreno-Navarrete JM, et al. Peroxisome Proliferator-Activated Receptor γ2 Controls the Rate of Adipose Tissue Lipid Storage and Determines Metabolic Flexibility. *Cell Rep*. 2018;24(8):2005-2012.e7. doi:10.1016/J.CELREP.2018.07.063

48. Medina-Gomez G, Gray SL, Yetukuri L, et al. PPAR gamma 2 prevents lipotoxicity by controlling adipose tissue expandability and peripheral lipid metabolism. *PLoS Genet*. 2007;3(4):0634-0647. doi:10.1371/JOURNAL.PGEN.0030064

49. He W. PPARγ2Pro12Ala Polymorphism and Human Health. *PPAR Res*. 2009;2009:15. doi:10.1155/2009/849538

50. Sherry ST, Ward MH, Kholodov M, et al. dbSNP: the NCBI database of genetic variation. *Nucleic Acids Res*. 2001;29(1):308. doi:10.1093/NAR/29.1.308

51. dbSNP. rs1801282. Accessed October 24, 2023. https://www.ncbi.nlm.nih.gov/snp/rs1801282

52. Deeb SS, Fajas L, Nemoto M, et al. A Pro12Ala substitution in PPARgamma2 associated with decreased receptor activity, lower body mass index and improved insulin sensitivity. *Nat Genet*. 1998;20(3):284-287. doi:10.1038/3099

53. Masugi J, Tamori Y, Mori H, Koike T, Kasuga M. Inhibitory effect of a proline-to-alanine substitution at codon 12 of peroxisome proliferator-activated receptor-gamma 2 on thiazolidinedione-induced adipogenesis. *Biochem Biophys Res Commun*. 2000;268(1):178-182. doi:10.1006/BBRC.2000.2096

54. Wan R, Ding Z, Xia S, Zheng L, Lu J. Effects of PPARγ2 Pro12Ala variant on adipocyte phenotype dependent of DHA. *Diabetes, Metabolic Syndrome and Obesity*. 2019;12:2273-2279. doi:10.2147/DMSO.S214526

55. Heikkinen S, Argmann C, Feige JN, et al. The Pro12Ala PPARγ2 Variant Determines Metabolism at the Gene-Environment Interface. *Cell Metab*. 2009;9(1):88-98. doi:10.1016/j.cmet.2008.11.007

56. Peraza MA, Burdick AD, Marin HE, Gonzalez FJ, Peters JM. The toxicology of ligands for peroxisome proliferator-activated receptors (PPAR). *Toxicol Sci*. 2006;90(2):269-295. doi:10.1093/TOXSCI/KFJ062

57. Liu Y, Yin T, Feng Y, et al. Mammalian models of chemically induced primary malignancies exploitable for imaging-based preclinical theragnostic research. *Quant Imaging Med Surg*. 2015;5(5):708-729. doi:10.3978/J.ISSN.2223-4292.2015.06.01

58. Kerdelhué B, Forest C, Coumoul X. Dimethyl-Benz(a)anthracene: A mammary carcinogen and a neuroendocrine disruptor. *Biochim Open*. 2016;3:49-55. doi:10.1016/J.BIOPEN.2016.09.003

59. Faustino-Rocha AI, Ferreira R, Oliveira PA, Gama A, Ginja M. N-Methyl-N-nitrosourea as a mammary carcinogenic agent. *Tumour Biol*. 2015;36(12):9095-9117. doi:10.1007/S13277-015-3973-2

60. Nicol CJ, Yoon M, Ward JM, et al. PPARγ influences susceptibility to DMBA-induced mammary, ovarian and skin carcinogenesis. *Carcinogenesis*. 2004;25(9):1747-1755. doi:10.1093/carcin/bgh160

61. Skelhorne-gross G, Reid AL, Apostoli AJ, et al. Stromal adipocyte PPARγ protects against breast tumorigenesis. *Carcinogenesis*. 2012;33(7):1412-1420. doi:10.1093/CARCIN/BGS173

62. Yin Y, Yuan H, Zeng X, Kopelovich L, Glazer RI. Inhibition of peroxisome proliferator-activated receptor gamma increases estrogen receptor-dependent tumor specification. 2009;(2):687-695. doi:10.1158/0008-5472.CAN-08-2446

63. Suh N, Wang Y, Charlotte R. Williams CR, et al. A new ligand for the peroxisome proliferator-activated receptor-gamma (PPAR-gamma), GW7845, inhibits rat mammary carcinogenesis. *Cancer Res*. 1999;59(22):5671-5673.

64. Yuan H, Kopelovich L, Yin Y, Lu J, Glazer RI. Drug-targeted inhibition of peroxisome proliferator-activated receptor-gamma enhances the chemopreventive effect of anti-estrogen therapy. *Oncotarget*. 2012;3(3).

65. Mehta RG, Williamson E, Patel MK, Koeffler HP. A ligand of peroxisome proliferator-activated receptor gamma, retinoids, and prevention of preneoplastic mammary lesions. *J Natl Cancer Inst*. 2000;92(5):418-423. doi:10.1093/JNCI/92.5.418

66. Mehta RG, Peng X, Roy S. PPAR c antagonist GW9662 induces functional estrogen receptor in mouse mammary organ culture : potential translational significance. Published online 2013:249-256. doi:10.1007/s11010-012-1466-9

67. Leesnitzer LM, Parks DJ, Bledsoe RK, et al. Functional consequences of cysteine modification in the ligand binding sites of peroxisome proliferator activated receptors by GW9662. *Biochemistry*. 2002;41(21):6640-6650. doi:10.1021/BI0159581

68. Gou Q, Gong X, Jin J, Shi J, Hou Y. Peroxisome proliferator-activated receptors (PPARs) are potential drug targets for cancer therapy. *Oncotarget*. 2017;8(36):60704-60709. doi:10.18632/ONCOTARGET.19610

69. Wang X, Wang G, Shi Y, et al. PPAR-delta promotes survival of breast cancer cells in harsh metabolic conditions. *Oncogenesis*. 2016;5(6):e232-e232. doi:10.1038/ONCSIS.2016.41

70. Mueller E, Sarraf P, Tontonoz P, et al. Terminal differentiation of human breast cancer through PPAR gamma. *Mol Cell*. 1998;1(3):465-470. doi:10.1016/S1097-2765(00)80047-7

71. Diamanti-Kandarakis E, Bourguignon JP, Giudice LC, et al. Endocrine-disrupting chemicals: an Endocrine Society scientific statement. *Endocr Rev*. 2009;30(4):293-342. doi:10.1210/ER.2009-0002

72. Lamminmäki M, Leivonen A, Heinävaara S, et al. A population-based cohort study on changes in breast, lung and colorectal cancer incidence and mortality among non-Western immigrant women. *BMC Cancer*. 2023;23(1). doi:10.1186/S12885-023-11140-6

73. Gupta R, Kumar P, Fahmi N, et al. Endocrine disruption and obesity: A current review on environmental obesogens. *Current Research in Green and Sustainable Chemistry*. 2020;3:100009. doi:10.1016/J.CRGSC.2020.06.002

74. Griffin MD, Pereira SR, DeBari MK, Abbott RD. Mechanisms of action, chemical characteristics, and model systems of obesogens. *BMC Biomed Eng*. 2020;2(1). doi:10.1186/S42490-020-00040-6

75. Chamorro-Garcia R, Blumberg B. Current Research Approaches and Challenges in the Obesogen Field. *Front Endocrinol (Lausanne)*. 2019;10(MAR). doi:10.3389/FENDO.2019.00167

76. Kanayama T, Kobayashi N, Mamiya S, Nakanishi T, Nishikawa JI. Organotin compounds promote adipocyte differentiation as agonists of the peroxisome proliferator-activated receptor gamma/retinoid X receptor pathway. *Mol Pharmacol*. 2005;67(3):766-774. doi:10.1124/MOL.104.008409

77. Grün F, Watanabe H, Zamanian Z, et al. Endocrine-disrupting organotin compounds are potent inducers of adipogenesis in vertebrates. *Mol Endocrinol*. 2006;20(9):2141-2155. doi:10.1210/ME.2005-0367

78. Milton FA, Lacerda MG, Sinoti SBP, et al. Dibutyltin Compounds Effects on PPARγ/RXRα Activity, Adipogenesis, and Inflammation in Mammalians Cells. *Front Pharmacol*. 2017;8(AUG). doi:10.3389/FPHAR.2017.00507

79. Watt J, Schlezinger JJ. Structurally-diverse, PPARγ-activating environmental toxicants induce adipogenesis and suppress osteogenesis in bone marrow mesenchymal stromal cells. *Toxicology*. 2015;331:66-77. doi:10.1016/J.TOX.2015.03.006

80. Pereira-Fernandes A, Demaegdt H, Vandermeiren K, et al. Evaluation of a screening system for obesogenic compounds: screening of endocrine disrupting compounds and evaluation of the PPAR dependency of the effect. *PLoS One*. 2013;8(10). doi:10.1371/JOURNAL.PONE.0077481

81. le Maire A, Grimaldi M, Roecklin D, et al. Activation of RXR-PPAR heterodimers by organotin environmental endocrine disruptors. *EMBO Rep*. 2009;10(4):367-373. doi:10.1038/EMBOR.2009.8

82. Harada S, Hiromori Y, Nakamura S, et al. Structural basis for PPARγ transactivation by endocrine-disrupting organotin compounds. *Sci Rep*. 2015;5. doi:10.1038/SREP08520

83. Grün F, Blumberg B. Environmental obesogens: organotins and endocrine disruption via nuclear receptor signaling. *Endocrinology*. 2006;147(6 Suppl). doi:10.1210/EN.2005-1129

84. Biemann R, Fischer B, Blüher M, Navarrete Santos A. Tributyltin affects adipogenic cell fate commitment in mesenchymal stem cells by a PPARγ independent mechanism. *Chem Biol Interact*. 2014;214(1):1-9. doi:10.1016/J.CBI.2014.01.021

85. Regnier SM, El-Hashani E, Kamau W, Zhang X, Massad NL, Sargis RM. Tributyltin differentially promotes development of a phenotypically distinct adipocyte. *Obesity (Silver Spring)*. 2015;23(9):1864-1871. doi:10.1002/OBY.21174

86. Lutfi E, Riera-Heredia N, Córdoba M, et al. Tributyltin and triphenyltin exposure promotes in vitro adipogenic differentiation but alters the adipocyte phenotype in rainbow trout. *Aquat Toxicol*. 2017;188:148-158. doi:10.1016/J.AQUATOX.2017.05.001

87. Kim S, Li A, Monti S, Schlezinger JJ. Tributyltin induces a transcriptional response without a brite adipocyte signature in adipocyte models. *Arch Toxicol*. 2018;92(9):2859-2874. doi:10.1007/S00204-018-2268-Y

88. Hurst CH, Waxman DJ. Activation of PPARalpha and PPARgamma by environmental phthalate monoesters. *Toxicol Sci*. 2003;74(2):297-308. doi:10.1093/TOXSCI/KFG145

89. Bility MT, Thompson JT, McKee RH, et al. Activation of mouse and human peroxisome proliferator-activated receptors (PPARs) by phthalate monoesters. *Toxicol Sci*. 2004;82(1):170-182. doi:10.1093/TOXSCI/KFH253

90. Feige JN, Gelman L, Rossi D, et al. The endocrine disruptor monoethyl-hexyl-phthalate is a selective peroxisome proliferator-activated receptor gamma modulator that promotes adipogenesis. *J Biol Chem*. 2007;282(26):19152-19166. doi:10.1074/JBC.M702724200

91. Maloney EK, Waxman DJ. trans-Activation of PPARalpha and PPARgamma by structurally diverse environmental chemicals. *Toxicol Appl Pharmacol*. 1999;161(2):209-218. doi:10.1006/TAAP.1999.8809

92. Riu A, Grimaldi M, le Maire A, et al. Peroxisome proliferator-activated receptor γ is a target for halogenated analogs of bisphenol A. *Environ Health Perspect*. 2011;119(9):1227-1232. doi:10.1289/EHP.1003328

93. Simon C, Onghena M, Covaci A, et al. Screening of endocrine activity of compounds migrating from plastic baby bottles using a multi-receptor panel of in vitro bioassays. *Toxicol In Vitro*. 2016;37:121-133. doi:10.1016/J.TIV.2016.09.008

94. Schaffert A, Krieg L, Weiner J, et al. Alternatives for the worse: Molecular insights into adverse effects of bisphenol a and substitutes during human adipocyte differentiation. *Environ Int*. 2021;156. doi:10.1016/J.ENVINT.2021.106730

95. Ahmed S, Atlas E. Bisphenol S- and bisphenol A-induced adipogenesis of murine preadipocytes occurs through direct peroxisome proliferator-activated receptor gamma activation. *Int J Obes (Lond)*. 2016;40(10):1566-1573. doi:10.1038/IJO.2016.95

96. Wang J, Sun B, Hou M, Pan X, Li X. The environmental obesogen bisphenol A promotes adipogenesis by increasing the amount of 11β-hydroxysteroid dehydrogenase type 1 in the adipose tissue of children. *Int J Obes (Lond)*. 2013;37(7):999-1005. doi:10.1038/IJO.2012.173

97. Boucher JG, Ahmed S, Atlas E. Bisphenol S Induces Adipogenesis in Primary Human Preadipocytes From Female Donors. *Endocrinology*. 2016;157(4):1397-1407. doi:10.1210/EN.2015-1872

98. Boucher JG, Boudreau A, Atlas E. Bisphenol A induces differentiation of human preadipocytes in the absence of glucocorticoid and is inhibited by an estrogen-receptor antagonist. *Nutr Diabetes*. 2014;4(1):e102. doi:10.1038/NUTD.2013.43

99. Reina-Pérez I, Olivas-Martínez A, Mustieles V, et al. Bisphenol F and bisphenol S promote lipid accumulation and adipogenesis in human adipose-derived stem cells. *Food Chem Toxicol*. 2021;152. doi:10.1016/J.FCT.2021.112216

100. Ariemma F, D'Esposito V, Liguoro D, et al. Low-Dose Bisphenol-A Impairs Adipogenesis and Generates Dysfunctional 3T3-L1 Adipocytes. *PLoS One*. 2016;11(3). doi:10.1371/JOURNAL.PONE.0150762

101. De Filippis E, Li T, Rosen ED. Exposure of adipocytes to bisphenol-A in vitro interferes with insulin action without enhancing adipogenesis. *PLoS One*. 2018;13(8). doi:10.1371/JOURNAL.PONE.0201122

102. Riu A, le Maire A, Grimaldi M, et al. Characterization of novel ligands of ERα, Erβ, and PPARγ: the case of halogenated bisphenol A and their conjugated metabolites. *Toxicol Sci*. 2011;122(2):372-382. doi:10.1093/TOXSCI/KFR132

103. Takeuchi S, Matsuda T, Kobayashi S, Takahashi T, Kojima H. In vitro screening of 200 pesticides for agonistic activity via mouse peroxisome proliferator-activated receptor (PPAR)alpha and PPARgamma and quantitative analysis of in vivo induction pathway. *Toxicol Appl Pharmacol*. 2006;217(3):235-244. doi:10.1016/J.TAAP.2006.08.011

104. Janesick AS, Dimastrogiovanni G, Vanek L, et al. On the Utility of ToxCast™ and ToxPi as Methods for Identifying New Obesogens. *Environ Health Perspect*. 2016;124(8):1214-1226. doi:10.1289/EHP.1510352

105. Kassotis CD, Hoffman K, Stapleton HM. Characterization of adipogenic activity of house dust extracts and semi-volatile indoor contaminants in 3T3-L1 cells. *Environ Sci Technol*. 2017;51(15):8735-8745. doi:10.1021/acs.est.7b01788

106. Foley B, Doheny DL, Black MB, et al. Screening ToxCast prioritized chemicals for PPARG function in a human adipose-derived stem cell model of adipogenesis. *Toxicological Sciences*. 2017;155(1):85-100. doi:10.1093/toxsci/kfw186

107. Routti H, Lille-Langoy R, Berg MK, et al. Environmental Chemicals Modulate Polar Bear (Ursus maritimus) Peroxisome Proliferator-Activated Receptor Gamma (PPARG) and Adipogenesis in Vitro. *Environ Sci Technol*. 2016;50(19):10708-10720. doi:10.1021/ACS.EST.6B03020

108. Huang R, Xia M, Cho MH, et al. Chemical genomics profiling of environmental chemical modulation of human nuclear receptors. *Environ Health Perspect*. 2011;119(8):1142-1148. doi:10.1289/EHP.1002952

109. Osada S, Nishikawa JI, Nakanishi T, Tanaka K, Nishihara T. Some organotin compounds enhance histone acetyltransferase activity. *Toxicol Lett*. 2005;155(2):329-335. doi:10.1016/J.TOXLET.2004.10.009

110. Audouze K, Juncker AS, Roque FJSSA, et al. Deciphering diseases and biological targets for environmental chemicals using toxicogenomics networks. *PLoS Comput Biol*. 2010;6(5):1-11. doi:10.1371/JOURNAL.PCBI.1000788

111. Rosenmai AK, Bengtström L, Taxvig C, et al. An effect-directed strategy for characterizing emerging chemicals in food contact materials made from paper and board. *Food Chem Toxicol*. 2017;106(Pt A):250-259. doi:10.1016/J.FCT.2017.05.061

112. Kassotis CD, Nagel SC, Stapleton HM. Unconventional oil and gas chemicals and wastewater-impacted water samples promote adipogenesis via PPARγ-dependent and independent mechanisms in 3T3-L1 cells. *Sci Total Environ*. 2018;640-641:1601-1610. doi:10.1016/J.SCITOTENV.2018.05.030

113. Colleluori G, Perugini J, Giordano A, Cinti S. From Obesity to Diabetes: The Role of the Adipose Organ. *Handb Exp Pharmacol*. 2022;274:75-92. doi:10.1007/164_2021_572

114. Kaur S, Auger C, Jeschke MG. Adipose Tissue Metabolic Function and Dysfunction: Impact of Burn Injury. *Front Cell Dev Biol*. 2020;8. doi:10.3389/FCELL.2020.599576

115. Sun K, Li X, Scherer PE. Extracellular Matrix (ECM) and Fibrosis in Adipose Tissue: Overview and Perspectives. *Compr Physiol*. 2023;13(1):4387-4407. doi:10.1002/CPHY.C220020

116. Ugurlu B, Karaoz E. Comparison of similar cells: Mesenchymal stromal cells and fibroblasts. *Acta Histochem*. 2020;122(8). doi:10.1016/J.ACTHIS.2020.151634

117. Audano M, Pedretti S, Caruso D, Crestani M, De Fabiani E, Mitro N. Regulatory mechanisms of the early phase of white adipocyte differentiation: an overview. *Cell Mol Life Sci*. 2022;79(3). doi:10.1007/S00018-022-04169-6

118. Giordano A, Smorlesi A, Frontini A, Barbatelli G, Cint S. White, brown and pink adipocytes: the extraordinary plasticity of the adipose organ. *Eur J Endocrinol*. 2014;170(5). doi:10.1530/EJE-13-0945

119. Steiner BM, Berry DC. The Regulation of Adipose Tissue Health by Estrogens. *Front Endocrinol (Lausanne)*. 2022;13. doi:10.3389/FENDO.2022.889923

120. Longo M, Zatterale F, Naderi J, et al. Adipose Tissue Dysfunction as Determinant of Obesity-Associated Metabolic Complications. *Int J Mol Sci*. 2019;20(9). doi:10.3390/IJMS20092358

121. Carobbio S, Pellegrinelli V, Vidal-Puig A. Adipose Tissue Function and Expandability as Determinants of Lipotoxicity and the Metabolic Syndrome. *Adv Exp Med Biol*. 2017;960:161-196. doi:10.1007/978-3-319-48382-5_7

122. Corrales P, Vidal-Puig A, Medina-Gómez G. PPARS and metabolic disorders associated with challenged adipose tissue plasticity. *Int J Mol Sci*. 2018;19(7). doi:10.3390/ijms19072124

123. Chait A, den Hartigh LJ. Adipose Tissue Distribution, Inflammation and Its Metabolic Consequences, Including Diabetes and Cardiovascular Disease. *Front Cardiovasc Med*. 2020;7. doi:10.3389/FCVM.2020.00022

124. Horwitz A, Birk R. Adipose Tissue Hyperplasia and Hypertrophy in Common and Syndromic Obesity-The Case of BBS Obesity. *Nutrients*. 2023;15(15). doi:10.3390/NU15153445

125. Nedungadi TP, Clegg DJ. Sexual dimorphism in body fat distribution and risk for cardiovascular diseases. *J Cardiovasc Transl Res*. 2009;2(3):321-327. doi:10.1007/S12265-009-9101-1

126. Nelson TR, Cerviño LI, Boone JM, Lindfors KK. Classification of breast computed tomography data. *Med Phys*. 2008;35(3):1078-1086. doi:10.1118/1.2839439

127. Simpson E, Rubin G, Clyne C, et al. Local estrogen biosynthesis in males and females. *Endocr Relat Cancer*. 1999;6(2):131-137. doi:10.1677/erc.0.0060131

128. Bulun SE, Chen D, Moy I, Brooks DC, Zhao H. Aromatase, breast cancer and obesity: A complex interaction. *Trends in Endocrinology and Metabolism*. 2012;23(2):83-89. doi:10.1016/j.tem.2011.10.003

129. Brown KA. Metabolic pathways in obesity-related breast cancer. *Nat Rev Endocrinol*. 2021;17(6):350-363. doi:10.1038/s41574-021-00487-0

130. Miller WL, Auchus RJ. The molecular biology, biochemistry, and physiology of human steroidogenesis and its disorders. *Endocr Rev*. 2011;32(1):81-151. doi:10.1210/ER.2010-0013

131. Li J, Papadopoulos V, Vihma V. Steroid biosynthesis in adipose tissue. *Steroids*. 2015;103:89-104. doi:10.1016/J.STEROIDS.2015.03.016

132. Simpson ER, Davis SR. Minireview: aromatase and the regulation of estrogen biosynthesis--some new perspectives. *Endocrinology*. 2001;142(11):4589-4594. doi:10.1210/ENDO.142.11.8547

133. Häggström M, Richfield D. Diagram of the pathways of human steroidogenesis. *WikiJournal of Medicine*. 2014;1(1). doi:10.15347/wjm/2014.005

134. Uruno A, Matsuda K, Noguchi N, et al. Peroxisome proliferator-activated receptor-{gamma} suppresses CYP11B2 expression and aldosterone production. *J Mol Endocrinol*. 2011;46(1):37-49. doi:10.1677/JME-10-0088

135. Kempná P, Hofer G, Mullis PE, Flück CE. Pioglitazone inhibits androgen production in NCI-H295R cells by regulating gene expression of CYP17 and HSD3B2. *Mol Pharmacol*. 2007;71(3):787-798. doi:10.1124/MOL.106.028902

136. Kwintkiewicz J, Nishi Y, Yanase T, Giudice LC. Peroxisome proliferator-activated receptor-γ mediates bisphenol A inhibition of FSH-stimulated IGF-1, aromatase, and estradiol in human granulosa cells. *Environ Health Perspect*. 2010;118(3):400-406. doi:10.1289/ehp.0901161

137. Lovekamp-Swan T, Jetten AM, Davis BJ. Dual activation of PPARα and PPARγ by mono-(2-ethylhexyl) phthalate in rat ovarian granulosa cells. *Mol Cell Endocrinol*. 2003;201(1-2):133-141. doi:10.1016/S0303-7207(02)00423-9

138. Ferst JG, Rovani MT, Dau AMP, et al. Activation of PPARG inhibits dominant follicle development in cattle. *Theriogenology*. 2020;142:276-283. doi:10.1016/J.THERIOGENOLOGY.2019.10.032

139. Puttabyatappa M, Lu C, Martin JD, Chazenbalk G, Dumesic D, Padmanabhan V. Developmental programming: Impact of prenatal testosterone excess on steroidal machinery and cell differentiation markers in visceral adipocytes of female sheep. *Reproductive Sciences*. 2018;25(7):1010-1023. doi:10.1177/1933719117746767

140. Etique N, Chardard D, Chesnel A, Merlin JL, Flament S, Grillier-Vuissoz I. Ethanol stimulates proliferation, ERalpha and aromatase expression in MCF-7 human breast cancer cells. *Int J Mol Med*. 2004;13(1):149-155. doi:10.3892/ijmm.13.1.149

141. Gordon GG, Southren AL, Vittek J, Lieber CS. The effect of alcohol ingestion on hepatic aromatase activity and plasma steroid hormones in the rat. *Metabolism*. 1979;28(1):20-24. doi:10.1016/0026-0495(79)90163-X

142. Monteiro R, Soares R, Guerreiro S, Pestana D, Calhau C, Azevedo I. Red wine increases adipose tissue aromatase expression and regulates body weight and adipocyte size. *Nutrition*. 2009;25(6):699-705. doi:10.1016/j.nut.2009.01.001

143. Ren L, Meldhahl A, Lech JJ. Dimethyl formamide (DMFA) and ethylene glycol (EG) are estrogenic in rainbow trout. *Chem Biol Interact*. 1996;102(1):63-67. doi:10.1016/0009-2797(96)03727-1

144. Zhao H, Zhou L, Shangguan AJ, Bulun SE. Aromatase expression and regulation in breast and endometrial cancer. *J Mol Endocrinol*. 2016;57(1):R19-R33. doi:10.1530/JME-15-0310

145. Brown KA, McInnes KJ, Hunger NI, Oakhill JS, Steinberg GR, Simpson ER. Subcellular localization of cyclic AMP-responsive element binding protein-regulated transcription coactivator 2 provides a link between obesity and breast cancer in postmenopausal women. *Cancer Res*. 2009;69(13):5392-5399. doi:10.1158/0008-5472.CAN-09-0108

146. Mihm M, Gangooly S, Muttukrishna S. The normal menstrual cycle in women. *Anim Reprod Sci*. 2011;124(3-4):229-236. doi:10.1016/J.ANIREPROSCI.2010.08.030

147. Fan W, Yanase T, Morinaga H, Mu YM, Nomura M, Okabe T. Activation of peroxisome proliferator-activated receptor-gamma and retinoid X receptor inhibits aromatase transcription via nuclear factor-kappaB. 2005;146(1):85-92. doi:10.1210/en.2004-1046

148. Graham FL, Smiley J, Russell WC, Nairn R. Characteristics of a human cell line transformed by DNA from human adenovirus type 5. *J Gen Virol*. 1977;36(1):59-72. doi:10.1099/0022-1317-36-1-59

149. Tan E, Chin CSH, Lim ZFS, Ng SK. HEK293 Cell Line as a Platform to Produce Recombinant Proteins and Viral Vectors. *Front Bioeng Biotechnol*. 2021;9. doi:10.3389/FBIOE.2021.796991

150. Schulman IG, Heyman RA. The flip side: Identifying small molecule regulators of nuclear receptors. *Chem Biol*. 2004;11(5):639-646. doi:10.1016/j.chembiol.2003.12.021

151. Promega. Reporter Genes and their Applications. Accessed October 22, 2023. https://dk.promega.com/resources/guides/cell-biology/bioluminescent-reporters/

152. Troy T, Jekic-McMullen D, Sambucetti L, Rice B. Quantitative comparison of the sensitivity of detection of fluorescent and bioluminescent reporters in animal models. *Mol Imaging*. 2004;3(1):153535002004031. doi:10.1162/15353500200403196

153. Tung JK, Berglund K, Gutekunst CA, Hochgeschwender U, Gross RE. Bioluminescence imaging in live cells and animals. *Neurophotonics*. 2016;3(2):1. doi:10.1117/1.NPH.3.2.025001

154. Borrel A, Huang R, Sakamuru S, et al. High-Throughput Screening to Predict Chemical-Assay Interference. *Sci Rep*. 2020;10(1). doi:10.1038/S41598-020-60747-3

155. Zhang Y, Chen X, Gueydan C, Han J. Plasma membrane changes during programmed cell deaths. *Cell Research 2017 28:1*. 2017;28(1):9-21. doi:10.1038/cr.2017.133

156. Chen T, Xie W, Agler M, Banks M. Coactivators in assay design for nuclear hormone receptor drug discovery. *Assay Drug Dev Technol*. 2003;1(6):835-842. doi:10.1089/154065803772613462

157. Signosis. PPAR-gamma LBD-Driven GAL4 Reporter HEK 293 Stable Cell Line. Accessed October 19, 2023. https://www.signosisinc.com/product-page/ppar-gamma-lbd-driven-gal4-reporter-hek-293-stable-cell-line

158. Signosis. Ultra Sensitive PPARgamma LBD-Driven GAL4 Reporter HEK293 Stable Cell Line. Accessed October 19, 2023. https://www.signosisinc.com/product-page/ultra-sensitive-ppargamma-lbd-driven-gal4-reporter-hek293-stable-cell-line

159. Xue R, Lynes MD, Dreyfuss JM, et al. Clonal analyses and gene profiling identify genetic biomarkers of the thermogenic potential of human brown and white preadipocytes. *Nat Med*. 2015;21(7):760-768. doi:10.1038/nm.3881

160. Sasaki MS, Kodama S. Establishment and some mutational characteristics of 3T3-like near-diploid mouse cell line. *J Cell Physiol*. 1987;131(1):114-122. doi:10.1002/jcp.1041310117

161. Wabitsch M, Brenner RE, Melzner I, et al. Characterization of a human preadipocyte cell strain with high capacity for adipose differentiation. *Int J Obes Relat Metab Disord*. 2001;25(1):8-15. doi:10.1038/SJ.IJO.0801520

162. Adi F. Gazdar, Herbert K. Oie, Cedric H. Shackleton, et al. Establishment and characterization of a human adrenocortical carcinoma cell line that expresses multiple pathways of steroid biosynthesis. *Cancer Res*. 1990;50(17):5488-5496.

163. Duranova H, Fialkova V, Valkova V, et al. Human adrenocortical carcinoma cell line (NCI-H295R): An in vitro screening model for the assessment of endocrine disruptors' actions on steroidogenesis with an emphasis on cell ultrastructural features. *Acta Histochem*. 2022;124(5). doi:10.1016/J.ACTHIS.2022.151912

164. Ye J, Coulouris G, Zaretskaya I, Cutcutache I, Rozen S, Madden TL. Primer-BLAST: a tool to design target-specific primers for polymerase chain reaction. *BMC Bioinformatics*. 2012;13(1):134. doi:10.1186/1471-2105-13-134/FIGURES/5

165. Watanabe M, Simpson ER, Pathirage N, Nakajin S, Clyne CD. Aromatase expression in the human fetal osteoblastic cell line SV-HFO. *J Mol Endocrinol*. 2004;32(2):533-545. doi:10.1677/JME.0.0320533

166. Berthing T, Holmfred E, Vidmar J, et al. Comparison of biodistribution of cerium oxide nanoparticles after repeated oral administration by gavage or snack in Sprague Dawley rats. *Environ Toxicol Pharmacol*. 2022;95. doi:10.1016/J.ETAP.2022.103939

167. Hestehave S, Munro G, Pedersen TB, Abelson KSP. Antinociceptive effects of voluntarily ingested buprenorphine in the hot-plate test in laboratory rats. *Lab Anim*. 2017;51(3):264-272. doi:10.1177/0023677216668553

168. Pap A, Cuaranta-Monroy I, Peloquin M, Nagy L. Is the Mouse a Good Model of Human PPARγ-Related Metabolic Diseases? *Int J Mol Sci*. 2016;17(8). doi:10.3390/IJMS17081236

169. Zhao H, Pearson EK, Brooks DC, et al. A humanized pattern of aromatase expression is associated with mammary hyperplasia in mice. *Endocrinology*. 2012;153(6):2701-2713. doi:10.1210/en.2011-1761

170. Zhao H, Tian Z, Hao J, Chen B. Extragonadal aromatization increases with time after ovariectomy in rats. *Reprod Biol Endocrinol*. 2005;3. doi:10.1186/1477-7827-3-6

171. Ye L, Leung LK. Effect of dioxin exposure on aromatase expression in ovariectomized rats. *Toxicol Appl Pharmacol*. 2008;229(1):102-108. doi:10.1016/J.TAAP.2008.01.003

172. Byeon HR, Lee SH. Expression of Steroidogenesis-related Genes in Rat Adipose Tissues. *Dev Reprod*. 2016;20(3):197-205. doi:10.12717/DR.2016.20.3.197

173. Monteiro R, Assunção M, Andrade JP, Neves D, Calhau C, Azevedo I. Chronic green tea consumption decreases body mass, induces aromatase expression, and changes proliferation and apoptosis in adult male rat adipose tissue. *J Nutr*. 2008;138(11):2156-2163. doi:10.1093/JN/138.11.2156

174. Gonçalves RM, Delgobo M, Agnes JP, et al. COX-2 promotes mammary adipose tissue inflammation, local estrogen biosynthesis, and carcinogenesis in high-sugar/fat diet treated mice. *Cancer Lett*. 2021;502:44-57. doi:10.1016/J.CANLET.2021.01.003

175. Song WS, Koh DH, Kim EY. Orthogonal assay for validation of Tox21 PPARγ data and applicability to in silico prediction model. *Toxicol In Vitro*. 2022;84. doi:10.1016/J.TIV.2022.105445

176. Auld D, Thorne N, Boxer M, et al. Understanding Enzymes as Reporters or Targets in Assays Using Quantitative High-throughput Screening (qHTS). In: Hicks MG, Kettner C, eds. *Proceedings of the 4th International Beilstein Symposium on Experimental Standard Conditions of Enzyme Characterizations*. ; 2010:21-43. Accessed September 26, 2023. https://www.beilstein-institut.de/en/publications/proceedings/escec-2009/

177. Illés P, Grycová A, Krasulová K, Dvořák Z. Effects of Flavored Nonalcoholic Beverages on Transcriptional Activities of Nuclear and Steroid Hormone Receptors: Proof of Concept for Novel Reporter Cell Line PAZ-PPARg. *J Agric Food Chem*. 2018;66(45):12066-12078. doi:10.1021/ACS.JAFC.8B05158

178. England CG, Ehlerding EB, Cai W. NanoLuc: A Small Luciferase Is Brightening Up the Field of Bioluminescence. *Bioconjug Chem*. 2016;27(5):1175-1187. doi:10.1021/ACS.BIOCONJCHEM.6B00112

179. Ma ZG, Yuan YP, Zhang X, Xu SC, Wang SS, Tang QZ. Piperine Attenuates Pathological Cardiac Fibrosis Via PPAR-γ/AKT Pathways. *EBioMedicine*. 2017;18:179-187. doi:10.1016/J.EBIOM.2017.03.021

180. Filho HVR, Videira NB, Bridi AV, et al. Screening for PPAR Non-Agonist Ligands Followed by Characterization of a Hit, AM-879, with Additional No-Adipogenic and cdk5-Mediated Phosphorylation Inhibition Properties. *Front Endocrinol (Lausanne)*. 2018;9(FEB). doi:10.3389/FENDO.2018.00011

181. Jang DM, Jang JY, Kim HJ, Han BW. Differential Effects of Cancer-Associated Mutations Enriched in Helix H3 of PPARγ. *Cancers (Basel)*. 2020;12(12):1-17. doi:10.3390/CANCERS12123580

182. Shang J, Kojetin DJ. Structural mechanism underlying ligand binding and activation of PPARγ. *Structure*. 2021;29(9):940-950.e4. doi:10.1016/J.STR.2021.02.006

183. Frkic RL, Marshall AC, Blayo AL, et al. PPARγ in Complex with an Antagonist and Inverse Agonist: a Tumble and Trap Mechanism of the Activation Helix. *iScience*. 2018;5:69-79. doi:10.1016/J.ISCI.2018.06.012

184. Brust R, Shang J, Fuhrmann J, et al. A structural mechanism for directing corepressor-selective inverse agonism of PPARγ. *Nat Commun*. 2018;9(1). doi:10.1038/S41467-018-07133-W

185. Pelletier G, Rigden M, Wang GS, et al. Comparison of tris(2-ethylhexyl) phosphate and di(2-ethylhexyl) phosphoric acid toxicities in a rat 28-day oral exposure study. *J Appl Toxicol*. 2020;40(5):600-618. doi:10.1002/JAT.3930

186. McInnes KJ, Brown KA, Knower KC, Chand AL, Clyne CD, Simpson ER. Characterisation of aromatase expression in the human adipocyte cell line SGBS. *Breast Cancer Res Treat*. 2008;112(3):429-435. doi:10.1007/s10549-007-9883-2

187. Madsen L, Petersen RK, Kristiansen K. Regulation of adipocyte differentiation and function by polyunsaturated fatty acids. *Biochim Biophys Acta*. 2005;1740(2):266-286. doi:10.1016/J.BBADIS.2005.03.001

188. Gamwell JM, Paphiti K, Hodson L, Karpe F, Pinnick KE, Todorčević M. An optimised protocol for the investigation of insulin signalling in a human cell culture model of adipogenesis. *Adipocyte*. 2023;12(1). doi:10.1080/21623945.2023.2179339

189. Kassotis CD, Masse L, Kim S, Schlezinger JJ, Webster TF, Stapleton HM. Characterization of Adipogenic Chemicals in Three Different Cell Culture Systems: Implications for Reproducibility Based on Cell Source and Handling. *Scientific Reports 2017 7:1*. 2017;7(1):1-17. doi:10.1038/srep42104

190. Hall JM, Powell HA, Rajic L, Korach KS. The Role of Dietary Phytoestrogens and the Nuclear Receptor PPARγ in Adipogenesis: An in Vitro Study. *Environ Health Perspect*. 2019;127(3):037007-1-037007-037013. doi:10.1289/EHP3444

191. Corvera S. Cellular Heterogeneity in Adipose Tissues. *Annu Rev Physiol*. 2021;83:257. doi:10.1146/ANNUREV-PHYSIOL-031620-095446

192. Yanase T, Mu YM, Nishi Y, et al. Regulation of aromatase by nuclear receptors. *Journal of Steroid Biochemistry and Molecular Biology*. 2001;79(1-5):187-192. doi:10.1016/S0960-0760(01)00161-3

193. Mu YM, Yanase T, Nishi Y, et al. A nuclear receptor system constituted by RAR and RXR induces aromatase activity in MCF-7 human breast cancer cells. *Mol Cell Endocrinol*. 2000;166(2):137-145. doi:10.1016/S0303-7207(00)00273-2

194. Wilde J, Erdmann M, Mertens M, Eiselt G, Schmidt M. Aromatase activity induction in human adipose fibroblasts by retinoic acids via retinoic acid receptor α. *J Mol Endocrinol*. 2013;51(2):247-260. doi:10.1530/JME-12-0129

195. Kamei Y, Kawada T, Kazuki R, Sugimoto E. Retinoic acid receptor gamma 2 gene expression is up-regulated by retinoic acid in 3T3-L1 preadipocytes. *Biochem J*. 1993;293 (Pt 3)(Pt 3):807-812. doi:10.1042/BJ2930807

196. Xue JC, Schwarz EJ, Chawla A, Lazar MA. Distinct stages in adipogenesis revealed by retinoid inhibition of differentiation after induction of PPARgamma. *Mol Cell Biol*. 1996;16(4):1567-1575. doi:10.1128/MCB.16.4.1567

197. Kawada T, Kamei Y, Fujita A, et al. Carotenoids and retinoids as suppressors on adipocyte differentiation via nuclear receptors. *Biofactors*. 2000;13(1-4):103-109. doi:10.1002/BIOF.5520130117

198. Mcilroy GD, Tammireddy SR, Maskrey BH, et al. Fenretinide mediated retinoic acid receptor signalling and inhibition of ceramide biosynthesis regulates adipogenesis, lipid accumulation, mitochondrial function and nutrient stress signalling in adipocytes and adipose tissue. *Biochem Pharmacol*. 2016;100:86-97. doi:10.1016/J.BCP.2015.11.017

199. Harris CA, Henttu P, Parker MG, Sumpter JP. The estrogenic activity of phthalate esters in vitro. *Environ Health Perspect*. 1997;105(8):802-811. doi:10.1289/ehp.97105802

200. Scippo ML, Argiris C, Van De Weerdt C, et al. Recombinant human estrogen, androgen and progesterone receptors for detection of potential endocrine disruptors. *Anal Bioanal Chem*. 2004;378(3):664-669. doi:10.1007/s00216-003-2251-0

201. Wang X, Ha D, Yoshitake R, Chan YS, Sadava D, Chen S. Exploring the biological activity and mechanism of xenoestrogens and phytoestrogens in cancers: Emerging methods and concepts. *Int J Mol Sci*. 2021;22(16). doi:10.3390/ijms22168798

202. Whitehead SA, Rice S. Endocrine-disrupting chemicals as modulators of sex steroid synthesis. *Best Pract Res Clin Endocrinol Metab*. 2006;20(1):45-61. doi:10.1016/j.beem.2005.09.003

203. Luz AL, Kassotis CD, Stapleton HM, Meyer JN. The high-production volume fungicide pyraclostrobin induces triglyceride accumulation associated with mitochondrial dysfunction, and promotes adipocyte differentiation independent of PPARγ activation, in 3T3-L1 cells. *Toxicology*. 2018;393:150-159. doi:10.1016/J.TOX.2017.11.010

204. Else PL. The highly unnatural fatty acid profile of cells in culture. *Prog Lipid Res*. 2020;77. doi:10.1016/J.PLIPRES.2019.101017

205. Weidner C, Wowro SJ, Rousseau M, et al. Antidiabetic effects of chamomile flowers extract in obese mice through transcriptional stimulation of nutrient sensors of the peroxisome proliferator-activated receptor (PPAR) family. *PLoS One*. 2013;8(11). doi:10.1371/JOURNAL.PONE.0080335

206. Nieto C, Bragado R, Municio C, et al. The Activin A-Peroxisome Proliferator-Activated Receptor Gamma Axis Contributes to the Transcriptome of GM-CSF-Conditioned Human Macrophages. *Front Immunol*. 2018;9(JAN). doi:10.3389/FIMMU.2018.00031

207. Baumann A, Burger K, Brandt A, et al. GW9662, a peroxisome proliferator-activated receptor gamma antagonist, attenuates the development of non-alcoholic fatty liver disease. *Metabolism*. 2022;133. doi:10.1016/J.METABOL.2022.155233

208. Nakano R, Kurosaki E, Yoshida S, et al. Antagonism of peroxisome proliferator-activated receptor gamma prevents high-fat diet-induced obesity in vivo. *Biochem Pharmacol*. 2006;72(1):42-52. doi:10.1016/J.BCP.2006.03.023

209. Sharma S, Sharma PM, Mistry DS, et al. PPARG regulates gonadotropin-releasing hormone signaling in LbetaT2 cells in vitro and pituitary gonadotroph function in vivo in mice. *Biol Reprod*. 2011;84(3):466-475. doi:10.1095/BIOLREPROD.110.088005

210. Ka NL, Lim GY, Kim S -S, et al. Type I IFN stimulates IFI16-mediated aromatase expression in adipocytes that promotes E2-dependent growth of ER-positive breast cancer. *Cell Mol Life Sci*. 2022;79(6). doi:10.1007/S00018-022-04333-Y

211. Odawara H, Iwasaki T, Horiguchi J, et al. Activation of aromatase expression by retinoic acid receptor-related orphan receptor (ROR) alpha in breast cancer cells: identification of a novel ROR response element. *J Biol Chem*. 2009;284(26):17711-17719. doi:10.1074/JBC.M109.009241

212. Yuan H, Zhang J, Yin X, et al. The protective role of corilagin on renal calcium oxalate crystal-induced oxidative stress, inflammatory response, and apoptosis via PPAR-γ and PI3K/Akt pathway in rats. *Biotechnol Appl Biochem*. 2021;68(6):1323-1331. doi:10.1002/bab.2054

213. Sun X, Tang Y, Tan X, et al. Activation of peroxisome proliferator-activated receptor-γ by rosiglitazone improves lipid homeostasis at the adipose tissue-liver axis in ethanol-fed mice. *Am J Physiol Gastrointest Liver Physiol*. 2012;302(5):548-557. doi:10.1152/ajpgi.00342.2011

214. Tian C, Jin X, Ye X, et al. Long term intake of 0.1% ethanol decreases serum adiponectin by suppressing PPARγ expression via p38 MAPK pathway. *Food and Chemical Toxicology*. 2014;65:329-334. doi:10.1016/j.fct.2014.01.007

215. Howard RJ, Slesinger PA, Davies DL, Das J, Trudell JR, Harris RA. Alcohol-binding sites in distinct brain proteins: The quest for atomic level resolution. *Alcohol Clin Exp Res*. 2011;35(9):1561-1573. doi:10.1111/j.1530-0277.2011.01502.x

216. Itoh T, Fairall L, Amin K, et al. Structural basis for the activation of PPARgamma by oxidized fatty acids. *Nat Struct Mol Biol*. 2008;15(9):924-931. doi:10.1038/NSMB.1474

217. Harris RA, Trudell JR, Mihic SJ. Ethanol's molecular targets. *Sci Signal*. 2008;1(28). doi:10.1126/scisignal.128re7

218. Ahmed FE. Toxicological effects of ethanol on human health. *Crit Rev Toxicol*. 1995;25(4):347-367. doi:10.3109/10408449509021614

219. Le Daré B, Lagente V, Gicquel T. Ethanol and its metabolites: update on toxicity, benefits, and focus on immunomodulatory effects. *Drug Metab Rev*. 2019;51(4):545-561. doi:10.1080/03602532.2019.1679169

220. You M, Arteel GE. Effect of ethanol on lipid metabolism. *J Hepatol*. 2019;70(2):237-248. doi:10.1016/J.JHEP.2018.10.037

221. Contreras-Zentella ML, Villalobos-García D, Hernández-Muñoz R. Ethanol Metabolism in the Liver, the Induction of Oxidant Stress, and the Antioxidant Defense System. *Antioxidants*. 2022;11(7). doi:10.3390/ANTIOX11071258

222. Zakhari S. Overview: How Is Alcohol Metabolized by the Body? *Alcohol Research & Health*. 2006;29(4):245. Accessed October 22, 2023. /pmc/articles/PMC6527027/

223. Crabb DW, Zeng Y, Liangpunsakul S, Jones RM, Considine R. Ethanol impairs differentiation of human adipocyte stromal cells in culture. *Alcohol Clin Exp Res*. 2011;35(9):1584-1592. doi:10.1111/j.1530-0277.2011.01504.x

224. Yi SJ, Jhun BH. Ethanol impairs insulin's actions through phosphatidylinositol 3-kinase. *J Med Food*. 2004;7(1):24-30. doi:10.1089/109662004322984662

225. Sikder K, Shukla SK, Patel N, Singh H, Rafiq K. High Fat Diet Upregulates Fatty Acid Oxidation and Ketogenesis via Intervention of PPAR-γ. *Cell Physiol Biochem*. 2018;48(3):1317-1331. doi:10.1159/000492091

226. Chatterjee A, Kusunoki H, Taniyama Y, Rakugi H, Morishita R. Improvement of metabolic syndrome by irbesartan via the PPARγ/HGF pathway in apolipoprotein E knockout mice. *Biomed Rep*. 2013;1(1):65-70. doi:10.3892/BR.2012.28

227. Su M, Sang S, Liang T, Li H. PPARG: A Novel Target for Yellow Tea in Kidney Stone Prevention. *Int J Mol Sci*. 2023;24(15). doi:10.3390/IJMS241511955

228. Gokina NI, Chan SL, Chapman AC, Oppenheimer K, Jetton TL, Cipolla MJ. Inhibition of PPARγ during rat pregnancy causes intrauterine growth restriction and attenuation of uterine vasodilation. *Front Physiol*. 2013;4. doi:10.3389/FPHYS.2013.00184

229. Liao L, Zhang XD, Li J, et al. Pioglitazone attenuates lipopolysaccharide-induced depression-like behaviors, modulates NF-κB/IL-6/STAT3, CREB/BDNF pathways and central serotonergic neurotransmission in mice. *Int Immunopharmacol*. 2017;49:178-186. doi:10.1016/J.INTIMP.2017.05.036

230. Barney TM, Vore AS, Deak T. Acute Ethanol Challenge Differentially Regulates Expression of Growth Factors and miRNA Expression Profile of Whole Tissue of the Dorsal Hippocampus. *Front Neurosci*. 2022;16. doi:10.3389/FNINS.2022.884197

231. Kapetanovic IM, Lyubimov A V., Kabirova E V., et al. Effects of bacterial and presystemic nitroreductase metabolism of 2-chloro-5-nitro-N-phenylbenzamide on its mutagenicity and bioavailability. *Chem Biol Interact*. 2012;197(1):16-22. doi:10.1016/J.CBI.2012.03.002

232. Patocka J, Hon Z. Ethylene glycol, hazardous substance in the household. *Acta Medica (Hradec Kralove)*. 2010;53(1):19-23. doi:10.14712/18059694.2016.58

233. Wilson DF, Matschinsky FM. Ethanol metabolism: The good, the bad, and the ugly. *Med Hypotheses*. 2020;140:109638. doi:10.1016/J.MEHY.2020.109638

234. Zhang W, Zhong W, Sun X, et al. Visceral White Adipose Tissue is Susceptible to Alcohol-Induced Lipodystrophy in Rats: Role of Acetaldehyde. *Alcohol Clin Exp Res*. 2015;39(3):416. doi:10.1111/ACER.12646

235. Cederbaum AI. Alcohol metabolism. *Clin Liver Dis*. 2012;16(4):667-685. doi:10.1016/J.CLD.2012.08.002

236. Pethig R, Kell DB. The passive electrical properties of biological systems: their significance in physiology, biophysics and biotechnology. *Phys Med Biol*. 1987;32(8):933-970. doi:10.1088/0031-9155/32/8/001

237. Stocco C. Aromatase Expression in the Ovary: Hormonal and Molecular Regulation. *Steroids*. 2008;73(5):473. doi:10.1016/J.STEROIDS.2008.01.017

238. Doody KJ, Lorence MC, Mason JI, Simpson ER. Expression of messenger ribonucleic acid species encoding steroidogenic enzymes in human follicles and corpora lutea throughout the menstrual cycle. *J Clin Endocrinol Metab*. 1990;70(4):1041-1045. doi:10.1210/JCEM-70-4-1041

239. Zhou Y, Yan H, Liu W, et al. A multi-tissue transcriptomic landscape of female mice in estrus and diestrus provides clues for precision medicine. *Front Cell Dev Biol*. 2022;10:983712. doi:10.3389/FCELL.2022.983712/BIBTEX

240. Gui Y, Cai Z, Silha J V., Murphy LJ. Variations in parametrial white adipose tissue mass during the mouse estrous cycle: relationship with the expression of peroxisome proliferator-activated receptor-gamma and retinoic acid receptor-alpha. *Can J Physiol Pharmacol*. 2006;84(8-9):887-892. doi:10.1139/Y06-032

241. Kadowaki K, Fukino K, Negishi E, Ueno K. Sex differences in PPARgamma expressions in rat adipose tissues. *Biol Pharm Bull*. 2007;30(4):818-820. doi:10.1248/BPB.30.818

242. Brown KA, Scherer PE. Update on Adipose Tissue and Cancer. *Endocr Rev*. 2023;(May):1-14. doi:10.1210/endrev/bnad015

243. Food and water intake. *Handb Behav Neurosci*. 1994;12(C):267-287. doi:10.1016/B978-0-444-81871-3.50019-9

244. Kang L, Sebastian BM, Pritchard MT, Pratt BT, Previs SF, Nagy LE. Chronic ethanol-induced insulin resistance is associated with macrophage infiltration into adipose tissue and altered expression of adipocytokines. *Alcohol Clin Exp Res*. 2007;31(9):1581-1588. doi:10.1111/J.1530-0277.2007.00452.X

245. He Z, Li M, Zheng D, Chen Q, Liu W, Feng L. Adipose tissue hypoxia and low-grade inflammation: A possible mechanism for ethanol-related glucose intolerance? *British Journal of Nutrition*. 2015;113(9):1355-1364. doi:10.1017/S000711451500077X

246. Krempler F, Breban D, Oberkofler H, et al. Leptin, peroxisome proliferator-activated receptor-gamma, and CCAAT/enhancer binding protein-alpha mRNA expression in adipose tissue of humans and their relation to cardiovascular risk factors. *Arterioscler Thromb Vasc Biol*. 2000;20(2):443-449. doi:10.1161/01.ATV.20.2.443

247. Wang L, Shao YY, Ballock RT. Leptin Antagonizes Peroxisome Proliferator-Activated Receptor-γ Signaling in Growth Plate Chondrocytes. *PPAR Res*. 2012;2012. doi:10.1155/2012/756198

248. Boberg J, Metzdorff S, Wortziger R, et al. Impact of diisobutyl phthalate and other PPAR agonists on steroidogenesis and plasma insulin and leptin levels in fetal rats. *Toxicology*. 2008;250(2-3):75-81. doi:10.1016/j.tox.2008.05.020

249. Lagathu C, Bastard JP, Auclair M, Maachi M, Capeau J, Caron M. Chronic interleukin-6 (IL-6) treatment increased IL-6 secretion and induced insulin resistance in adipocyte: prevention by rosiglitazone. *Biochem Biophys Res Commun*. 2003;311(2):372-379. doi:10.1016/J.BBRC.2003.10.013

250. Rotter V, Nagaev I, Smith U. Interleukin-6 (IL-6) Induces Insulin Resistance in 3T3-L1 Adipocytes and Is, Like IL-8 and Tumor Necrosis Factor-α, Overexpressed in Human Fat Cells from Insulin-resistant Subjects. *Journal of Biological Chemistry*. 2003;278(46):45777-45784. doi:10.1074/JBC.M301977200

251. Assi M, Kenawi M, Ropars M, Rébillard A. Interleukin-6, C/EBP-β and PPAR-γ expression correlates with intramuscular liposarcoma growth in mice: The impact of voluntary physical activity levels. *Biochem Biophys Res Commun*. 2017;490(3):1026-1032. doi:10.1016/J.BBRC.2017.06.158

252. Cui H, Zhao G, Wen J, Tong W. Follicle-stimulating hormone promotes the transformation of cholesterol to estrogen in mouse adipose tissue. *Biochem Biophys Res Commun*. 2018;495(3):2331-2337. doi:10.1016/j.bbrc.2017.12.120

253. Chen D, Zhao H, Coon JS, Ono M, Pearson EK, Bulun SE. Weight gain increases human aromatase expression in mammary gland. *Mol Cell Endocrinol*. 2012;355(1):114-120. doi:10.1016/J.MCE.2012.01.027

Appendix I

Comparison of the effect of cell density on the luminescent signal in the PPARγ reporter assay.

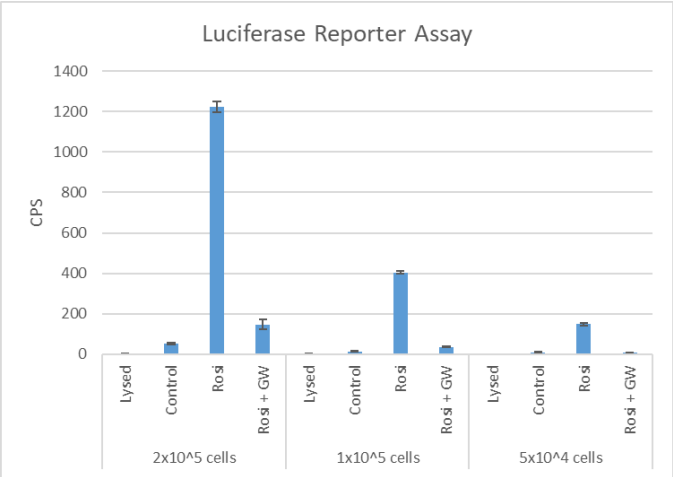

CPS: counts per second.

Lysed:	2% Triton X-100 was used to lyse the cells
Control:	0.0006% DMSO was used as control
Rosi:	100 nM rosiglitazone was used to activate PPARγ
Rosi + GW:	100 nM GW9662 was used to inhibit PPARγ activation induced by 100 nM rosiglitazone

The graph shows means of 3 technical replicates (different wells in the same plate) ± SEM.

Appendix II

Pre-adipocyte differentiation protocols.

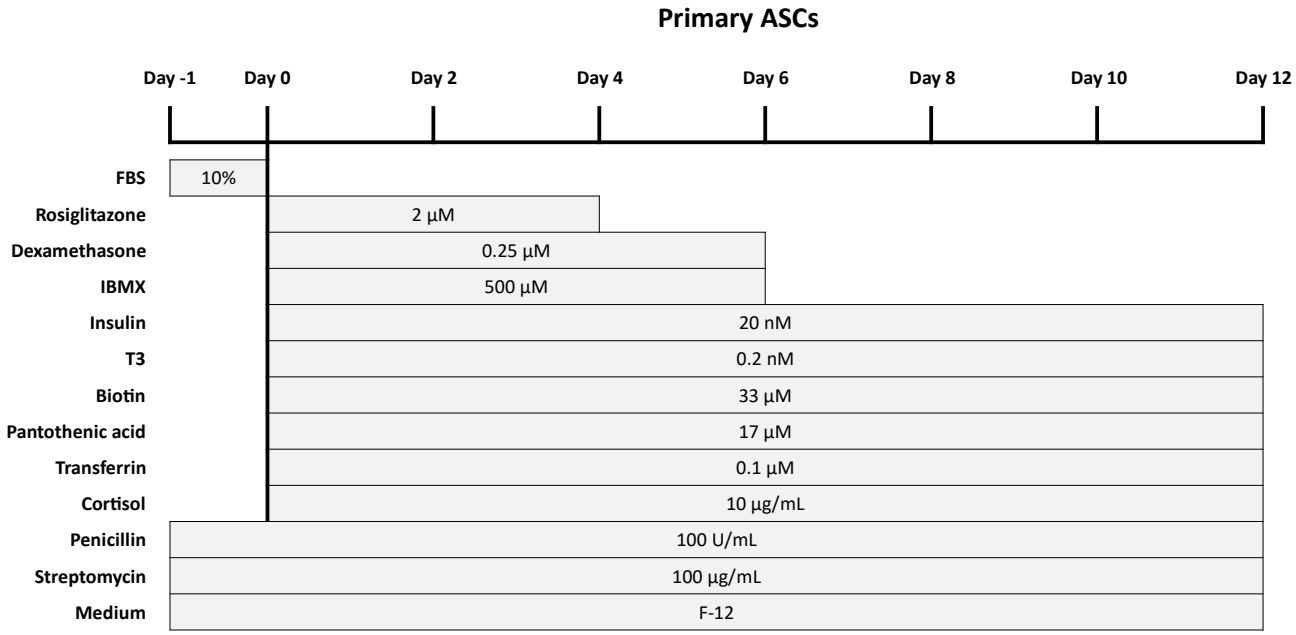

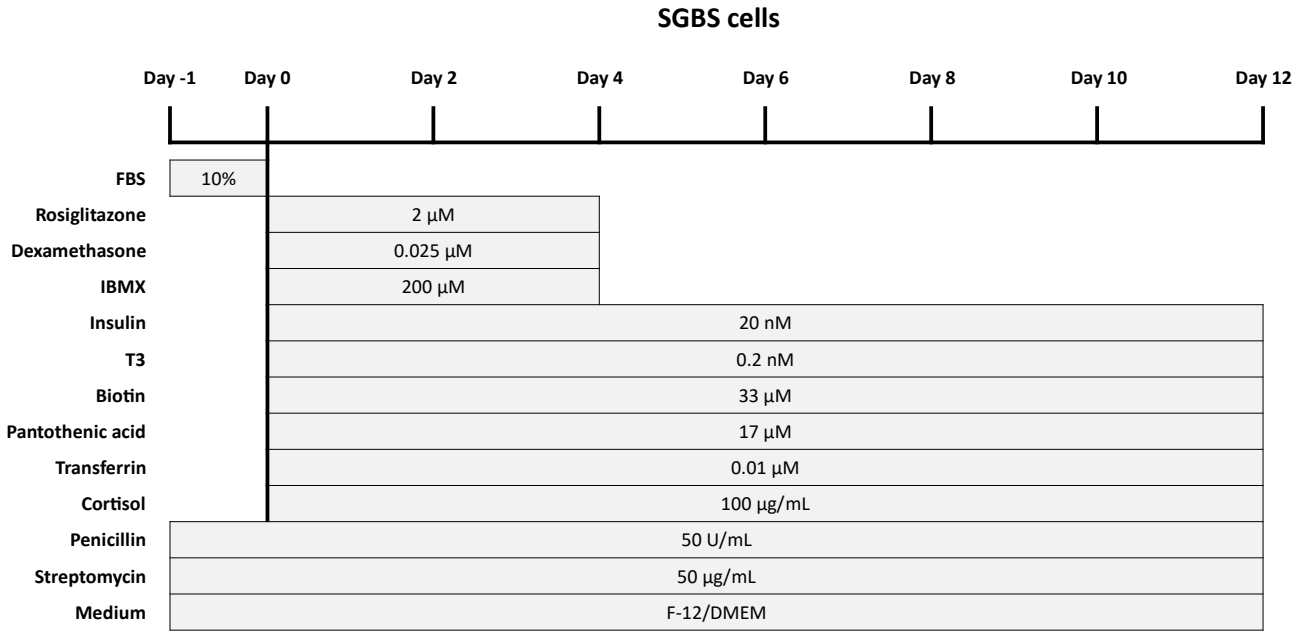

A41 cells

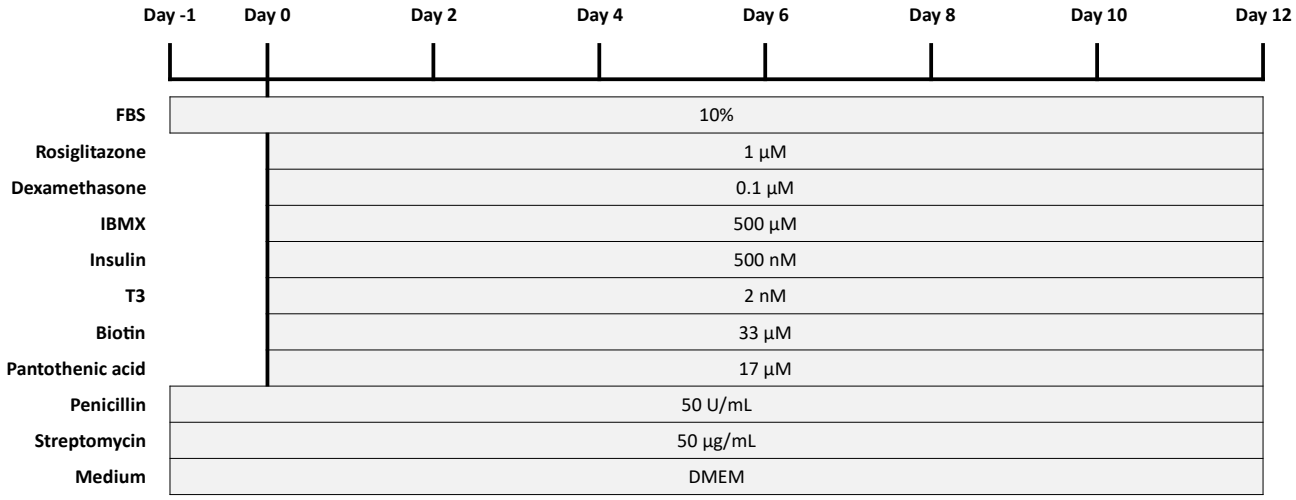

C3H10T1/2 cells

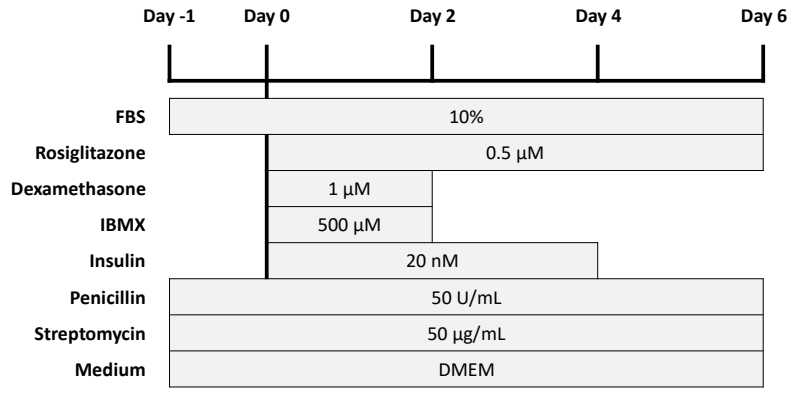

Appendix III

Primer sets were tested using RT-qPCR. JA1 and JA2 were designed for this study. They were compared to a commonly used aromatase primer set (RT7/RT8). The primers were tested in primary human adipose stromal cells treated with forskolin and PMA for 24 h in serum-free medium. The graph shows means of 3 technical qPCR replicates ± SEM. The JA1 primer set was selected for further studies due to lowest C_t values.

NT No treatment
Vehicle Solvent control (0.05% EtOH, 0.0021% DMSO)
FSK1 4 nM PMA, 1 µM forskolin
FSK5 4 nM PMA, 5 µM forskolin
FSK25 4 nM PMA, 25 µM forskolin

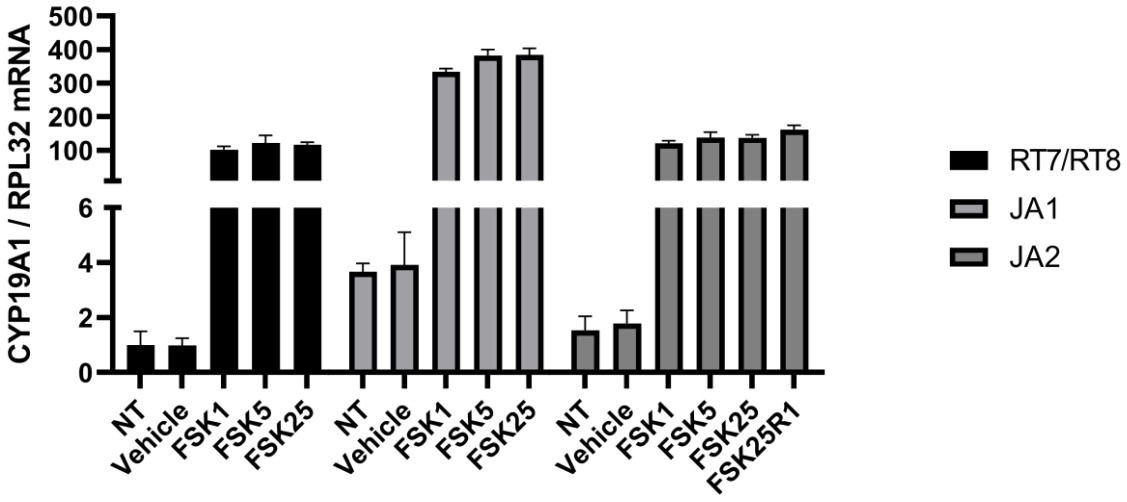

C_t values

	NT	Vehicle	FSK 1	FSK 5	FSK 25	FSK 25 R1
RPL32	20.2	19.9	20.2	20.5	20.3	20.4
RT7/RT8	34.4	34.1	27.7	27.7	27.6	27.3
JA1	32.4	32.1	25.9	26.0	25.9	25.9
JA2	33.7	33.3	27.4	27.5	27.3	27.2

qPCR primers

Primer	Sequence	T_m	GC%	SC	3' SC
RT7	TTGGAAATGCTGAACCCGAT	57.79	45.00	2.00	2.00
RT8	CAGGAATCTGCCGTGGGAGA	61.62	60.00	6.00	6.00

Primer	Sequence	T_m	GC%	SC	3' SC
JA1 F	TTGACCCTTCTGCGTCGTGT	62.02	55.00	3.00	0.00
JA1 R	AGGAGAGCTTGCCATGCATCA	62.14	52.38	6.00	3.00

Primer	Sequence	T_m	GC%	SC	3' SC
JA2 F	ATTCGGCAGCAAACTTGGGC	62.16	55.00	4.00	2.00
JA2 R	GGGGCCTGACAGAGCTTTCATA	62.07	54.55	6.00	2.00

T_m Melting temperature
GC% Guanine-cytosine content
SC Self complementarity
3' SC Self 3' complementarity

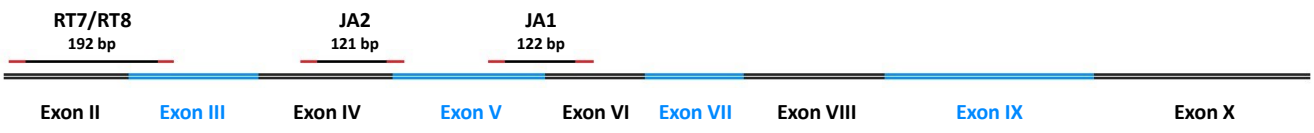

CYP19A1 coding region

Appendix IV

Agarose gel electrophoresis of *CYP19A1* RT-qPCR products from A41 cell lysates amplified using the JA1 primers.